

## University of Southampton Research Repository

Copyright © and Moral Rights for this thesis and, where applicable, any accompanying data are retained by the author and/or other copyright owners. A copy can be downloaded for personal non-commercial research or study, without prior permission or charge. This thesis and the accompanying data cannot be reproduced or quoted extensively from without first obtaining permission in writing from the copyright holder/s. The content of the thesis and accompanying research data (where applicable) must not be changed in any way or sold commercially in any format or medium without the formal permission of the copyright holder/s.

When referring to this thesis and any accompanying data, full bibliographic details must be given, e.g.

Thesis: Author (Year of Submission) "Full thesis title", University of Southampton, name of the University Faculty or School or Department, PhD Thesis, pagination.

Data: Author (Year) Title. URI [dataset]



**University of Southampton**

Faculty of Medicine

Cancer Science Unit – Antibody and Vaccine Group

**Role of the Akt Signalling Pathway in CD8 T Cell Immune Response**

by

**Thomas James Bailey**

Thesis for the degree of Doctor of Philosophy

September 2018



# University of Southampton

## Abstract

Faculty of Medicine

Cancer Sciences Unit – Antibody and Vaccine Group

Thesis for the degree of Doctor of Philosophy

Role of the Akt Signalling Pathway in CD8 T Cell Immune Response

by

Thomas James Bailey

Understanding the signalling pathways controlling activation and differentiation of CD8 T cells will facilitate their exploitation for anti-cancer therapy. The Akt/PKB signalling pathway influences CD8 T cell function and differentiation but published data are discrepant. Utilising a PDK<sup>K465E</sup> knock-in mutant mouse model, in which T cells exhibit impaired Akt activity, data presented here show that sub-optimal Akt activity limits CD8 T cell IFN- $\gamma$  and IL-2 production, granzyme B expression and cellular cytotoxicity. Additional chemical inhibition of Akt further hindered cytotoxicity and granzyme B expression. Microarray and confirmatory qPCR showed reduced expression of transcripts encoding the membrane trafficking protein BAIAP3 in PDK<sup>K465E</sup> cells which may be responsible for some of these effects.

Previous data from the group showed that PDK<sup>K465E</sup> CD8 T cells have a skewed memory population. Here single cell RNA sequencing and unsupervised clustering was used to define 7 cell subsets at the peak of *Listeria Monocytogenes* infection and in which a memory precursor effector cell-like phenotype was favoured by PDK<sup>K465E</sup> cells. Additionally, mRNA encoding ribosomal proteins was enriched in PDK<sup>K465E</sup> compared with WT CD8 T cells, and also in more memory-like cells across both samples. PDK<sup>K465E</sup> cells also exhibited enrichment in OXPHOS-related transcripts, a feature previously correlated with a memory phenotype.

Use of PDK<sup>K465E</sup> mutant cells, pharmacological inhibition (Akti) and a constitutive form of Akt (Myr-Akt), allowed further examination of effects of altered Akt activity on oxidative phosphorylation. These data showed no significant improvement in spare respiratory capacity (SRC) in Akt-inhibited WT CD8 T cells cultured in IL-2 although Akt inhibition in PDK<sup>K465E</sup> CD8 T cells resulted in a significant improvement in SRC. Enforced Akt activity in CD8 T cells cultured in IL-15 reduced SRC. However, SRC remained higher than IL-2-treated cells, indicating that whilst increased Akt activity impairs oxidative phosphorylation, there are aspects of IL-15 signalling that cannot be overcome by constitutive Akt activity. Despite a beneficial metabolic and cytotoxic profile, Myr-Akt transduced IL-15 treated CD8 T cells were only marginally superior to IL-15 treated controls cells at conferring tumour therapy.

SGK1, a kinase sharing homology with Akt, was also examined for its effects in CD8 T cells. Under stimulation with normal or restrictive concentrations of IL-2, pharmacological inhibition of SGK1 had negative effects on cellular proliferation. Further, stimulation of SGK1 through increased NaCl concentrations in culture media caused increased survival of CD8 T cells in both cytokine replete and limiting conditions.

Together the data presented in this thesis show that reduced Akt signalling causes a defect in the cytotoxic capacity of CD8 T cells *in vitro* and alters the transcriptome of CD8 T cells at the peak of an immune response, inducing a more MPEC phenotype. In addition, new subsets of CD8 T cells were identified through Drop-Seq. Mitochondrial oxidative phosphorylation was shown to be negatively regulated by Akt activity. Lastly, SGK1 was shown to increase survival and proliferation of CD8 T cells. These data have implications for CD8 T cell differentiation and treatments aimed at manipulating Akt for therapeutic benefit.



# Table of Contents

<b>Table of Contents</b> .....	<b>i</b>
<b>Table of Figures</b> .....	<b>v</b>
<b>Research Thesis: Declaration of Authorship</b> .....	<b>ix</b>
<b>Acknowledgements</b> .....	<b>xi</b>
<b>Definitions and Abbreviations</b> .....	<b>xiii</b>
<b>Chapter 1 Introduction</b> .....	<b>1</b>
1.1 The Immune System.....	1
1.1.1 Innate Immunity.....	1
1.1.2 Adaptive Immunity.....	2
1.2 T Cell Development and Activation.....	3
1.2.1 Maturation .....	3
1.2.1.1 DN1-4.....	3
1.2.1.2 DP-SP .....	4
1.2.2 Activation .....	5
1.2.2.1 Signal 1 - T Cell Receptor .....	5
1.2.2.2 Signal 2 - Co-stimulation.....	8
1.2.2.3 Signal 3 - Cytokines.....	10
1.2.2.4 CD4 T cells.....	12
1.2.2.5 CD8 T cells.....	14
1.2.3 CD8 T Cell Subsets .....	17
1.2.3.1 SLECs and MPECs.....	17
1.2.3.2 Effector Memory and Central Memory.....	18
1.2.3.3 Resident Memory .....	18
1.2.3.4 Stem-cell Like Memory.....	19
1.2.4 Models of Differentiation.....	19
1.2.4.1 Decreasing Potential Model .....	19
1.2.4.2 Signal Strength Model .....	20
1.2.4.3 Asymmetric Cell Division .....	20

## Table of Contents

1.2.5	$\gamma\delta$ T Cells .....	21
1.3	PI3K-Akt Signalling Pathway .....	21
1.3.1	PI3K .....	23
1.3.2	PKD1 .....	25
1.3.3	Akt .....	26
1.4	Cancer Immunology .....	27
1.5	Immunotherapies .....	31
1.5.1	Monoclonal Antibodies .....	31
1.5.1.1	Passive Monoclonal Antibodies .....	31
1.5.1.2	Active Monoclonal Antibodies .....	33
1.5.2	Adoptive Cell Transfer .....	35
1.5.3	Cancer Vaccines .....	37
1.6	Aims and Hypotheses .....	39
<b>Chapter 2</b>	<b>Methods .....</b>	<b>41</b>
2.1	Mice .....	41
2.2	Reagents .....	41
2.3	Cell Lines .....	41
2.4	qPCR .....	42
2.5	ELISA .....	43
2.6	CFSE Proliferation Assay .....	44
2.7	Thymidine Proliferation Assay .....	44
2.8	Microscopy .....	44
2.9	Flow Cytometry .....	45
2.10	Cytotoxicity Assay .....	46
2.11	Plasmid Cloning .....	47
2.12	Metabolism Assays .....	47
2.13	Western Blots .....	48
2.14	Transfection .....	49
2.15	Transduction .....	49
2.16	Cell Sorting .....	50
2.17	Tumour Challenges .....	50

2.18 Drop-Seq.....	51
2.19 Statistical and Computational Analysis .....	51
<b>Chapter 3 Effect of Akt Signalling on Effector Functions of CD8 T Cells in vitro .....</b>	<b>53</b>
3.1 Introduction.....	53
3.2 Results .....	57
3.2.1 Effect of Akt Signalling on CD8 T Cell Cytokine Expression.....	57
3.2.2 Effects of Akt Signalling on CD8 T Cell Cytotoxicity .....	63
3.2.3 Potential Role of Akt in the Regulation of Secretion in CD8 T Cells.....	71
3.3 Summation and Discussion .....	75
<b>Chapter 4 Effects of Akt Signalling on CD8 Effector T Cell Differentiation Determined by Single Cell RNA Sequencing.....</b>	<b>81</b>
4.1 Introduction.....	81
4.2 Results .....	83
4.2.1 Drop-Seq Analysis of the Effects of the PDK <sup>K465E</sup> Mutation on CD8 T cell Differentiation .....	85
4.2.2 Gene Set Enrichment Analysis.....	96
4.2.2.1 Comparison of WT SLEC Subsets.....	98
4.2.2.2 Effects of PDK <sup>K465E</sup> Mutation on Metabolic Processes .....	100
4.2.2.3 Effect of the PDK <sup>K465E</sup> Mutation on SLECs .....	100
4.2.2.4 Comparison of MPEC Subsets .....	102
4.3 Summation and Discussion .....	105
<b>Chapter 5 Effect of Akt Signalling on CD8 T Cell Metabolism and Adoptive Cell Therapy of Cancer .....</b>	<b>111</b>
5.1 Introduction.....	111
5.2 Results .....	117
5.3 Summation and Discussion .....	133
<b>Chapter 6 The Role of SGK in CD8 T Cells .....</b>	<b>139</b>
6.1 Introduction.....	139
6.1.1 SGK .....	139

Table of Contents

6.2	Results.....	143
6.3	Summation and Discussion.....	154
<b>Chapter 7</b>	<b>Discussion.....</b>	<b>157</b>
7.1	Models of CD8 T Cell Differentiation .....	157
7.2	The Role of Akt in CD8 T Cell Differentiation.....	160
7.2.1	Epigenetic Modification by Akt in T Cells.....	160
7.2.2	Regulation of Transcription Factor Activity by Akt in T Cells.....	163
7.2.3	Influence of Akt Signalling on CD8 T Cell Metabolism.....	166
7.3	Summation.....	168
<b>Chapter 8</b>	<b>Data Appendix.....</b>	<b>171</b>
	<b>List of References .....</b>	<b>173</b>

## Table of Figures

Figure 1-1 – Mechanism of Antigen Processing and Presentation .....	7
Figure 1-2 – Three Signal Mechanism of T Cell Activation.....	11
Figure 1-3 – The TCR – PI3K/Akt Signalling Pathway in CD8 T Cells .....	22
Figure 2-1 - Antibody Source Table.....	45
Figure 3-1 – Effect of PDK <sup>K465E</sup> mutation on IFN $\gamma$ secretion by CD8 <sup>+</sup> T cells.....	57
Figure 3-2– Effect of restimulating with peptides of different affinities on WT and PDK <sup>K465E</sup> CD8 <sup>+</sup> T cells. ....	59
Figure 3-3 – Effect of initial SIIQFEKL stimulation on IFN $\gamma$ secretion by WT and PDK <sup>K465E</sup> CD8 <sup>+</sup> T cells.....	60
Figure 3-4 – Gating strategy for intracellular cytokine staining .....	61
Figure 3-5 – Intracellular production of IFN $\gamma$ in WT and PDK <sup>K465E</sup> CD8 <sup>+</sup> T cells.....	62
Figure 3-6 – Intracellular production of IL-2 in WT and PDK <sup>K465E</sup> CD8 <sup>+</sup> T cells. ....	63
Figure 3-7 – Optimisation of PKH26 and CFSE staining protocol and cytotoxicity assay proof of concept.....	64
Figure 3-8 – Effects of Peptide Affinity on Cytotoxicity .....	66
Figure 3-9 – Effects of Akt Inhibition on Cytotoxicity .....	68
Figure 3-10 – Effect of the PDK Mutation on CD8 T cell Cytotoxicity.....	70
Figure 3-11 – Difference in <i>Baiap3</i> expression in WT and PDK <sup>K465E</sup> mutant CD8 <sup>+</sup> T cells.....	72
Figure 3-12 – Immunofluorescent assessment of Baiap3 protein expression by fluorescence microscopy and flow cytometry .....	73
Figure 4-1 – Analysis of phenotypic markers in CD8 T cells 45 hours post <i>in vivo</i> stimulation with listeria-OVA. ....	84
Figure 4-2 – Schematic of Drop-Seq mechanism for single cell RNA capture. ....	87

Table of Figures

Figure 4-3 – Schematic of molecular biology processes between single cell capture and next generation sequencing post Drop-Seq.....	88
Figure 4-4 – Quality control assessment of PCR and Tagmentation products.....	90
Figure 4-5 – Drop-Seq analysis of WT and PDK OT-1 CD8 T cells 6 days post <i>in vivo</i> stimulation with listeria-OVA .....	92
Figure 4-6 – Population distribution of t-SNE plot clusters in Drop-Seq analysis.....	93
Figure 4-7 – Phenotypic violin plots of cells analysed from Drop-Seq experiment.....	94
Figure 4-8 – Classification of Drop-Seq clusters based on existing phenotypic markers .....	95
Figure 4-9 – Genes Encoding Ribosomal protein Gene Set Enrichment Analysis (GSEA) of Drop-Seq data set. ....	97
Figure 4-10 – Gene Set Enrichment Analysis (GSEA) comparison of clusters 6 and 3. ....	99
Figure 4-11 – Gene Set Enrichment Analysis (GSEA) of Oxidative Phosphorylation. ....	100
Figure 4-12 – Gene Set Enrichment Analysis (GSEA) comparing cluster 6 with cluster 2. ....	102
Figure 4-13 – Gene Set Enrichment Analysis (GSEA) comparing clusters 4, 7 and 8 .....	103
Figure 5-1 – Metabolic Pathways in CD8 T cells.....	114
Figure 5-2 – Effect of Akt activity on oxidative phosphorylation on CD8 <sup>+</sup> T cells.....	118
Figure 5-3 – Effect of PDK <sup>K465E</sup> mutation on oxidative phosphorylation in CD8 <sup>+</sup> T cells. ....	119
Figure 5-4 – Schematic of Myristoylated Akt and pMP71 Sequence. ....	121
Figure 5-5 – Representative Expression of CD62L and GFP Post Transduction with Myr-Akt.....	123
Figure 5-6 – Effect of transduced myristoylated Akt on oxidative phosphorylation in CD8 <sup>+</sup> T cells .....	125
Figure 5-7 – Effect of transduced myristoylated Akt on CD8 T cell cytotoxicity.....	126
Figure 5-8 – Adoptive cell transfer utilising Myr-Akt transduction for tumour therapy.....	128
Figure 5-9 – Tracking survival of Myr-Akt transduced cells.....	130
Figure 5-10 – Phenotype of tracked Myr-Akt transduced cells.....	131
Figure 6-1 – The SGK Signalling Pathway. ....	141

<b>Figure 6-2 – Effects of SGKi on NDRG1 phosphorylation in CD8<sup>+</sup> T cells. ....</b>	<b>143</b>
<b>Figure 6-3 – Effects of SGKi on Tritiated Thymidine Incorporation by CD8<sup>+</sup> T cells. ....</b>	<b>144</b>
<b>Figure 6-4 – SGKi prevents cellular proliferation and reduces survival in naïve cells. ....</b>	<b>146</b>
<b>Figure 6-5 – NaCl protects CD8 T cells under cytokine deprived conditions.....</b>	<b>148</b>
<b>Figure 6-6 – SGK and pMP71 Vector Maps.....</b>	<b>150</b>
<b>Figure 6-7 – Restriction digest of SGK DN and SGK CA .....</b>	<b>151</b>
<b>Figure 6-8 – Restriction digest of SGK DN, pMP71 and SGK CA samples .....</b>	<b>152</b>
<b>Figure 6-9 – Effect of dominant negative and constitutively active SGK transduction on CD8 T cells.....</b>	<b>153</b>
<b>Figure 7-1 – Models of Differentiation.....</b>	<b>158</b>
<b>Figure 7-2 – Akt signalling pathway.....</b>	<b>162</b>
<b>Figure 8-1 – Expression of CD8a in t-SNE clusters.....</b>	<b>171</b>



## Research Thesis: Declaration of Authorship

Print name: Thomas James Bailey

Title of thesis: Role of the Akt Signalling Pathway in CD8 T Cell Immune Response

I declare that this thesis and the work presented in it are my own and has been generated by me as the result of my own original research.

I confirm that:

1. This work was done wholly or mainly while in candidature for a research degree at this University;
2. Where any part of this thesis has previously been submitted for a degree or any other qualification at this University or any other institution, this has been clearly stated;
3. Where I have consulted the published work of others, this is always clearly attributed;
4. Where I have quoted from the work of others, the source is always given. With the exception of such quotations, this thesis is entirely my own work;
5. I have acknowledged all main sources of help;
6. Where the thesis is based on work done by myself jointly with others, I have made clear exactly what was done by others and what I have contributed myself;
7. None of this work has been published before submission:

Signature:

Date: 25/09/2018



## Acknowledgements

I would like to begin this section by thanking Professor Aymen Al-Shamkhani. You did not have to provide me with the opportunity of this PhD, and as such, I am eternally grateful to you for allowing me to join your lab group. Your guidance over the course of my PhD has been invaluable. Your encouragement to learn new techniques such as Drop-Seq and the coding required to analyse it, will only come to serve well in my future career. So for all your advice over the past four years, thank you sincerely.

I am deeply grateful to my secondary supervisor Dr Sarah Buchan for her support throughout the course of this PhD. From training me in the lab at the start of this PhD, to giving final editing advice on this thesis, I could always count on you to answer any question I had. Without your critical eye I am certain my writing over the course of this PhD would not have improved in the slightest. For that and so much more, thank you.

I am very confident when stating the fact that there is no harder-working, nor more dedicated scientist than Dr Anne Rogel. Demonstrated by the fact that for the first few months I was convinced she never left the lab. Please know Anne that you are a constant source of inspiration for me to work harder, even though I am not sure it is possible to match the effort you put in.

I would like to acknowledge and thank everyone who worked in the antibody and vaccine group in the Tenovus building. From the administrative staff to the lab technicians and the BRF staff. You all helped make these four years of work easier by being so warm and welcoming. I am particularly grateful to both Dr Matthew Rose-Zerilli for his help in my work with Drop-Seq, and Dr Steve Thirdborough for his bioinformatics analysis of my Drop-Seq data.

Lastly, I would like to sincerely thank my family for their support over the last four years. They were a great source of encouragement and aid over these last 4 months during my writing of this thesis. I truly appreciate all the support afforded to me.



## Definitions and Abbreviations

2-ME	2-Mercaptoethanol
3GP	3-Phosphoglyceric Acid
β2M	β2-Microglobulin
ABD	Adaptor Binding Domain
ACT	Adoptive Cell Transfer
ADCC	Antibody-Dependent Cellular Cytotoxicity
AICD	Activation Induced Cell Death
AKT	Protein Kinase B (PKB)
AMPK	AMP Activated Protein Kinase
APC	Antigen Presenting Cell
BAI1	Brain-specific Angiogenesis Inhibitor
BAIAP3	Brain-specific Angiogenesis Inhibitor Associated Protein 3
BCR	B Cell Receptor
CAF	Cancer Associated Fibroblast
CAR	Chimeric Antigen Receptor
Cas	CRISPR Associated Protein
CDC	Complement-Dependent Cytotoxicity
CFSE	Carboxyfluorescein Succinimidyl Ester
CPT1α	Carnitine Palmitoyl Transferase 1 α
CRISPR	Clustered Regularly Interspaced Short Palindromic Repeat
cTEC	Cortical Thymic Epithelial Cells
CTL	Cytotoxic T Lymphocyte
CTLA-4	Cytotoxicity T Lymphocyte-associated Antigen 4

## Definitions and Abbreviations

CX3CR1	CX3C chemokine receptor 1
D	Diversity
DAG	Diacylglycerol
DAMP	Damage/Danger Associated Molecular Pattern
DN	Double Negative
DNMT1	DNA Methyltransferase 1
DP	Double Positive
DSRCT	Desmoplastic Small Round Cell Tumour
ECACC	European Collection of Cell Cultures
ECAR	Extracellular Acidification Rate
EGFR	Epidermal Growth Factor Receptor
EMT	Epithelial to Mesenchymal Transition
ENaC	Epithelial Sodium Channel
EOMES	Eomesodermin
ERAP	Endoplasmic Reticulum Aminopeptidase
ERK	Extracellular Signal-Regulated Kinase
EZH2	Enhancer of Zeste Homologue 2
FAO	Fatty Acid Oxidation
FCCP	Carbonyl Cyanide-4-(Trifluoromethoxy) Phenylhydrazone
FDR	False Discovery Rate
FHL	Familial Haemophagocytic Lymphohistiocytosis
FOXO	Family Forkhead Box O
G6P	Glucose-6-Phosphate
GAPDH	Glyceraldehyde 3-Phosphate Dehydrogenase

GFP	Green Fluorescent Protein
GLUT1	Glucose Transporter 1
GM-CSF	Granulocyte-Macrophage Colony-Stimulating Factor
GSEA	Gene Set Enrichment Analysis
GSK3	Glycogen Synthase Kinase 3
Gzmb	Granzyme B
HDF	Human Dermal Fibroblast
HIF	Hypoxia Inducible Factor
ID	Inhibitor of DNA binding
IDT	Integrated DNA Technologies
IP <sub>3</sub>	Inositol Trisphosphate
ITAM	Immunoreceptor Tyrosine-based Activation Motif
iT <sub>regs</sub>	Induced T <sub>regs</sub>
J	Joining
KLF2	Krüppel-like Factor 2
KRAS	Kirsten Rat Sarcoma virus
LAT	Linker of Activated T cells
LBP	Lipopolysaccharide Binding Protein
LCMV	Lymphocytic Choriomeningitis Virus
LDH	Lactate Dehydrogenase
LM-OVA	OVA-expressing <i>Listeria Monocytogenes</i>
LPS	Lipopolysaccharide
mAb	Monoclonal Antibodies
MAPK	Mitogen Activated Protein Kinase

## Definitions and Abbreviations

mCRC	Metastatic Colorectal Cancer
MDSC	Myeloid Derived Suppressor Cell
MFN	Mitofusion
MHC	Major Histocompatibility Complex
MMP	Matrix Metalloproteinase
MPEC	Memory Precursor Effector Cell
mRCC	Metastatic Renal Cell Carcinoma
Myr-Akt	Myristoylated Akt
NDRG1	N-myc Down-Regulated Gene 1
Nedd4-2	Neural precursor cell Expressed Developmentally Downregulated gene 4-like
NES	Normalised Enrichment Score
NF- $\kappa$ B	Nuclear Factor kappa-light-chain-enhancer of activated B cell
NFAT	Nuclear Factor of Activated T Cells
NGS	Next Generation Sequencing
NK	Natural Killer
NSCLC	Non-Small Cell Lung Cancer
nT <sub>regs</sub>	Natural (Thymic) T <sub>regs</sub>
NTreg	Natural Regulatory T Cells
OCR	Oxygen Consumption Rate
Opa1	Optic Atrophy 1
OVA	Ovalbumin
OXPPOS	Oxidative Phosphorylation
PAMP	Pathogen-Associated Molecular Pattern
PD-1	Programmed Death 1

PDGF	Platelet Derived Growth Factor
PDHK1	Pyruvate Dehydrogenase
PDK	Phosphoinositide Dependent Protein Kinase
PDK1	Phosphoinositide Dependent Protein Kinase-1
PFA	Paraformaldehyde
PFS	Progression Free Survival
PH	Pleckstrin Homology
PHLPP	PH Domain Leucine-Rich Repeat Phosphatase
PIP	Phosphatidylinositol Phosphate
PKA	Protein Kinase A
PKC	Protein Kinase C
PLC	Peptide Loading Complex
PLC	Phospholipase C
PLL	Poly-L-Lysine
PP2	Protein Phosphatase 2
PRC	Polycomb-repressive complex 2
PRDM1	PR domain zinc finger protein 1
PRR	Pattern Recognition Receptor
PX	Phox Homology Domain
PYAP	Phospho-Yes Associated Protein
RAG	Recombination Activating Gene
RBD	Ras-Binding Domain
RNA	Ribonucleic Acid
ROS	Reactive Oxygen Species

## Definitions and Abbreviations

S1PR5	Sphingosine-1-phosphate receptor 5
SCCHN	Squamous Cell Carcinoma of the Head and Neck
scRNA	Single Cell RNA sequencing
SGK	Serum/Glucocorticoid-regulated Kinase
SGLT1	Sodium-Glucose Cotransporter
SHP	Src Homology Phosphatase
shRNA	Short/small Hairpin RNA
SLEC	Short Lived Effector Cell
SP	Single Positive
SRC	Spare Respiratory Capacity
SREBP	Sterol Regulatory Element Binding Protein
TAP	Transporter associated with Antigen Processing
TCA	Tricarboxylic Acid Cycle
TCF7	Transcription Factor 7
T <sub>CM</sub>	Central Memory T Cells
TCR	T Cell Receptor
T <sub>EM</sub>	Effector Memory T Cells
TIL	Tumour Infiltrating Lymphocyte
TLR	Toll-Like Receptor
TLR4	Toll-Like Receptor 4
TME	Tumour Microenvironment
TNFRSF	Tumour Necrosis Factor Receptor Superfamily
T <sub>SCM</sub>	Stem-cell Like Memory CD8 T cells
t-SNE	T-distributed Stochastic Neighbour Embedding

UMI	Unique Molecular Identifier
V	Variable
VACV	Vaccinia Virus
VEGF	Vascular Endothelial Growth Factors
VEGF-A	Vascular Endothelial Growth Factor Alpha
VHL	Von Hippel-Lindau
WT	Wild Type
YAP	Yes Associated Protein



# Chapter 1 Introduction

In recent years there has been a shift in the way cancers are treated. Now entering the mainstream, immunotherapies are beginning to replace chemotherapy and radiation treatments as primary therapy options. Immunotherapy is an umbrella term that covers many different treatments, including antibody therapy, vaccines and adoptive immune cell transfers. T cell based immunotherapies hinge on the ability to not only generate CD8<sup>+</sup> T cells capable of eradicating the patients' cancer cells, but also to generate a memory response that will protect the patient in the long term. As such, understanding the signalling pathways and molecular mechanisms of memory generation within CD8<sup>+</sup> T cells is critical to future development of CD8 T cell based therapies.

## 1.1 The Immune System

The immune system protects the host against disease instigated by foreign pathogens as well as internal aberrations such as cancer, and can be further subcategorised into innate and adaptive immune responses.

### 1.1.1 Innate Immunity

In mammalian systems, the innate immune system represents the first active line of defence against infectious pathogens. The innate immune system is comprised of many different cell types including; neutrophils, eosinophils, basophils, mast cells, monocytes, macrophages, NK cells and dendritic cells to name but a few<sup>2</sup>. The primary function of the innate immune system is to respond swiftly to pathogenic infection, and initiate the immune response<sup>3</sup>. Innate immunity is reliant on pathogen-associated molecular patterns (PAMPs); these are expressed on many common pathogens. For example, both lipopolysaccharide (LPS) and flagellin are considered PAMPs, as both are evolutionarily conserved molecules found in multiple bacterial species. Pattern recognition receptors (PRRs), which identify PAMPs, have evolved over the past 750 million years to recognize common biological signs of infection<sup>4</sup>. As such, the innate immune system is activated by a combination of PAMPs through toll-like receptors (TLRs) and PRRs to recruit the adaptive arm of the immune system. One such recruitment mechanism is through the secretion of chemokines that act as chemo-attractants.

## Chapter 1

Specific aspects considered to be part of the innate immune system act indirectly upon the adaptive immune system. LPS is an excellent example of one such aspect. LPS is recognized by the innate toll-like receptor 4 (TLR4), a PRR along with CD14, LPS binding protein (LBP) and lymphocyte antigen 96 (MD-2), which bind the surface lipid present in all gram-negative bacteria as a complex. Upon binding to dendritic cells LPS causes their activation and enhances their expression of costimulatory factors such as CD80, CD86 and CD40, as well as inducing the secretion of inflammatory cytokines such as IL-12<sup>5</sup>. Upregulation of these factors will contribute greatly to an effective response from the adaptive immune system.

In addition to PAMPs, which have evolved over time to detect external signals such as those of flagellin or LPS, there also exist damage/danger associated molecular patterns or DAMPs. DAMPs are biomolecules generated from internal host damaged cells and tissue, through necrosis or apoptosis. Hence, in a similar manner to how PRRs have evolved over time to recognise LPS, so have other receptors evolved to recognise markers of damage to host cells. Examples of DAMPs include HMGB1, DNA/RNA, S100 proteins, as well as purine metabolites such as ATP, adenosine and uric acid<sup>6</sup>. These factors are well known to induce classical inflammatory responses. Fragmented RNA released from UV-radiation damaged cells activates TLR3 on keratinocytes, the subsequent inflammation caused by this pathway has been shown to be responsible for the effects of sunburn<sup>7</sup>. Similarly, excessive levels of uric acid can induce gout, an extreme inflammatory form of arthritis<sup>8</sup>.

In summary, the innate immune system orchestrates an immediate response to pathogens and internal cellular damage, displaying evolutionarily conserved molecular sequences that are recognized by receptors with a limited repertoire. This can induce a primary immune response to contain the infection or address the internal damage, whilst simultaneously activating the adaptive immune system.

### 1.1.2 Adaptive Immunity

Unlike the innate immune system which is a rapid, non-specific response, the adaptive immune system is slower and exceptionally specific. The adaptive immune system is primarily represented by two cell types, B cells and T cells. The primary difference between the innate and adaptive immune system is the ability of B and T cells to rearrange their antigen receptors. Both the B cell

receptor (BCR) and T cell receptor (TCR) are capable of undergoing a form of genetic recombination in order to increase the diversity of their receptor repertoire. Typical  $\alpha\beta$  TCRs, for example, are formed from the recombination of one of each gene segments; 70-80 Variable (V) segments with 61 possible Joining (J) segments in the  $\alpha$  chain and 52 V segments, 13 J segments and 2 Diversity (D) segments in the  $\beta$  chain<sup>9</sup>. The number of potential TCR variants is thought to be between  $10^{15}$  and  $10^{20}$ , although not all of these possible TCRs can be expressed simultaneously<sup>10</sup>. This level of diversity enables T cells to respond to virtually any antigen that may present itself to the immune system.

## 1.2 T Cell Development and Activation

T cells represent the cell-mediated arm of the adaptive immune response, they are specialised for the clearance of viral infections as well as optimal activation of B cells among other functions. T cells can be subcategorised; the most typical variant are  $\alpha\beta$  T cells, which can be split further into  $CD4^+$  T cells and  $CD8^+$  T cells. An atypical variant T cell subset also exists, known as  $\gamma\delta$  T cells. This section will cover the development and activation of typical mouse  $\alpha\beta$  T cells.

### 1.2.1 Maturation

T cells, B cells and NK cells all originate from a common lymphoid progenitor cell that is derived from the bone marrow. During early immune development, some of these common lymphoid progenitor cells migrate to the thymus gland, situated above the heart where they undergo a development process to generate functional, self-tolerant and mature T cells. Initially, lymphoid progenitor cells in the thymus are known as early immature thymocytes and are designated as double negative cells (DN), due to a lack of CD4 and CD8 expression.

#### 1.2.1.1 DN1-4

There are 4 stages of development that DN cells progress through whilst in the thymus, called DN1-4. At the DN1 stage the thymocytes have yet to rearrange the  $\alpha$  and  $\beta$  chains of their T cell receptors (TCR), hence the TCR is not expressed. During the transition from DN1 to DN2, the RAG enzymes catalyse rearrangement of genes encoding the diversity (D) and joint (J) regions of the TCR  $\beta$  chain<sup>11</sup>. The joining of the variable (V) region to the DJ region occurs once the cells have

## Chapter 1

transitioned into the DN3 stage. The defining feature of the DN4 stage is expression of the pre-TCR, which is comprised of a fully rearranged TCR  $\beta$  chain covalently bonded to the pre- $\alpha$  chain, a transmembrane protein belonging to the immunoglobulin superfamily<sup>12</sup>. The stimulation transduced through the pre-TCR, is sufficient to promote survival in those cells with an effective rearrangement of the  $\beta$  chain, in a process known as  $\beta$  selection<sup>13</sup>. Furthermore, pre-TCR signalling initiates the recombination of the TCR  $\alpha$  chain, as well as disrupting any further TCR  $\beta$  chain rearrangement through allelic exclusion<sup>14</sup>. During the DN4 stage there is a rapid proliferation of thymocytes which also coincides with the upregulation of CD4 and CD8, and the expression of the rearranged TCR  $\alpha$  chain, which supplants the pre- $\alpha$  chain<sup>14</sup>. These thymocytes now express a complete  $\alpha\beta$  TCR as well as both of the co-receptors, CD4 and CD8; they are now considered to be double positive cells (DP).

### 1.2.1.2 DP-SP

These DP cells move into the cortex of the thymus and undergo positive selection. During this process, DP cells are presented peptides derived from self-antigens on MHC class I and II molecules by the cortical thymic epithelial cells (cTEC). Only cells that bind with the appropriate affinity to either peptide/MHC molecule complex will receive the necessary survival signals; cells that have an inappropriate binding affinity are neglected and die. It is during this process that the vast majority of DP cells are eliminated from the potential T cell pool<sup>15</sup>. During positive selection the fate of the DP cells is also determined; if they react to self-antigen bound to MHC class I molecules they are destined to become CD8 T cells, conversely a reaction with MHC class II molecules indicates a future CD4 T cell lineage<sup>15</sup>. The cells that survive the positive selection process are now considered single positive cells (SP), as their interactions in the thymic cortex cause the downregulation of either CD4 or CD8.

These SP cells migrate to the medulla of the thymus for negative selection. Negative selection eliminates cells that react too strongly to self-antigens, which minimises release of T cells that could potentially cause autoimmune reactions<sup>16</sup> resulting in central tolerance. Cells that have a weak affinity for self-antigen/MHC exit the thymus and become fully functional CD4 and CD8 T cells. However, certain CD4 T cells possess an intermediate affinity for self-antigen. These cells differentiate into natural regulatory T cells, or nTregs. These nTreg cells contribute to peripheral tolerance by suppressing excessive or unnecessary immune responses in the periphery.

### 1.2.2 Activation

Once CD4<sup>+</sup> and CD8<sup>+</sup> T cells have exited the thymus they circulate throughout the host entering secondary lymphoid tissues. To become fully activated, T cells must receive three signals. Signal 1 is triggered through peptide-presenting MHC class I molecules interacting with the TCR. Signal 2 follows recognition of costimulatory molecules such as CD80/86 binding to CD28 on T cells. Signal 3 is in the form of cytokine stimulation. These three signals not only assist in activation of CD8 T cells but also influence differentiation and their eventual fate. Coordination of these signals controls the immune response. This response is typically divided into three phases<sup>17</sup>. The first phase is expansion. This immediate reaction to a presented antigen is rapid clonal expansion of naïve immune cells in combination with differentiation of the cells to a more effector phenotype. This leads to the peak of the response where the numbers of antigen-specific cytotoxic effector cells are at their highest. Second comes the contraction phase. This occurs after the peak of the response and once the antigen has been cleared. The effector cells begin to die off via a combination of activation induced cell death (AICD) and/or from lacking the appropriate survival signals to persist into the final stage<sup>18</sup>. This process of contraction typically causes the death of 90% of antigen-specific cells<sup>19</sup>. Lastly, there is the memory phase. Cells that have survived contraction have differentiated to a state where they can mediate their survival in an antigen independent mechanism. These cells are now considered to be in a primed state and will react substantially faster than naïve cells upon re-exposure to the same antigen.

#### 1.2.2.1 Signal 1 - T Cell Receptor

Conventional CD4<sup>+</sup> and CD8<sup>+</sup> T cells possess an  $\alpha\beta$  TCR as well as the co-receptor CD4 or CD8, which allows interactions with appropriate peptide-presenting MHC class II and class I molecules respectively. Upon entering a lymph node, T cells have the potential to encounter APCs, usually dendritic cells, which can present peptides that are complementary to the TCR of that T cell.

The mechanism of antigen presentation is therefore critical for proper activation of T cells. For a professional antigen presenting cell such as a dendritic cell, in the context of MHC class I molecules, the process starts with the proteasome<sup>20</sup>. Proteasomes are cytoplasmic protein complexes that degrade damaged, misfolded and foreign proteins through proteolytic mechanisms<sup>21</sup>. Upon encountering a pathogen, such as a virus, dendritic cells are capable of small acts of phagocytosis<sup>22</sup>. This allows them to acquire pathogen proteins, which are subsequently ubiquitinated, marking them for proteasomal degradation<sup>23</sup>. This degradation produces peptides

## Chapter 1

of variable length, typically peptides between 8-11 amino acids in length are the most suitable for MHC class I binding<sup>24</sup>. As peptides are not constantly generated at the correct length, ERAP1/2 also act to fine tune peptides produced by the proteasome, cleaving N-terminal amino acids to generate peptides of the correct length<sup>25</sup>. Construction of the MHC class I complex begins within the lumen of endoplasmic reticulum. A single heavy  $\alpha$ -chain, consisting of three domains, and  $\beta$ 2-microglobulin ( $\beta$ 2M) comprise the MHC class I molecule<sup>26</sup>. Before their association, calnexin acts to stabilise the  $\alpha$ -chain, which is inherently unstable alone<sup>27</sup>. ERp57 also aids in stabilising the complex, which allows the formation of the peptide binding groove between the  $\alpha$ 1 and  $\alpha$ 2 domains of the  $\alpha$ -chain and releases calnexin<sup>28</sup>. Calreticulin binds to the proto-MHC molecule, forming the peptide loading complex (PLC)<sup>29</sup>. The PLC then binds to the peptide transport protein TAP and the protein tapasin<sup>29</sup>. TAP, in an ATP dependent mechanism, transports peptides from the cytosol into the lumen<sup>30</sup>. The orientation of the PLC ensures the maximal chance that peptides will bind to the groove formed by the  $\alpha$ 1 and  $\alpha$ 2 domains<sup>31</sup>. Once a peptide of significantly high affinity is bound, the complex disassociates, the completed peptide bound MHC class I structure is transported to the cell surface through vesicle transport<sup>32</sup>. Thus, an MHC class I molecule presenting a peptide of sufficient affinity will be bound by a TCR on the surface of a CD8 cell, leading to T cell activation. This process is outlined in *Figure 1-1*. This process of dendritic cells phagocytosing extracellular antigens, before processing them for display through MHC class I molecules is termed cross-presentation<sup>33</sup>. Cross-presentation is an essential mechanism for activation of the adaptive immune system in cases of viral infections that do not target dendritic cells directly, or with tumour cells<sup>34</sup>. This process is also required for successful induction of cytotoxic immunity through vaccination.

There is debate as to how the MHC-TCR interaction leads to T cell activation. One model is based on conformational change of the TCR following MHC binding. This model posits that the residues that are phosphorylated by the TCR-activating kinase Lck are sequestered and hidden within the plasma membrane<sup>35</sup>. Upon MHC-TCR interaction, these residues are released from the membrane and are then available for phosphorylation by Lck<sup>36</sup>. Another model of TCR activation suggests that TCRs are kept in a state of inactivity by the action of CD45, a transmembrane phosphatase enzyme. Upon MHC interaction with the TCR, the receptor is then associated into lipid rafts that contain a high density of co-receptors and co-stimulatory molecules that spatially occlude the large extracellular domain of CD45 from interfering with TCR activation<sup>37</sup>.

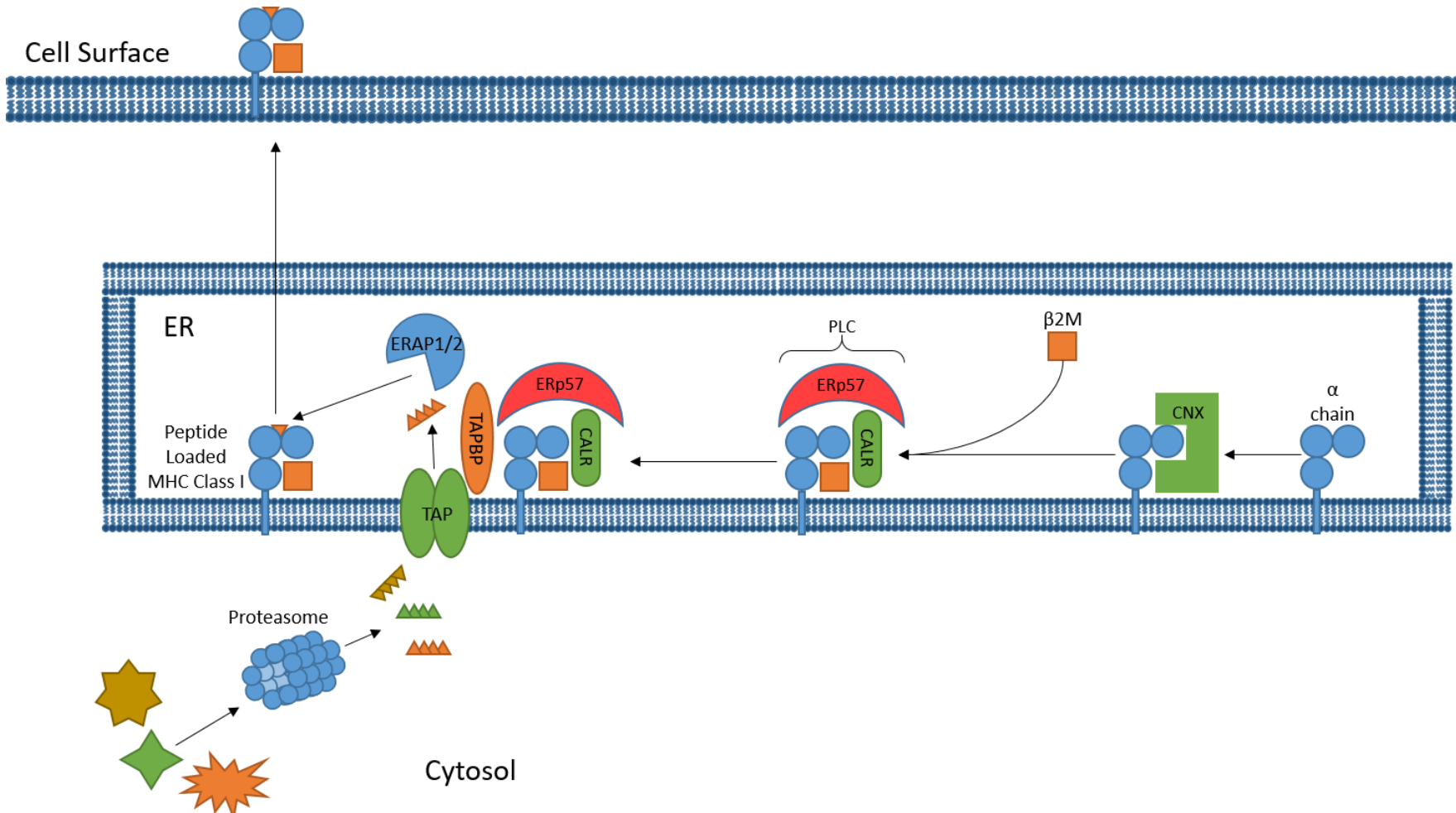


**Figure 1-1 – Mechanism of Antigen Processing and Presentation**

$\alpha$  chain of MHC class I is stabilised by the binding of calnexin (CNX).  $\beta$ 2M associates with the  $\alpha$  chain. ERp57 binds the proto-MHC class I molecule, releasing calnexin. Calreticulin also binds to form the peptide loading complex (PLC). The PLC then binds the peptide transport channel TAP, and its binding protein Tapasin (TAPBP). Peptides generated by the proteasome are transported into the endoplasmic reticulum (ER), they are then trimmed by ERAP1/2 to create peptides that are able to bind the MHC class I molecule. This peptide loaded MHC class I molecule is transported to the cell surface for recognition by TCR of CD8 T cells.

## Chapter 1

Regardless of the specific mechanism behind MHC-TCR interaction, following TCR/peptide/MHC interaction, Lck phosphorylates the immunoreceptor tyrosine-based activation motifs (ITAMs) of CD3 and the  $\zeta$  chains<sup>38</sup>. These phosphorylated ITAMs allow binding of the ZAP70 kinase and its subsequent activation. Activated ZAP70 phosphorylates adaptor proteins such as linker of activated T cells (LAT). LAT allows the recruitment of various downstream signalling molecules that all contribute to the activation of T cells, such as PLC $\gamma$ 1 and PI3K<sup>35,38</sup>. PLC $\gamma$ 1 subsequently converts PIP<sub>2</sub> into inositol trisphosphate (IP<sub>3</sub>) and diacylglycerol (DAG). IP<sub>3</sub> binds to receptors on the endoplasmic reticulum and induces intracellular calcium release, which in turn induces NFAT nuclear translocation. The presence of DAG leads to the activation of PKC, NF- $\kappa$ B, RAS and MAPK<sup>35</sup>.

In certain environments, it is also possible for T cells to receive TCR stimulation, but be deprived of the necessary co-stimulation required for complete activation. This forces T cells into a state where their proliferation and effector functions are inhibited, known as anergy. Anergic T cells are held in a hypo-responsive state until either they receive the necessary stimuli or succumb to eventual cell death<sup>39</sup>. Anergy exists as a peripheral tolerance mechanism and limits the activation of CD4<sup>+</sup> and CD8<sup>+</sup> T cells to those sites that express both co-stimulatory molecules and TCR-stimulating antigens.

### 1.2.2.2 Signal 2 - Co-stimulation

Perhaps the best documented co-stimulatory molecules are CD80 and CD86, also known as B7-1 and B7-2, which interact with CD28<sup>40</sup>. CD28 is expressed on resting naïve CD8 T cells, whereas CD80 and CD86 are expressed on APCs such as dendritic cells. Upon dendritic cell activation, in conjunction with peptide presentation, CD80 and CD86 are upregulated; thus, presenting naïve CD8 T cells with both signals 1 and 2. CD28 is a key co-stimulatory molecule as it contains two key structural motifs in its cytoplasmic tail: YMNM and PYAP<sup>41</sup>. YMNM binds to the p85 subunit of PI3K whereas PYAP facilitates the activation of Ras, ERK and NFAT<sup>40</sup>. The combination of these two signalling pathways acts to enhance CD8 T cell survival, through upregulation of anti-apoptotic factors such as Bcl-X<sub>L</sub><sup>41</sup>. Through PI3K mediated Akt signalling, GLUT1 expression and thereby glucose uptake is also enhanced, this allows newly activated CD8 T cells to meet the new metabolic demands induced by activation<sup>42</sup>.

The interaction of CD28 with CD80/86 are not the only co-stimulatory molecules to be involved in T cell activation. The tumour necrosis factor receptor superfamily (TNFRSF) contains multiple proteins that can provide co-stimulation such as CD27, OX40, DR3 and 4-1BB<sup>43</sup>. The TNFRSF consists of 27 receptors that can bind TNF like molecules. The vast majority of TNF ligands are trimeric membrane bound structures, as this is when they are capable of providing the most effective stimulation<sup>44,45</sup>. TNFRSF members can be bound as a single receptor but are also typically engaged in a trimeric state<sup>45</sup>. Whilst some TNFRs are expressed constitutively on T cells such as CD27, others such as DR3, 4-1BB and OX40 are inducible; only becoming expressed upon TCR engagement, CD28 cross-linking or exposure to certain cytokines<sup>44</sup>. Upon binding their cognate ligand, TNFRSF proteins largely interact with TRAF adaptor proteins, which can activate the canonical, and in some cases non-canonical NF- $\kappa$ B pathways. As well as activating NF- $\kappa$ B, TNFRSF proteins can also increase the expression of the anti-apoptotic proteins BCL-2 and BCL-XL<sup>43,46,47</sup>. Knockout studies have also demonstrated the importance of TNFRSF members. When CD70, the ligand for CD27, was knocked out, it was shown that the interaction between these two molecules is important for a robust primary response but inconsequential for the recall response of CD8 T cells to lymphocytic choriomeningitis virus (LCMV)<sup>48</sup>. However, CD27, 4-1BB and OX40 have all been shown to be critical in shaping the CD8 T cell memory pool<sup>49</sup>.

Similarly, 4-1BB has been shown to be key for activation of CD8 T cells. As shown by 4-1BBL<sup>-/-</sup> mice, the absence of cognate ligand causes a substantial reduction in number of primary effector cells in response to LCMV infection following peptide immunization<sup>50</sup>. The lack of 4-1BB signalling also impacts memory, as the same 4-1BBL<sup>-/-</sup> study demonstrated a compromised ability of cells to respond to secondary infection<sup>50</sup>. Use of anti-4-1BB Ab has shown that it induces increased proliferation of CD8 T cells in response to infection with attenuated vaccinia virus (VACV)<sup>51</sup>. However, excessive signalling has also been shown to impair the development of memory CD8 T cells, indicating a balance of 4-1BB stimulation is required for optimised CD8 T cell function<sup>51</sup>.

OX40 was initially identified as a marker of T cell activation<sup>52</sup>, before later being shown to act as a costimulatory molecule with its cognate ligand OX40L<sup>53</sup>. Unlike CD40, which is constitutively expressed on dendritic cells, OX40L is not expressed by dendritic cells unless it has undergone prior stimulation by CD40-CD40L interaction or TLR induction<sup>54</sup>. Similarly, T cells do not express OX40 unless they have also undergone TCR activation, but they require co-stimulation through CD28 in order to sustain this expression<sup>55</sup>. Much like 4-1BB and the other TNFRSF proteins, OX40-OX40L interaction promotes proliferation and survival in CD8 T cells<sup>56</sup>.

Members of the TNFRSF have also been implicated in having an important role in the contraction phase of T cell activation. These molecules assist in inducing the cell death required to pair back the T cell population in order to give rise to the memory population of T cells<sup>57</sup>.

As part of the peripheral tolerance mechanism, co-inhibition can also restrain activation of T cells. This allows for regulation of hyperactive T cells and also assists in preventing inappropriate activation. Molecules such as cytotoxicity T-lymphocyte-associated antigen 4 (CTLA-4) and programmed death 1 (PD-1) act as negative forms of co-stimulation<sup>58</sup>. CTLA-4 is homologous to CD28 and possesses an even higher affinity for CD80/CD86 than CD28. This increased affinity allows CTLA-4 to displace CD28 and sequester CD80/CD86. Aside from competitive binding with CD28, CTLA-4 also signals by activating the phosphatases SHP2 and PP2A<sup>59</sup>. These deactivate the major signalling nodes, such as Akt and PLC, downstream of TCR signalling, thus abrogating CD8 T cell activation. PD1/PD-L1 signalling works in a similar manner, by activating SHP, another phosphatase. PD-1 can also inhibit PI3K and PKC signalling; two critical enzymes in T cell activation<sup>60</sup>.

### 1.2.2.3 Signal 3 - Cytokines

Broadly, cytokines are small immunomodulatory proteins involved in activation and modulation of immune cells. There are many classes of cytokine, such as interleukins, chemokines, interferons and members of the tumour necrosis family of proteins, many of which have unique roles depending on the cell type they are affecting. CD4<sup>+</sup> and CD8<sup>+</sup> T cells are both heavily influenced by cytokines released over the course of an immune response.

Cytokines such as IL-12, IFN- $\gamma$ , IL-4, and IL-10 can induce CD4<sup>+</sup> T cells to differentiate into different phenotypes that can be pro-inflammatory, anti-inflammatory or even display auto-immune effects.

Cytokines can also greatly impact the activation and differentiation of CD8<sup>+</sup> T cells. There are pro-inflammatory cytokines such as IL-2 and IL-12 that promote terminal differentiation and enhanced effector functions. As well as IL-7 and IL-15 that are required by naïve CD8<sup>+</sup> T cells for survival. The

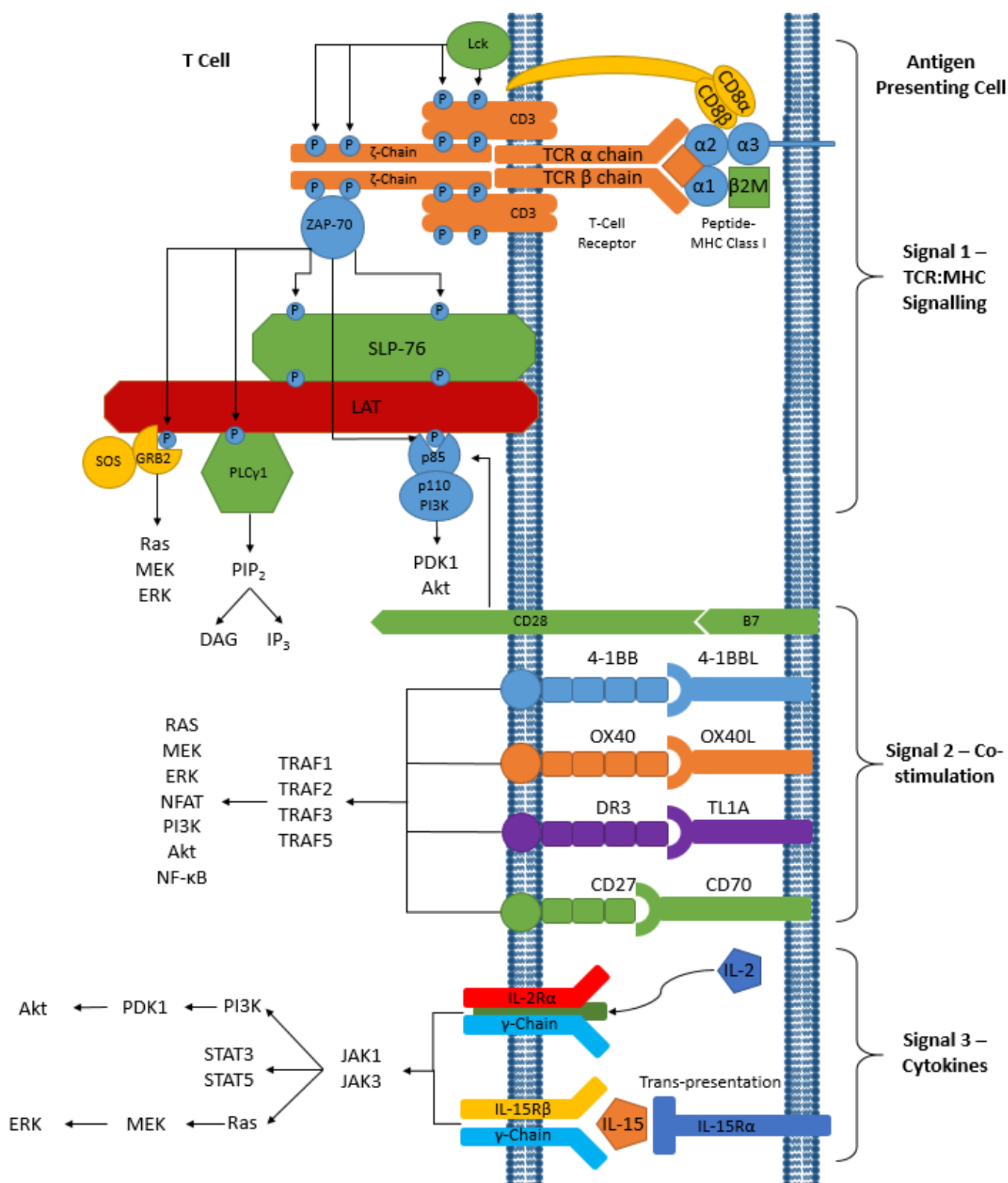


**Figure 1-2 – Three Signal Mechanism of T Cell Activation.**

Peptide presented by MHC class I molecule is bound by the T cell receptor, with CD8 aiding with the interaction by affixing to the  $\alpha 3$  domain of MHC class I molecule. This interaction allows Lck phosphorylation of CD3 and  $\zeta$ -chain sites. This allows recruitment and activation of the kinase ZAP-70. ZAP-70 phosphorylates the adaptor proteins LAT and SLP-76. These proteins allow the binding and activation of signal transduction enzymes PI3K, PDK1, Akt, PLC $\gamma$ , Ras. CD28 is the standard example of a co-stimulatory molecule that also feeds into PI3K stimulation. TNFRSF proteins 4-1BB, OX40, DR3 and CD27 also contribute to multiple T cell stimulatory pathways through TRAF adapter proteins. Common  $\gamma$ -chain cytokine receptors can bind soluble cytokines, in the case of IL-2, or they can be presented by another cell, IL-15 is an example of this trans-presentation. This figure displays an overview of the three primary signals necessary for full T cell activation.

## Chapter 1

transition of these cells into the memory phase, which will be discussed in a later section (1.2.3.2). CD4 and CD8 T Cells. An overall display of these signals is displayed in *Figure 1-2*.

### 1.2.2.4 CD4 T cells

Effector CD4 T cells, more commonly referred to as T helper cells ( $T_h$  cells), are capable of differentiating into a broad range of subtypes upon activation; each with their own profile of chemokine receptors and secreted cytokines. There are eight  $T_h$  cell subsets currently recognized, however only five of them,  $T_h1$ ,  $T_h2$ ,  $T_h17$ ,  $T_{fh}$  and  $T_{regs}$ , have been extensively studied<sup>61</sup>.

The  $T_h1$  subset is characterised by the upregulation of the transcription factor Tbet, the secretion of IFN $\gamma$  and the expression of CXCR3; a chemokine receptor<sup>62,63</sup>. Development of the  $T_h1$  subtype is induced by IL-12 and IFN $\gamma$ <sup>64</sup>. IL-12 signals through the transcription factor STAT4, which generates a positive feedback loop by causing increased IFN $\gamma$  production<sup>65</sup>.  $T_h1$  cells are primarily involved with assisting CD8<sup>+</sup> T cells responses against intracellular pathogens such as influenza, vaccinia and mycobacteria.

$T_h2$  cells express GATA-3 as their signature transcription factor and secrete IL-4, IL-5 and IL-13<sup>66</sup>.  $T_h2$  cells contribute to immune responses against extracellular parasites such as helminths. IL-4 induces GATA-3 by upregulating STAT6; increased expression of these transcription factors also suppresses the  $T_h1$  subtype by downregulating STAT4<sup>67</sup>. The  $T_h2$  subset is also involved in the allergic response, as it is able to promote the production of IgE from B cells, as well as activating mast cells; both are critical to the allergic response.

$T_h17$  cells are functionally responsible for host defence against fungi and extracellular bacteria, but are also implicated in many pathogenic inflammatory and auto-immune conditions. The combination of TGF- $\beta$ , IL-6, IL-21 and/or IL-23 can induce the  $T_h17$  subtype, and it is primarily characterised by the expression of ROR $\gamma$ t transcription factor and the secretion of IL-17<sup>68</sup>.

T follicular helper ( $T_{fh}$ ) cells are a unique subset of CD4 T cells that specialize in assisting B cells during their reactions in the germinal centre. The route of differentiation for  $T_{fh}$  is reliant on a

multistage process, unlike the previous subsets mentioned which can be induced by exposure to specific cytokines. During initial priming of naïve CD4 T cells by dendritic cells a fate determining decision occurs based on the expression of the chemokine receptor CXCR5<sup>69</sup>. CD4 T cells expressing CXCR5 then migrate to B cell follicles, where they will undergo further differentiation to generate T<sub>fh</sub> cells. During dendritic cell priming it is the interaction of IL-6, ICOS (CD278), IL-2 and TCR signalling that determines initial CXCR5 expression<sup>69</sup>.

There also exists a subset of CD4<sup>+</sup> T cells known as regulatory T cells, or T<sub>regs</sub>. T<sub>regs</sub> themselves can be split into thymic T<sub>regs</sub> (nT<sub>regs</sub>) and peripherally induced T<sub>regs</sub> (iT<sub>regs</sub>), depending on their point of origin<sup>70</sup>. Natural T<sub>regs</sub> arise from the population of CD4<sup>+</sup> T cells in the thymus that bind MHC class II molecules with an intermediate affinity but not so high as to be eliminated through negative selection. Induced T<sub>regs</sub> arise from stimulation of CD4<sup>+</sup> T cells with TGF-β in the periphery<sup>71</sup>. Whilst functionally comparable to nT<sub>regs</sub>, and expressing similar molecules such as the Foxp3 transcription factor and the alpha chain of the IL-2 receptor, CD25, iT<sub>regs</sub> form an important non-redundant subset of regulatory T cells that work in concert with nT<sub>regs</sub> to impose peripheral tolerance<sup>72</sup>.

As previously mentioned these are only the most common CD4<sup>+</sup> subsets, there are also Th22, Th9, Tr1 and Th3. However, these subsets have only been discovered in the past 5 years, and hence there is much less information available about them. It should be noted that new CD4<sup>+</sup> T cell subsets continue to be proposed as research continues, it is likely that this list will continue to expand over the coming years.

CD4<sup>+</sup> T cells also play a role in the optimal priming of CD8<sup>+</sup> T cells, in a process termed CD4 licensing<sup>73</sup>. This process is mediated through interaction of the costimulatory protein CD40 with its cognate ligand CD40L<sup>74</sup>. CD40 is constitutively expressed at low levels on dendritic cells<sup>74</sup>. CD40L is induced upon CD4<sup>+</sup> T cells following binding of their TCR to peptide bound MHC class II molecules. The effect of this CD40-CD40L interaction effectively 'licenses' dendritic cells, increasing their expression of costimulatory molecules such as CD70 and also increasing the production of cytokines<sup>75</sup>. This licensing allows dendritic cells to augment CD8<sup>+</sup> T cell activation, this does impact the primary response, but has also been shown to be critical for development of substantive memory populations<sup>76</sup>. Whilst the generally accepted model is that of CD4<sup>+</sup> T cells

## Chapter 1

stimulating CD40 on dendritic cells, it has also been proposed that dendritic cells may act as a docking station for CD4<sup>+</sup> T cells to stimulate CD40 on CD8<sup>+</sup> T cell directly<sup>77</sup>.

Whilst known to support the CD8<sup>+</sup> T cell immune response, it has more recently been demonstrated that CD4<sup>+</sup> T cells can possess potent MHC class II dependent anti-tumour activity<sup>78</sup>. However, this has been shown to primarily occur in melanoma models or in specifically abnormal immunological settings such as radiation associated lymphopenia<sup>79</sup>. The ability of CD4<sup>+</sup> T cells to directly contribute to the cytotoxic destruction of melanoma associated tumours is due to the fact that, unlike most cancerous cells, melanoma do not lack MHC class II expression<sup>80</sup>.

### 1.2.2.5 CD8 T cells

Whilst CD4 T cells can enhance the eradication of certain cancers<sup>81</sup>, it is the primary role of CD8 T cells to target both cancerous and other infected or non-self cells for elimination<sup>82</sup>.

#### 1.2.2.5.1 CD8 T cell activation

CD8 T cells are initially activated following TCR recognition of an appropriate peptide-MHC class I molecule complex on the surface of antigen-presenting cells (APCs). This activation process is also influenced by the presence of costimulatory molecules and inflammatory conditions found in peripheral lymph nodes. During this activation process, CD8 T cells undergo extensive clonal expansion and migrate into the periphery. MHC class I molecules are expressed on the surface of nearly all nucleated cells and generally present fragments of normal cytosolic proteins, created through the mechanism of antigen processing. This identifies the cells as self and due to the mechanisms of central and peripheral tolerance, CD8 T cells should not target these cells. However, in the case of viral infection, for example, intracellular viral proteins are degraded by the proteasome, leading to viral peptide fragments being presented on MHC class I molecules. This presentation will initiate the process by which CD8 T cells, known at this point as cytotoxic T lymphocytes (CTLs), will eliminate the infected cells. The presentation of altered or non-self peptides can also occur in cancerous tissues, where the deregulation of certain signalling pathways leads to the production of aberrant proteins, which are subsequently processed and presented on MHC class I molecules.

#### 1.2.2.5.2 CD8+ T cell effector mechanisms

CTLs are capable of destroying their target cells through a range of different mechanisms. The predominant method is the release of cytotoxic granules, which contain an assortment of granzymes and perforin<sup>83</sup>. Perforin oligomerises and inserts itself into the membrane of the target cell and generates pores to allow the entry of the granzymes. Whilst perforin is capable of inducing cell death by itself, granzymes are the primary molecules utilised in order to induce apoptosis. Granzymes are serine proteases that interrupt the fundamental functions of a cell to cause death by apoptosis. Granzyme B, for example, cleaves and activates caspase-3, an enzyme responsible for activating a Dnase enzyme which then proceeds to cleave the DNA in the nucleus into unusable fragments. Granzyme B can also cleave Bid, this protein in its cleaved form can recruit proteins to the mitochondrial membrane and cause its permeability<sup>83</sup>. The increased permeability of the mitochondria releases cytochrome c which is a critical component of the apoptosome, a multi-protein complex which activates another caspase enzyme. This cascade of caspase enzyme activation essentially terminates all critical processes; shredding the DNA prevents protein production and cell division, and disrupting the integrity of the mitochondrial membrane prevents production of ATP. CTLs can also induce targeted apoptosis through Fas ligand, which causes apoptosis through binding to Fas and induction of the death-induced signalling complex.

#### 1.2.2.5.3 Phases of CD8+ T-cell activation and differentiation

A typical CD8 T cell immune response consists of three main phases, expansion, contraction and memory<sup>84</sup>. For example, in response to a viral infection, CD8 T cells will clonally expand, rapidly increasing their numbers in order to combat the virus. After approximately one week, CTLs enter a programmed contraction phase when the vast majority (>90%) of cells are terminally differentiated and die by apoptosis<sup>84-86</sup>. After approximately a month the remaining cells become known as memory CD8 T cells and are characterised by decreased immediate effector functions and an increased capacity for proliferation upon re-exposure to antigen. These memory CD8 T cells can persist for the lifespan of an organism, providing long term protection against subsequent infections. The manner in which memory cells are maintained is antigen-independent and relies primarily on the cytokines IL-7 and IL-15 to induce self-renewal. Cytokines influence CD8+ T cells throughout all stages of their activation and differentiation and a more detailed description of the effects of key cytokines on CD8+ T cells therefore follows.

#### 1.2.2.5.4 Influence of cytokines on CD8<sup>+</sup> T cells

Upon infection PAMPs are recognised by the innate immune system, primarily dendritic cells and macrophages, causing release of the pro-inflammatory cytokine IL-12<sup>87</sup>. IL-12 induces the expression of transcription factors such as T-bet, in CD8 T cells that correlate with increased effector functions and differentiation into short lived effector cells (SLECs)<sup>88</sup>, which will be discussed later (chapter 1.2.4.1). Strong inflammatory conditions induced by IL-12 and other pro-inflammatory cytokines can preclude the development of memory cells, as they heavily enforce the SLEC phenotype.

IL-2 is another key cytokine influencing CD8 T cell responses. IL-2 contributes at all stages of CD8 T cell activation, it produces robust proliferation in CD8 T cells during the primary response, but also helps shape the memory population<sup>89</sup>. IL-2 signals through receptors composed of chains CD25, CD122 (which is shared with the IL-15 receptor) and CD132 which is frequently referred to as the common- $\gamma$  chain. CD132 is present in a number of other cytokine receptors, such as those binding to IL-4, IL-7, IL-9, IL-15 and IL-21<sup>90</sup>. CD25 is not expressed by resting CD8 T cells and is only upregulated upon stimulation with inflammatory cytokines such as IL-12 or even IL-2 itself. The expression of CD25, provides the initial binding interaction for IL-2<sup>91</sup>. The interaction of CD25 and IL-2 promotes formation of the heterotrimeric IL-2 receptor with CD122 and CD132, which in turn stimulates signalling through the transcription factor STAT5 as well as PI3K and MAPK pathways<sup>91,92</sup>. As such, an increase in the expression of CD25 causes cells to become more sensitive to the presence of IL-2<sup>93</sup>. The expression of CD25 is not uniform amongst CD8 T cells, those that express more CD25 are likely to have received more IL-2 stimulation and display a more terminally differentiated phenotype. These CD25<sup>high</sup> cells display greater expression of the transcription factors T-bet and Blimp-1 as well as the effector molecules granzyme B, IFN $\gamma$  and perforin<sup>94</sup>. Conversely, CD8 T cells that express less CD25 favour expression of Bcl-6 and CD62L, two early signs of memory development and persistence<sup>95</sup>. As such, IL-2 drives massive expansion of the CD8 T cell population whilst also inducing a more effector like phenotype. However, as exposure to the cytokine increases, the potential for memory decreases; hence the regulation of the high affinity receptor CD25 is critical for an effective immune response.

IL-7 and IL-15 are two more common- $\gamma$  chain cytokines that regulate the function of CD8 T cells. Unlike IL-2 and IL-12, these cytokines are not associated with inflammation and driving an effector phenotype, but regulate CD8 T cell homeostatic proliferation and survival. IL-7 is a key component

of homeostasis of the naïve CD8 T cell pool, allowing proliferation without activation<sup>96</sup>. As mentioned in the section above, IL-15 and IL-2 share the receptor subunits CD122 and CD132. However, they differ in their high affinity subunit, which is IL-15R $\alpha$  for IL-15. IL-15R $\alpha$  is constitutively expressed at very low levels on CD8 T cells, although it can be induced by IL-2<sup>97</sup>. Signalling through IL-15 is transduced through STAT3 and STAT5, as well as the MAP kinase pathway, leading to induction of Bcl-2; a critical pro-survival protein<sup>98</sup>.

Not all cytokines act to promote CD8 T cell mediated immune responses. IL-10 and TGF- $\beta$  are anti-inflammatory cytokines that have an inhibitory role in T cell responses. These cytokines are commonly secreted by T<sub>regs</sub> as a mechanism to inhibit inappropriately activated immune cells.

### 1.2.3 CD8 T Cell Subsets

#### 1.2.3.1 SLECs and MPECs

The fates of CD8 T cells are determined during the initial immune response. Before the peak of the response, CD8 T cells can already be separated into two distinct precursors; short lived effector cells (SLECs) and memory precursor effector cells (MPECs). These two cell subsets are distinguished based on their expression of IL-7R and KLRG1, with SLECs expressing a KLRG1<sup>high</sup> IL-7R<sup>low</sup> phenotype and MPECs expressing the inverse; KLRG1<sup>low</sup> IL-7R<sup>high</sup><sup>88</sup>. SLECs represent the population of CD8 T cells that make up the majority of the initial immune response, are destined to become terminally differentiated and undergo apoptosis during the contraction phase. MPECs comprise the population of effectors that retain enough plasticity to give rise to the entire pool of memory CD8 T cells<sup>99</sup>.

The mechanisms that lead to the SLEC and MPEC phenotypes have yet to be fully understood and some models will be discussed in later chapters. However, the transcription factors T-bet and Eomesodermin (Eomes) are central to the early differentiation process<sup>84</sup>. Expression of T-bet, as induced by IL-12, sets up a gradient of effector like properties; with CD8 T cells expressing high levels of T-bet favouring SLEC differentiation and low T-bet expressing cells developing into MPECs<sup>88</sup>. Thus, CD8 T cells lacking T-bet expression subsequently fail to form SLECs during an immune response<sup>88</sup>. Eomes-deficient CD8 T cells display no impairment in developing the MPEC

## Chapter 1

phenotype. However, after progression into the memory phase they show an inability to properly express CD122, CD62L and CXCR3, all of which are critical for IL-15 maintenance and homing to the lymph nodes. Due to the lack of these proteins, Eomes-deficient CD8 T cells show diminished central memory formation, reduction in long-term survival and decreased homeostatic proliferation<sup>100</sup>.

### 1.2.3.2 Effector Memory and Central Memory

In early studies memory CD8 T cells were separated into two distinct phenotypes based on the expression CD62L, an adhesion molecule and CCR7, a chemokine receptor which regulates the ability of naïve and memory CD8 T cells to enter lymph nodes<sup>101</sup>. Memory CD8 T cells expressing both these molecules are termed central memory cells ( $T_{CM}$ ), whereas cells lacking these molecules are known as effector memory cells ( $T_{EM}$ ). Due to the differential expressions of CD62L and CCR7,  $T_{CM}$  cells primarily migrate towards lymph nodes and the spleen, whereas  $T_{EM}$  cells circulate through the blood and also through non-lymphoid tissue<sup>102</sup>.

$T_{CM}$  cells act as progenitor cells in secondary immune responses, they possess the capacity to self-renew and differentiate into effector cells upon antigen restimulation<sup>103</sup>. Whilst  $T_{CM}$  cells are able to secrete IFN $\gamma$  and IL-2, they lack immediate effector functions<sup>104</sup>. However, the lack of effector functions is balanced by an increased proliferative potential<sup>105</sup>. Hence, the generation of  $T_{CM}$  is critical to long term immunity. Conversely,  $T_{EM}$  cells provide an immediate effector response, achieved by continual expression of cytotoxic granules, as well as the ability to secrete increased quantities of TNF- $\alpha$  and IFN $\gamma$ <sup>106</sup>.  $T_{EM}$  cells compared to  $T_{CM}$  cells show a significantly decreased proliferative ability and do not have the capacity for long-term self-renewal.

Whilst  $T_{CM}$  and  $T_{EM}$  subsets were identified some time ago, two more memory subsets have been recently proposed and will be discussed in the sections below.

### 1.2.3.3 Resident Memory

It was noted recently that there is a population of  $T_{EM}$  that do not circulate through the blood and instead reside within non-lymphoid tissues such as the skin, gut and lungs<sup>84</sup>. These non-circulating  $T_{EM}$  cells are termed resident memory cells or  $T_{RM}$ . Aside from their reduced migratory ability, they

are functionally comparable to  $T_{EM}^{107}$ . They do possess some unique characteristics such as increased expression of CD69 and CD103, as well as tissue specific integrins and chemokine receptors to enhance their tissue residency<sup>108</sup>.

#### 1.2.3.4 Stem-cell Like Memory

Stem-cell like memory CD8 T cells, or  $T_{SCM}$ , were first identified by Gattinoni *et al* in 2009<sup>109</sup> who showed that by activating the Wnt- $\beta$ -catenin signalling pathway during CD8 T cell activation, it was possible to arrest the differentiation of naïve CD8 T cells into effectors. This generated a unique subset of CD8 T cells that presented with a  $CD44^{low}$   $CD62L^{high}$   $Sca-1^{high}$   $CD122^{high}$   $Bcl-2^{high}$  phenotype. These  $T_{SCM}$  cells were self-renewing multipotent CD8 memory cells with proliferative and anti-tumour abilities that exceed that of both the  $T_{CM}$  and  $T_{EM}$  subtypes.  $T_{SCM}$  cells also display an ability to differentiate into all subsequent CD8 memory subtypes<sup>110</sup>. Given that this  $T_{SCM}$  subset has recently been found in patients that received vaccinations for yellow fever 35 years previously<sup>111</sup>, and that their proliferative and anti-tumour capabilities exceed that of typical memory subsets, these cells would be ideal for adoptive cell therapies in cancer treatment.

#### 1.2.4 Models of Differentiation

Whilst some of the signals and transcription factors required to generate each particular subset of CD8 T cells are known, the precise mechanisms of differentiation have remained elusive. Initially, it was believed that all T cells were fated to either effector or memory cells during development in the thymus. However, studies have determined that each individual T cell is multipotent, capable of generating all possible phenotypes available<sup>112,113</sup>. Due to these studies, the separate precursor model as it was known has largely been dismissed. However, there still remain multiple theories for CD8 T cell differentiation some of which are discussed below.

##### 1.2.4.1 Decreasing Potential Model

This model states that repetitive stimulation of T cells with antigen and pro-inflammatory cytokines drives terminal differentiation. With each successive round of stimulation, T cells acquire a greater level of effector function and cytotoxic capability but lose the features of memory cells, such as longevity and proliferative ability. Thus, T cells that receive minimal repetitive stimulation form MPECs and eventually populate the CD8 memory cell pool, whereas

## Chapter 1

cells that receive multiple stimulations favour SLECs and terminal differentiation. There is evidence to support this model, as restricting the amount of antigen or inflammatory cytokines, and hence reducing the number of repeated stimulations, can lead to accelerated memory formation<sup>114</sup>.

### 1.2.4.2 Signal Strength Model

This model is similar to the decreasing potential model described in the previous section except that instead of successive rounds of stimulation leading to a loss of multipotency, it posits that the overall strength/intensity of the initial stimulatory signal determines eventual fate. Studies show that stimulation with a weak antigen can cause anergy, whereas after strong antigen stimulation, activation induced death can occur<sup>115</sup>. This model has been shown to be dependent upon a minimum of three different parameters; antigen affinity, co-stimulation and duration<sup>116</sup>. To a certain extent these factors can compensate for each other, for example, a weak affinity antigen can be compensated for by an increased level of co-stimulation or prolonged duration of stimulation<sup>116</sup>.

### 1.2.4.3 Asymmetric Cell Division

Typically, cell division is symmetrical; all aspects of the cell such as organelles and signalling pathway enzymes are divided equally, generating two equivalent daughter cells. However, in asymmetric cell division, structures such as organelles and key signalling pathway enzymes are not divided equally. There is evidence that certain molecules critical to CD8 T cell development are asymmetrically inherited, such that daughter cells proximal to the APC inherit more CD8, TCR, T-bet, Myc and mTORC1, whilst the distal daughter cell will lack these factors<sup>117,118</sup>. This, therefore, generates a proximal cell that contains more factors associated with the SLEC phenotype and a distal cell that retains a more MPEC phenotype. As asymmetric cell division can theoretically occur at each cell division, this may explain why some CD8 T cells show plasticity in their ability to interconvert between the SLEC and MPEC phenotype. If this theory is taken to its logical extreme, it would suggest that spatial division of the factors that regulate effector vs memory phenotype is a key mechanism in determining the final fate of a CD8 T cell.

### 1.2.5 $\gamma\delta$ T Cells

$\gamma\delta$  T cells are often referred to as a bridge between innate and adaptive immune systems<sup>119</sup>. This is because they display features associated with each system. The TCR receptors of these  $\gamma\delta$  T cells are composed of the corresponding  $\gamma$  and  $\delta$  chains. Much like the conventional  $\alpha$  and  $\beta$  chains, these  $\gamma$  and  $\delta$  chains also undergo recombination as part of their maturation process<sup>120</sup>. Unlike  $\alpha\beta$  T cells, however, their TCR repertoire is significantly restricted in its recognition of antigens<sup>119</sup>.  $\gamma\delta$  T cells are considered atypical primarily due to their ability to recognise non-MHC restricted antigens<sup>121</sup>. In addition to this,  $\gamma\delta$  T cells also are found at higher concentrations in different biological sites, particularly in the skin as well as the gut mucosa, as part of the intraepithelial lymphocyte population<sup>121,122</sup>.

## 1.3 PI3K-Akt Signalling Pathway

Whilst TCR engagement with MHC molecules, co-stimulation and cytokines drive the activation and differentiation of CD8 T cells, ultimately, it is the network of downstream signalling pathways and transcription factors that they induce which determines the fate and function of CD8 T cells. Multiple factors contribute to the process and not all can be covered in this thesis. The work completed in this thesis primarily covers the enzymes downstream of the PI3K signalling pathway, in particular PDK and Akt, as well as the various transcription factors that they regulate. Understanding the underlying signalling pathways of CD8 T cells and more importantly how they can be manipulated, will aid the design of more effective treatments for cancer and viral infections. A summarised form of this pathway is shown in *Figure 1-3*.

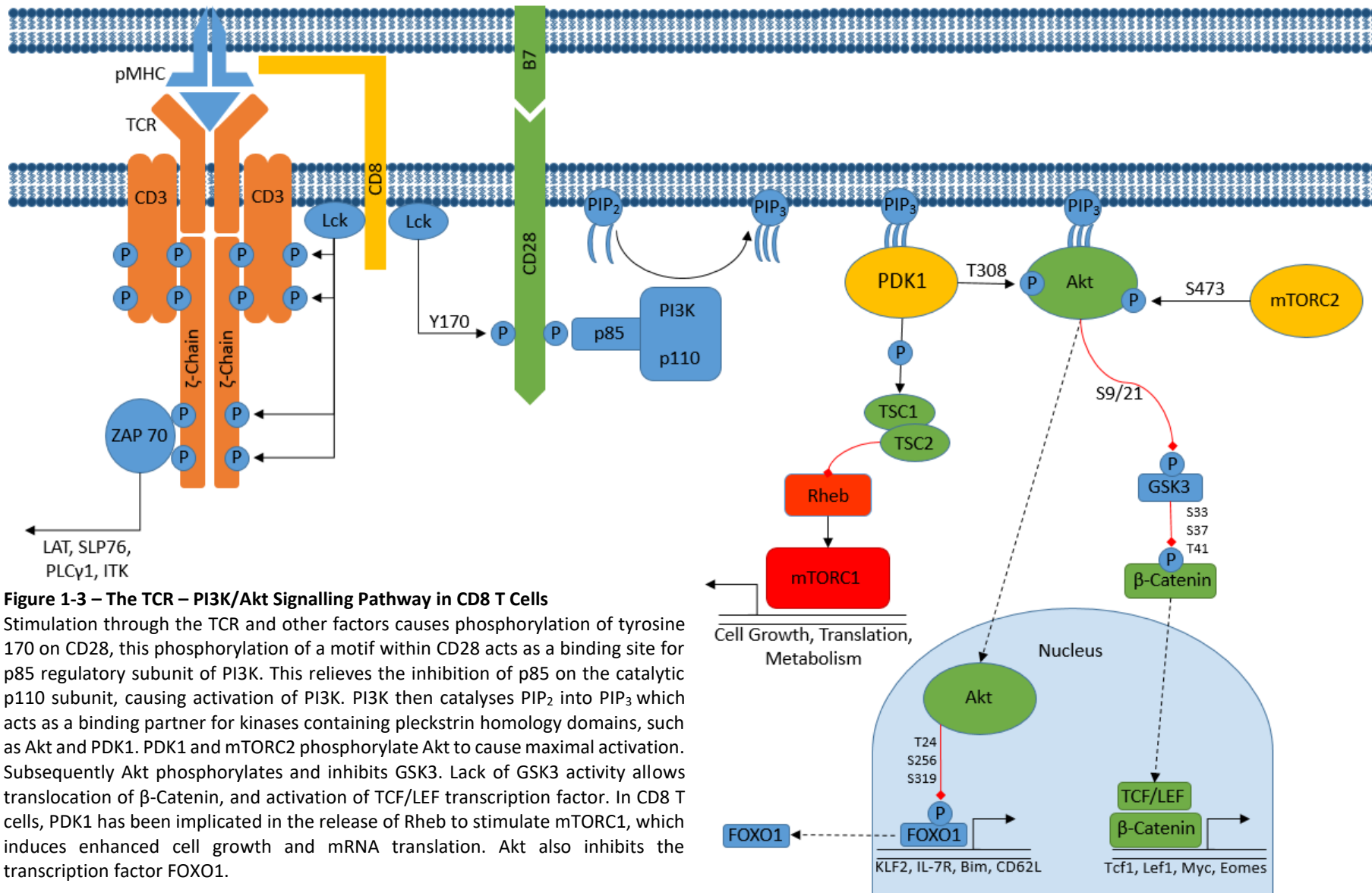


**Figure 1-3 – The TCR – PI3K/Akt Signalling Pathway in CD8 T Cells**

Stimulation through the TCR and other factors causes phosphorylation of tyrosine 170 on CD28, this phosphorylation of a motif within CD28 acts as a binding site for p85 regulatory subunit of PI3K. This relieves the inhibition of p85 on the catalytic p110 subunit, causing activation of PI3K. PI3K then catalyses PIP<sub>2</sub> into PIP<sub>3</sub> which acts as a binding partner for kinases containing pleckstrin homology domains, such as Akt and PDK1. PDK1 and mTORC2 phosphorylate Akt to cause maximal activation. Subsequently Akt phosphorylates and inhibits GSK3. Lack of GSK3 activity allows translocation of β-Catenin, and activation of TCF/LEF transcription factor. In CD8 T cells, PDK1 has been implicated in the release of Rheb to stimulate mTORC1, which induces enhanced cell growth and mRNA translation. Akt also inhibits the transcription factor FOXO1.

### 1.3.1 PI3K

The PI3K pathway receives signals from various environmental inputs including growth factors, TCR stimulation, cytokines, insulin and other hormones. Further, PI3K has considerable control over the numerous cellular activities that those environmental inputs induce including growth, proliferation, glucose uptake, survival, differentiation and ribosomal efficiency. Hence, PI3K itself, as well as its major downstream signalling elements PDK, Akt and the mTOR complexes are important for CD8 T cell function<sup>123,124</sup>. Multiple studies confirm that impairing PI3K activity in T cells can cause a myriad of functional defects in CD8 T cells, from diminished primary and secondary responses to altered cell trafficking, defective proliferation, cytokine production and even preventing T cells from maturing and exiting the thymus<sup>125-127</sup>.

Different classes of PI3K have been described, defined by the combination of proteins that come together to form the heterodimer. Class I PI3Ks are by far the most common form of the enzyme found in mammals and comprise an isoform of the p110 catalytic subunit bound to a regulatory subunit. The p110 catalytic subunit has four distinct isoforms designated  $\alpha$ ,  $\beta$ ,  $\gamma$  and  $\delta$ , each with different downstream functions and tissue expression patterns. Class I PI3Ks can be further split into class IA and IB based on the combination of the subunits. Class IA PI3Ks contain p110 $\alpha$ ,  $\beta$  or  $\delta$  commonly bound to the regulatory subunit known as p85, or its splice variants<sup>128</sup>. Whereas, class IB PI3Ks are formed by the interaction between the p110 $\gamma$  subunit with either p101 or p84/p87 acting as a regulatory subunit<sup>128</sup>. p110 $\alpha$  and p110 $\beta$  are expressed in virtually all tissue. Conversely, p110 $\gamma$  and p110 $\delta$  are more restricted in expression, present at highest levels in the leukocyte population<sup>129</sup>.

The crystal structures of the catalytic and regulatory subunits have provided insights into the mechanics of their interaction. Whilst there is some variation in their structure, broadly the catalytic p110 subunits possess a conserved domain structure. The p110 structure consists of an adaptor binding domain (ABD), a Ras-binding domain (RBD), a C2 domain (for membrane lipid association), and a helical motif leading into the kinase domain which itself is split into an N-terminal and C-terminal lobe<sup>130</sup>. The typical p85 structure consists of an N-terminal SH3 domain, a Bar cluster region homology (BH) domain, followed by the core signature of PI3K regulatory subunits, two Src homology 2 domains (nSH2 and cSH2) separated by a coiled-coil domain (iSH2) that promotes binding to p110<sup>130,131</sup>. The iSH2 domain of p85 is bound by residues found in the

## Chapter 1

kinase domain, the ABD and C2 domains of p110<sup>132</sup>. The contact between iSH2 and ABD is high affinity, however the strength of the bond between iSH2 and the C2 is variable due to differences in sequence in the p110 isoforms. This variable interaction between iSH2 and C2 domains helps to explain the differential sensitivity that PI3K isoforms have for the inhibitory p85<sup>133</sup>. The cSH2 domain of p85 is critical to the inhibition of p110 isoforms as it binds between two helices of the kinase domain<sup>130</sup>. During T cell activation, phosphorylated tyrosine sequences from costimulatory molecules such as CD28 bind to the SH2 domains of p85. This relieves the inhibitory pressure on p110, allowing its kinase domain to function and for it to associate with phosphatidylinositol 4, 5-bisphosphate (PIP<sub>2</sub>) rich membranes<sup>134</sup>.

PI3Ks phosphorylate the inositol molecule phosphatidylinositol 4,5-bisphosphate (PIP<sub>2</sub>) to generate phosphatidylinositol 3,4,5-trisphosphate (PIP<sub>3</sub>)<sup>135</sup>. This PIP<sub>3</sub> molecule acts as a second messenger and docking platform for downstream molecules in this pathway. Many proteins can bind and be activated by PIP<sub>3</sub> including IRS-1, dynamin and phospholipase C (PLC). However, most studies on CD8 T cells have focussed on the PI3K targets PDK and Akt. Excessive PI3K activity has been associated with multiple cancers and PI3K is thus considered an oncogene. PI3K is negatively regulated by the phosphatase enzyme PTEN and PTEN is often downregulated in cancer.

The balance of PI3K signalling is critical for the maturation process of CD8 T cells in the thymus. It has been demonstrated that when PI3K $\delta$  is deleted in CD8 T cells there is compensation in the form of PI3K $\gamma$ , which acts in a redundant manner to allow progression of developing thymocytes<sup>136</sup>. When both of these PI3K isoforms are deleted there is a profound block between the DN3-DN4 transition<sup>136</sup>. This block is indicative of a lack of progression past  $\beta$  selection, due to a lack of the pre-TCR signal that would be typically transduced through the PI3K signalling pathway. This results in a substantial reduction in the number of peripheral T cells, DP T cells in the thymus, as well as the size of the thymus itself<sup>136</sup>. T cells that manage to transition into the DP state with co-expression of CD4 and CD8 also displayed significant reduction in survival, which was attributed to reduced expression of proteins from the Bcl2 family of pro-survival proteins, leading to increased apoptosis mediated by BIM<sup>136</sup>. Conversely, the deletion of PTEN, the negative regulator of PI3K, causes excessive activity in the PI3K signalling pathway<sup>137</sup>. This increased PI3K activity can allow T cells to effectively bypass the checkpoint of  $\beta$  selection, allowing T cells to progress to DP stage<sup>137</sup>. As such, PI3K and the proper function of its signalling pathway is key to the development of functional peripheral T cells.

### 1.3.2 PDK1

3-phosphoinositide dependent protein kinase-1, also known as PDK1, is immediately downstream of PI3K in its signalling pathway. It acts as an intermediary protein kinase, transducing activation signals received by PI3K. PDK1 is known to be a master regulator of multiple AGC kinase family members such as Akt, PKC, S6K, RSK and SGK<sup>138</sup>. PDK1 consists of an N-terminal kinase catalytic domain, with a C-terminal pleckstrin homology (PH) domain<sup>139</sup>. The PH domain mediates binding to the product of activated PI3K, PIP<sub>3</sub><sup>140</sup>. This association of PDK1 and PIP<sub>3</sub> mediates localisation of PDK1 to the plasma membrane. Whilst PDK1 lacks a self-inhibitory domain, and is therefore considered constitutively active, it is dependent on this localisation to be able to mediate its effects through phosphorylation of Akt<sup>138</sup>. However, this is not the only mechanism of action available. PDK1 is also capable of activating a variety of other AGC kinase family members through PIF pocket interaction. Most AGC kinases possess a highly hydrophobic motif in the C-terminus of their catalytic domains. It has been shown that interaction of enzymes such as S6K, SGK and RSK with PDK1 and their subsequent activation is greatly increased if this hydrophobic motif is phosphorylated<sup>141</sup>. PDK1 has been found to also possess a hydrophobic pocket, which has been shown to interact with phosphorylated hydrophobic motifs of the other AGC kinases<sup>142</sup>. This pocket, now known as the PIF pocket, is a mechanism of non-PI3K dependent activation of AGC kinases downstream of PDK1<sup>139</sup>. In this regard, Akt can be considered unique, as it is the only AGC kinase that also requires PIP<sub>3</sub> to be activated by PDK1 phosphorylation.

Within CD8 T cells, PDK1 has been shown to be a major metabolic regulator, as it mediates both glucose and amino acid uptake required to meet the metabolic demands of an activated CD8 T cell<sup>143</sup>. This metabolic control is imperative in CD8 T cell differentiation, as increased glucose uptake and glycolysis is considered a metabolic switch that favours the generation of SLECs and terminally differentiated cells<sup>144,145</sup>. It has also been demonstrated that within CD8 T cells there is an alternate non-canonical pathway for mTORC1 activation, which is dependent on PDK1 but not Akt or PI3K. This pathway was shown by Finlay *et al* through a use of Akt and PI3K $\delta$  inhibitors, as well as PDK1 conditional knockout studies in CD8 T cells<sup>146</sup>. This PI3K and Akt independent regulation of mTORC1 is not typically observed in other cells types, as canonically Akt is the immediate upstream regulator of mTORC1 activity.

### 1.3.3 Akt

Protein kinase B (PKB), more commonly referred to as Akt, is a serine/threonine kinase and a member of the AGC family of kinases. Originally identified as the first transducer of PI3K activity following stimulation with insulin, Akt is now recognised as one of the primary mediators of the PI3K signalling pathway<sup>147,148</sup>. As such, across multiple cell types it is typically linked to crucial cellular functions such as regulation of cell size, cell cycle progression, cellular survival, metabolism, transcription and protein synthesis. Akt has three isoforms, known as Akt1, Akt2 and Akt3 respectively. Akt1 is ubiquitously expressed in virtually all tissues, where it is implicated in cell growth and survival<sup>149</sup>. Akt2 is still broadly expressed, but has been associated particularly with insulin signalling and glucose homeostasis in muscle and adipocytes<sup>150</sup>. Akt3 shows more specific tissue restriction, in particular the brain and testes<sup>151</sup>. The base structure of Akt is similar to that of protein kinase A and C, it contains a PH domain at the N-terminus, to facilitate binding of PIP<sub>3</sub>; a kinase domain, similar to that of other AGC family kinases; and a hydrophobic regulatory domain at the C-terminus, which acts to prevent Akt activity when in a dephosphorylated state. Phosphorylation of two key residues are required for complete Akt activation, threonine at position 308 and serine at position 473, phosphorylation of these sites are mediated by PDK1 and mTORC2 respectively. The threonine residue lies within the T-loop, of the catalytic kinase domain of Akt, whereas the serine residue lies within the regulatory domain. Whilst the phosphorylation at Thr308 is responsible for activation of Akt kinase activity, the Ser473 phosphorylation is required for Akt to reach its maximal activity<sup>152</sup>. Negative regulation of these two phosphorylation sites is mediated by protein phosphatase 2 (PP2) and PH domain leucine-rich repeat phosphatase (PHLPP), targeting Thr308 and Ser473 respectively<sup>153,154</sup>.

Akt is responsible for the induction of a transcriptional profile that drives the cytotoxic and effector functions of CD8 T cells<sup>143</sup>. As such, loss of Akt signalling *in vitro* causes a decrease in the expression of IFN $\gamma$ , perforin and granzyme B and upregulation of markers preferentially found in the memory pool, such as CD27<sup>155,156</sup>. Akt exists as three different isoforms, all of which are widely expressed in virtually all tissues including T cells<sup>157</sup>. Whilst they have similar structure, their variation in tissue expression and target specificities lead to differential and non-redundant effects. Akt is critical for early T cell development and survival, particularly the Akt1/2 isoforms, which when knocked out cause substantial reduction in the total number of lymphocytes<sup>158</sup>. Akt influences CD8 T cells primarily through the transcription factor family forkhead box O, or FOXO. FOXO1 and FOXO3a are critical in CD8 T cells and both are constitutively active in the nucleus of naïve CD8 T cells. Akt phosphorylation of FOXOs causes their exclusion from the nucleus and loss

of transcriptional activity. FOXO1 induces the expression of CD127, Bcl-2, CD62L and CCR7<sup>159</sup>. These factors enable naïve CD8 T cells to persist in the absence of antigen and to enter lymph nodes. Whilst FOXO1-deficient mice are embryonically lethal, mice in which FOXO1 is specifically knocked out in CD8 T cells show a decrease in the number of naïve CD8 T cells, primarily due to the loss of CD127 and CD62L<sup>160</sup>. Signalling through Akt, therefore, decreases expression of CD62L and CCR7; this impacts the trafficking of CD8 T cells, directing them away from secondary lymphoid organs and towards peripheral sites of inflammation<sup>161</sup>.

Another key function of FOXO1 mediated signalling is the repression of T-bet expression<sup>162</sup>. Pro-inflammatory cytokines such as IL-12 activate Akt, and, through phosphorylation and inactivation of FOXO1, induce T-bet expression. IL-12 also causes a loss in total FOXO1 protein, acting to further re-enforce T-bet expression. This directly links Akt to the effector differentiation of CD8 T cells. Hence, cells that display minimal Akt activity express less T-bet and skew towards MPEC formation, whilst cells with high levels of Akt activity have increased levels of T-bet and are skewed towards terminal differentiation<sup>163</sup>. This correlates with studies using constitutively active forms of Akt in CD8 T cells, which show reduction in expression of CD127, CD122 and Bcl-2 and subsequent loss of the MPEC phenotype<sup>164</sup>. Less is known about FOXO3a, however, it has been shown to regulate the initial expansion phase of the primary CD8 T cell response whilst being uninvolved with the development of memory<sup>165</sup>.

## 1.4 Cancer Immunology

As stated above (section 1.2.3.2), one of the functions of CD8 T cells is to eliminate cancerous cells through constant immunosurveillance. It has been known for some time that introduction of carcinogens into immunodeficient hosts is linked to a higher incidence of cancer<sup>166-168</sup>. Conversely, patients that present with high frequencies of tumour infiltrating lymphocytes (TILs) are more likely to have a positive outcome<sup>169</sup>. It is clear, therefore, that intratumoral CD8 T cells are critical to the successful elimination of tumours.

Upon the emergence of cancerous cells, there is a process of immune cell interaction with these cells known as immunoediting. The immunoediting process can have profound effects on tumours, as it has been shown that tumours grown in immunodeficient mice are more immunogenic than those that develop within immunocompetent mice<sup>168</sup>. There are three stages of immunoediting; elimination, equilibrium and escape. Elimination is the first stage. When cancerous cells develop they can, through integration of the innate responses of NK cells and the adaptive responses of CD8 T cells, be targeted for destruction. However, this elimination phase

## Chapter 1

does not always occur, certain cancers have been known to proceed immediately to the equilibrium phase<sup>168</sup>. Based on the studies in immunodeficient mice, it would seem that the elimination phase is capable of minimizing the rate of occurrence of many types of cancerous cells<sup>170</sup>. However, cancerous cells that manage to survive the initial immune reaction can progress into the second stage; equilibrium. The equilibrium phase is defined by a balance between the immune system and the tumour. The balance of tumour cell expansion and destruction of the tumour by the immune system keeps the tumour in a suspended state where there is no growth in the tumour overall. However, individual cells undergo mutation and selection. This selective pressure on cancer cells favours those that are more resistant to the effects of this immune system and those that mutate to resist cytotoxic T cells<sup>169</sup>. This stage can last for many years and in the case of solid tumours as many as 20 years between initial cancer cell emergence and detection of a tumour<sup>171</sup>. After this prolonged state of genetic instability, some tumour cells become able to subvert the immune system. This is the third phase, escape, and can be achieved through multiple mechanisms e.g. down regulation of MHC molecules<sup>172</sup>, loss of NK activating ligands<sup>173</sup>, resistance to the effects of IFN $\gamma$ , increased secretion of the immunosuppressive cytokines IL-10 and TGF- $\beta$  and cultivation of a supportive, immunosuppressive microenvironment. After entering the escape phase, tumours can become capable of expanding at an accelerated rate as they are no longer constrained by the immune system.

It should be noted that there is only a small amount of direct evidence for *in vivo* eradication of premalignant lesions<sup>170</sup>. Knock-out of specific genes such as *Rag2*, *Ifng*, *Prf*, *Stat1* and *Gmcsf* have been shown to cause spontaneous tumour development in mice<sup>170</sup>. This, at minimum, implies that the impairment of the immune system that follows these specific knock-outs, aids in the development of tumours that would normally be controlled and most likely eliminated upon their emergence. Additionally, patients that receive immunosuppression therapy as part of organ transplantation have also been shown to have a significantly increased incidence of cancers of both viral and non-viral origin<sup>174</sup>. In a similar manner to the specific gene knock-outs in mice, it can be inferred from the data from transplant recipients that the immune system aids in eliminating cells that would potential become malignant. The majority of this data is provided by the phenomenon of spontaneous tumour regression that occurs in concert with clonal T cell expansion, which suggests a tumour specific immune response<sup>175,176</sup>. Whilst spontaneous tumour regression can occur without a known cause, historically it has been shown that it can occur as a result of bacterial infection<sup>177</sup>. Most notably was the treatment regimen developed by Dr William Coley during the late 19<sup>th</sup> and early 20<sup>th</sup> century. After observing a patient develop a *Streptococcus pyogenes* infection at the site of a partial tumour excision, it was noted that as the

infection continued to recur over the next few weeks, the tumour shrank<sup>178</sup>. Following this observation, Coley went on to develop a vaccine containing two dead bacterial species (Coley's Toxins) which, when injected into the tumour site repeatedly over a time course of a month, successfully treated inoperable cases of sarcoma<sup>178</sup>. However, due to the advent of post-operative antibiotics, and the emergence of chemotherapy and radiotherapy as primary cancer treatments, the use of Coley's Toxins fell into decline. In addition, more recent studies have also demonstrated the effect of using bacteria to induce T cell immune responses to tumours<sup>179</sup>.

Evidence for the equilibrium phase has been shown in cases of monoclonal gammaopathy of undetermined significance (MGUS). MGUS is a premalignant plasma cell proliferative disorder, eventually progressing to the cancerous condition of multiple myeloma<sup>180</sup>. Patients develop vigorous effector T cell responses specific for the premalignant plasma cells responsible for MGUS<sup>181</sup>, although this immune response is not observed in subsequent multiple myeloma, suggesting that the cells responsible for MGUS were in a state of equilibrium with the immune system<sup>181</sup>. Melanoma has provided excellent evidence of the escape mechanism, with large numbers of patients showing tumour-specific immune responses that are unable to provide beneficial anti-tumour effects<sup>182</sup>. In summary, whilst elimination is difficult to observe directly, the overall evidence for immunosurveillance as a hypothesis is robust<sup>183</sup>.

Malignant tumour cells are not the only cell types involved in the progression of cancerous tumours. The progression is also directly related to a complex network of non-malignant cells that cultivate and support the tumour, termed the tumour microenvironment (TME)<sup>184</sup>. The TME consists of tumour cells, a variety of immune cells and can also contain cancer associated fibroblasts (CAFs), endothelial cells supporting new vasculature and an extracellular matrix. This basic structure of TMEs is not universal; certain cancers such as leukaemias, which do not typically form tumours, possess entirely different forms of microenvironment within the bone marrow<sup>185</sup>. As such, the TME can be just as unique as each specific cancer.

Fibroblasts are cellular components of the tissue stroma, critical for the wound healing process through the production and secretion of an extracellular matrix scaffold for tissue regeneration<sup>186</sup>. Fibroblasts can be activated through multiple mechanisms, growth factors such as TGF- $\beta$ , adhesion molecules and reactive oxygen species (ROS)<sup>187</sup>. The conversion of typical fibroblasts in CAFs occurs due to a perpetually activated state, induced by factors released by tumour cells. This phenotype prevents apoptosis and in a reciprocal manner supports the development of the

## Chapter 1

tumour microenvironment. CAFs support tumour progression by increased production of growth factors and cytokines, as well as the production of matrix metalloproteinases (MMPs)<sup>188</sup>. MMPs are capable of altering the extracellular matrix, loosening the structure and promoting epithelial to mesenchymal transition (EMT)<sup>189</sup>. The EMT enhances the ability of tumour cells to invade surrounding tissues and at later stages, promotes metastatic spread. CAFs also aid in localised immunosuppression through expression of PD-L1 and PD-L2, which act to inhibit effector cells expressing PD-1<sup>190</sup>.

Tumours, like any tissue, require nutrients from the blood, however due to their rapid expansion they must also cultivate an expanded vasculature to meet their metabolic demands. This demand is met primarily through the hypoxia inducible factor (HIF) signalling pathways<sup>191</sup>. Typically, HIF1 $\alpha$  is activated in response to nutrient deprivation, hypoxic and stress conditions. However, in tumours, the regulatory components that control HIF1 $\alpha$  often become uncoupled, allowing constitutive activation<sup>191</sup>. This induces a cascade of angiogenic factors such as vascular endothelial growth factors (VEGF) and platelet derived growth factor (PDGF), which promote the formation of new vessels and expansions of new ones<sup>192</sup>. HIF1 $\alpha$  also enhances the primary metabolic process of tumour cells, glycolysis<sup>193</sup>. Beyond the immediate benefit of improved supply of glucose and sustained metabolism, this also acts as an immunosuppressive mechanism through nutrient deprivation. It has been shown that tumours actively drain glucose from their immediate microenvironment, which can directly impair the activity of CD8<sup>+</sup> effector T cells, which are similarly dependent on glycolysis<sup>194</sup>. This new vasculature production, as well as the general tissue alteration, can cause increased interstitial fluid pressure. This increased pressure can compress and impair lymphatic system drainage, further preventing interaction with potentially beneficial effector cells, thus aiding in the production of an immunosuppressive environment<sup>195</sup>.

Overall, tumour cells mutating under the selective pressure of the immune system can lead to their learning to evade the immune system. In addition to the direct effects on the tumour cells, tumours can also drastically alter their immediate microenvironment. Through manipulation of localised endothelial cells and fibroblasts, tumours can produce an immunosuppressive environment, as well as support their own expansion through metabolic alteration and increased angiogenesis.

## 1.5 Immunotherapies

The fact that the elimination phase is capable of preventing the progression of cancerous cells through immunosurveillance demonstrates the effectiveness of the immune system<sup>196</sup>. Thus, in recent years research has been directed at harnessing the ability of the immune system to clear cancers, termed immunotherapy. There are different forms of immunotherapy including both passive and active antibody therapy, vaccination and adoptive cell transfer. However, the mechanism of tumour escape can influence their relative effectiveness. Escape can occur through a variety of mechanisms, e.g. increased expression of checkpoint molecules such as PD-L1, downregulation of MHC class I molecules and by promotion of local immunosuppression by T<sub>regs</sub> and/or myeloid derived suppressor cells (MDSCs). Each mechanism alters the approach that would be most effective. For example, a lack of MHC class I molecules impairs the response of cytotoxic CD8 T cells<sup>197</sup>. However, NK cells act independently of MHC molecules and as such, therapies boosting their capabilities might be more effective in this setting<sup>198</sup>.

### 1.5.1 Monoclonal Antibodies

Monoclonal antibodies (mAb) have shown great promise since the approval of the first anti-cancer therapy with rituximab in 1997. Whilst the mechanism of action can vary between each mAb, they are generally split into two categories; passive and active. Passive mAb therapies generally target the tumour, and do not directly activate the hosts' immune system, whereas, active mAb therapies instead target the host immune system using either increased stimulation or relieved inhibition to achieve their effects.

#### 1.5.1.1 Passive Monoclonal Antibodies

The prime example of a passive mAb is rituximab, a chimeric mouse/human anti-CD20 antibody. As CD20 is expressed primarily on B cells, excluding early pro-B cells in bone marrow and activated plasma cells, it is an ideal target for many malignancies derived from B cells<sup>199</sup>. It can be utilised as a single agent treatment or in combination with chemotherapy<sup>200</sup>. It was initially used for the treatment of non-Hodgkin's lymphoma. However, since its approval in 1997, it is now used for other conditions such as chronic lymphocytic leukaemia and rheumatoid arthritis. Rituximab has also been utilised off-label for other B cell-implicated conditions such as multiple sclerosis, system lupus erythematosus and non-malignant lymphoproliferative disorders<sup>201-203</sup>. Rituximab

## Chapter 1

can induce B cell death through multiple different mechanisms including antibody-dependent cellular cytotoxicity (ADCC), complement-dependent cytotoxicity (CDC), induction of apoptosis and through sensitization to chemotherapy<sup>204</sup>. Despite the efficacy of rituximab, it still possess some harmful side effects such as severe infusion reaction and cytokine release syndrome<sup>205</sup>. These side effects are a consequence of the chimeric mouse/human structure, which can induce adverse immune reactions. As such, second generation anti-CD20 antibodies have now been generated to minimize the negative effects. mAbs such as ofatumumab, ocrelizumab and veltuzumab have been either humanized or are fully human antibodies targeting CD20 and as such are less likely to induce known side effects<sup>199</sup>.

Other examples of passive mAbs include trastuzumab, cetuximab and bevacizumab. These mAb target the HER2/neu receptor, epidermal growth factor receptor (EGFR) and vascular endothelial growth factor alpha (VEGF-A) respectively. These targets are less cancer specific, instead they target processes considered hallmarks of cancer development and progression, namely sustained signalling through growth factor and angiogenic pathways<sup>184</sup>.

HER2/neu is a member of the human EGFR family, which can signal through the mitogen-activated protein kinase (MAPK), PI3K/Akt, protein kinase C and STAT pathways, all of which are associated with cellular survival and proliferation. Up to 30% of breast cancers present with overexpression of the HER2/neu receptor, hence making it a good target for antibody therapy<sup>206</sup>. The humanized antibody trastuzumab, in combination with chemotherapy, improves survival in HER2/neu receptor positive breast cancer compared to chemotherapy alone<sup>206</sup>. By binding and preventing dimerization of the HER2/neu receptor with other members of the receptor family, trastuzumab is able to inhibit the signalling effects of the receptor<sup>207</sup>. The subsequent lack of pro-survival signals sensitises cancer cells to chemotherapy, hence why the combination is effective. In addition to the increase in chemotherapy sensitivity, trastuzumab can also induce ADCC<sup>207</sup>.

Cetuximab, a chimeric human/mouse antibody against the EGFR, is utilised against metastatic colorectal cancer (mCRC) and squamous cell carcinoma of the head and neck (SCCHN)<sup>208</sup>. As it targets a receptor in the same family as the HER2/neu receptor, the mechanism of action is similar to that of trastuzumab. It inhibits pro-survival, proliferation signalling pathways, causing ADCC as well as sensitisation to radiation and chemotherapy<sup>208</sup>. It should be noted that targeting

EGFR for anti-cancer effect has been shown to be effective only if KRAS is not mutated downstream of the receptor<sup>209</sup>.

Tumours need to develop their own vasculature in order to continue receiving oxygen and nutrients to support their accelerated proliferation. This is achieved through excessive induction of angiogenic pathways<sup>184</sup>. One of the more notable factors to contribute to this is VEGF-A. This deregulated angiogenesis is known to occur early in the development of cancerous tumours, as it has been shown to be one of the first factors visible in pre-malignant growths<sup>210</sup>. The overexpression of VEGF-A induces aberrant production of blood vessels within tumour masses. The vessels are typically characterised by unnecessary branching, increased size with minor haemorrhaging and leakiness<sup>211</sup>. As such, targeting the excessively activated angiogenic pathways in tumours in order to deprive them of basic metabolic requirements is a valid strategy for therapy. Bevacizumab is a humanized mAb derived from mouse, that targets VEGF-A, and was the first anti-angiogenic based therapy for cancer<sup>212</sup>. Bevacizumab was initially authorised in the treatment of mCRC in combination with 5-fluorouracil-based chemotherapy in 2004<sup>213</sup>. However, since then it has also been approved for use in non-small cell lung cancer (NSCLC), metastatic renal cell carcinoma (mRCC) as well as glioblastoma multiforme<sup>212</sup>. Whilst bevacizumab inhibits the pro-angiogenic pathways more directly it should be noted that inhibition of EGFR by cetuximab and trastuzumab, can also decrease VEGF-A expression<sup>214,215</sup>.

#### 1.5.1.2 Active Monoclonal Antibodies

Active mAbs aim to activate the immune system directly but there are inhibitory systems that prevent the full effect of stimulatory antibodies. Some of these proteins that inhibit immune response are now targets of active mAbs. Currently only antibodies against three target molecules have been approved for clinical use. These molecules are CTLA-4, PD-1 and PD-L1<sup>216</sup>. CTLA-4 is an inhibitory molecule, which is expressed on CD8 T cells following activation and constitutively expressed by T<sub>regs</sub><sup>217</sup>. The function of CTLA-4 derives from its higher binding affinity and avidity for CD80 and CD86 compared to CD28. This makes CTLA-4 a competitive antagonist for binding of CD80 and CD86, thus depriving CD8 T cells of co-stimulation. CTLA-4 has also been shown to signal through phosphatases to further dampen TCR responses<sup>59</sup>.

The receptor PD-1 and one of its cognate ligands PD-L1 represent the other two current targets of immune checkpoint therapy. PD-1 is expressed transiently on activated CD8 T cells, but under chronic antigenic stimulation this expression is increased and persists for longer. Generation of

## Chapter 1

the first *Pdcd1*<sup>-/-</sup> mouse in 1998 led to the discovery that the absence of PD-1 causes excessive proliferation of B cells and splenomegaly in response to stimulation<sup>218</sup>. Subsequent identification of its cognate ligand, PD-L1, demonstrated that engagement of PD-1 inhibited T cell proliferation and cytokine production upon stimulation with an anti-CD3 antibody<sup>219</sup>. Structural analysis of PD-1 revealed a type I transmembrane glycoprotein possessing an IgV-like extracellular domain showing limited homology to the CD28 and CTLA-4 family of co-stimulatory/co-inhibitory receptors<sup>220</sup>. The cytoplasmic tails of PD-1 were shown to contain both an immunoreceptor tyrosine-based inhibition motif (ITIM) and immunoreceptor tyrosine-based switch motif (ITSM). These motifs act as docking points for the phosphatases SHP-1 and SHP-2, which dephosphorylate the tyrosine residues of proteins within the signalling pathways downstream of the TCR signalling complex, such as the  $\zeta$ -chain of CD3, in order to inhibit stimulatory signals<sup>221</sup>. In terms of exhaustion, PD-1 signalling in activated CD8 T cells induces a highly dysfunctional effector phenotype. This is characterised primarily by an inability to effectively produce cytokines, such as IFN- $\gamma$  or IL-2, or to degranulate for effective cytotoxicity, as well as impaired proliferation and survival<sup>222</sup>.

Whilst the ligands for CTLA-4 are largely restricted to professional APCs, the ligands of PD-1 are more widely expressed<sup>217</sup>. PD-L1 can be found on many non-lymphoid tissues and is found to be present in many cancerous tumours, the higher expression of which is correlated to a poorer prognosis<sup>58</sup>. Both CTLA-4 and PD-1 function to attenuate CD8 T cell responses as part of the mechanisms of peripheral tolerance, which can be through the induction of exhaustion<sup>217</sup>.

Clinically, ipilimumab has been used to target CTLA-4 and nivolumab to target PD-1, although other CTLA-4 and PD-1/L1 blockers are used in patients. Ipilimumab is a fully human mAb, and was the first checkpoint inhibitor to be approved in 2011 for use in metastatic melanoma<sup>223</sup>. The mechanism of this antibody is not just to block the interaction of CTLA-4 with CD80/86 but also to deplete T<sub>regs</sub> that express CTLA-4 at constitutively higher levels<sup>224</sup>. The resulting change in T<sub>reg</sub>/T<sub>eff</sub> balance aids in anti-tumour effect. Nivolumab is a fully human mAb, initially used as a monotherapy for melanoma, but now also approved for squamous cell lung cancer and renal cell cancers. Like ipilimumab, nivolumab acts in part by blocking its target receptor and relieving inhibitory signalling in CD8 T cells. This allows the reactivation of exhausted antigen specific TILs to occur, now free from these inhibitory pathways<sup>225</sup>. Combination of ipilimumab and nivolumab showed notable success in the treatment of metastatic melanoma<sup>226</sup> and resulted in progression

free survival (PFS) of 11.5 months, compared to just 2.9 and 6.9 months for ipilimumab and nivolumab monotherapy respectively<sup>226</sup>, suggesting synergistic effects of combination therapy.

While the successes of active mAbs have been impressive<sup>226</sup>, only a subset of patients respond to anti-PD1/PD-L1 therapy. Meta-analysis estimates that approximately 20% of patients show complete or partial responses to anti-PD-1/PD-L1 therapy<sup>227</sup>, but in individual studies the response rate to nivolumab can be as high as 40%<sup>226</sup>. This incomplete response is due in part to a lack of a repertoire of T cells specific for the tumour, absence of cells capable of infiltrating the tumour and reduced immunogenicity of target tumour cells<sup>228</sup>. Adoptive cell transfer can allow infusion of *ex vivo* expanded and genetically modified cells, which can overcome these limitations.

### 1.5.2 Adoptive Cell Transfer

Adoptive cell transfer (ACT) of autologous TILs was shown to be an effective treatment for metastatic melanoma as early as 1988<sup>229</sup>. This process involves the transfer of substantial numbers of *ex vivo* expanded antitumor lymphocytes (up to  $10^{11}$ ) back into patients, with IL-2 being administered concurrently.

Since this time, advances have been made in ACT therapy. A key development was the discovery that non-myeloablative chemotherapy prior to ACT led to a more profound regression of metastatic melanoma tumours and persistent repopulation of T cells<sup>230</sup>. The standard methodology for ACT of autologous TILs involves excision and fragmentation of tumours and culturing in high dose IL-2. Over two weeks, lymphocytes expand and destroy the tumour fragments, and, through co-culture assays it is then possible to identify tumour specific cells, which can be subsequently expanded with feeder cells, anti-CD3 stimulation and IL-2. Following lymphodepletion, patients then receive an infusion of these expanded cells. It was initially thought that lymphodepletion enhanced the effectiveness of ACT therapy by the elimination of immunosuppressive T<sub>regs</sub>. However, it has been shown that lymphodepletion, through chemotherapy or radiotherapy, eliminates cellular sinks<sup>231</sup> of NK or other immune cells that reduce the availability of homeostatic cytokines such as IL-7 and IL-15<sup>231</sup>. Lymphodepletion, therefore allows greater availability of these cytokines to augment the effectiveness of ACT therapy<sup>231</sup>.

This process of lymphodepletion followed by ACT has shown great effect in metastatic melanoma. In one study of 93 patients with metastatic melanoma who had received some form of pre-treatment, this process was able to induce objective response rates in 50-70% of patients, with 20% displaying complete tumour regression<sup>232</sup>. The patients showing complete responses went on to have three and five year survival rates of 100% and 93% respectively<sup>232</sup>. Given that the five year survival rate for patients in this stage of metastatic melanoma with conventional treatments is approximately 5%, this is a clear demonstration that ACT therapy can be highly effective<sup>232,233</sup>. This study also showed that factors that were most associated with objective responses were the percentage of CD8<sup>+</sup> CD27<sup>+</sup> cells infused, telomere length and persistence of cells past one month post infusion. All of these factors are markers of a memory-like phenotype, indicating that the differentiation state of infused cells is key.

ACT is not without drawbacks, such as the requirement for lymphodepletion either by chemotherapy or radiotherapy, the subsequent patient exhaustion, the financial cost, and the fact that generating T cells with prolonged longevity has proved challenging<sup>234</sup>. All of these factors must be considered in designing more effective ACT protocols. Ideally, one would want to improve the effectiveness of ACT so that it not only increases the response and regression rate, but can also be applied to more forms of cancer. One way to achieve this is to genetically alter the CD8 T cells during *ex vivo* expansion to enhance their abilities. This can be done by introducing chimeric antigen receptors (CARs) and/or by overexpressing or inhibiting key molecular signalling pathways. Hence, an understanding of the pathways that control CD8 T cell activation and differentiation are critical for the development of more effective ACT protocols. This thesis is focussed on understanding the PI3K-PDK-Akt signalling pathway, which is important for the regulation of CD8 T cell metabolism, cytotoxicity, differentiation, proliferation and survival. However, it is unclear whether this pathway can be manipulated to improve T cell cytotoxicity and survival without compromising other key aspects such as metabolism or differentiation. It is hoped that with an increased understanding of the roles of their downstream enzymes and transcription factors one might be able to find the best combination of factors to elicit maximal therapeutic benefit.

### 1.5.3 Cancer Vaccines

Despite the success of vaccines in immunizing and in some cases eradicating disease, translating the potential of cancer vaccines into efficacious therapies has been difficult<sup>235</sup>. Currently, the two most beneficial vaccines to treat cancer are prophylactic in nature and target viruses that can cause cancer to develop. These vaccines target the liver cancer causing hepatitis B virus and the human papillomavirus, which accounts for up to 70% of cervical cancers<sup>235</sup>.

Regardless of the lack of success shown by therapeutic cancer vaccines in clinical trials, many remain in development. Combining cancer vaccines with immunotherapies have shown promising effects. For example, GVAX is a cancer vaccine created by conferring autologous tumour cells the ability to secrete granulocyte-macrophage colony-stimulating factor (GM-CSF), followed by irradiation to prevent proliferation<sup>236</sup>. In combination with anti-CTLA-4 antibody GVAX demonstrated effective elimination of B16 melanoma cell line in mice<sup>237</sup>. This effect was mediated through increased infiltration of both CD4 and CD8 T cells, as well as an increase in the CD4 effector/regulatory ratio<sup>237</sup>. Other studies have also demonstrated the effectiveness of GVAX as well as another autologous tumour cell vaccine FVAX<sup>238</sup>. Generation of FVAX follows the same method but involves transduction with genes encoding FTL-3 ligand in place of GM-CSF. In this study by Curran *et al*<sup>238</sup>, FVAX in combination with anti-CTLA-4, anti-PD-1 and anti-PD-L1 showed remarkable synergistic effects against B16 melanoma tumours in mice.

Other cancer vaccine models continue to be tested. These include dendritic cell vaccines, tumour associated antigen vaccines, as well as DNA and RNA vaccines<sup>235</sup>. Neo-antigen vaccinations have been shown in a clinical setting to have some benefit. The combination of injecting multiple long peptides with an adjuvant of poly-ICLC (a TLR3 stimulator), was capable of eliciting strong T cell responses<sup>239</sup>. These long peptides were derived from excised tumour cells and identified through whole exome sequencing (WES) compared to healthy tissue. This vaccination system was designed with the intent of overcoming two limitations of cancer therapy: tumour heterogeneity and selectively targeting tumour cells relative to normal cells<sup>239</sup>. Whilst this trial demonstrates the ability of neo-antigen vaccines to generate new T cell responses to a vast array of cancer antigens, it is still very limited in its ability to effectively eliminate tumours as a monotherapies.

## Chapter 1

Many vaccination methods are capable of inducing responses but one of the prime obstacles to their success is the inability to overcome the immunosuppressive effects of the tumour microenvironment<sup>235</sup>. This might explain why combinations of vaccines such as GVAX and FVAX, with checkpoint inhibition, show some synergistic effects. However, as it stands, cancer vaccines as monotherapies remain unlikely.

## 1.6 Aims and Hypotheses

The overall aim of this PhD was to better understand the role that the Akt signalling pathway plays in CD8 T cells, including in regulating effector function, differentiation, metabolism and ACT therapy. This was investigated primarily using the PDK<sup>K465E</sup> mutant mouse model described above, as well as by pharmacological inhibition of Akt.

We aimed to address discrepancies found in the literature between reported effects of the PDK<sup>K465E</sup> mutation on T cells *in vitro* and *in vivo*. Specifically, Akt inhibition or PDK<sup>K465E</sup> mutant cells demonstrate reduced granzyme B and IFN- $\gamma$  expression *in vitro* suggesting that restricting Akt activity has a negative effect on CD8 T cell cytotoxicity yet this is not observed with *in vivo* tumour and infection models which are controlled effectively by both WT and PDK<sup>K465E</sup> CD8 T cells<sup>240</sup>. We therefore sought to clarify the effect of Akt on effector functions of CD8 T cells, primarily through analysis of cytokine production and assessment of direct cytotoxic capacity of PDK<sup>K465E</sup> CD8 T cells *in vitro*. These results are shown in Chapter 3.

Akt acts as a nexus for converging signals that influence the differentiation pathway of CD8 T cells. However, the temporal effects of Akt activity on CD8 T cell differentiation are not well defined. Thus we aimed to investigate when differential Akt activity begins to influence CD8 T cell differentiation and what effects the PDK<sup>K465E</sup> mutation has on this process. To this end we utilised both PDK<sup>K465E</sup> mutant mice and a single cell RNA sequencing technique known as Drop-Seq. This was the focus of Chapter 4.

Whilst Akt has previously been reported to increase expression of proteins that promote glycolysis<sup>241</sup> its role in oxidative phosphorylation of CD8 T cells has not yet been established. However, both glycolysis and oxidative phosphorylation are key to activation and differentiation processes of CD8 T cells. Glycolysis generates metabolic intermediates that are utilised to support the rapid clonal expansion and macromolecule production that are required by effector cells, whereas, oxidative phosphorylation plays a critical role in the metabolic state of memory cells, aiding in their long term persistence<sup>1</sup>. Data shown in Chapter 5 sought to determine the role of

## Chapter 1

Akt in modifying oxidative phosphorylation using a constitutively active form of Akt, in addition to PDK<sup>K465E</sup> mutant mice and pharmacological inhibition.

Given the homology of the kinase domains of SGK and Akt<sup>242</sup>, we decided to investigate if SGK functions similarly to Akt within CD8 T cells. SGK currently is poorly characterised in CD8 T cells. However, its function in CD4 cells suggests it may have similar effects as Akt<sup>243</sup>. As such, we felt it warranted further investigation to see what role, if any, it plays in CD8 T cells. Chapter 6 displays results from these experiments.

The specific aims of my thesis were:

- 1 – To determine the influence of sub-optimal Akt signalling on CD8 T cells, through testing cytotoxic capacity and cytokine production.
- 2 – To characterise the effect of Akt signalling on CD8 T cell differentiation, utilising Drop-Seq to gain greater insight.
- 3 – To identify the effect of graded Akt activity on mitochondrial oxidative phosphorylation and whether this can be utilised for improved ACT therapy against tumours.
- 4 – To investigate the role that SGK, a homologous kinase to Akt, plays in CD8 T cells.

## Chapter 2 Methods

### 2.1 Mice

Polyclonal wild-type C57BL/6 and OT-1 TCR transgenic mice were purchased from Charles River. PDK1 (K465E) mutant mice on a C57BL/6 background were initially generated by Alessi *et al*<sup>244</sup> and gifted by Professor Doreen Cantrell (University of Dundee). PDK1 mutant mice were subsequently cross-bred with C57BL/6 mice, in house, to generate mice with a polyclonal T cell repertoire, and were also bred with OT-1 mice to generate a strain of mice with T cell specificity for ovalbumin harbouring this PDK1 mutation. All animal experiments were carried out according to UK Home Office Licence guidelines and were approved by the University of Southampton's ethical committee.

### 2.2 Reagents

RPMI 1640 Medium (Cat# 21875091) was purchased from Invitrogen. PE-labelled Tetramers were produced in house. Ovalbumin (OVA) protein was purchased from Sigma. OVA-derived peptides SIINFEKL and SIIQFEKL were purchased from ProImmune (Oxford, UK) or Peptide Protein Research (Peptide Synthetics, Hampshire, UK). All cytokines utilised in cell culture were purchased from Peprotech unless otherwise stated. Akt Inhibitor VIII (Akti-1/2) is produced by Calbiochem, and was purchased through Merck. SGK inhibitor, GSK650394, was acquired from Selleckchem (Strattech Scientific, Cambridgeshire, UK). Carboxyfluorescein succinimidyl ester (CFSE) and PKH26 cell dyes were purchased from Sigma-Aldrich (now Merck, Dorset, UK)

### 2.3 Cell Lines

Cell lines used in this study were the epithelial cell line stably expressing chicken OVA and B7 (MecSig OVA-B7), the T cell hybridoma cell line B3Z, the T cell lymphoma derived EL4, EG7-OVA an EL4 derivative that expresses OVA and Phoenix-ECO, a HEK 293T/17 derived cell line transformed to express ecotropic envelope proteins from retrovirus genes. The MecSig OVA-B7 cell line originates from the European Collection of Cell Cultures (ECACC) and was cultured in DMEM

## Chapter 2

media supplemented with 10% FCS, 2% glutamine and sodium pyruvate, 1% penicillin/streptomycin, 150µg/ml of geneticin (G418) and Hygromycin B. Phoenix-ECO cells were also grown in DMEM media as above, but without penicillin, streptomycin, geneticin or Hygromycin-B. EG7-OVA cells were cultured in RPMI 1640 media with 10% FCS, 2% glutamine and sodium pyruvate and 1% penicillin/streptomycin (hereafter referred to as complete RPMI media) supplemented with 400µg/ml of geneticin (G418). Both the B3Z and EL4 cell lines were cultured in complete RPMI media alone. Attenuated OVA-expressing *Listeria Monocytogenes* ( $\Delta$ ActA-LM-OVA, hereafter referred to as LM-OVA, from H. Shen, University of Pennsylvania Perelman School of Medicine, Philadelphia) was grown in brain heart infusion (BHI) media. Spectrophotometer was used to quantify colony forming units (CFU) of LM-OVA cultures for *in vivo* infection challenges.

### 2.4 qPCR

For isolation of CD8<sup>+</sup> T cells, spleens were taken from mice, homogenized to release splenocytes and treated with 2-3ml red cell lysis buffer solution (155mM NH<sub>4</sub>Cl, 10mM KHCO<sub>3</sub> in 1L of deionized water) for 5 minutes. Splenocytes were then washed in PBS and resuspended in complete RPMI media, supplemented with 50µM 2-mercaptoethanol (2-ME). Isolation of CD8<sup>+</sup> T cells from the splenocyte pool was achieved by negative selection, using the mouse CD8a<sup>+</sup> T Cell Isolation Kit (Miltenyi biotech, Surrey, UK). Purity of CD8<sup>+</sup> samples was assessed by flow cytometry following staining with anti-CD8-APC Cy7 (eBioscience, now ThermoFisher). From this pure CD8<sup>+</sup> T cell sample, RNA extraction was performed using RNeasy Mini Kits and QIAshredder Kits (Qiagen); the concentration and purity of the mRNA was then analysed using a Nanodrop 2000 Spectrophotometer. Absorbance at the 260nm wavelength on the spectrophotometer was used to determine mRNA concentration, with the ratio of absorbance between 260/280nm wavelengths determining the presence of protein contaminants from the RNA extraction process. The mRNA was either used immediately or stored at -80°C in order to prevent degradation and was converted to cDNA through the use of the SuperScript III First-Strand Synthesis System (Invitrogen, now ThermoFisher) using 200ng of RNA in the initial reaction, with random hexamers provided in the kit as the primer, according to the manufacturer's instructions. All primers and probes for subsequent qPCR were purchased from Integrated DNA Technologies (IDT, Belgium), primers were selected to cross exon-exon boundaries to improve target specificity. For qPCR, all samples were plated in triplicate in a 96-well plate (Bio-Rad); each well contained a final volume of 20µl, consisting of 10µl PCR SuperMix-UDG (Invitrogen, now ThermoFisher), 1µl of a 20x stock of the primer/probe mixture (yielding a final concentration of 500nM primer and 250nM probe), 0.5µl of cDNA and 8.5µl of water (sterilised by UV radiation). The qPCR was performed using a

C1000 Thermal Cycler with CFX96 Real Time system (Bio-Rad, Hertfordshire, UK) with the following protocol: 4 minutes at 95°C to initiate the process, followed by cycles of 15 seconds at 95°C and 45 seconds at 60°C, with the plate being read at the end of each of these cycles. The process terminated following 40 cycles unless otherwise stated. Cycle threshold ( $C_t$ ) from qPCR reaction was determined by plotting the logarithmic intensity of fluorescent probe against the qPCR cycle number and setting the threshold at the linear point of this amplification plot. From this  $\Delta C_t$  was calculated based on the difference between the  $C_t$  of the target gene and the reference gene,  $\beta 2M$ . From this,  $\Delta \Delta C_t$  can be calculated based on the difference between the  $\Delta C_t$  of two different biological samples. From this, fold change can be established with the formula –  $2^{((WT \Delta C_t)-(PDK \Delta C_t))}$ .

## 2.5 ELISA

96-well MaxiSorp plates (eBioscience, now ThermoFisher) were coated with purified rat anti-IFN $\gamma$  antibody (BD Pharmingen, Oxford, UK) diluted in a 50mM bicarbonate buffer (1.59g Na<sub>2</sub>CO<sub>3</sub>, 2.93g NaHCO<sub>3</sub> in 1L dH<sub>2</sub>O) to 4 $\mu$ g/ml. 100 $\mu$ l of this solution was applied to each well and allowed to incubate overnight at room temperature. Plates were then blocked with PBS/1%BSA for 1 hour, followed by 3 washes with PBS/0.05%Tween-20. Mouse IFN $\gamma$  standards and samples were then applied to the plate; IFN $\gamma$  standards were used in two-fold dilutions starting at 4ng/ml with the lowest point being 62.5pg/ml. Samples were then incubated in plates for 1.5 hours followed by 3 washes with PBS/0.05%Tween-20. Detecting biotinylated rat anti-mouse IFN $\gamma$  antibody (eBiosciences, now ThermoFisher) was then added at a concentration of 1.25 $\mu$ g/ml, and incubated for 1 hour. Plates were then washed 3 times and streptavidin-HRP (Invitrogen, now ThermoFisher) was applied at a dilution of 1:2500 (1 $\mu$ g/ml), followed by a 30 minute incubation at room temperature. Finally, plates were washed 3 times and OPD substrate mixture was applied (consisting of 1 OPD tablet (Sigma-Aldrich, Dorset, UK) in 25ml citrate buffer (19.2 citric acid/L of water), 25ml phosphate buffer (28.4g Na<sub>2</sub>HPO<sub>4</sub>/L of water), 50ml of water and 20 $\mu$ l of H<sub>2</sub>O<sub>2</sub>). Once the wells containing the standards had changed colour the reaction was halted using 40 $\mu$ l 2.5M H<sub>2</sub>SO<sub>4</sub>. Plates were read on an ELISA plate reader measuring detection at the 425nm wavelength.

## 2.6 CFSE Proliferation Assay

To measure CD8<sup>+</sup> T cell proliferation, purified CD8<sup>+</sup> T cells were resuspended at  $50 \times 10^6$ /ml in PBS/0.1%BSA containing 10 $\mu$ M CFSE from a stock solution of 10mM and incubated for 5 minutes at 37°C. Cells were then washed with complete RPMI media three times before being plated at  $2 \times 10^5$  cells per well in a 96-well plate, under various stimulatory conditions. Stimuli included anti-CD3 (clone 2C11), anti-CD28 (clone 37.51) and EG7 cells as indicated. In some assays the SGK inhibitor GSK650394 (Selleckchem, Stratech Scientific, Cambridgeshire, UK) was also used. CFSE proliferation assays were performed in triplicate. The degree of CFSE dilution was assessed using a BD FACSCanto II or equivalent, after counter staining as indicated; CFSE fluorescence is visible on the FITC channel.

## 2.7 Thymidine Proliferation Assay

Purified CD8<sup>+</sup> T cells were plated at a concentration of  $2 \times 10^6$ /ml in 96-well plates in a total volume of 200 $\mu$ l/well. Stimulatory conditions in the plate varied but included plate-bound anti-CD3 with soluble anti-CD28 or the EG7 cell line. At 56 hours after initial stimulation, 1 $\mu$ Ci of tritiated thymidine was added to each well in a volume of <20 $\mu$ l. Subsequently, at 72 hours after stimulation, cells were ruptured using distilled water and cell fragments and DNA collected on a filter plate. Scintillation fluid (40 $\mu$ l) was added to each well of the filter plate and radiation measured in a  $\beta$ -emission counter. Increased  $\beta$ -emission correlates with increased tritiated thymidine incorporation and hence increased proliferation.

## 2.8 Microscopy

Coverslips were coated with poly-L-Lysine (PLL) by 5 minute incubation of PLL on glass coverslips, followed by a 5 minute wash with water. PLL coverslips were then incubated with  $1 \times 10^6$ /ml cell suspension for 40 minutes in a 12-well plate. Media was then removed and 1ml of cold 4% Paraformaldehyde (PFA) was added into the well coating the coverslip. Plates were left on ice for 15 minutes in order to fix cells. Once fixed, the PFA was removed and wells washed 3 times gently with PBS. To permeabilise cells, 1ml of a solution of 0.25% Triton X-100 was applied to each coverslip for 10 minutes, followed by 3 further washes with PBS. PBS/2.5%BSA/0.05%Tween-20 was then used to block the coverslip for 1 hour. Antibody stocks of goat anti-baiap3 (Santa Cruz

Biotechnology, SC-163726, now discontinued, 2µg/ml) and a control goat IgG isotype (Santa Cruz Biotechnology, SC-3887, now discontinued, 2µg/ml) were then applied to the bottom of a 6 well plate in a volume of 100µl. The non-coated sides of the coverslips were then dried with filter paper and coverslips, with the cells facing down, were placed on top of the droplet of primary antibody and incubated at room temperature for 1 hour, protected from light. After primary incubation coverslips were placed back into the wells, facing upwards again. Coverslips were washed with PBS 3 times and the staining process repeated using the secondary antibodies (donkey anti-goat Alexa488; ThermoFisher Scientific, 2µg/ml), incubating for only 30 minutes. After antibody staining and washing, DAPI counterstain was applied for 5 minutes, before mounting coverslips on glass microscopy slides. Coverslips were mounted in Vectashield and cells were viewed under an Olympus CKX41 inverted microscope at 20x magnification.

## 2.9 Flow Cytometry

For flow cytometry staining, all cell samples were washed with 3ml PBS/0.1% BSA, and centrifuged at 400g for 5 minutes. For surface staining, cells were first blocked with 10µg/ml 2.4G2 anti-FcγR mAbs for 10 minutes, prior to addition of antibodies, as indicated, for a minimum of 30 minutes at 4°C. For intracellular staining, the Foxp3/Transcription Factor Staining Buffer Set from eBioscience was used for fixation and permeabilisation using the manufacturer's protocol. For intracellular cytokine measurement, 1x10<sup>6</sup> CTLs were resuspended in 100µl of media and cultured in 96-well plates. 100µl of media containing peptide for restimulation and GolgiPlug (BD Bioscience 555029, Berkshire, UK) was then added to these cells for 4 hours. GolgiPlug was added at a final dilution of 1/1000 per well. Following this restimulation, cells were washed with PBS before being fixed and permeabilised using the buffer set described above. All antibodies used for flow cytometry are listed in *Figure 2-1* below.

**Figure 2-1 - Antibody Source Table**

Target	Fluorophore	Clone	Source
CD8α	APC-Cy7	53-6.7	eBioscience
CD62L	eFluor450	MEL-14	eBioscience
CD62L	PerCP-Cy5.5	MEL-14	eBioscience
IL-2	PE	JES6-5H4	eBioscience
IFNγ	APC	XMG1.2	eBioscience

CD45.1	eFluor450	A20	eBioscience
CD25	PE-Cy7	PC61.5	eBioscience
KLRG1	APC	2F1	eBioscience
Granzyme B	APC	GB11	Molecular Probes
Baiap3	Unconjugated	E-14	Santa Cruz Biotechnology
Goat IgG	FITC	sc-2024	Santa Cruz Biotechnology
Goat IgG Control	Unconjugated	sc-3887	Santa Cruz Biotechnology
Rat IgG2a $\kappa$ Isotype	eFluor450	eBR2a	eBioscience
Mouse IgG1	APC	P3.6.2.8.1	eBioscience
Rat IgG2b $\kappa$ Isotype	PE	eB149/10H5	eBioscience
Rat IgG1 $\kappa$ Isotype	APC	eBRG1	eBioscience
Syrian Hamster IgG	APC	2F1	eBioscience
Rat IgG1 $\kappa$ Isotype	PE-CY7	eBRG1	eBioscience
Mouse IgG2a	eFluor450	eBM2a	eBioscience
Rat IgG2a $\kappa$ Isotype	PerCP-Cy5.5	eBR2a	eBioscience
Donkey Anti-Goat IgG	Alexa488	Polyclonal	ThermoFisher Scientific

## 2.10 Cytotoxicity Assay

To measure cytotoxic capacity of T cells, separate samples of EL4 cell targets were stained with 5 $\mu$ M of CFSE and PKH26 (Sigma-Aldrich). CFSE stained cells were subsequently pulsed with peptide by incubating for 1 hour in media containing the peptide indicated at the concentrations shown in the relevant Figures. The peptide pulsed CFSE-stained and non-peptide pulsed PKH26-stained cells were then mixed at a 1:1 ratio, which was confirmed by flow cytometry. The 1:1 mixture was then combined with cytotoxic T lymphocytes (CTLs) at varying ratios and incubated for 6 hours at 37°C. The resulting samples were then analysed via flow cytometry, and the ratio of CFSE-stained cells to PKH26-stained cells compared to a control sample in order to assess the cytotoxic capacity of the CTLs. Unless otherwise stated, CTLs were generated from OT-1 derived splenocytes previously stimulated with 20pM SIINFEKL peptide for 2 days, followed by 3 days in IL-2 at 10ng/ml.

## 2.11 Plasmid Cloning

All genetic constructs were designed in and provided by GeneArt Synthesis from ThermoFisher Scientific. The original pMP71 vector was generously gifted by Professor Hans Stauss (University College London). All restriction enzymes and associated buffers were purchased from Promega. All restriction digestions were carried out in 20µl reactions, with 0.5U of restriction enzyme, 2µl appropriate 10x buffer and water. Reactions were allowed to proceed for 2-3 hours at 37°C before analysis on a 1% agarose gel. Products were resolved by gel electrophoresis and relevant DNA bands extracted using the QIAquick Gel Extraction Kit from Qiagen, using the manufacturers' protocols. Fragments for ligation were mixed at a molar ratio of 3:1 insert to vector, with T4 Ligase enzyme (Promega), 10x Ligase buffer (Promega) and water, up to a final volume of 15µl. Ligation reactions were left at room temperature for 3 hours and 2µl of final ligation reaction used to transform One Shot STBL3 bacteria by heat shock (ThermoFisher Scientific). Subsequently, transformed bacteria were expanded in LB broth with 100µg/ml ampicillin before plasmid extraction using Qiagen Plasmid Maxi Kit, following manufacturers' recommended protocols.

## 2.12 Metabolism Assays

To study metabolic changes in CD8<sup>+</sup> T cells, a Seahorse XF Analyser (Agilent, Cheshire, UK) was used. For these assays Cell-Tak plates were prepared by diluting Cell-Tak to 25µg/ml in filter sterilised 0.1M sodium bicarbonate buffer. Once diluted, 25µl of solution was dispensed per well immediately. Cell-Tak solution was incubated in 96-well plates from Seahorse Biosciences at RT for 30 minutes. Solutions were flicked or aspirated off and plates washed twice with 200µl of sterile water before allowing to air-dry and storing at 4°C. Once stored, Cell-Tak coated plates were used within 1 week. One day before performing the assay, the sensor cartridge was hydrated by adding 200µl of calibrant fluid to each of the wells and incubating in a non-CO<sub>2</sub> incubator at 37°C. DMEM media lacking glucose, glutamine, phenol red, pyruvate and sodium bicarbonate, was utilised as the base XF media for the assay. Using one vial of powdered media (DMEM, Sigma-Aldrich, Dorset, UK), 1L was reconstituted with distilled water; glucose (to 25mM), glutamine (to 2mM) and sodium pyruvate (to 1mM) was then added to 200ml of this media and warmed to 37°C. At this temperature, the pH of the solution was adjusted using HCl and NaOH to between 7.35 and 7.4, the media was filter sterilised, used in all future steps and referred to as XF media.

## Chapter 2

On the day of the assay, the Cell-Tak plate was removed and allow to reach room temperature. Target cells were washed twice in XF media, resuspended at  $4 \times 10^6$ /ml and plated at 400,000 cells per well with six replicate wells per condition tested; 100 $\mu$ l of the XF media was added to the control wells, which comprise the first and last column of the plate. Following plating of the cells the plate was centrifuged (200xg with the brake set to zero for 10 seconds) to bind cells to the Cell-Tak adhesive. The plates were then incubated in a non-CO<sub>2</sub> incubator at 37°C for 30 minutes before starting the assay. Inhibitors were diluted in XF media to 8x, 9x and 10x concentrated stocks for oligomycin, carbonyl cyanide-*p*-trifluoromethoxyphenylhydrazone (FCCP) and rotenone with antimycin-A (AA) respectively and 25 $\mu$ l of each of these were then added to the associate ports in the sensor cartridge. The plate and cartridge were then introduced to the XF analyser to begin calibration. During calibration, 75 $\mu$ l of the XF media was added to the control and sample wells to a final volume of 175 $\mu$ l before the assay. The protocol for the assay was then entered into the XFe96 analyser. This protocol comprised a cycle of two minutes of mixing, followed by three minutes of measurement, followed by injection of the relevant inhibitor port after every third measurement in the order: Oligomycin – FCCP – Rotenone/AA. Oligomycin acts to inhibit ATP synthase by blocking its proton channel, which causes a decrease in oxygen consumption rate (OCR). FCCP is an uncoupling agent, which causes proton permeability in the mitochondrial membranes and effectively uncouples ATP from the electron transport chain. The overall effect of FCCP is to cause maximal consumption of oxygen through proton export. Rotenone and antimycin A inhibit complexes 1 and 3 in the electron transport chain respectively, terminating the reaction and causing complete abrogation of oxygen consumption.

Corning Cell-Tak adhesive was purchased from ThermoFisher Scientific (Cat# - 10317081). FluxPaks including the 96-well plate sensor cartridges and cell culture microplates as well as Seahorse XF Calibrant solution were purchased from Seahorse Biosciences, through Agilent (102601-100). Oligomycin, FCCP, Rotenone and Antimycin A reagents were purchased as part of the Seahorse XF Cell Mito Stress Test Kit (103015-100), again from Seahorse Bioscience, Agilent. Final concentration of reagents was as follows: Oligomycin 1 $\mu$ M, FCCP 1.5 $\mu$ M, Rotenone 100nM and Antimycin A 1 $\mu$ M. DMEM media, in powder form, was purchased from Sigma-Aldrich (D5030-10X1L). All metabolism assays were performed using Seahorse XFe96 Analysers.

### 2.13 Western Blots

For western blots,  $1 \times 10^6$  cells were lysed in protein solubilisation buffer (160mmol/L, 6.4 mol/L urea, 1.6% SDS, 0.08% bromophenol blue, pH8). Lysates were sonicated briefly before being

resolved on NuPAGE Novex 10% Bis-Tris Gels (ThermoFisher Scientific). Proteins were subsequently transferred to Immobilon-P membranes (Millipore) using a transfer buffer (12.5mM Tris, 96mM Glycine, 10% ethanol, solution in H<sub>2</sub>O), then incubated with antibodies against phospho-NDRG1 (Thr346, Clone D98G11, Rabbit mAb), NDRG1 (Clone D6C2, Rabbit mAb), both from Cell Signalling Technologies and actin (Clone C-11, Goat polyclonal Ab, Santa Cruz Biotechnology). Membranes are blocked in 1xTBS buffer (10mM Tris, 150mM NaCl, 0.1% Tween-20, solution in H<sub>2</sub>O) with 5% milk. Between blocking the membrane, incubating with primary and secondary antibodies, the membrane was washed three times with 1xTBS buffer for 5 minutes. Blots were visualised using HRP-conjugated anti-rabbit (GE Healthcare) or anti-goat (Santa Cruz Biotechnology) secondary antibodies with Supersignal West Pico Chemiluminescent Substrate (ThermoFisher Scientific). An acidic glycine buffer (25mM glycine, 1% SDS, solution in H<sub>2</sub>O, 2pH) was used to strip the membrane of bound antibodies in order to allow re-probing of transferred proteins with new antibodies.

## 2.14 Transfection

To transfect cells to generate retroviral particles for subsequent transduction, three days before transfection, Phoenix-ECO cells were cultured to achieve a confluency of between 50-70% in 3ml of DMEM media in a small flask (containing 10% FCS, 2% Glutamine/Pyruvate, antibiotic free). On the day of transfection, the media was gently replaced so as not to displace cells and 4µg of the vector to be transfected and 4µg of pCL-Eco (Addgene, Cambridge MA, USA) was mixed with 135µl DMEM media and 15µl of FuGENE HD Transfection Reagent (Promega). The mixture was then incubated at RT for 10 minutes. Subsequently, 150µl of the vector mixture was added to the final 3ml Phoenix-ECO cell culture. Cells were cultured for a further 48 hours at 37°C, before the supernatant was used for transduction. The supernatant from each transfection reaction was used to transduce 10x10<sup>6</sup> splenocytes. All experiments contained a positive control of pMP71 control vector transduced cells.

## 2.15 Transduction

Unless otherwise stated, wild-type (WT) OT-1 splenocytes were utilised in all transductions. Retronectin (Takara Bio Inc., Clontech in Europe, Cat# T100A/B) coated plates were prepared beforehand according to manufacturers' instructions.

Splenocytes were harvested 24 hours before transduction and  $10 \times 10^6$  splenocytes cultured in 5ml of complete RPMI media, supplemented with  $2 \mu\text{g/ml}$  ConA (ThermoFisher),  $1 \text{ng/ml}$  IL-7 (PeproTech, London, UK) and  $5 \text{ng/ml}$  IL-12 (PeproTech, London, UK) in six-well plates, for 18-24 hours. Retronectin solution was removed from plates and stored for repeat use. Retronectin coated plates were blocked with 2ml of sterile PBS/BSA (2%) per well for 30 minutes. Viral supernatants from transfection reactions were collected by centrifuging Phoenix-ECO cell cultures at 490g for 10 minutes to remove any cells. Splenocytes to be transduced were centrifuged at 400g for 10 minutes and the supernatant discarded. The splenocytes were then resuspended in the collected viral supernatant and an additional  $10 \text{ng/ml}$  of IL-2 (PeproTech, London, UK) was added. The PBS/BSA solution was removed from the Retronectin coated plates and replaced with splenocytes in viral supernatant. The plates were wrapped in parafilm and spininfected at 700g for 90 minutes at  $32^\circ\text{C}$  with the brake off. Post spin transduction, cells were incubated at  $37^\circ\text{C}$  for a further 24 hours, before the transduced cells were purified from the total population as follows.

### 2.16 Cell Sorting

Following transduction, cells were sorted using a FACS Aria to retrieve only GFP<sup>+</sup> transduced cells. Cells were washed to remove the cytokine-containing media, resuspended in filter sterilised PBS/BSA (1% BSA) and stained with anti-CD8 $\alpha$ -APC-Cy7 antibody in order to gate on only transduced CD8 T cells. In the case of cells going forward for *in vivo* experiments CD45.1<sup>+</sup> WT OT-1 T cells were utilised, in which case cells were also stained with eFluor450 conjugated anti-CD45.1 antibody. Fluorophores were selected to prevent issues with compensation. Following antibody staining, cells were washed and resuspended at a concentration of approximately  $12\text{-}14 \times 10^6/\text{ml}$ . Prior to sorting, this suspension was passed through a  $20 \mu\text{m}$  mesh to filter out clumped cells or debris that could impair the Aria. Once cells were sorted and purified, samples were cross-checked by flow cytometry to confirm purity levels.

### 2.17 Tumour Challenges

To determine whether adoptive cell therapy of transduced cells protect mice from tumour growth, groups of age and sex matched C57BL/6 mice were injected subcutaneously with  $0.5 \times 10^6$  EG7-OVA cells. EG7-OVA cells grown in culture for at least one week but less than 3 months were

washed the day before use in order to remove G418 and then re-seeded in complete medium. The day of challenge cells were washed three times in PBS, a single cell suspension obtained and cell counts and viability confirmed by visualising trypan blue exclusion and counting using a haemocytometer. Tumours were allowed to grow for 1 week in the mice before treatments began. Transduced cells were given at i.v. 7 days post tumour injection at a concentration of  $1 \times 10^6$  cells in 200  $\mu$ l. The threshold for culling mice was limited to an average tumour measurement of 15mmx15mm or average area of 225mm<sup>2</sup>, whichever was reached first. Tumours were measured every other day.

## 2.18 Drop-Seq

The protocol for Drop-Seq was developed by Evan Macosko and Melissa Goldman from Steve McCarroll's lab, out of Harvard Medical School and is freely available from the McCarroll Lab (<http://mccarrolllab.com/dropseq/>); this is regularly updated with the latest refinements to the methodology. The protocol was followed at all times unless otherwise stated. All primers and custom DNA segments were acquired from Integrated DNA Technologies (IDT, Belgium). All other reagents are listed in the digital protocol (linked above, direct download - <http://mccarrolllab.org/download/905/>). Initial testing of the PCR library indicated a requirement for increased cycle number to compensate for low transcriptional activity of CD8 T cells (data not shown). As such a total of 16 PCR cycles was utilised to improve yield, with the second round of PCR cycles in the digital protocol being increased to 12. I would like to acknowledge the assistance of Dr Matthew Rose-Zerilli and Dr Rachel Parker, who taught and supervised the Drop-Seq process.

## 2.19 Statistical and Computational Analysis

Unless otherwise stated, all statistical analysis was performed in GraphPad Prism. Two-tailed student's t-test was primarily used to calculate statistical significance. p-values stated in each figure.

For Drop-Seq analysis, R-studio and associate packages were employed. The scater package (<https://bioconductor.org/packages/release/bioc/html/scater.html>) was used to perform quality control on single cell data recovered, to identify features with the highest expression, to highlight

## Chapter 2

the most influential principle components and was also used to detect features that may distort the analysis, such as differential library sizes. Normalisation of data through deconvolution was undertaken using Scran (<https://bioconductor.org/packages/release/bioc/html/scrn.html>), which allows differential library size to be taken into account. Zinbwave (<https://bioconductor.org/packages/release/bioc/html/zinbwave.html>) was used to perform dimensional reduction, which reduces the number of variables being analysed and aids in removing redundant or unnecessary information. Hierarchical clustering was performed using the hclust and the Ward.D2 algorithm, which assigned cells into their initial clusters. Cutreedynamic was used to define the clusters by adjusting branches of the dendrograms produced by the hierarchical clustering. RandomForest (1000 trees) allowed reassignment of sub-optimally clustered cells through repeated comparison. This comparison of groups of randomly chosen cells over multiple iterations allows for optimisation of their clustering. Random forest proximity was used as a distance measure for subsequent t-distributed stochastic neighbour embedding (t-SNE) plots. Finally, elements of edgeR (<https://bioconductor.org/packages/release/bioc/html/edgeR.html>) of Seurat (<https://satijalab.org/seurat/install.html>) were used for generation of differential gene expression lists and production of t-SNE plots, violin plots and heatmaps. I would like to acknowledge Dr Steve Thirdborough who performed the conversion of the data from the next generation sequencer output into a t-SNE plot, utilising the packages described above.

## Chapter 3 Effect of Akt Signalling on Effector Functions of CD8 T Cells in vitro

### 3.1 Introduction

Given the importance of Akt and its associated signalling pathways during CD8 T cell differentiation in both memory and effector subtypes, multiple studies have been conducted to better characterise the effects of Akt in the differentiation process. This group has conducted experiments previously in this field using a mouse model first described by Bayasas *et al*<sup>244</sup>. This mouse contains a mutated knock-in version of the PDK1 enzyme, specifically a lysine conversion to glutamate at position 465, known as PDK<sup>K465E</sup>. This prevents the PDK1 PH domain binding phosphoinositides, resulting in decreased phosphorylation at Thr308, and hence decreased activation of Akt. Whilst Akt activity is substantially decreased in this model, the functions of other PDK1 targets are unimpaired<sup>244</sup>. Akt does still retain its basal activity; it merely cannot be induced through stimuli such as TCR activation. This causes a multitude of effects on mice bearing the knock-in mutation, including significantly reduced size and insulin resistance<sup>244</sup>.

Previous studies utilising either combined PI3K $\delta/\gamma$  or PDK1 knockouts show a severe block in T cell development before expression of CD4 and CD8<sup>245,246</sup>. As such, these knockout mice demonstrate a substantially diminished thymus gland, containing a population comprised of immature DN T cells, in addition to a near complete lack of peripheral T cells. These effects can be primarily linked to the lack of Akt signalling that would be present in these knockout models, due to the critical role of that signalling pathway in  $\beta$  selection during T cell development<sup>247</sup>. Waugh *et al*<sup>248</sup> examined the effect of the PDK<sup>K465E</sup> mutation, and hence significantly reduced Akt activity, on the development of T cells. The primary contrast between the PDK<sup>K465E</sup> mutant and a PDK1 knockout mouse, is that the relative frequencies of each T cell subset within the thymus of PDK<sup>K465E</sup> mutants are equivalent to their WT counterparts; demonstrating that the basal activity of Akt present in the PDK<sup>K465E</sup> mutant model is sufficient for the transition of immature DN T cells through to mature peripheral CD4 and CD8 T cells. Akt knockout mice display disrupted transitions at the DN3-DN4 stage, which in turn impairs the population of DP and SP T cells in the thymus<sup>248-250</sup>. As the PDK<sup>K465E</sup> mutation does not impact the development of CD8 T cells<sup>248</sup>, the PDK<sup>K465E</sup> mouse model offers an effective mechanism for analysing the impact of Akt signalling in mature peripheral CD8 T cells. Another advantage of the PDK<sup>K465E</sup> mutant compared to a conditional

## Chapter 3

knockout is the normal physiological expression of both PDK and Akt. For other proteins that interact with these kinases, such as mTORC2 with Akt, there is no shift in the quantity of their interactions. Therefore, mTORC2 is unlikely to have a relative increase in activity against its other targets. Whereas in a conditional knockout system, the absence of Akt may increase the availability of mTORC2 to interact and phosphorylate its other target proteins.

Further experimentation with the PDK<sup>K465E</sup> mutant revealed that T cells show no impairment in proliferation following *in vitro* culture with peptide<sup>248</sup>. Lastly, this study also presented that PDK<sup>K465E</sup> T cells displayed increased expression of CD62L and CCR7; two molecules that are involved with lymphocyte migration between lymphoid and non-lymphoid tissues. The expression of CD62L and CCR7 in T cells is dictated by the transcription factors KLF2 and FOXOs, which are regulated by Akt activity, hence the increased expression of these molecules is due to the reduced activity of Akt found in the PDK<sup>K465E</sup> model. Follow-up experiments with the PDK<sup>K465E</sup> model by Macintyre *et al*<sup>143</sup> have demonstrated that the upregulation of CD62L and CCR7 expression in PDK<sup>K465E</sup> CD8 T cells does induce retention of these cells within lymph nodes<sup>143</sup>. Using ELISA it was also demonstrated that there was an impairment of IFN $\gamma$  release from PDK<sup>K465E</sup> CD8 T cells, at least in a P14 transgenic mouse setting<sup>143</sup>.

This group has previously conducted experiments aimed at investigating the effects of this PDK<sup>K465E</sup> mutation on CD8 T cell activation and differentiation in an *in vivo* setting. As such, two experimental systems were used with this mouse model. The first involved a challenge of mice with a recombinant form of *Listeria monocytogenes* whilst the second was based on a vaccination model. For each setting, both WT and PDK<sup>K465E</sup> mutant mice were cross-bred onto an OT-1 background. OT-1 mice are genetically modified to contain a skewed T cell repertoire in which all CD8 T cells possess an identical TCR that responds to OVA, or OVA-derived peptides. In the infection model, WT or PDK<sup>K465E</sup> OT-1 CD8 T cells were adoptively transferred into WT hosts that were subsequently challenged with an OVA-expressing strain of *Listeria Monocytogenes*. Both the WT and PDK<sup>K465E</sup> mutant recipients displayed equal effectiveness in eliminating the pathogen, but during the contraction phase the CD8 T<sub>EM</sub> subtypes were absent in the PDK<sup>K465E</sup> mutant recipients. No excessive apoptosis was observed in the infection model, indicating that the lack of the T<sub>EM</sub> subtype was most likely due to a skewed differentiation process that favoured the T<sub>CM</sub> subtype.

The vaccination model similarly involved challenging WT mice previously adoptively transferred with WT or PDK mutant T cells, with an agonist anti-CD40 antibody, LPS and OVA. In this model, whilst again the initial immune responses in both the WT and PDK mutant recipients were comparable, there was no development of memory CD8 T cells in mice receiving PDK mutant cells. Whilst the protein Bim was increased in the PDK<sup>K465E</sup> CD8 T cells compared to WT CD8 T cells, a comprehensive explanation for this lack of memory in the vaccination model is yet to be established. It is, however, possible that the vaccination simply cannot provide sufficient stimulatory factors necessary to generate a memory response in the same way that a live pathogen can, such as *Listeria Monocytogenes*.

These data prompted the instigation of the experiments in this chapter. As has been shown in the Immunity paper by Macintyre *et al*<sup>143</sup>, the transcriptional profile of Akt inhibited CTLs generated *in vitro* display deficits in effector molecules such as IFN $\gamma$ , granzymes and perforin. However, *in vivo* studies from this group<sup>240</sup> have demonstrated that the PDK<sup>K465E</sup> T cells were as effective as WT cells in the elimination of tumour cells. In addition, intracellular IFN $\gamma$  production was unaffected in *in vivo* models, which is in contrast to published data from *in vitro* stimulated T cells<sup>143</sup>. It is possible that previously reported data using *in vitro* stimulated cells may have been confounded by the non-specific effects of a chemical inhibitor of Akt. As such, the aim of the experiments shown here was to utilise the PDK<sup>K465E</sup> mutant model to better understand the role of Akt signalling in controlling effector functions in CD8 T cells.



## 3.2 Results

### 3.2.1 Effect of Akt Signalling on CD8 T Cell Cytokine Expression

To begin to investigate the role of Akt in regulating the effector activity of CD8 T cells, the production of cytokine was compared between WT and PDK1<sup>K465E</sup> CD8 T cells. To increase cytokine production by CD8 T cells, WT and PDK1<sup>K465E</sup> OT-1 splenocytes were stimulated with SIINFEKL peptide for 2 days, followed by 10ng/ml IL-2 for 3 days. After culture the percentage of CD8<sup>+</sup> cells was above 98% in all experiments. Subsequently,  $1 \times 10^6$  CTLs were restimulated with a range of SIINFEKL concentrations for 4 hours, supernatants were then harvested and IFN $\gamma$  concentrations assessed by ELISA. *Figure 3-1* shows that PDK1<sup>K465E</sup> CD8 T cell supernatants contain approximately 50% of the concentration of IFN $\gamma$  contained in cultures from WT CD8 T cells.

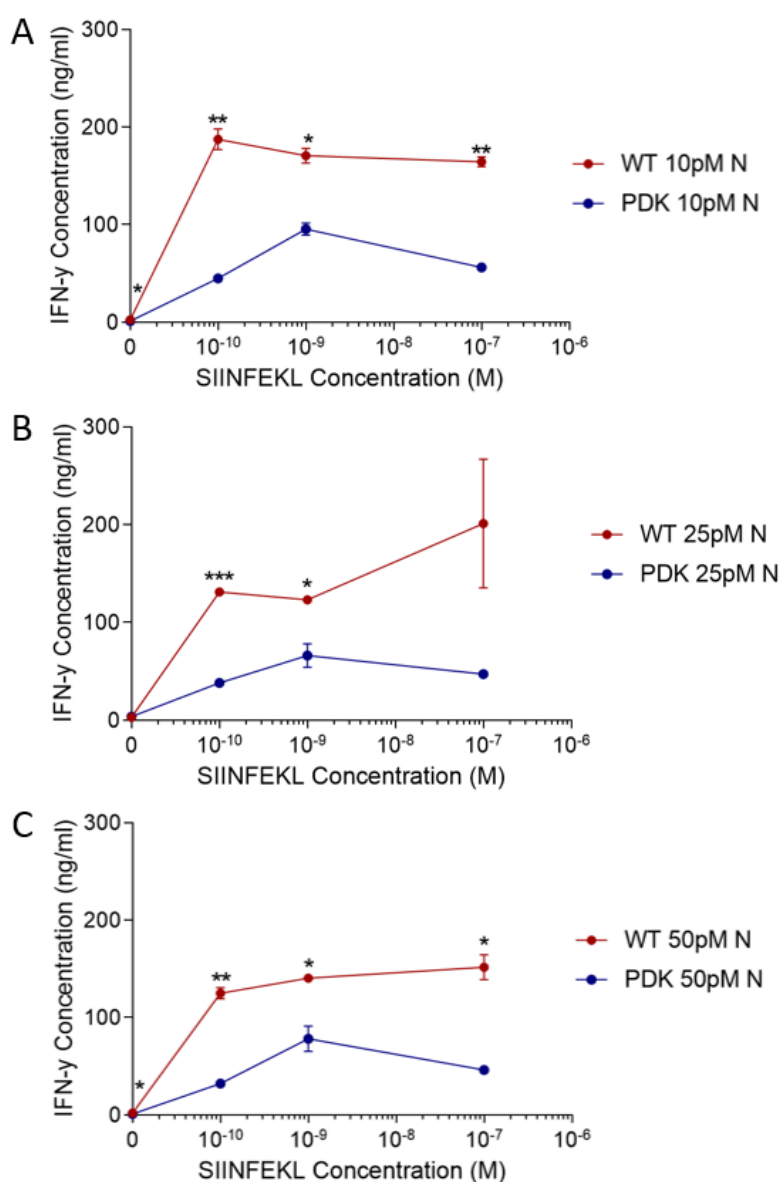


**Figure 3-1 – Effect of PDK<sup>K465E</sup> mutation on IFN $\gamma$  secretion by CD8<sup>+</sup> T cells.**

WT and PDK1 mutant splenocytes were stimulated with either 10pM, 25pM or 50pM SIINFEKL for 2 days (A, B and C respectively) followed by 3 days stimulation with IL-2 at 10ng/ml.  $1 \times 10^6$  cells were subsequently treated with a range of concentrations of SIINFEKL (restimulation concentration shown on x-axis) for 4 hours before harvesting the supernatants for IFN $\gamma$  analysis by ELISA. Mean and SEM of two duplicate wells from a single experiment shown. Student's two-tailed t-test applied to each restimulation concentration. p-value of \* $<0.05$ , \*\* $<0.005$ , \*\*\* $<0.0005$

## Chapter 3

This difference appears to be independent of the initial stimulatory concentration of SIINFEKL. It would seem that as long as the initial stimulating concentration is enough to cause activation of the CD8 T cells, increasing the concentration does not substantially increase the amount of IFN $\gamma$  in the supernatant.

To investigate the role of peptide affinity on the ability of WT and PDK1<sup>K465E</sup> CD8 T cells to secrete IFN $\gamma$ , the experiment was repeated, but cells were restimulated with either the parental SIINFEKL peptide or with SIIQFEKL. SIIQFEKL is a variant of the OVA peptide SIINFEKL, however it possesses an approximate 20-fold reduced affinity for the OT-1 TCR when compared to SIINFEKL, but a similar affinity for MHC class I molecules<sup>251</sup>. *Figure 3-2* shows that when cells are restimulated with SIINFEKL (*Figure 3-2A*) or SIIQFEKL (*Figure 3-2B*) peptide, WT cell supernatants contain more IFN $\gamma$  than their PDK<sup>K465E</sup> counterparts at each concentration tested.

On average, when restimulated with SIINFEKL peptide, the PDK<sup>K465E</sup> mutant cells produced approximately 50% as much IFN $\gamma$  as their WT counterparts. Interestingly, this difference was more pronounced when SIIQFEKL was used to restimulate the cells instead of SIINFEKL, with the PDK1<sup>K465E</sup> cells only secreting 38% as much IFN $\gamma$  on average compared to the WT cells. Also, when restimulating with SIIQFEKL instead of SIINFEKL, the overall amount of IFN $\gamma$  secreted by each cell type decreased by approximately 30% in the WT and 50% in the PDK<sup>K465E</sup>.

*Figure 3-2* showed differences in the amounts of IFN $\gamma$  secreted by T cells when cells were restimulated with SIIQFEKL instead of SIINFEKL. As peptide-TCR affinity is known to influence CD8 T cell activation, the next line of investigation was to study whether the amount of IFN $\gamma$  in the supernatants of WT and PDK<sup>K465E</sup> mutant cells was altered when SIIQFEKL was used as the initial stimulation.

*Figure 3-3* shows that when CD8 T cells were primed with SIIQFEKL, the amount of IFN $\gamma$  present in the supernatant upon restimulation was dramatically reduced when compared to SIINFEKL primed cells in *Figure 3-2*. The y-axes of the graphs in *Figures 3-2* and *3-3* are locked to the same

scale to demonstrate the differences in IFN $\gamma$  secretion. On a background of SIIQFEKL priming, the amount of IFN $\gamma$  present was independent of whether SIIQFEKL or SIINFEKL peptide was used to restimulate the cells. This could be an indication that SIIQFEKL is not a strong enough stimulus to fully differentiate naïve OT-1 CD8 T cells, or an indication that the difference is only observable when the cells are primed with a high affinity antigen.

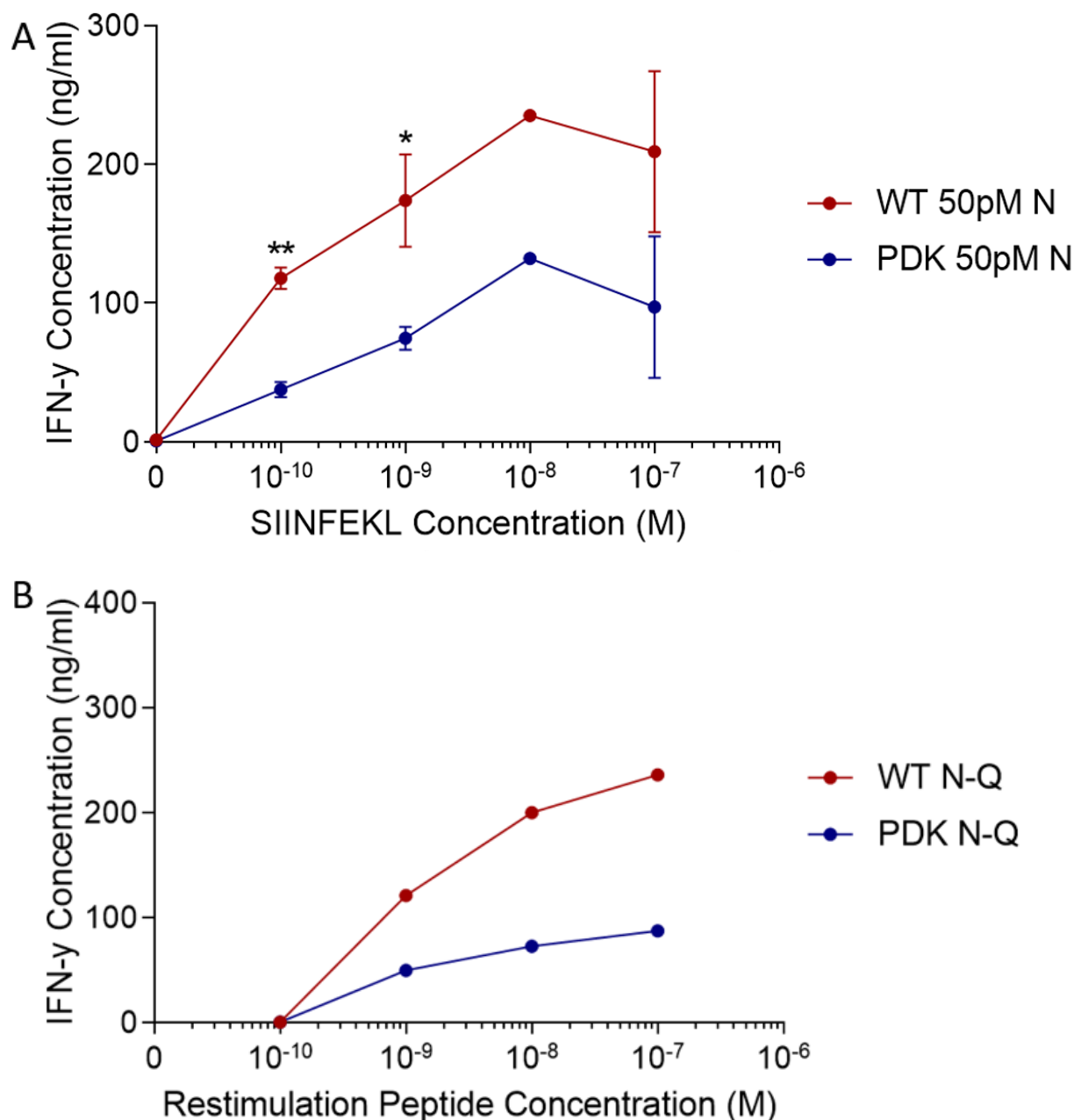


**Figure 3-2– Effect of restimulating with peptides of different affinities on WT and PDK<sup>K465E</sup> CD8<sup>+</sup> T cells.**

WT and PDK<sup>K465E</sup> OT-1 splenocytes were stimulated with 50pM SIINFEKL for 2 days, followed by 3 days stimulation with IL-2 10ng/ml to generate CTLs.  $1 \times 10^6$  CTLs were subsequently restimulated with a range of either SIINFEKL (A) or SIIQFEKL (B) peptide for 4 hours. Supernatants were then harvested and IFN $\gamma$  measured by ELISA. Data points combined from independent experiments in A, mean and SEM displayed where possible,  $n=3$ . Otherwise data is from a single experiment. \* $<0.05$ , \*\* $<0.005$ , by Students two-tailed t-test.

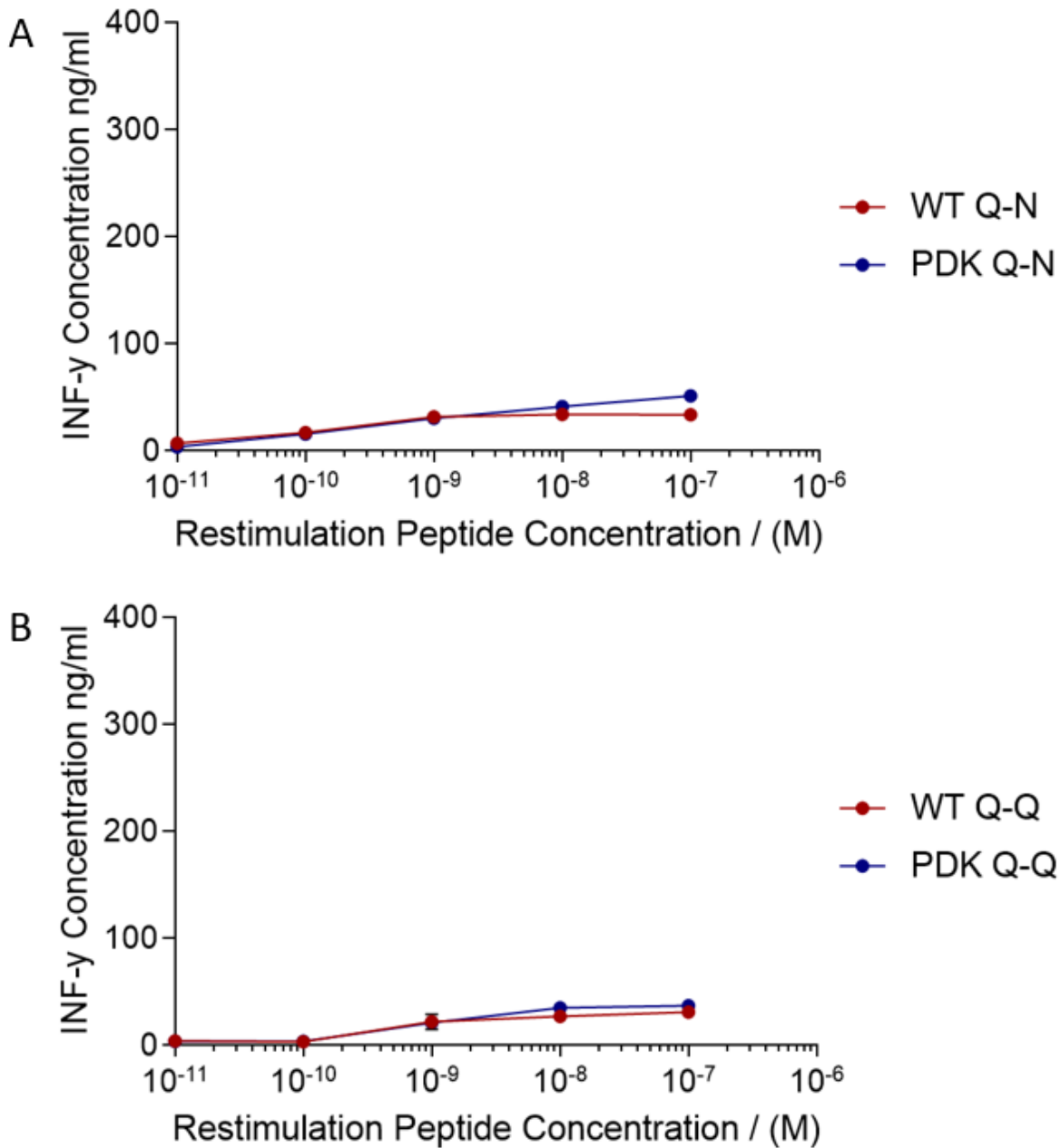


**Figure 3-3 – Effect of initial SIQFEKL stimulation on IFN $\gamma$  secretion by WT and PDK<sup>K465E</sup> CD8<sup>+</sup> T cells.** WT and PDK<sup>K465E</sup> OT-1 splenocytes were initially stimulated with 5nM SIQFEKL for 2 days followed by IL-2 at 10ng/ml for 3 days, before subsequent restimulation of 1x10<sup>6</sup> cells with **A** - SIINFEKL (Q-N) or **B** - SIQFEKL (Q-Q) for 4 hours. Supernatants were retained and ELISA was performed. Data displayed three replicates across two experiments, mean and SEM displayed.

As initial peptide stimulation by the high affinity peptide SIINFEKL highlighted less IFN $\gamma$  in the supernatants of PDK<sup>K465E</sup> compared with WT T cell cultures, it was interesting to determine whether the PDK<sup>K465E</sup> mutation affects the amount of IFN $\gamma$  produced, or only its secretion. To that end, intracellular production of cytokines was investigated by analysing the levels of IFN $\gamma$  and IL-2 using flow cytometry. Splenocytes were taken from WT and PDK<sup>K465E</sup> OT-1 mice and stimulated for 2 days with either 10pM, 25pM or 50pM SIINFEKL peptide, followed by 10ng/ml IL-2 for 3 days to generate CTLs before being washed to remove excess IL-2. Equal numbers of CTLs were then restimulated in fresh media containing 100pM, 1nM or 100nM concentrations of SIINFEKL.

Following 4 hours of restimulation, the CTLs were then fixed and permeabilized, before intracellular staining for IFN $\gamma$  and IL-2. The gating strategy for subsequent experiments is shown in *Figure 3-4*.

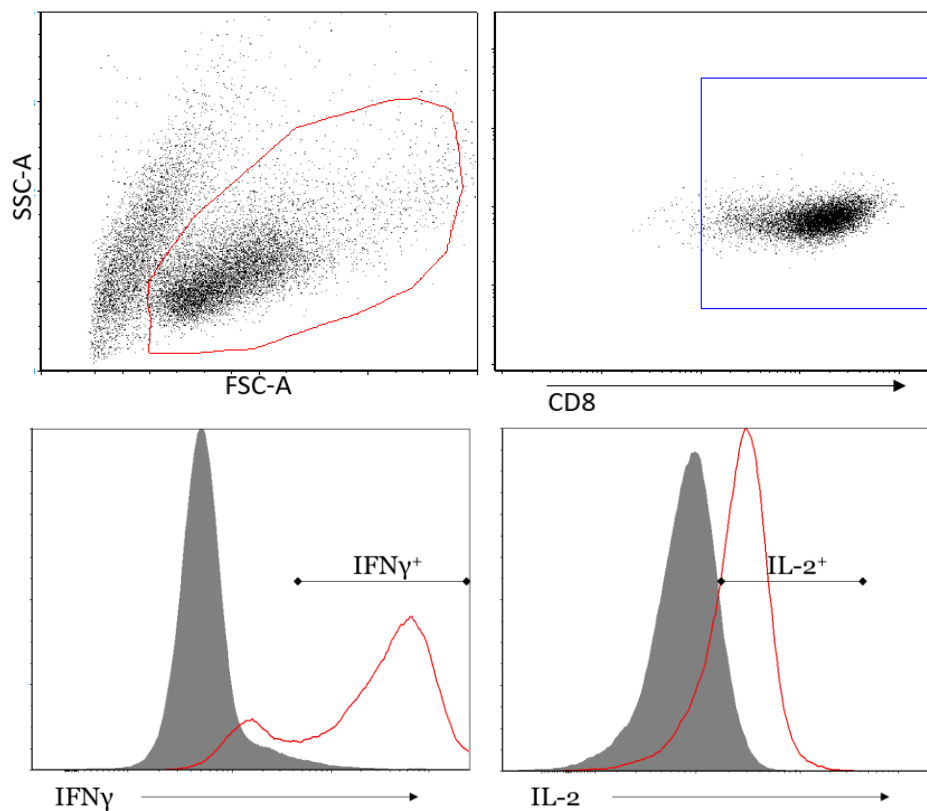


**Figure 3-4 – Gating strategy for intracellular cytokine staining**

Live cells gated on forward scatter, side scatter plots (top left panel). Subsequently live cells were gated on expression of CD8 (top right panel). Lastly, these CD8 positive cells were gated on their expressions of IFN $\gamma$  and IL-2 (bottom panels, left and right). Grey – Isotype control, Red – Representative example of cytokine staining.

The data collected from this experiment are shown in *Figures 3-5 and 3-6*. *Figure 3-5A* shows that the percentage of IFN $\gamma^{\text{high}}$  cells was similar between WT and PDK<sup>K465E</sup> cells. *Figure 3-5B* displays the mean fluorescence intensity of IFN $\gamma$  gated on IFN $\gamma^{\text{high}}$  cells taken from the WT and PDK<sup>K465E</sup> mice. At the highest peptide concentrations used for restimulation, 1nM and 100nM SIINFEKL, there was a statistically significant decrease in the amount of IFN $\gamma$  found in PDK<sup>K465E</sup> CD8 T cells compared to WT CD8 T cells. These data indicate that the decreased IFN $\gamma$  in PDK mutant cultures is likely due, not to a function of a smaller number of cells producing IFN $\gamma$ , but rather a function of each individual cell producing less IFN $\gamma$ .

Unfortunately, without an accurate or reliable method to convert MFI into an actual concentration of IFN $\gamma$ , it is difficult to gauge whether the decreased accumulation of IFN $\gamma$  in

stimulated PDK mutant cells is responsible for the reduced concentrations in culture supernatants.

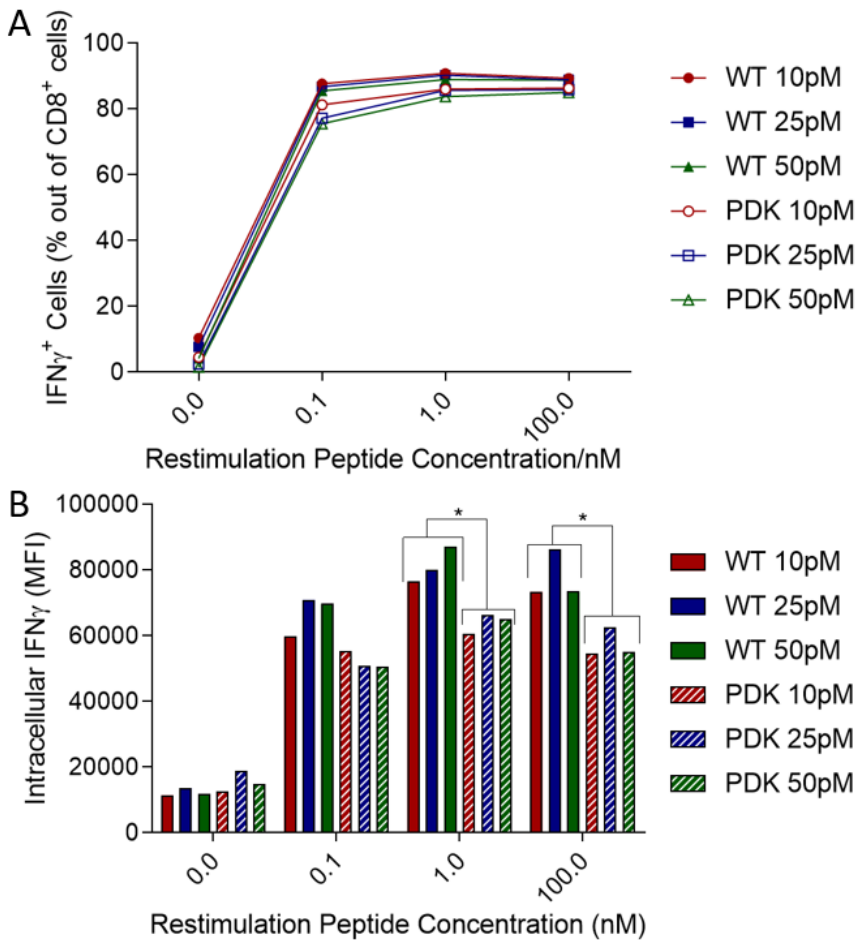


**Figure 3-5 – Intracellular production of IFN $\gamma$  in WT and PDK<sup>K465E</sup> CD8<sup>+</sup> T cells.**

The splenocytes of a single WT and PDK mutant OT-1 mouse were stimulated with 10pM, 25pM or 50pM SIINFEKL peptide for 2 days followed by 3 days in IL-2 10ng/ml to generate CTLs. 1x10<sup>6</sup> CTLs were then restimulated with a range of SIINFEKL peptide concentrations. The intracellular levels of IFN $\gamma$  expression were analysed by flow cytometry. **A** – Shows the percentage of cells considered IFN $\gamma^{\text{high}}$  across each condition, based on gating in Figure 3-5. **B** - Displays the mean fluorescence intensity (MFI) of IFN $\gamma$  following 4 hours of restimulation with SIINFEKL, gated on cells designated IFN $\gamma^{\text{high}}$ . Student's two-tailed t-test performed on collective WT and PDK at each restimulation concentration, total of 3 samples. p-value \* $<0.05$ . Data from single experiment displayed

In this experiment, the levels of IL-2 contained within WT and PDK<sup>K465E</sup> cells were also investigated. Interestingly, the frequency of cells that are IL-2<sup>high</sup> were diminished by approximately 50% in PDK<sup>K465E</sup> compared with WT cells, as shown in *Figure 3-6A*. In *Figure 3-6B* it is evident that in all restimulatory conditions the amount of IL-2 in IL-2 producing PDK mutant cells was significantly decreased compared to WT cells.

In summary, whilst there was no change in the percentage of WT and PDK<sup>K465E</sup> mutant T cells producing IFN $\gamma$ , each cell is secreting less IFN $\gamma$ . In the case of IL-2, the frequency of cells producing IL-2 was reduced by approximately 50% and the amount of IL-2 secreted per cell was also diminished. However, without an accurate way to determine intracellular protein concentration,

it would be erroneous to assume that the decrease in IFN $\gamma$  production is the cause of the decreased concentration of this cytokine seen in the ELISA of *Figures 3-1* and *3-2*.

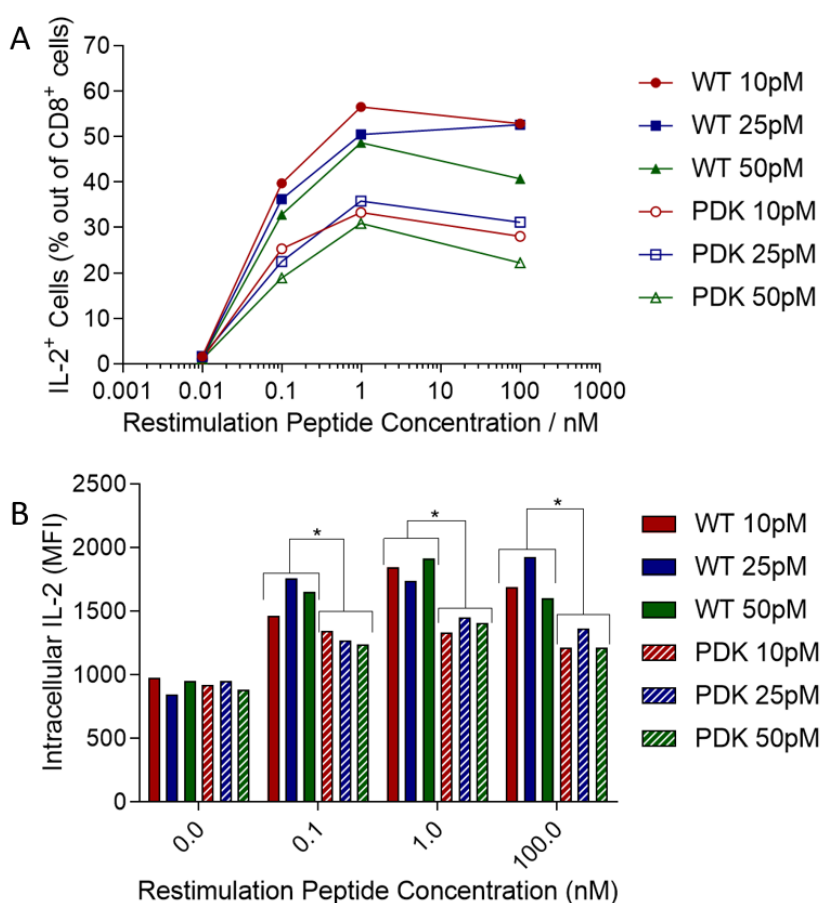


**Figure 3-6 – Intracellular production of IL-2 in WT and PDK<sup>K465E</sup> CD8<sup>+</sup> T cells.**

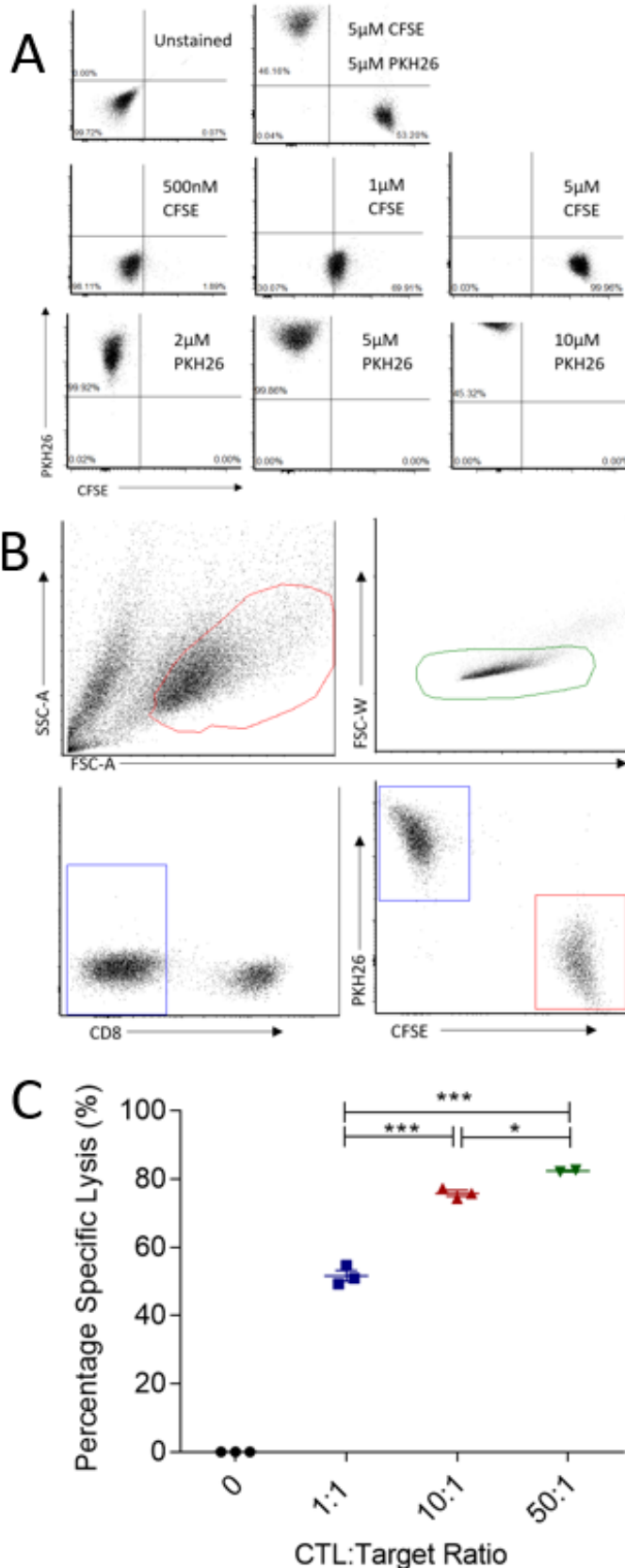
The splenocytes of a single WT and PDK<sup>K465E</sup> OT-1 mouse were stimulated with 10pM, 25pM or 50pM SIINFEKL peptide for 2 days followed by 3 days in IL-2 10ng/ml to generate CTLs.  $1 \times 10^6$  CTLs were restimulated with a range of SIINFEKL peptide concentrations. IL-2 expression was then analysed by intracellular flow cytometry. **A** – Shows the percentage of cells considered IL-2<sup>high</sup> across each condition, based on gating in Figure 3-5. **B** – Displays the MFI of IL-2, gated on cells designated IL-2<sup>high</sup>. Student's two-tailed t-test performed on collective WT and PDK at each restimulation concentration, a total of 3 samples. p-value  $* < 0.05$ . Data from single experiment.

### 3.2.2 Effects of Akt Signalling on CD8 T Cell Cytotoxicity

To more directly investigate the influence of the PDK<sup>K465E</sup> knock-in mutation on the development of cytotoxic function in CD8 T cells we modified a published protocol by Reeves *et al*<sup>252</sup>, which is not reliant on the traditional radioactive chromium release method. Instead, this protocol is reliant on separating target cells into two groups, in which one population is pulsed with a relevant target peptide and stained with the dye CFSE, and the second population is left unpulsed with peptide and stained with another dye, PKH26. *Figure 3-7A* displays the optimisation steps of the CFSE and PKH26 staining on the EL4 cell line that served as target cells for cytotoxicity assays. A range of CFSE and PKH26 concentrations were used in order to determine the ideal concentration for detection by flow cytometry. This pilot experiment also examined which concentrations allowed adequate compensation, as the wavelengths at which CFSE and PKH26 emit overlap. The result of this optimisation demonstrated that 5 $\mu$ M of both CFSE and PKH26

gave significant staining above background by flow cytometry. There was also no excessive compensation between these two groups when mixed at a 1:1 ratio.

**Figure 3-7 – Optimisation of PKH26 and CFSE staining protocol and cytotoxicity assay proof of concept.**



**A** - Unpulsed EL4 target cells were stained with either 500nM, 1µM or 5µM of CFSE for 5 minutes (middle row). A separate population of unpulsed EL4 target cells were also stained with PKH26 at concentrations of 2µM, 5µM or 10µM for 4 minutes (bottom row). These EL4 cells were then analysed by flow cytometry to assess the homogeneity and magnitude of cell membrane staining. 1:1 cultures of each CFSE and PKH26 concentration were also analysed (top row, right hand panel) to determine the ideal mixture to be used in future cytotoxicity assays. **B+C** - CTLs generated by incubating OT-1 splenocytes with 10pM of SIINFEKL peptide for 2 days followed by 3 days stimulation with 10ng/ml IL-2. 10x10<sup>6</sup> EL4 cells were stained with 5µM CFSE for 5 minutes or 5µM PKH26 for 4 minutes, following subsequent wash CFSE stained cells were then pulsed with 1µM SIINFEKL peptide. Homogeneity of the CFSE and PKH26 stains were determined by flow cytometry, the 1:1 ratio of CFSE:PKH26 cells was also confirmed at this time (B; lower right panel). Subsequently 2x10<sup>5</sup> cells of the 1:1 ratio cell mixture were incubated at 37°C for 6 hours with CTLs at a ratio of 50:1, 10:1 and 1:1 as well as a target mixture alone as a negative control. Cultures were subsequently analysed by flow cytometry. **B** – Dot plots displaying gating strategy for this cytotoxicity assay. Cells were initially gated on live cells (B, top left panel), followed by singlets (B, top right panel), then gated on the CD8 negative population which represents the remaining live EL4 target cells (B, bottom left panel). Subsequently EL4 cells were gated based on CFSE and PKH26 (B, bottom right panel). **C** – Percentage specific lysis of EL4 target cells as determined by the equation described in the main text below. All samples were in triplicate from a single biological sample and individual values are represented by the symbols, groups mean and SEM displayed, all p values < 0.015 with Students two-tailed t-test.

A preliminary cytotoxicity assay was then conducted, as shown in *Figure 3-7B+C*, in order to determine whether this protocol would provide an accurate assessment of the cytotoxic capabilities of CD8 T cells. OT-1 splenocytes were stimulated with 10pM SIINFEKL for two days, before being cultured in 10ng/ml IL-2 for a further 3 days to generate CTLs. These CTLs were then mixed at a range of ratios relative to the target cell mixture, which itself was comprised of a 1:1 ratio of 1µM SIINFEKL-peptide pulsed (CFSE) to non-peptide pulsed (PKH26) EL4 cells. To assess the level of cytotoxicity, live singlet EL4 cells were identified based on their FSC/SSC profile, FSC-W/FSC-A (to identify singlets) and the absence of CD8; the ratio of CFSE to PKH26 in the experimental samples versus the control samples was then compared. *Figure 3-7B* displays the gating strategy employed to examine the EL4 target cells; *Figure 3-7C* shows the extent of peptide-specific EL4 cell lysis across the different CTL:target ratios tested. The equation for calculating the specific cell lysis was:

$$\text{Target Cell Specific Lysis} = \left( \left( 1 - \left( \frac{\text{Experimental CFSE cells}}{\text{Experimental PKH26 cells}} \right) / \left( \frac{\text{Control CFSE cells}}{\text{Control PKH26 cells}} \right) \right) \right) \times 100$$

In the above equation, 'experimental CFSE cells' and 'experimental PKH26 cells' refer to the number of cells within the CFSE<sup>+</sup> and PKH26<sup>+</sup> gates of the EL4 cells in the CTL and target EL4 co-cultures samples, whereas, 'control CFSE cells' and 'control PKH26 cells' are the number of cells within the CFSE<sup>+</sup> and PKH26<sup>+</sup> gates of the EL4 cells in the EL4 alone cultures. This allowed for correction of any baseline differential cell death occurring in the CFSE- and PKH26-labelled EL4 cells during the 6 hour incubation period. From *Figure 3-7C* a ratio of 10:1 CTLs to EL4 target cells induced approximately 80% killing of peptide pulsed CFSE-labelled EL4 target cells.

At the 1:1 ratio of CTLs to EL4s, 50% of target cells were observed undergoing apoptosis. This was increased significantly at the 10:1 ratio, to approximately 75% target cell lysis. Whilst increasing the ratio of effector to target cells in the 50:1 group did increase target cell lysis significantly, it was not a substantial increase over the 10:1 group. This assay also displayed reliability between technical replicates, with less than 5% difference between individual samples.

Stimulation of OT-1 cells with either high or low affinity peptide induced similar expression of activation markers such as CD44 and granzyme B<sup>251</sup>. However, stimulation with low affinity peptide led to reduced cellular proliferation and decreased expression of the IL-2 receptor, CD25<sup>251</sup>. To address the question of how affinity may impact cytotoxicity, the cytotoxicity of CTLs

targeting cell targets pulsed with SIIQFEKL or SIINFEKL peptides was compared using the new assay established above.

Thus, CFSE stained EL4 cells were pulsed with a range of concentrations of either SIINFEKL or SIIQFEKL peptide, before then combining them with PKH26 stained control EL4 cells at a 1:1 ratio. This EL4 cell mixture was then combined with CTLs at a ratio of 10:1 (CTL:EL4). The results of this assay are displayed in *Figure 3-8*. At a peptide concentration of 1 $\mu$ M the levels of cytotoxicity observed towards SIINFEKL or SIIQFEKL pulsed target cells were significantly but not substantially different. As the concentration of SIIQFEKL decreased to 100nM, 10nM and 1nM there was a significant and noticeable reduction in the extent of EL4 cell lysis. Conversely, 100nM and 10nM SIINFEKL-pulsed EL4 cells were killed to a similar extent as the 1 $\mu$ M SIINFEKL pulsed EL4 target cells.

As mentioned in the introduction to this chapter, the effect of Akt signalling on cytotoxicity has not been extensively studied *in vitro*, and its effects have mostly been inferred from granzyme B expression or tumour regression studies. To investigate the effect of Akt on CD8 T cell cytotoxicity and markers of effector function, the PDK<sup>K465E</sup> mutant model was utilised, as well as small molecule Akt Inhibitor VIII from Calbiochem (also known as Akt-1/2, hereafter referred to as Akti). This is a cell-permeable and reversible inhibitor that significantly inhibits the two primary isoforms

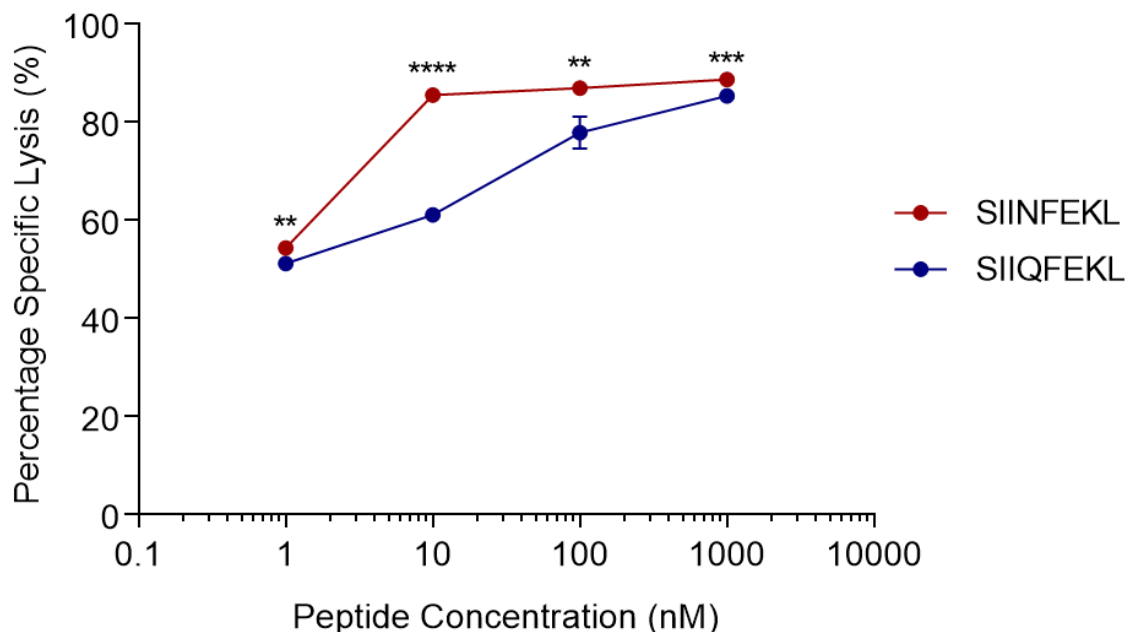


**Figure 3-8 – Effects of Peptide Affinity on Cytotoxicity**

Cytotoxicity assay performed as previously described using the dual staining method of PKH26 and CFSE. In this assay, a serial dilution of both SIINFEKL and SIIQFEKL peptide was used to pulse the CFSE stained target cells. All samples consist of 10:1 CTL:EL4 target cells. n=3 samples in triplicate from a single biological sample, mean values and SEM are displayed. Student's two-tailed t-test performed for each peptide concentration. p-value \*\*\*\*<0.0001, \*\*\*<0.0005, \*\*<0.005.

of Akt at nanomolar concentrations<sup>253</sup>. Whereas the PDK<sup>K465E</sup> mutation inhibits physiological Akt activation, there remains low level activity<sup>244</sup>. To assess the role of Akt in T cell cytotoxicity, WT OT-1 splenocytes were cultured with SIINFEKL peptide at 10pM in the presence or absence of 1µM Akti for 2 days, followed by 3 days stimulation with 10ng/ml IL-2 +/- 1µM Akti. The concentration for the Akti was based on previous experiments within our lab as well as in reported literature<sup>143</sup>. CTLs were subsequently analysed by flow cytometry one day prior to their use in cytotoxicity assays, to examine the expression of CD62L. CD62L, also known as L-selectin, is an adhesion molecule whose expression is associated with naïve and memory CD8 T cells. The expression of CD62L is kept at high levels by the FOXO transcription factors, but upon T cell stimulation or IL-2 treatment, Akt inhibits FOXOs causing decreased expression of CD62L. As such, in the Akt inhibited group CD62L expression should remain high throughout exposure to IL-2, making it an ideal marker for assessing the effectiveness of the inhibitor<sup>156</sup>. During the cytotoxicity assay however, no Akti was added to the media, and hence any difference observed will be due to the altered effects that reduced Akt signalling had on the CD8 T cells during their activation. It should be noted that during the culture, the Akti had no effect on either the proliferation or survival of the CD8 T cells (data not shown).

*Figure 3-9A* demonstrates that, as expected, CD62L did as predicted and compared to isotype controls, the Akti maintained a higher expression of CD62L on CD8 T cells. At the same time as assessing CD62L, granzyme B expression was examined. *Figure 3-9B* reveals that the expression of granzyme B was reduced by approximately 10-fold in the presence of the Akti.

To assess the effects of this Akti on the cytotoxic capabilities of CTLs as before, both SIINFEKL and SIIQFEKL peptide were used to pulse the target cells. However, this time, the concentration of peptide was restricted to 100nM as this concentration still showed a high level of killing in the previous assay (*Figure 3-8*). As before, a range of CTL to target cell ratios were included within this experiment. *Figure 3-9C* shows that in the Akti untreated groups there was no substantial difference in the ability of SIINFEKL and SIIQFEKL to induce cytotoxicity, which correlates with the previous results at this peptide concentration and E:T ratio (*Figure 3-8*).

However, treating CD8 T cells with the Akti induced a highly significant and extensive reduction in the extent of target cell lysis observed in both peptides. The reduction in cytotoxic activity from approximately 95% to below 20% demonstrates the critical role Akt plays in CD8 T cell signalling

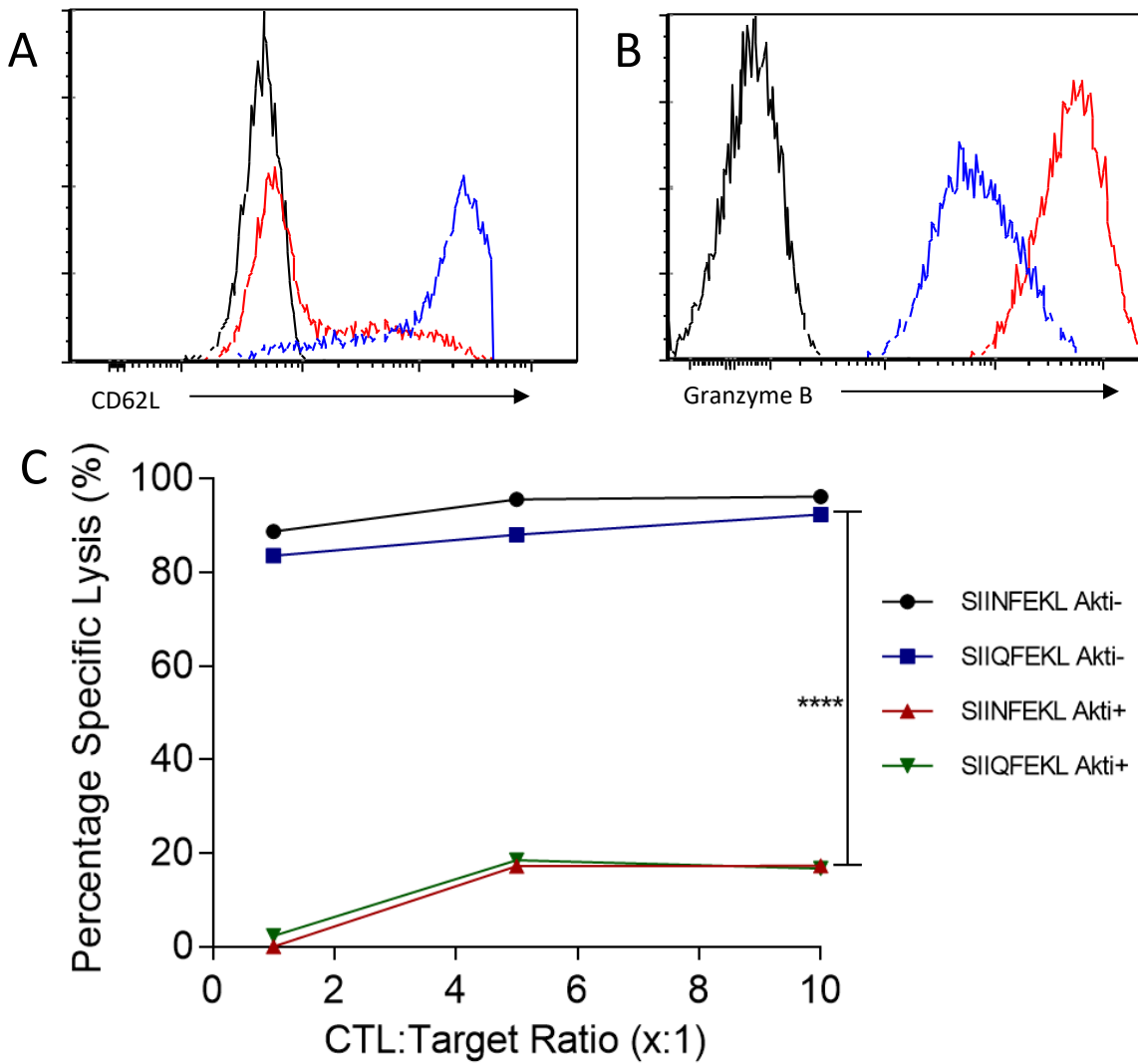


**Figure 3-9 – Effects of Akt Inhibition on Cytotoxicity**

OT-1 splenocytes cultured as previously described in the absence or presence of 1µM of the Akt inhibitor (Akt inhibitor VIII from Calbiochem). Cytotoxicity assay performed as previously described using the dual staining method of PKH26 and CFSE, with 100nM SIINFEKL pulsed target cells. n=3 samples in triplicate, mean values and SEM are displayed, p=0.0003. **A** - CD62L expression on CD8 T cells was measured by flow cytometry on day 4 post activation. **B** - granzyme B was assessed in CTL samples following cytotoxicity assay. Black line – Isotype Control, red line – Akti untreated group and blue line – Akti treated group. **C** – Result of cytotoxicity assay described above. Student’s two-tailed t-test performed at each CTL:Target ratio. p-value \*\*\*\*<0.0001, n=3, triplicates from a single biological sample.

and the acquisition of effector functions. The significantly decreased expression of granzyme B correlates with the reduced cytotoxic capacity of Akti treated CTLs.

Given these data, next compared were PDK<sup>K465E</sup> and WT CD8 T cells in these cytotoxicity assays. As stated previously, the PDK<sup>K465E</sup> has a non-functional pleckstrin homology (PH) domain. This prevents PDK from co-localizing with Akt and other downstream targets at the plasma membrane, and hence prevents the activation induced activity of Akt<sup>244</sup>. PDK<sup>K465E</sup> T cells still possess basal Akt activity and it was therefore hypothesised that the cytotoxic activity of these PDK<sup>K465E</sup> CD8 T cells would be somewhere between that of WT cells and Akti-treated cells.

However, work done by peers within the same lab, has shown that adoptively transferred PDK<sup>K465E</sup> CD8 T cells are capable of controlling and eliminating tumours<sup>240</sup>. This result raises three further questions of the PDK<sup>K465E</sup> CD8 T cells. Do they retain full effector function *in vivo* despite a reduced cytotoxic capacity? Do the large number of CTLs utilised in these experiments obscure the effects of Akt inhibition on CTL function? Is basal Akt activity all that is required for maximal CD8 T cell effector functions *in vivo*?

To begin to address these points, OT-1 splenocytes from both WT and PDK<sup>K465E</sup> mice were differentiated into CTLs in the presence or absence of 1 $\mu$ M Akti and their cytotoxicity tested. The results of this assay are shown in *Figure 3-10A*. As in the previous experiment (*Figure 3-9*), WT CD8 T cells expanded in the absence of the inhibitor were capable of eliminating over 90% of the SIINFEKL-pulsed target cells, but as before, this was reduced to less than 20% when cells were cultured with the Akti. At the highest effector to target ratio, PDK<sup>K465E</sup> CTLs eliminated approximately 60% of targets; a reduction of 30% compared to WT CD8 T cells at the same E:T ratio. As with the prior assays, decreasing the effector to target ratio caused modest reductions in cytotoxic capability, following a similar trend to the WT cells. Interestingly, treatment of the PDK<sup>K465E</sup> CTLs with the Akti entirely abrogated the cytotoxic effect of the cells. In this assay, the expression of granzyme B was also studied. *Figure 3-10B* displays a representative overlay of granzyme B expression from multiple experimental samples, whereas *Figure 3-10C* shows granzyme B expression in treated CTLs across multiple experiments.

There was a significant reduction in the expression of granzyme B in WT CTLs treated with the Akti compared to their untreated counterparts. When treated with the Akti, PDK<sup>K465E</sup> CTLs showed a similar substantial decrease in the expression of granzyme B. When comparing untreated WT and PDK<sup>K465E</sup> CTLs, PDK<sup>K465E</sup> CTLs showed substantially reduced expression of granzyme B. Similarly, Akti-treated PDK<sup>K465E</sup> CTLs expressed less granzyme B than Akti-treated WT CTLs. However, Akti-treated PDK<sup>K465E</sup> cells expressed less granzyme B than WT cells, which may indicate that the inhibitor has a more pronounced effect on the PDK<sup>K465E</sup> cells due to lower basal Akt activity. *Figure 3-10C* also shows an interesting observation, that the expression of granzyme B parallels the results of the cytotoxicity assay in *Figure 3-10A*. This would indicate that granzyme B expression and cytotoxic capacity may be directly related to the level of Akt activity.

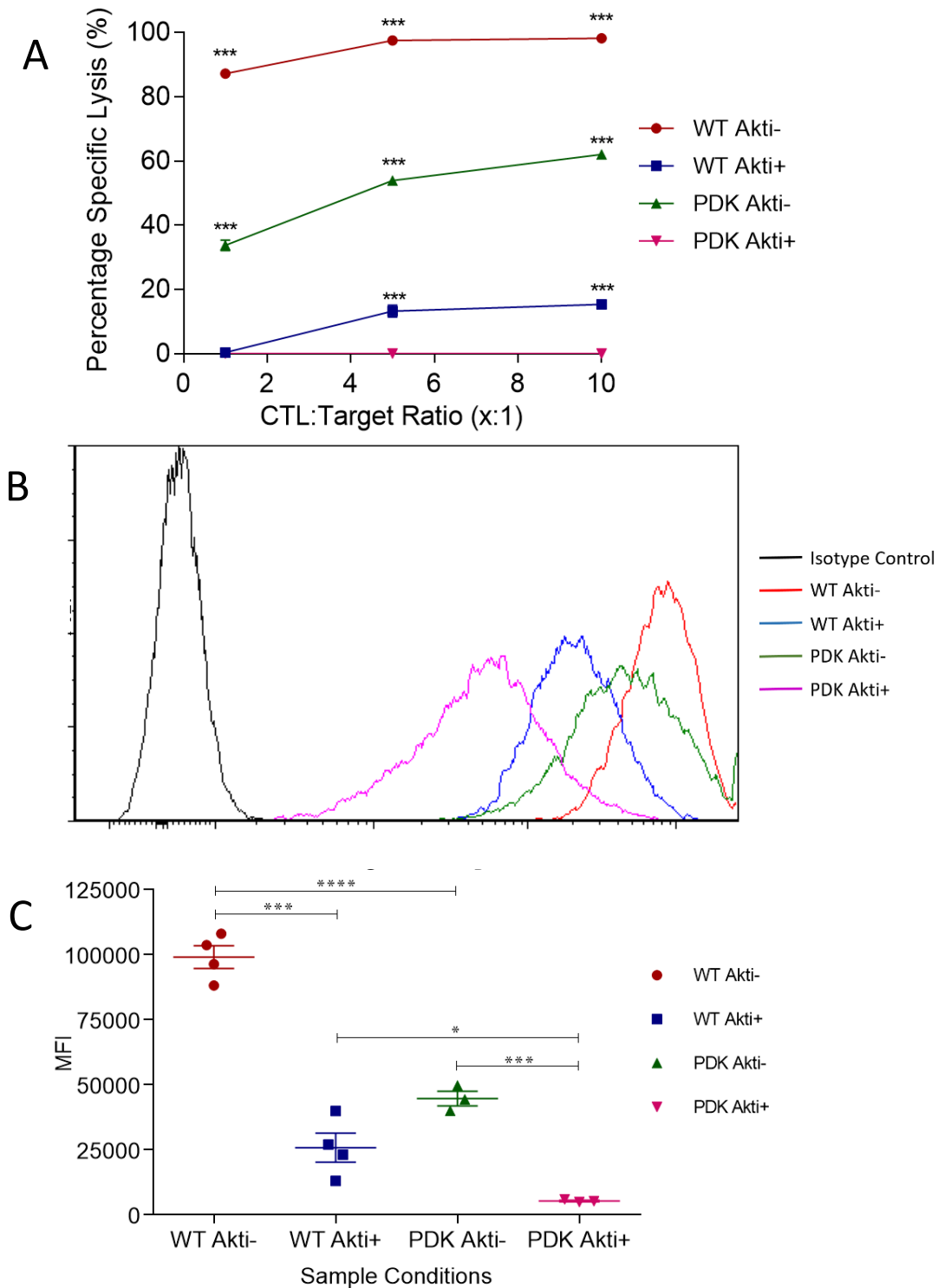


**Figure 3-10 – Effect of the PDK Mutation on CD8 T cell Cytotoxicity.**

**A** – WT and PDK<sup>K465E</sup> OT-1 splenocytes were activated with 20pM SIINFEKL for 2 days followed by 10ng/ml IL-2 for 3 days in the presence and absence of 1μM Akti, to generate CTLs. These CTLs were then subjected to the aforementioned cytotoxicity assay protocol, n=3 triplicates from a single biological sample. Mean and SEM displayed. **B** – Representative granzyme B expression plot from WT and PDK<sup>K465E</sup> CTLs both with and without exposure to the Akti. These plots are representative of multiple experimental samples under the same stimulatory conditions and isotypes were equivalent across all samples. **C** - MFI of granzyme B expression across independent experiments, five with the WT and three with the PDK, all using the same stimulatory conditions, isotype controls equivalent across samples. p-value \*\*\*\* = <0.0001, \*\*\* = <0.002, \* = 0.05.

### 3.2.3 Potential Role of Akt in the Regulation of Secretion in CD8 T Cells

Akt could potentially influence the cytotoxicity and effector functions of CD8 T cells through regulation of secretory pathways. To this end, previous experiments performed in this lab compared the transcriptomes of adoptively transferred OT-1 WT and PDK1<sup>K465E</sup> CD8 T cells on day 6 after challenge with OVA and anti-CD40 antibody. The results from this microarray experiment (data not shown) highlighted over 100 genes with altered levels of expression between the two groups. The gene *Baiap3* showed a greater than 20-fold reduction in mRNA expression in the PDK1<sup>K465E</sup> cells compared with WT cells. A recently discovered paralogue to Munc13-4, *Baiap3* is the fifth member of this Munc13 family of proteins. The Munc13 proteins have been shown to regulate vesicle-priming in neuronal and endocrine cells<sup>254</sup>. Munc13-4 has also been shown to be required for polarised exocytosis of lytic granules in CTLs and NK cells<sup>255</sup>. *Baiap3* is a relatively understudied protein, however, it possesses homologous sequences and structures to Munc13-4 and synaptotagmin; two proteins involved in vesicle priming and secretion<sup>256</sup>. As such, it seemed appropriate to investigate whether the pattern of *Baiap3* expression could explain some of the differences observed between WT and PDK<sup>K465E</sup> CD8 T cells in cytotoxicity and cytokine secretion.

Initially, the expression of *Baiap3* was examined by qPCR in the samples used for the microarray (WT and PDK vaccination samples in *Figure 3-11*) to confirm that *Baiap3* was in fact decreased in the PDK1<sup>K465E</sup> T cells. The data in *Figure 3-11* showed a significant 5.345  $C_t$  difference between the *Baiap3* mRNA in the PDK<sup>K465E</sup> samples compared to the WT. Following calculation of the  $\Delta\Delta C_t$  this translated to a near 60-fold decrease in the PDK<sup>K465E</sup> sample, thereby confirming the microarray data. The expression of *Baiap3* was also examined in naïve CD8 T cells extracted from independent WT and PDK<sup>K465E</sup> mice. The aim was to determine whether the difference was due to differential activation or reflected a pre-existing difference between naïve WT and PDK1<sup>K465E</sup> cells. Naïve CD8 T cells also showed a 15-fold difference on average between WT and PDK<sup>K465E</sup>, again with the PDK<sup>K465E</sup> cells expressing significantly less *Baiap3*-encoding mRNA. *In vitro* generated CTLs were also examined for their expression of *Baiap3* by qPCR. For this, OT-1 WT and PDK1<sup>K465E</sup> splenocytes were stimulated with either 50pM SIINFEKL or 5nM SIQFEKL for 2 days, followed by treatment with IL-2 at 10ng/ml for 3 days. After this time, >96% of cells were antigen-specific CD8 T cells. The data in *Figure 3-12* showed that regardless of whether a high or low affinity peptide was used, the PDK<sup>K465E</sup> cells still displayed over 50-fold less *Baiap3* mRNA compared to WT cells. From these data, it can be concluded that irrespective of the stimulatory conditions, the PDK<sup>K465E</sup> mutation caused a significant decrease in the production of *Baiap3* mRNA when compared to WT CD8 T cells. This decrease was more pronounced once T cells had been activated. Overall, the data

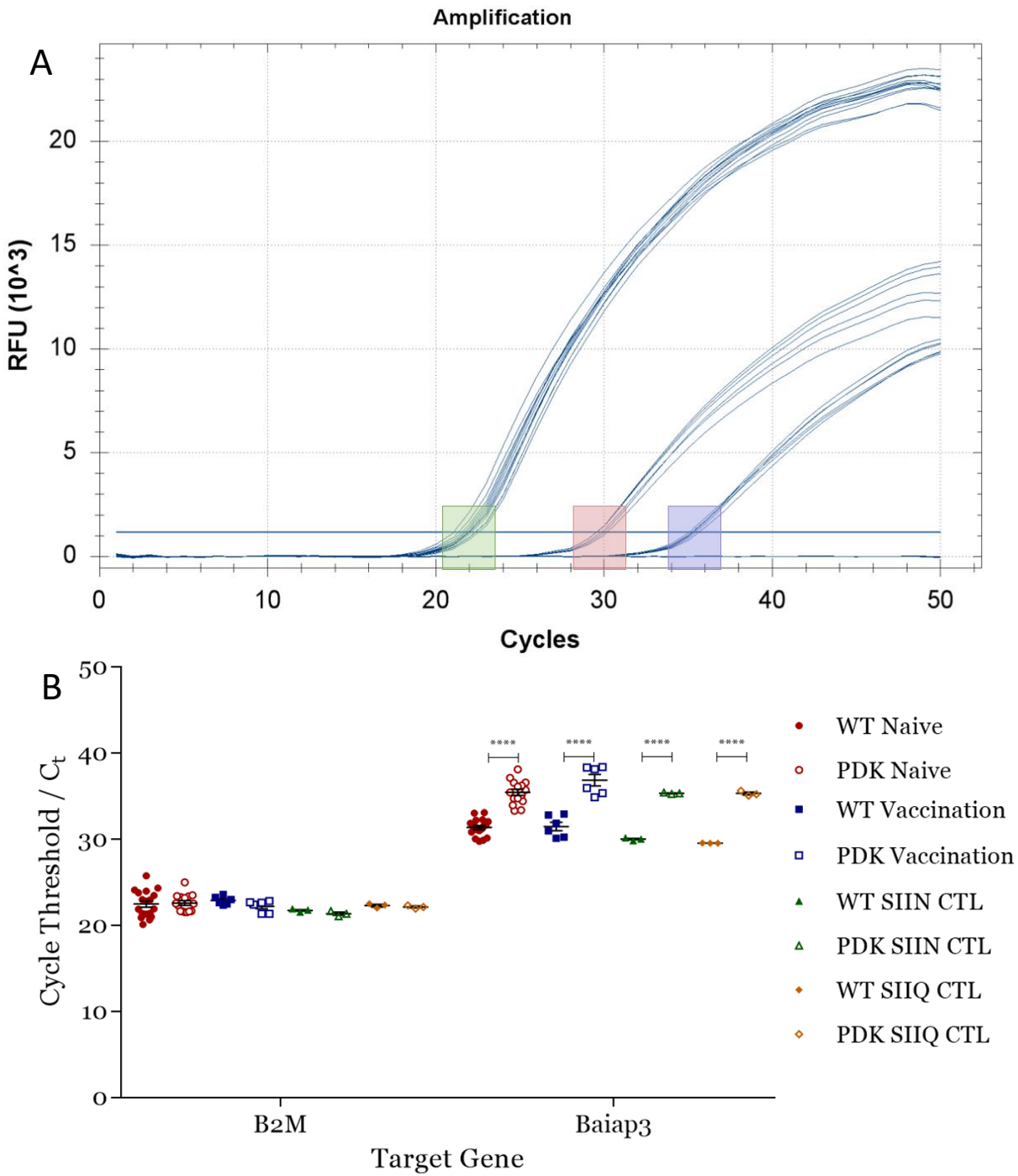


**Figure 3-11 – Difference in *Baiap3* expression in WT and PDK<sup>K465E</sup> mutant CD8<sup>+</sup> T cells**

Naive CD8 cell samples were negatively purified using MACS selection kits. Vaccination samples were generated from WT and PDK mutant OT-1 cells that were adoptively transferred into recipient mice before being challenged with OVA,  $\alpha$ CD40 antibody and LPS. CTL samples were obtained from splenocytes from WT or PDK mutant OT-1 mice stimulated with either 50pM SIINFEKL or 5nM SIIQFEKL for 2 days followed by CTL generation with 10ng/ml IL-2 for 3 days. CD8 purity was >85% across all samples. RNA was isolated and 200ng of RNA was used to generate all cDNA samples. qPCR was then performed using probes specific for *Baiap3* and a housekeeping gene,  $\beta_2M$ . **A** – Representative qPCR replication curves, highlighted areas indicated cycle thresholds, green – WT and PDK  $\beta_2M$ , red – WT *Baiap3* and blue – PDK *Baiap3*. **B** – Graph showing cycle threshold of  $\beta_2M$  and *Baiap3* across multiple samples. Cycle threshold represents the number of qPCR cycles required to reach the threshold of detection, set as the linear section of the logarithmic amplification plot described in the methods section. Mean and SEM are displayed. Student’s two-tailed t-test performed, p-value \*\*\*\* <0.005. Replicates vary between conditions, naïve samples n=18, four biological samples; vaccination samples n=6, two biological samples; CTL samples n=3, single biological sample.

caused a significant reduction in the expression of *Baiap3* mRNA.

To confirm that the near 60-fold reduction in *Baiap3* mRNA between WT and PDK<sup>K465E</sup> vaccination samples translates into a difference at the protein level, Baiap3 protein expression was assessed in CTLs from both WT and PDK<sup>K465E</sup> mice by fluorescence microscopy using a commercially available Baiap3 antibody and a fluorescently-labelled secondary antibody.

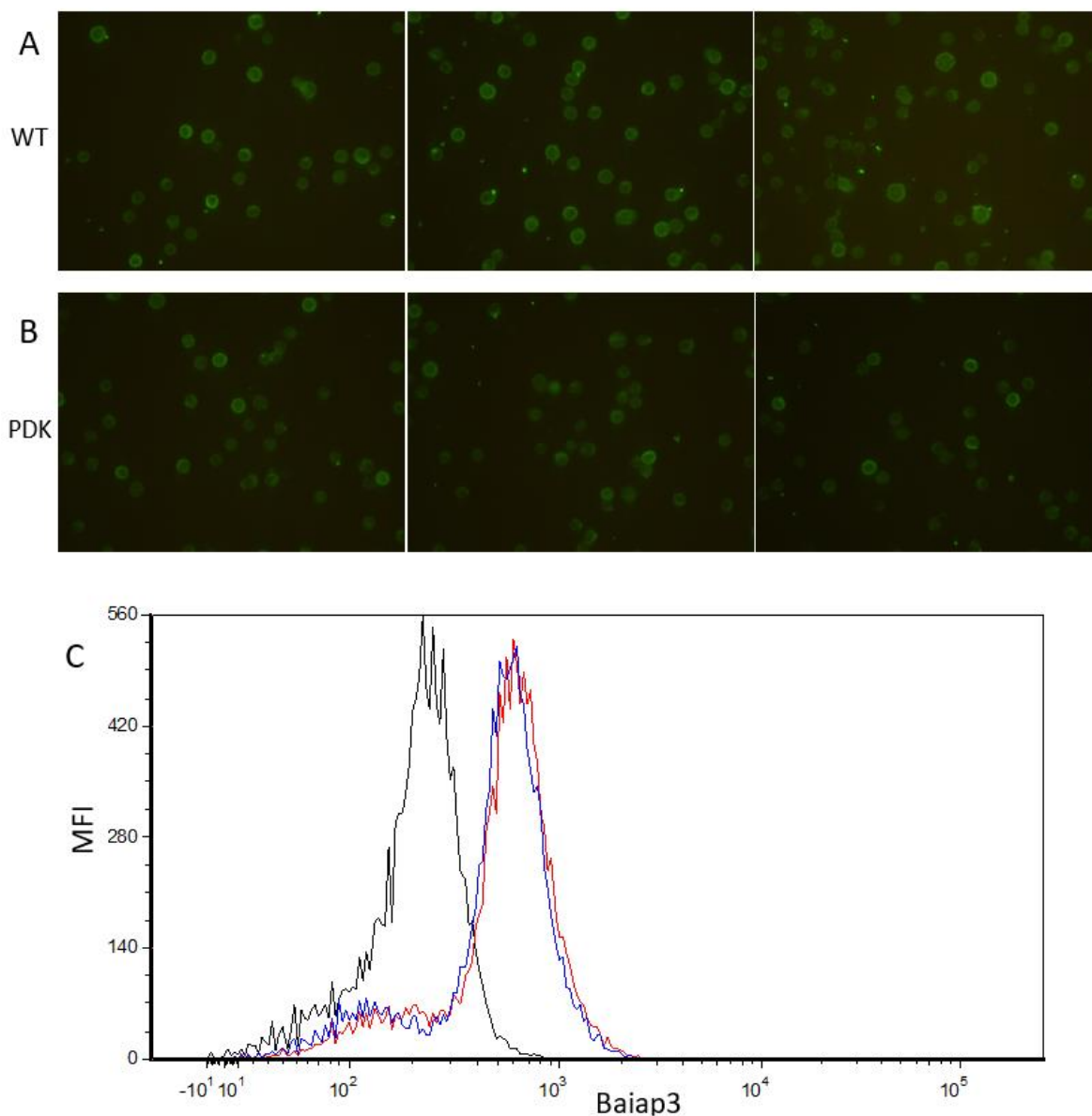


**Figure 3-12 – Immunofluorescent assessment of Baiap3 protein expression by fluorescence microscopy and flow cytometry**

WT and PDK mutant splenocytes activated for 2 days with 50pM SIINFEKL peptide, followed by 3 days IL-2 10ng/ml to generate CTLs. **A** – Representative images taken from WT CTLs fixed, permeabilised and stained with a goat anti-Baiap3 primary antibody, followed by donkey anti-goat Alexa488 secondary antibody. **B** – Representative images from PDK<sup>K465E</sup> mutant CTLs treated as in (A). **C** – Intracellular staining of Baiap3 as assessed by flow cytometry in CTLs generated as described above, black – goat IgG control antibody, red – WT CTLs Baiap3 expression, blue – PDK<sup>K465E</sup> mutant CTLs Baiap3 expression, data from a single biological sample.

## Chapter 3

Based on comparison of microscopy images in *Figures 3-12A and B*, although there was a clear difference in *Baiap3* mRNA production between WT and PDK<sup>K465E</sup> CD8 T cells (*Figure 3-11*), this difference was not clear at the protein level. These microscopy images also indicate that *Baiap3* is likely expressed on the intracellular side of the plasma membrane. To obtain more quantitative data regarding the expression of *Baiap3*, protein expression was analysed by flow cytometry. As shown in *Figure 3-12C* the levels of *Baiap3* in both WT and PDK<sup>K465E</sup> mutant CTLs were virtually identical, indicating that *Baiap3* protein is expressed equally across both cell types. An attempt was made to perform Western blotting to confirm that this commercial antibody recognised only one protein product of the correct size. Unfortunately, there was too much background intensity for the blot to be reliable. This indicates that the antibody might be binding other, non-specific targets, within the T cells. Given the relatively understudied nature of *Baiap3* at the time, only one *Baiap3* antibody was available.

Together the data in this chapter have revealed that the reduced Akt activity caused by the PDK<sup>K465E</sup> mutation causes substantive reductions in CD8 T cell effector functions *in vitro*.

### 3.3 Summation and Discussion

It has been known for some time that the PI3K/Akt signalling pathway has regulatory control over elements of CD8 T cell differentiation. PDK1 has been shown to be responsible for increased proliferation and glucose uptake, whilst Akt is required for sustained expression of effector molecules such as granzyme B and IFN $\gamma$  in multiple *in vitro* systems<sup>143,144</sup>. Reducing Akt activity in CD8 T cells should therefore cause reduced expression of granzyme B and hence may decrease their cytotoxic capability. However, work done by colleagues in this lab has showed that PDK<sup>K465E</sup> CD8 T cells are capable of combating and eliminating tumours<sup>240</sup>. These cells do show some defects in secondary re-challenge, but this may be due to altered differentiation of the memory population. Given the discrepancy between the reported *in vitro* data and in-house *in vivo* observations, the question remains: what are the effects of Akt activity on CD8 T cell effector functions?

In this chapter, an attempt has been made to address this question, by examining CD8 T cell cytokine production and cytotoxicity in WT and PDK<sup>K465E</sup> mutant CD8 T cells. OT-1 transgenic mice were utilised, in which T cells are specific for a peptide derived from OVA, SIINFEKL and which also respond to the lower affinity peptide SIIQFEKL<sup>251</sup>. First to be examined was cytokine production. Initial priming and restimulation with SIINFEKL demonstrated that PDK<sup>K465E</sup> T cells display an approximate 50% reduction in the amount of IFN $\gamma$  secreted. Further, when SIIQFEKL was used to restimulate cells, the overall amount of IFN $\gamma$  was reduced. Furthermore, it was found that if SIIQFEKL was used as the priming peptide, the resultant IFN $\gamma$  would be greatly reduced; regardless of the restimulatory peptide. Subsequently, intracellular IFN $\gamma$  and IL-2 were examined, to determine if the reduction in secreted cytokines observed was due to impaired production or expression. From these data, it was seen that WT and PDK<sup>K465E</sup> CD8 T cells had an equivalent percentage of cells registering as IFN $\gamma$ <sup>high</sup>. However, the MFI and inferred expression was reduced at higher restimulatory conditions, implying that this could be the cause of the difference. Although it cannot be considered to be the only circumstance affecting the secretion, as the overall reduction of intracellular expression in the PDK<sup>K465E</sup> cells, whilst significant, was substantially smaller than the observed difference in secretion. Also examined was IL-2, to investigate if cytokines were being equally affected. This data shows a similar reduction of IL-2 MFI expression. However, unlike IFN $\gamma$ , there is a near 50% reduction in the number of cells that register as IL-2<sup>high</sup>. As both IL-2 and IFN $\gamma$  are a sign of T cell activation and drive towards the effector response, it is possible that the reduced Akt activity of the PDK<sup>K465E</sup> mutants contributes

to the decrease observed in the secretion of these cytokines. Although this does not explain why there were less IL-2<sup>high</sup> cells present in the PDK<sup>K465E</sup> mutant.

However, perturbations in cytokine production have been reported previously in CD4 T cells with impaired or ablated PDK enzymes<sup>257</sup>. Specifically, it has been shown that PDK1 is capable of activating the IL-4 promoter, independently of Akt in CD4 T cells, primarily through PKA and NFAT<sup>258</sup>. Ablation of PDK1 was also shown to cause defects in IL-2 production whilst leaving IFN $\gamma$  production intact in CD4 T cells<sup>257</sup>. Perhaps this is also true in CD8 T cells, as this shows similarities to the data presented here. Given that these reductions in IFN $\gamma$  expression are not observed in the previously reported *in vivo* data from this group<sup>240</sup>, it is possible that the presence of inflammatory cytokines and co-stimulation *in vivo* can overcome the inherent defect caused by the PDK<sup>K465E</sup> mutation. Likewise, IL-2 is not decreased in *in vivo* experiments as it is *in vitro*<sup>240</sup>. Overall, this suggests the cytokine production under optimal priming conditions of an *in vivo* immune reaction is not dependent on Akt activity.

A published cytotoxicity assay was adapted. This was shown to be a good replacement for the current cytotoxicity assay that is dependent on radioactive isotopes. Initially, the effects of peptide affinity on T cell cytotoxicity were studied. The data from these experiments revealed that SIINFEKL-pulsed target cells were maximally killed when pulsed at a peptide concentration of 10nM. Lowering the concentration of SIINFEKL to less than 10nM caused a drop in the level of cytotoxicity, consistent with previous work<sup>259</sup>. Target cells pulsed with the lower affinity peptide, SIIQFEKL, showed equal susceptibility to killing as SIINFEKL-pulsed targets at 1 $\mu$ M, but became less susceptible once the peptide concentration was lowered. This shows that maximal cytotoxicity directed against lower affinity peptides requires a higher peptide concentration than that of higher affinity peptides, at least in an OT-1 setting. This could tie into the threshold model of T cell activation, where interactions between the MHC complex and TCR are required to spatially occlude inhibitory phosphatases such as CD45. Peptides with weaker affinities may not be able to form as many interactions to induce this occlusion of phosphatases when compared to their higher affinity counterparts. In turn, this could lead to reduced cytotoxic activity<sup>132</sup>.

Next, the role of Akt in T cell cytotoxicity was examined using an Akt inhibitor. The concentration of this Akt inhibitor was chosen based on a previous study examining both the inhibitor and PDK<sup>K465E</sup> mutant mouse model<sup>143</sup>. Both SIINFEKL and SIIQFEKL peptides were used as targets in

order to assess whether Akt plays any role in regulating the cytotoxic response to peptides of different affinities. This experiment showed that inhibition of Akt during CTL differentiation causes a significant and substantial decrease in the level of cytotoxicity, although the inhibition did not differentially affect the cytotoxicity induced by the two different affinity peptides. It is possible that phosphatases play a more integral part in distinguishing the responses to antigens of different affinities than Akt<sup>260,261</sup>. This same experiment also showed a near 10-fold reduction in expression of granzyme B when CD8 T cells were cultured in the presence of the Akti. This could be the primary explanation for the reduced cytotoxicity observed. However, it has been reported that granzyme B expression is substantially higher than the threshold required for cytotoxicity<sup>83</sup>. Therefore, a 10-fold reduction may not have significantly impacted its killing ability.

Given that Akt drives maximal granzyme B and killing activity, the PDK<sup>K465E</sup> mutant CD8 T cells were used to establish whether reduced Akt activity would have a similar effect. This group has previously demonstrated that *in vivo* generated effector PDK<sup>K465E</sup> CD8 T cells are capable of controlling tumours, so it is interesting to see that these cells do show a reduced cytotoxic capability *in vitro* in *Figure 3-10*. The reduction is statistically significant and substantial, ranging from a reduction of 30-60% depending on effector to target ratios. The untreated PDK<sup>K465E</sup> CD8 T cells also display a reduced expression of granzyme B, but not to the same extent as Akti-treated WT cells. This is consistent with the only partial Akt inhibition in PDK<sup>K465E</sup> cells but more complete knock-down in Akti treated cells. Considering the PDK<sup>K465E</sup> CD8 T cells show reduced cytotoxic capacity and a reduced granzyme B expression, it is curious that they are still capable of controlling tumours. It is possible that the basal Akt activity that is present in the PDK<sup>K465E</sup> CD8 T cells, whilst not enough to induce maximal killing, is sufficient when targeting an *in vivo* tumour model. Additionally, within an *in vivo* system there may be a facet of granzyme B expression that is independent of Akt activity, thus explaining why PDK<sup>K465E</sup> CD8 T cells are competent in our group's tumour challenge experiments. One factor not considered is cell number; in an *in vivo* tumour model the high number of cells involved could possibly compensate for individual cytotoxic impairment. The inflammatory conditions of the *in vivo* listeria infection used in these experiments may also determine whether these PDK<sup>K465E</sup> CD8 T cells control primary tumours. As shown earlier in the chapter, PDK<sup>K465E</sup> cells do show a decreased production of cytokines such as IFN $\gamma$  and IL-2 in an *in vitro* setting, perhaps this is also compensated for under the more inflammatory conditions of an *in vivo* listeria infection. It should also be noted that despite the Akti being classified as a reversible allosteric inhibitor of Akt 1 and 2, there is no reference to its half-life in cell culture. As such, it cannot be ruled out that the inhibitor was still present within

## Chapter 3

cells during these cytotoxicity experiments. Therefore, it is a possibility that the result observed is a direct effect of Akt being inhibited rather than the alteration in differentiation during culture.

Brain-specific angiogenesis inhibitor (BAI1) associated protein 3 (*Baiap3*) was first identified by Shiratsuchi *et al* in 1998 as one of three binding proteins to BAI1<sup>262</sup>. *Baiap3* contains two Munc-like C2 domains, thought to be involved in a form of phospholipid binding. *Baiap3* also contains homologous sequences to that of Munc13-4 and synaptotagmin<sup>262</sup>. Synaptotagmin is a pre-synaptic protein that is key in neurotransmitter vesicle release in neurones<sup>263</sup>. Synaptotagmin binds with SNARE proteins holding vesicles in a primed position at the membrane, and acts as a critical regulator that will only allow fusion and exocytosis of the vesicle once it has bound calcium ions through its C2 domains<sup>263</sup>. Munc13-4 is a protein also involved in the regulated exocytosis of vesicles via interaction with SNARE proteins<sup>264</sup>. Mutations in *Munc13-4* have also been associated with familial haemophagocytic lymphohistiocytosis (FHL) subtype 3, an immune disorder associated with dysregulated cytotoxic granule and cytokine release. In desmoplastic small round cell tumours (DSRCTs), a cancer characterised by the chimeric fusion of the Ewing's Sarcoma and Wilms' tumour genes creating the novel transcription factor EWS-WT1, *Baiap3* is overexpressed. This overexpression of *Baiap3* was shown to accelerate the regulated exocytosis pathway that resulted in the increased secretion of growth factors, which are one of the primary oncogenic factors of DSRCTs<sup>265</sup>. It has also been shown that overexpression of *Baiap3* in human melanoma cell lines causes enhanced proliferation at limiting serum concentrations<sup>266</sup>.

Due to its suspected role in regulated exocytosis and the pronounced change in gene expression between PDK<sup>K465E</sup> and WT cells in the microarray, it seemed worthy of investigation. The experiments in this chapter demonstrate that expression of *Baiap3* appears fundamentally altered in PDK<sup>K465E</sup> T cells. *In vitro* activated samples and naïve cell samples, both show a minimum of a 30-fold reduction in *Baiap3* expression in PDK<sup>K465E</sup> T cells compared with WT T cells. Whilst the difference between WT and PDK<sup>K465E</sup> expression of *Baiap3* does increase between the naïve cells and either of the *in vitro* or *in vivo* activated samples, it is clear that *Baiap3* is radically downregulated in PDK<sup>K465E</sup> CD8 T cells. However, subsequent experiments have shown that this transcriptomic difference does not translate to a difference at the protein level. This maybe, however, due to the lack of an effective commercial antibody at the time of performing these experiments; particularly when noting the inability to retrieve a successful western blot using this antibody.

More recently, Baiap3 was shown to be a calcium sensitive protein, that regulates the retrograde trafficking of secretory vesicles back to the trans-Golgi network<sup>267</sup>. Critically, it was shown that the absence of Baiap3 impaired secretory vesicle formation and caused their degradation<sup>268</sup>. This more detailed information would seem to indicate that if Baiap3 were to be altered in the CD8 T cells of PDK<sup>K465E</sup> it could impair cytokine and cytotoxic granule production, possibly explaining the data shown in this chapter.

If this work concerning the role of Baiap3 was to be continued in future experiments, it is my opinion that overexpression and knockdown models should be the primary methodology utilised. These methods are not without their own advantages and disadvantages. As it stands, our current system for overexpression using retroviral transduction is likely to prove difficult, due to the large size of the Baiap3 transcript, at 3451 nucleotides in length. Typically, retroviral transduction systems are limited to a maximum size of approximately 8kb in length before reducing in transduction efficiency<sup>269</sup>. Introduction of Baiap3 into our pMP71 vector would put the size of the complete vector at nearly 10kb, thus rendering it unlikely to be capable of stable cellular transduction. As such, methods that focus on suppressing the expression of Baiap3 are more likely to be successful. shRNA mediated knockdown is a possible method of examining the effect of reducing Baiap3 expression in CD8 T cells. However, shRNA methods do have the disadvantage of not providing complete silencing of the gene product. Given its more recent accessibility, utilising the CRISPR/Cas9 system would present a more effective way to completely silence the Baiap3 gene, as the non-homologous end joining mechanism could cause knockout of the target gene. If Baiap3 were to be knocked out in WT CD8 T cells through gene editing by CRISPR/Cas9, it could be possible to observe a similar reduction in cytotoxic capacity, as seen in the PDK<sup>K465E</sup> mutant cells.



# Chapter 4 Effects of Akt Signalling on CD8 Effector T Cell Differentiation Determined by Single Cell RNA Sequencing

## 4.1 Introduction

As discussed in the introduction to this thesis, many mechanisms of differentiation have been proposed. Mathematical and computational models focussing on these mechanisms such as asymmetric cell division, or the decreasing potential models have been unable to clarify a clear process for CD8 T cell differentiation<sup>270</sup>. This not only recognises the complexity of the issue of CD8 T cell differentiation, but also points to a solution that combines these models.

The role of Akt in the differentiation has been partially defined. Currently, it is known that Akt, through the inhibition of the FOXO family of transcription factors and upregulation of transcription factors such as Bach2 and T-bet, induces a more cytotoxic phenotype at the cost of cellular longevity<sup>271</sup>. Those cells that display the highest levels of Akt activity are destined to become terminally differentiated SLECs and eventually be deleted as part of the contraction phase of the immune response<sup>164</sup>. However, the effect of Akt on the differentiation of memory cells is more in dispute.

Crompton *et al*<sup>156</sup> demonstrated that Akti inhibition causes upregulation of CD62L, promotes homing to lymphoid tissues, enhances oxidative phosphorylation and increased survival post adoptive transfer. These are all factors strongly associated with a more memory like phenotype. Whilst these experiments were conducted using isolated human tumour infiltrating lymphocytes cultured *ex vivo* (TILs), it is still indicative that greatly reducing Akt activity induces a memory phenotype.

Work by Rogel *et al*<sup>240</sup> in this lab also examined the effects of Akt activity on CD8 T cells in an *in vivo* setting. As discussed previously, this lab group utilises a knock-in PDK<sup>K465E</sup> model that

## Chapter 4

prevents maximal Akt activity by preventing PDK1 association with PIP<sub>3</sub> at the plasma membrane. This prevents the co-localisation of PDK1 with Akt and its subsequent activation. These data demonstrate that the limiting Akt activity in PDK<sup>K465E</sup> CD8 T cells does not impair the generation of primary effector cells or clearance of tumours. Interestingly, in response either OVA-expressing *Listeria Monocytogenes* (LM-OVA) or vaccination with OVA, anti-CD40 mAb and LPS, PDK<sup>K465E</sup> cells demonstrate an alteration in the transition from effector to memory cells. The T<sub>EM</sub> subset, denoted by the lack of CXCR3 and CD43 expression, is reduced in PDK<sup>K465E</sup> cells. Additionally, the vaccination model described above, caused an accelerated cell death phase during contraction of the effector responses. This led to a reduction in the total memory population formed by the PDK<sup>K465E</sup> cells. Co-transfer experiments in this vaccination model also demonstrated that an equal transfer of WT and PDK<sup>K465E</sup> CD8 T cells showed an inability of WT cells to rescue the PDK<sup>K465E</sup> cells. Indicating that the lack of survival and/or transition into memory is due to cell intrinsic factors. This indicates that reduced Akt activity can affect the differentiation process, which can go on to impair long term memory.

In this chapter, the aim is to use single cell RNA sequencing techniques to gain a more thorough understanding of the differentiation process that leads to the generation of effector and memory subsets; and to define, in greater detail, how Akt signalling impacts on this complex process.

## 4.2 Results

To examine the temporal effects of Akt activity on CD8 T cell differentiation an infection model was used in which congenically marked OT-1 cells were transferred into congenic recipients, before infection with LM-OVA 24 hours later. Phenotypic differences were examined in CD8 T cells at two distinct time points either 45 hours or six days; 45 hours provided an opportunity to capture the initial division step to see if differential Akt activity caused by the PDK<sup>K465E</sup> mutation affected early markers of functional differentiation. Six days post stimulation represents the peak of the CD8 T cell response in this infection model, as has been determined by previous work published by our lab<sup>240</sup>, and thus allowed study Akt-induced changes at a later stage when the key fate decision in CD8 T cells are becoming more stable. It has also been clarified that at this time point there is clear heterogeneity in the effector population. Based on expression of KLRG1 and CD127, MPECs and SLECS can be demarcated.

To examine T cells at the 45 hour time point, splenocytes were harvested from WT and PDK<sup>K465E</sup> OT-1<sup>+</sup>, CD45.1<sup>+</sup> congenic mice. The splenocytes were then stained with 5 $\mu$ M CFSE to track cellular division. These splenocytes were then injected into recipient C57BL/6 mice, so that each mouse received the equivalent of 3x10<sup>6</sup> naïve CD8 T cells. 24 hours after receiving the transferred cells, the recipient mice were infected with 2x10<sup>6</sup> CFUs of LM-OVA. Spleens from recipient mice, 45 hours post infection, were harvested and processed for analysis by flow cytometry. *Figure 4-1* displays the data from this experiment. From the CFSE staining shown in *Figure 4-1A* there was no clear difference in the level of cellular proliferation between WT and PDK<sup>K465E</sup> CD8 T cells at this early time point. There was also no significant difference in the expression of the MPEC markers CD62L, TCF7 and IL-7R at this time point (*Figure 4-1B*). Markers of increased effector functions such as Granzyme B, T-bet and CD25 were similar between WT and PDK<sup>K465E</sup> T cells (*Figure 4-1B*). Representative histogram plots of these effector and MPEC phenotypic markers are shown in *Figure 4-1C*.

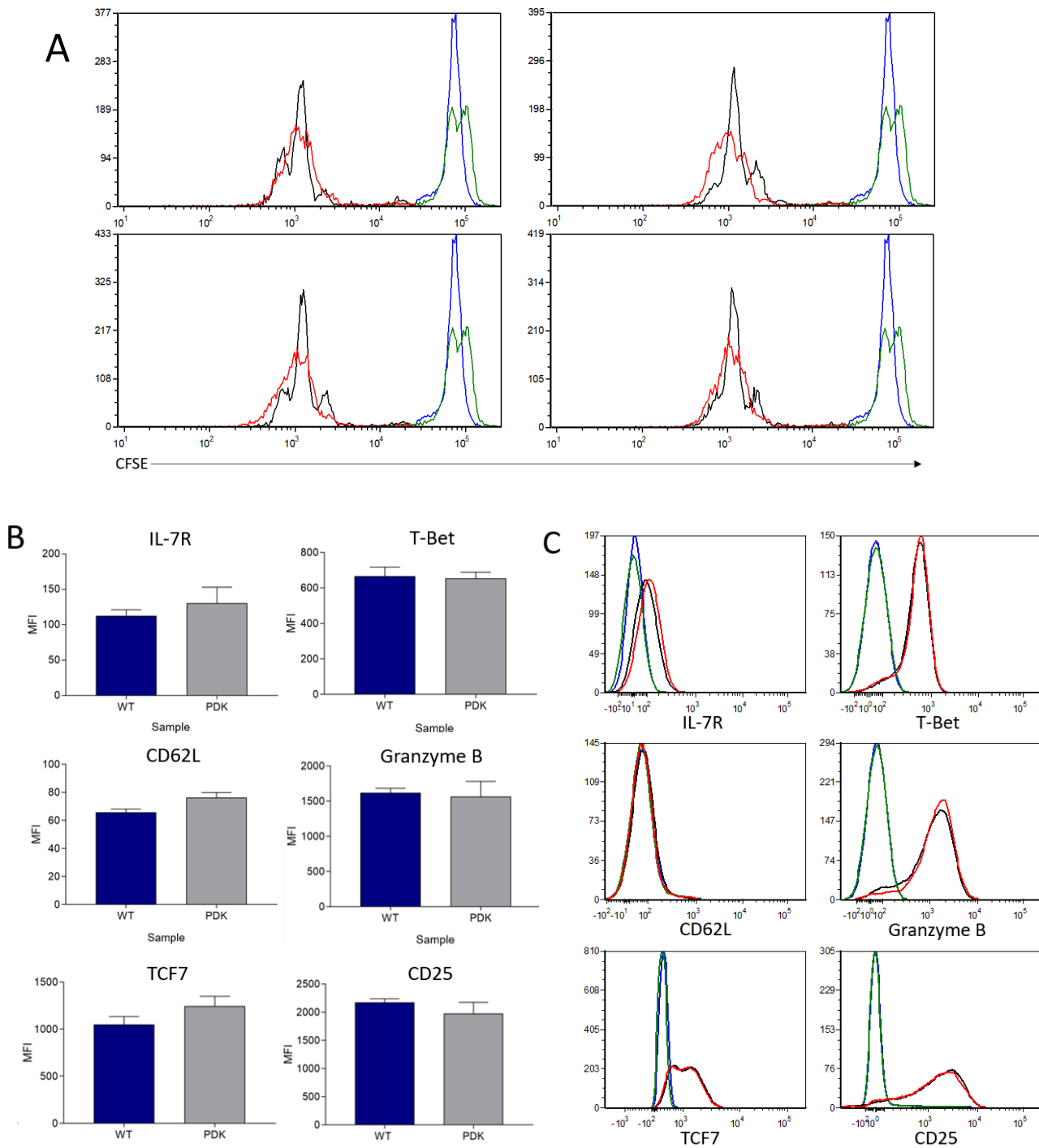


**Figure 4-1 – Analysis of phenotypic markers in CD8 T cells 45 hours post *in vivo* stimulation with listeria-OVA.**

WT and PDK<sup>K465E</sup> CD45.1<sup>+</sup> OT-1 splenocytes were labelled with 5µM CFSE before being introduced intravenously to recipient C57BL/6 mice, 4 mice for each group. After 24 hours, recipient mice were infected intravenously with 2x10<sup>6</sup> CFUs of attenuated OVA-expressing *Listeria Monocytogenes*. 45 hours post infection with Listeria-OVA, recipient splenocytes were harvested and phenotypic markers analysed by flow cytometry. **A** – Representative histograms showing CFSE dilution of CD8 T cells 45 hours post Listeria-OVA infection from four individual mice, red – WT at 45hrs, black – PDK<sup>K465E</sup> at 45hrs, green – WT post CFSE staining, blue – PDK<sup>K465E</sup> post CFSE staining. **B** – MFI of phenotypic markers related to differentiation state of CD8 T cells at 45 hour post stimulation with listeria-OVA, n=4, MFI taken from total CD8<sup>+</sup> CD45.1<sup>+</sup> population, isotypes for all samples were equivalent. **C** – Representative histograms of phenotypic markers from B.

#### 4.2.1 Drop-Seq Analysis of the Effects of the PDK<sup>K465E</sup> Mutation on CD8 T cell Differentiation

The next step was to investigate the effects that PDK<sup>K465E</sup> mutation had on differentiation at the later time point of six days post stimulation. Previous work in this group by Rogel *et al*<sup>240</sup> showed expression of some of these markers at day six post infection. PDK<sup>K465E</sup> CD8 T cells displayed approximately three-fold greater frequency of CD62L<sup>hi</sup> cells compared with WT CD8 T cells at this point. In addition, the frequency of CD127<sup>hi</sup> cells (IL-7R $\alpha$ ) in PDK<sup>K465E</sup> CD8 T cell populations was two-fold higher than that of WT CD8 T cells. PDK<sup>K465E</sup> CD8 T cells, did however, display approximately 20% fewer granzyme B positive cells following the response to this LM-OVA infection. In this setting expression of T-bet was also unchanged between WT and PDK<sup>K465E</sup> CD8 T cells. Expression of CD25 and TCF7 was not examined.

Flow cytometric processes can yield valuable insights into intracellular and surface protein expression. However, as they are based on targeting a limited number of already known proteins, they are restricted in their scope; preventing the study of more comprehensive profiles and discovery of novel factors. In recent years the advent of transcriptomic methodologies has allowed for a much broader analysis of gene expression. In particular single cell RNA sequencing (scRNA-Seq) has been shown to allow effective analysis of transcriptomes across multiple cells whilst maintaining both accuracy and sensitivity<sup>272</sup>. The availability of high throughput techniques allows profiling of thousands of cells in parallel, which affords an unbiased assessment of heterogeneity of single cells within a population<sup>273</sup>. As such, scRNA-Seq, specifically Drop-Seq, will be utilised in order to gain further insights into any changes in differentiation that have occurred as a results of Akt signalling in PDK<sup>K465E</sup> CD8 T cells. Drop-Seq, due to being newel available to this lab group, was decided as a methodology of examining the changes in differentiation that had occurred at six days post stimulation. The process would allow us to see a greater number of variables in the population that at this stage would not be clearly defined by flow cytometry. The established subsets at this time point will serve as a standard for the Drop-Seq analysis to hopefully build upon. At this time point the transferred cells have expanded to peak numbers, which aids in their subsequent isolation and purification for this process. This Drop-Seq process is still a relatively new development and as such the knowledge of the mechanics are not commonplace. Thus, *Figure 4-2* displays a schematic of the key processes that define Drop-Seq. The process involves passing three separate reagents across a flow cell to generate droplets that

## Chapter 4

ideally contain 1 mRNA capture bead with a single cell of interest; in this instance flow sorted OVA-specific OT-1 CD8 T cells, recovered six days post stimulation.

*Figure 4-2A* displays the inner workings of the flow cell during the Drop-Seq protocol. mRNA capture beads, suspended in a cellular lysis buffer, are injected into a flow cell. At two points in the flow cell, the target cells resuspended in a PBS/0.01% BSA solution, meet the capture beads. The flow rate has been optimised to maximise the number of single cells captured and also to reduce the rate of doublets (two cells per bead). Immediately after the cells are injected, the combined solution encounters an oil flow. The design of the flow cell at this point encourages the formation of a droplet, which due to the flow rate has been optimised to contain one bead and one cell.

As shown in *Figure 4-2B*, the capture arms of the beads are made up of four distinct domains; oligo-dT repeats, unique molecular identifiers (UMIs), cell barcode and a PCR handle. Once captured within the droplet, the lysis buffer causes the target cell to rupture releasing the mRNA within. The oligo-dT segment of the capture bead binds to any poly-adenylated mRNA present in the lysate. Unique molecular identifier (UMI) is a unique string of nucleotides that identifies each capture arm on the bead and allows sequencing to distinguish between two different mRNA molecules encoding the same gene on the same bead. Cellular barcode is another marker, but this only differs between beads. When single cells are captured, the mRNA from that cell in further processing steps will include this cell barcode, allowing mRNA to be assigned to its cell of origin at the sequencing step. Lastly, the PCR handle is a nucleotide sequence that allows for all the previous segments of the capture arms to be included in downstream processes to prepare for genetic sequencing.

An overall flowchart of the molecular biology processes from single cell droplet to NGS is shown in *Figure 4-3*. Post droplet generation, the mRNA capture beads are processed for genetic sequencing. This process first involves a reverse transcription step. This method converts the captured mRNA into more stable cDNA by utilising a template switch oligomer. This then allows for the template switch, whereby the reverse transcriptase switches strands and proceeds with secondary strand synthesis, overwriting the captured mRNA. At this point, the cDNA conjugated beads can be stored safely at -20°C.

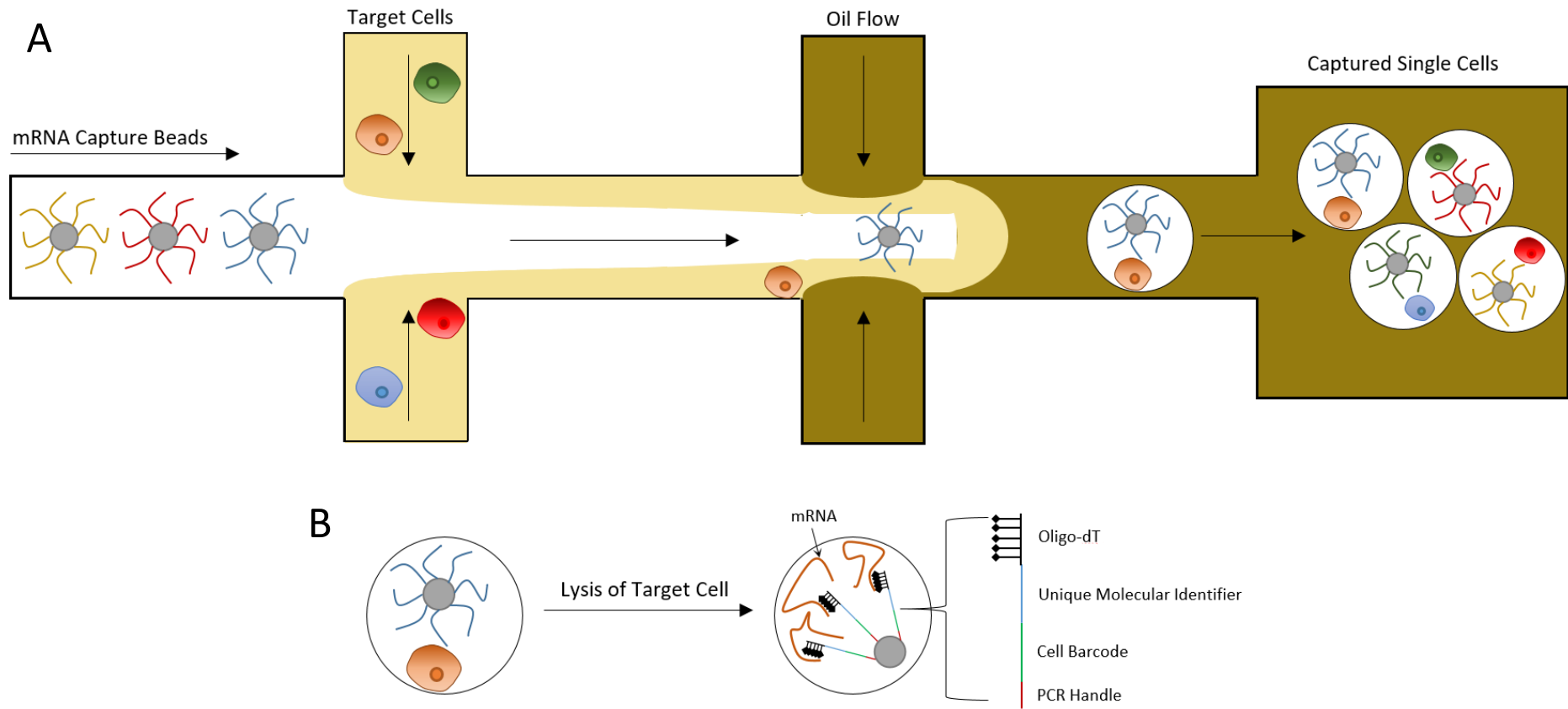


**Figure 4-2 – Schematic of Drop-Seq mechanism for single cell RNA capture.**

**A** – Internal flow cell process, demonstrates the single cell capture and droplet formation process that occurs as part of the Drop-Seq protocol. **B** – mRNA capture bead structure and process of mRNA capture post droplet formation

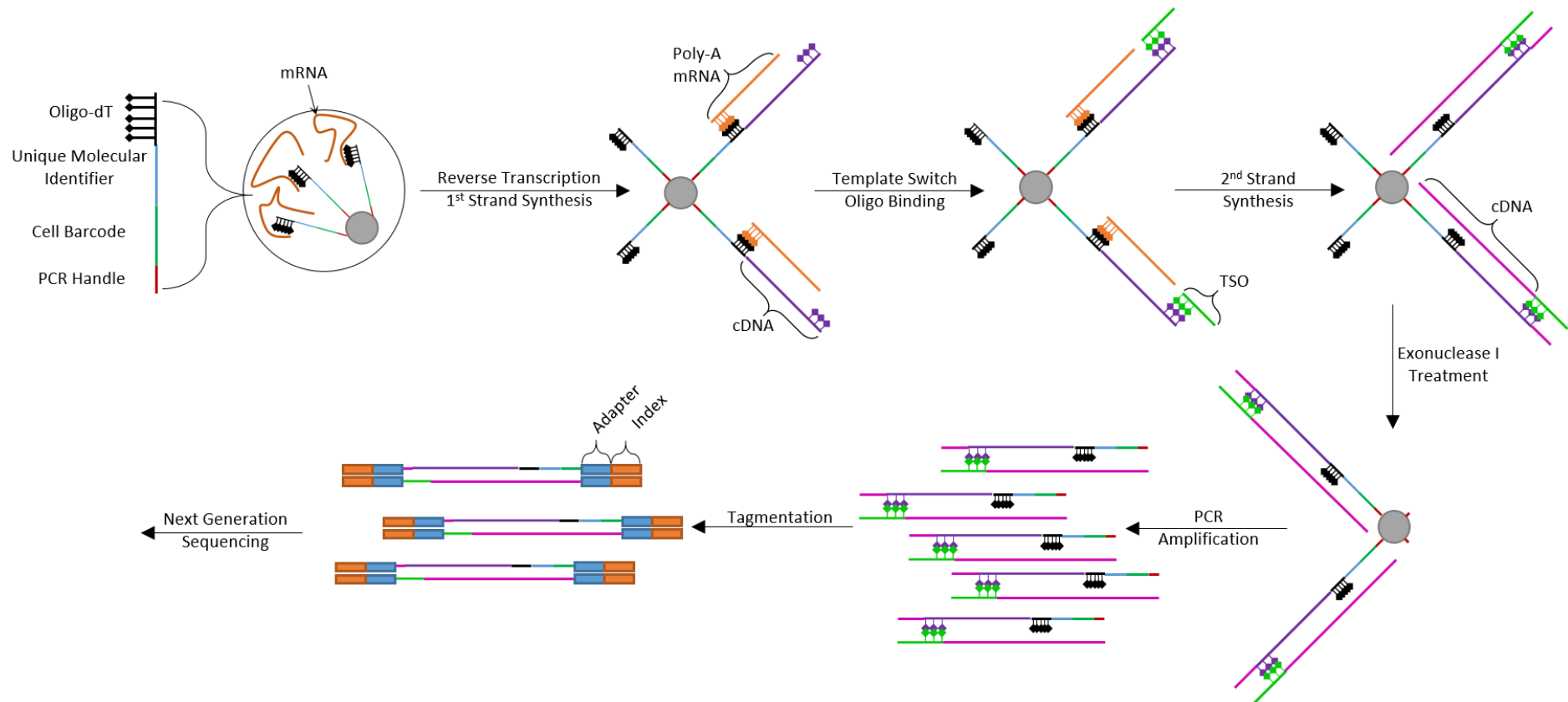


**Figure 4-3 – Schematic of molecular biology processes between single cell capture and next generation sequencing post Drop-Seq.**

Reverse transcription extends bead capture arm producing complementary DNA (cDNA) to the captured mRNA. Reverse transcriptase enzyme is engineered to terminate sequence with multiple cytosine residues. These residues act as docking point for the template switch oligomer (TSO). This TSO acts as another primer site allowing extension of the cDNA on the opposing strand, effectively overwriting the captured mRNA. Once this process is finished the beads are now only bound to cDNA and as such are more stable, allowing for long term storage at  $-20^{\circ}\text{C}$ . Subsequently the beads are treated with an exonuclease enzyme. This exonuclease cleaves unbound mRNA capture arms present on the beads. cDNA bound to beads is amplified through PCR. Following this the cDNA undergoes tagmentation, an enzymatic reaction that fragments the cDNA, and binds adaptors to both ends of the cDNA fragments. Indexes are added to these adaptors. Indexes are short identifying sequences of DNA that cap the fragments that allow for multiplex sequencing.

Following the reverse transcriptase step, an exonuclease enzyme is employed to cleave the remaining bead capture arms that did not bind to any poly-adenylated mRNA. This prevents the carryover of these blank sequences, which upon PCR amplification, would contaminate the final genetic library. Following several rounds of PCR to amplify the captured material, the cDNA library is purified. After the cDNA library has been purified, its concentration and overall quality is assessed on a BioAnalyzer. A good understanding of the typical range expected for cDNA length is based on previous Drop-Seq experiments. The concentration is a more variable factor and is very much dependent on the cell type that is being analysed. Once a cDNA library has been purified, it undergoes tagmentation in order to fragment and cap the cDNA with adaptor sequences and indices that allow recognition by next generation sequencing (NGS) instruments. Subsequent output of this NGS is run through an in-house customised development pipeline utilising our institutions supercomputing network, before being analysed in R Studio using the Seurat package; developed by the inventors of this Drop-Seq technique.

For analysis at this later time point,  $10^4$  CD45.1<sup>+</sup> OT-1 cells from either WT or PDK<sup>K465E</sup> mice were intravenously injected into recipient mice, before being challenged with LM-OVA 24 hours later. Six days post stimulation with this listeria strain, the spleens of the recipient mice were harvested and OVA-specific CD8<sup>+</sup> CD45.1<sup>+</sup> T cells were purified by cell sorting, prior to the Drop-Seq procedure described above.

Following reverse transcription and exonuclease treatment of captured beads the process of PCR began. For the initial PCR reaction, 8 tubes each containing 4000 beads from both the WT and PDK<sup>K465E</sup> T cells underwent 16 cycles of PCR. After purification, the PCR product was quantified utilising a BioAnalyzer. These data can be seen in *Figure 4-4A*.

Average size for cDNA libraries typically ranges between 1300-2000 base pairs (bp). This is seen in both the WT and PDK<sup>K465E</sup> pooled PCR reactions, at 1550bp and 1728bp respectively. A sample (500pg) of pooled PCR product was utilised for a tagmentation reaction. The result of this tagmentation reaction is shown in *Figure 4-4B*. Post tagmentation, the average library size typically decreases to between 500-700bp, although libraries can sit outside this average and still be successfully sequenced. There is also a corresponding increase in concentration of the library, which is seen in the WT product.

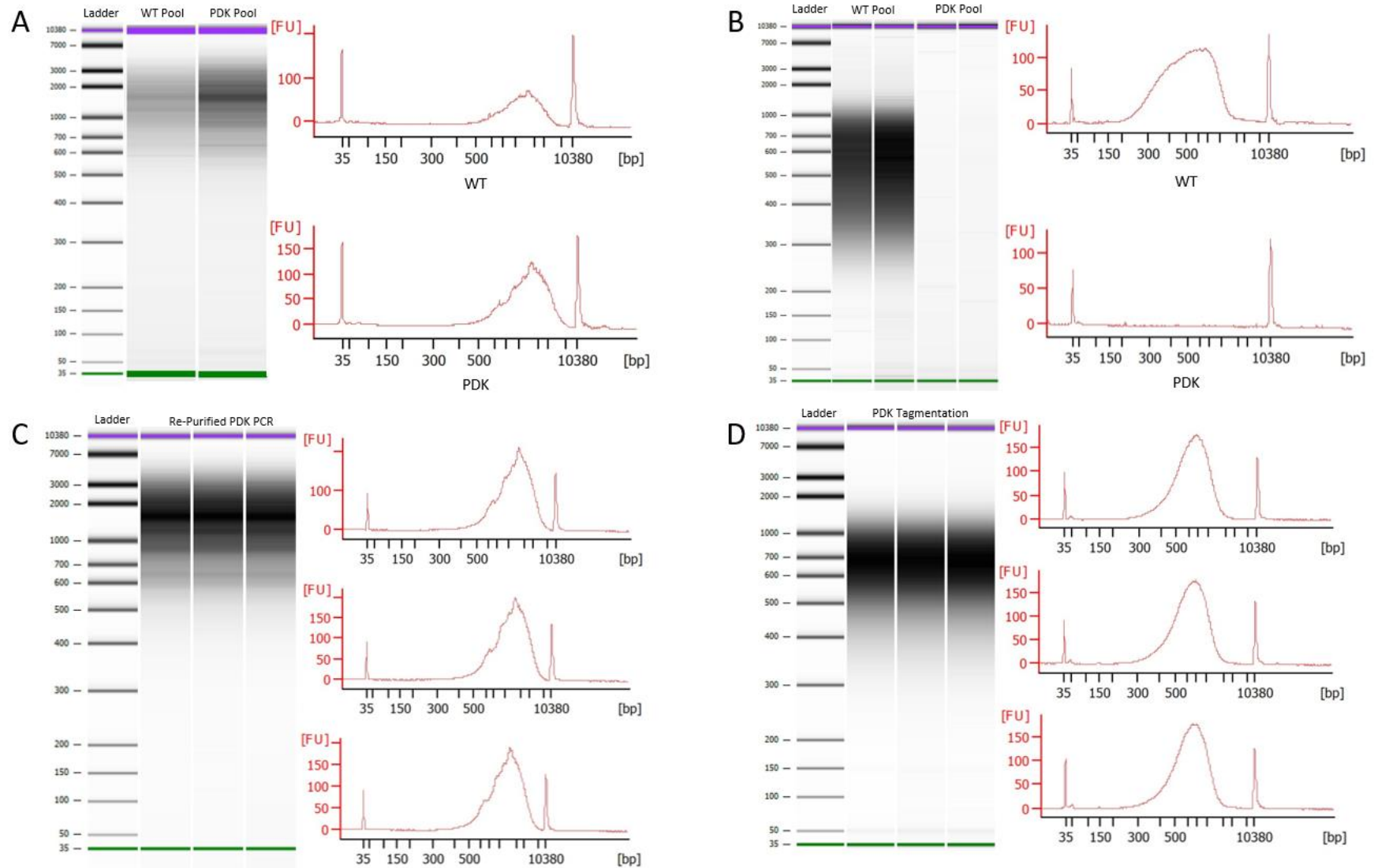


**Figure 4-4 – Quality control assessment of PCR and Tagmentation products**

**A** – BioAnalyzer traces of combined PCR pool of WT and PDK cells. **B** – BioAnalyzer traces of initial tagmentation reaction. **C** – BioAnalyzer traces of PDK PCR product after re-purification. **D** – BioAnalyzer traces of product from secondary PDK tagmentation reaction using re-purified PDK PCR product.

However, the PDK<sup>K465E</sup> sample did not generate a product post-tagmentation. Typically, lack of a tagmentation product, is due to contamination from carry-over reagents during purification. As such, the old PCR product was re-purified in an attempt to remove any contaminating reagents, then analysed once again. The new plots are shown in *Figure 4-4C*. As previously, the average size of the library was consistent with prior PCR product at approximately 1650bp, and was slightly more concentrated than before. Proceeding with tagmentation using this new PCR product yielded a successful final library. The average size of the PDK<sup>K465E</sup> pool post tagmentation was slightly larger than that of the WT, 720bp compared to 580bp respectively, as shown in *Figure 4-4D*. However, in the cases of both the WT and PDK<sup>K465E</sup>, the final tagmented libraries were sufficient in both quality and concentration to proceed to next generation sequencing. In both WT and PDK<sup>K465E</sup> samples, between 500-1200 genes were recovered per cell, with an average of approximately 850 genes and a total of 3146 unique genes being sequenced. A minimum of 200,000 reads per cell was achieved. A total of 1997 single cells were sequenced; 1118 WT and 879 PDK<sup>K465E</sup>. *Figure 4-5* shows two t-distributed stochastic neighbourhood embedding (t-SNE) plots displaying the clustering of these sequenced cells. *Figure 4-5A* represents clustering based on the differential gene expression in both WT and PDK<sup>K465E</sup> cells using the Random Forest algorithm.

This analysis package identified 7 defined populations, as well as an eighth (cluster 5) which represents cells that were unable to be associated with a particular cluster due to threshold constraints that were set as part of this analysis. This sub-threshold clustering is most likely representative of the multiple transitive cellular populations between the more defined differentiation states. As such, cluster 5 will not be included when discussing the differential gene expression patterns of each cluster later in the chapter. *Figure 4-5B* shows the same cell clustering, but the t-SNE plot has been re-assigned to show the origin of the cell type, WT or PDK<sup>K465E</sup>. By integrating the data from these two plots it is possible to assess the relative populations of the WT and PDK<sup>K465E</sup> cells in these clusters. Confirmation of CD8 expression is shown in appendix *Figure 8-1*.

In most cases, each of the clusters defined in *Figure 4-5A* heavily favour a particular cellular origin. Clusters 3, 6 and 8 were almost exclusively comprised of WT cells; conversely clusters 2, 4 and 7 were primarily cells of PDK<sup>K465E</sup> origin. Clusters 1 and 5 were the exceptions as they contained significant numbers of both WT and PDK<sup>K465E</sup> cells. The overall breakdown of the clusters in terms of their relative numbers can be seen in *Figure 4-6*.

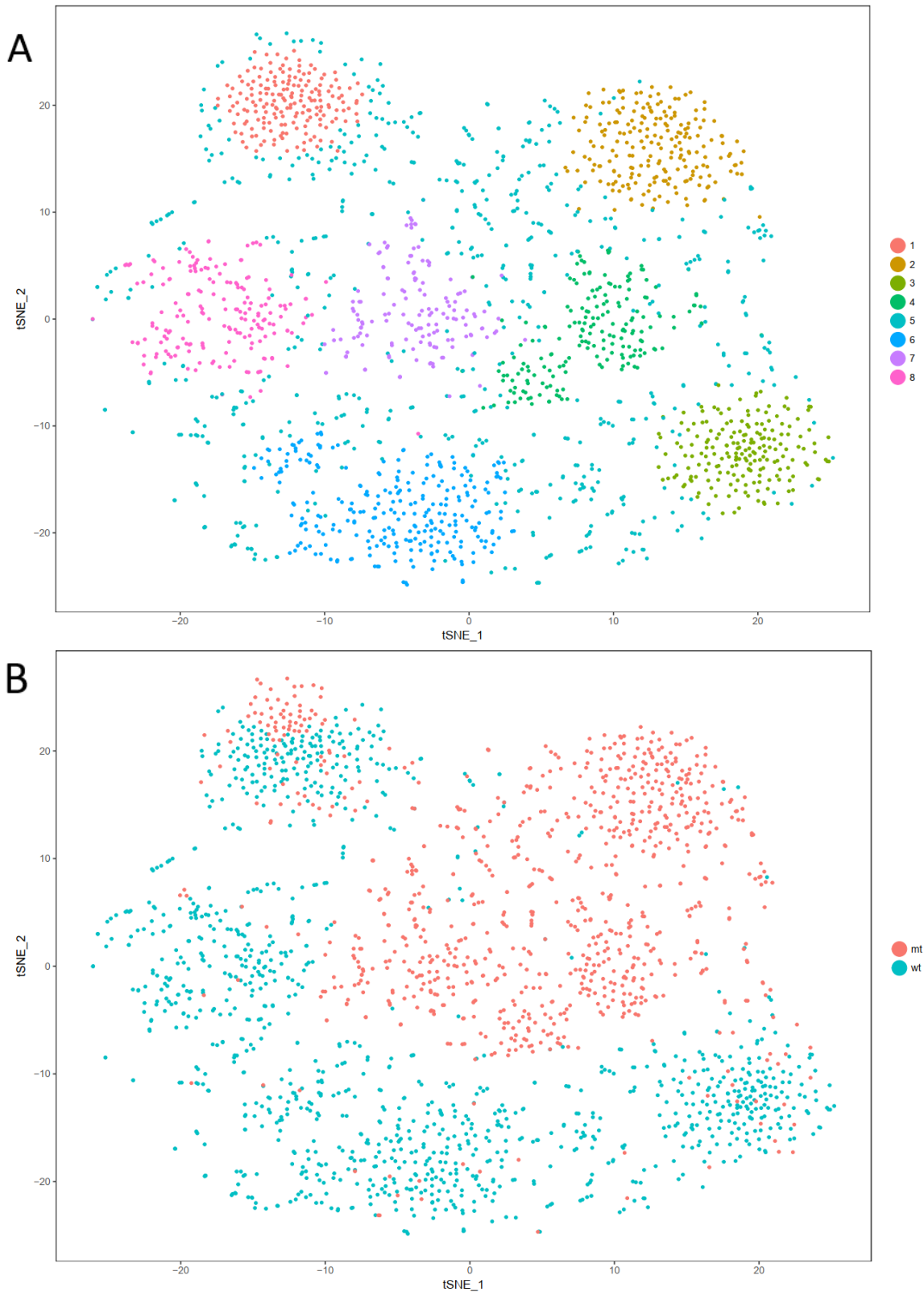


**Figure 4-5 – Drop-Seq analysis of WT and PDK OT-1 CD8 T cells 6 days post *in vivo* stimulation with listeria-OVA**

WT and PDK<sup>K465E</sup> OT-1 splenocytes were harvested and transferred into recipient C57BL/6 mice, which were subsequently challenged with  $10^6$  CFUs of  $\Delta$ ActA-LM-OVA 1 day later. 6 days after listeria infection spleens were harvested, purified by Macs CD8 negative selection kits before sorting using flow cytometry to purify the OVA-specific CD8 T cells. These OVA-reactive CD8 T cells were then subjected to the Drop-Seq protocol as described in more detail in chapter 2. Following Drop-Seq and genetic sequencing, data was processed in R studio using the Seurat package. **A** – t-SNE plot showing clustering of both WT and PDK CD8 T cells based on differential genetic expression, clusters 1-8 generated by Random Forest software. PDK<sup>K465E</sup> – mt, WT – wt. **B** – t-SNE plot showing clustering based on cellular origin type. I acknowledge Steve Thirdborough for his aid in creation of these t-SNE plots.

Assigned Cluster	WT	PDK
1	128	56
2	3	209
3	178	16
4	4	183
5	371	253
6	257	10
7	1	147
8	176	5
<b>Total</b>	<b>1118</b>	<b>879</b>

**Figure 4-6 – Population distribution of t-SNE plot clusters in Drop-Seq analysis**

Table displaying the numbers of cells present in each of the clusters of the t-SNE plot, as well as their origin phenotype.

Preliminary factors that are commonly used to determine the phenotype of CD8 T cells during an immune response were examined utilising the edgeR and Seurat packages within R studio. The focus was on the expression of transcripts encoding TCF7, IL-7R (CD127), Granzyme B, MKi-67, EZH2 and KLRG1. TCF7 and IL-7R are more commonly expressed by cells that are developing towards an MPEC phenotype compared with a SLEC phenotype. Granzyme B and KLRG1 are highly expressed on cells that display increased effector function, hence transcripts encoding these proteins are more likely to be represented in clusters favouring the SLEC phenotype. Whilst EZH2 has been associated with both effector and memory phenotypes, when combined with MKi-67, it is indicative of cells that are still actively proliferating.

This preliminary marker data is presented in *Figure 4-7*. Short of Mki-67, cluster 5 shows expression of all of these factors. As this cluster represents a loosely grouped cohort of cells, this is to be expected as they are present across the t-SNE plot and would hence likely have a broad expression of markers. Clusters 4, 7 and 8 are enriched for transcripts encoding TCF7 and IL-7R. Interestingly, this classifies three MPEC-like populations with two being of PDK<sup>K465E</sup> origin and one of WT origin.

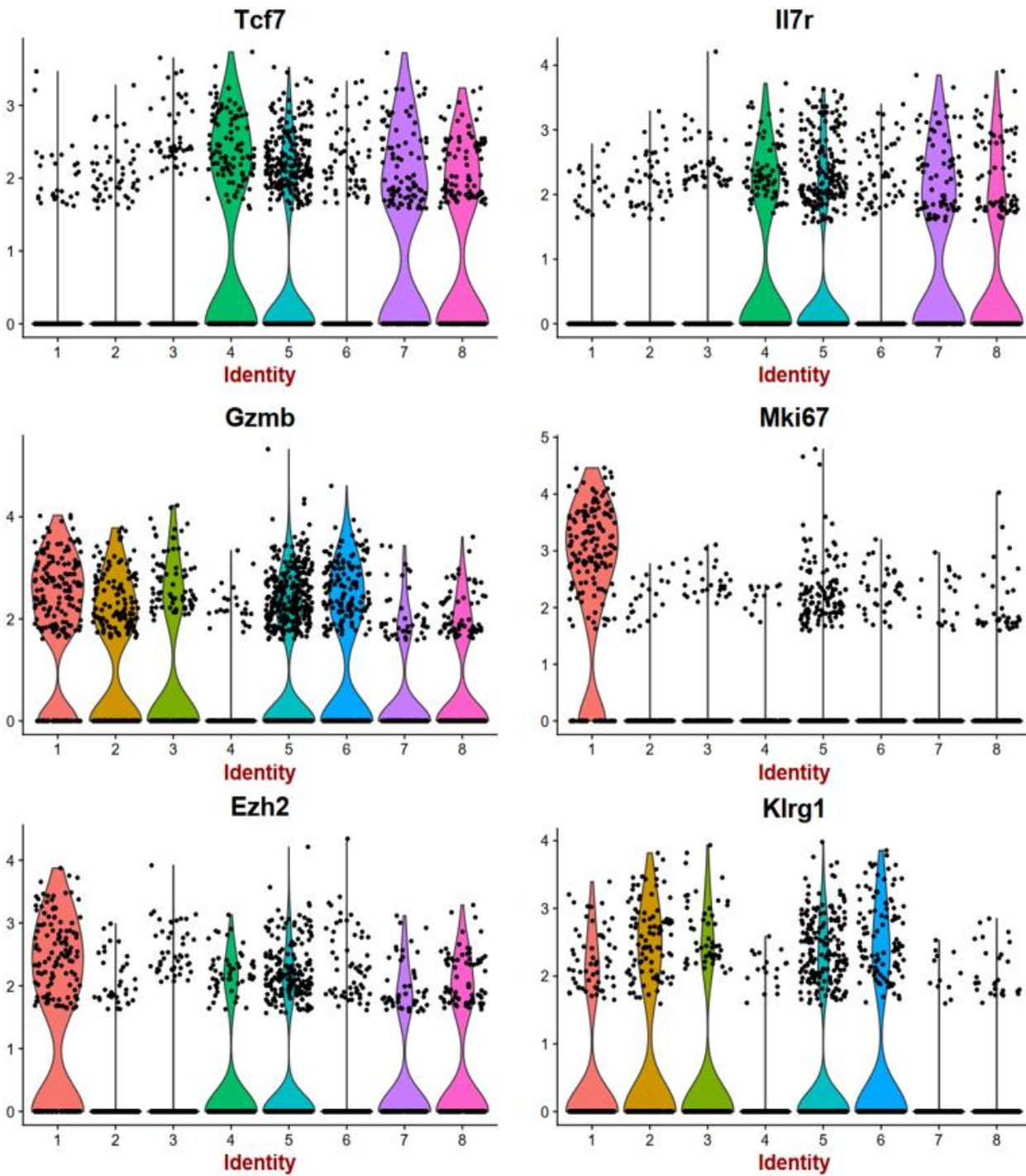


**Figure 4-7 – Phenotypic violin plots of cells analysed from Drop-Seq experiment**

Factor array used to categorise identified clusters in the t-SNE plot from *Figure 4-3* into existing known differentiation states. TCF7 and IL-7R expression is frequently associated with the MPEC phenotype. Whereas granzyme B and KLRG1 are commonly more highly expressed in SLEC phenotype compared to MPECs. Finally MKi67 and EZH2 are used to differentiate the cell cycle phase of effector cells. X-axes display cluster identity from t-SNE plots, y-axes display relative expression of these factors. Each dot represents a cell, width of violin plot is relative to the number of cells expressing the factor at that level.

Cluster 1, which is comprised of significant numbers of cells from both samples, is enriched for transcripts encoding granzyme B, EZH2 and Mki-67. This indicates not only an effector/SLEC like phenotype but that these cells are still very much in active cell cycle progression. As these cells were taken near the peak of an immune response, it is unsurprising that we find a proportion of

cells that have yet to enter the contraction phase of the response. Lastly, clusters 2, 3 and 6 show a similar enhanced expression of Granzyme B but without the corresponding expression of EZH2 and Mki-67. These three clusters also show an increase in the expression of KLRG1, a marker correlated with a more terminally differentiated effector phenotype. As such, clusters 2, 3 and 6 are more likely to form the contingent of SLECs in this immune cell pool. It is noteworthy that two of the three clusters in this SLEC like phenotype belong to predominantly WT cells, which inverts the pattern seen in the more MPEC inclined cells.

Based on these preliminary markers of differentiation, the cells in each group were classified to known existing differentiation states. These data are displayed in *Figure 4-8*, which shows that there is an overall increase in the percentage of cells favouring a more SLEC like phenotype in the WT cells. Despite there being no difference in proliferation of WT versus PDK<sup>K465E</sup> cells in any *in vitro* or *in vivo* experiments performed, the number of cells displaying signs of proliferation (i.e. EZH2 and MKi-67) are decreased in the PDK<sup>K465E</sup> cells. The most substantial difference between the two groups is in regard to the percentage of cells favouring the MPEC phenotype. The PDK<sup>K465E</sup> mutant CD8 T cells display a more than 100% increase in the number of cells preferentially

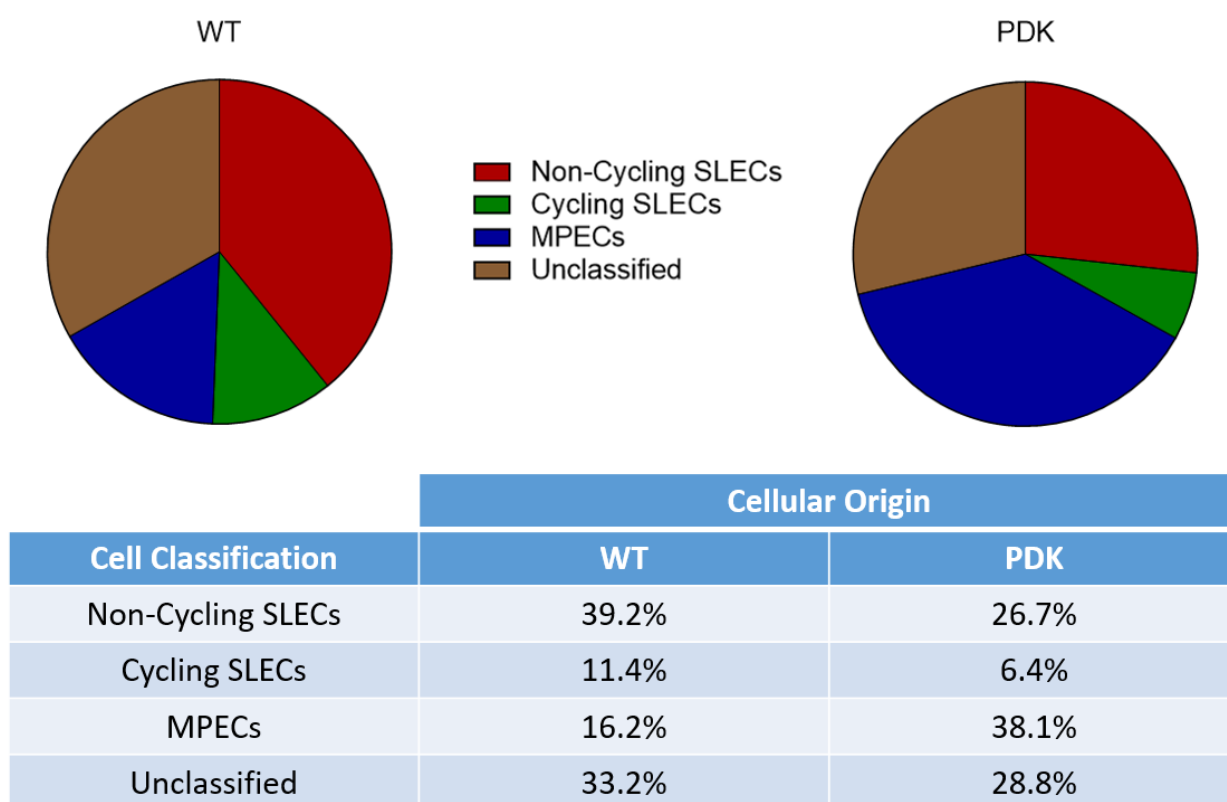


**Figure 4-8 – Classification of Drop-Seq clusters based on existing phenotypic markers**

Based on the differentiation markers utilised in *Figure 4-5* the cells are assigned to each of the classifications shown above. Non-cycling SLECs – Clusters 2, 3 + 6, Cycling SLECs – Cluster 1, MPECs – Clusters 4, 7 + 8, Unclassified – Cluster 5

expressing more factors associated with an MPEC phenotype. Overall, this suggests that the PDK<sup>K465E</sup> mutation alters the differentiation process to favour MPECs over SLECs.

### 4.2.2 Gene Set Enrichment Analysis

To compare individual clusters in more detail and using the tools available in R studio, differential gene expression was performed using the edgeR and Seurat software packages. The comparative gene lists generated through this process were then converted and sorted into a format compatible for Gene Set Enrichment Analysis (GSEA). GSEA is a computational algorithm designed to detect statistically differences between two phenotypes based on a list of input genes. This GSEA was primarily targeted at the Hallmark, Kegg and Immunological datasets from the Molecular Signatures Database (MSigDB). The Hallmark dataset is formed from aggregation of multiple sets to best represent well defined biological systems. The Kegg (Kyoto encyclopaedia of genes and genomes) dataset links genomes to specific biological pathways. Lastly the immunological dataset is derived from microarray data from studies of immune cells specifically. The combination of these databases should provide greater insight into the precise molecular process that are affected by the mutation and hopefully provide comparisons to existing analyses of CD8 T cells.

From this analysis, an intriguing trend emerged. Any comparison looking at WT vs PDK<sup>K465E</sup> clusters displayed an enrichment of genes encoding ribosomal proteins. Representative GSEA plots of this enrichment are shown in *Figure 4-9A*. *Figure 4-9B* displays a heat map of the genes encoding ribosomal proteins identified by the GSEA, ranked in order of the clusters identified in the t-SNE plots. For this and subsequent analyses cluster 5 was excluded because this cluster consists of both WT and PDK<sup>K465E</sup> cells that have failed to meet the base threshold set by the RandomForest and cutreeDynamic software, which defines the primary clusters. As such, the expression pattern of this cluster is atypical, as it contains cells that are similar to every other cluster within the TSNE plot.

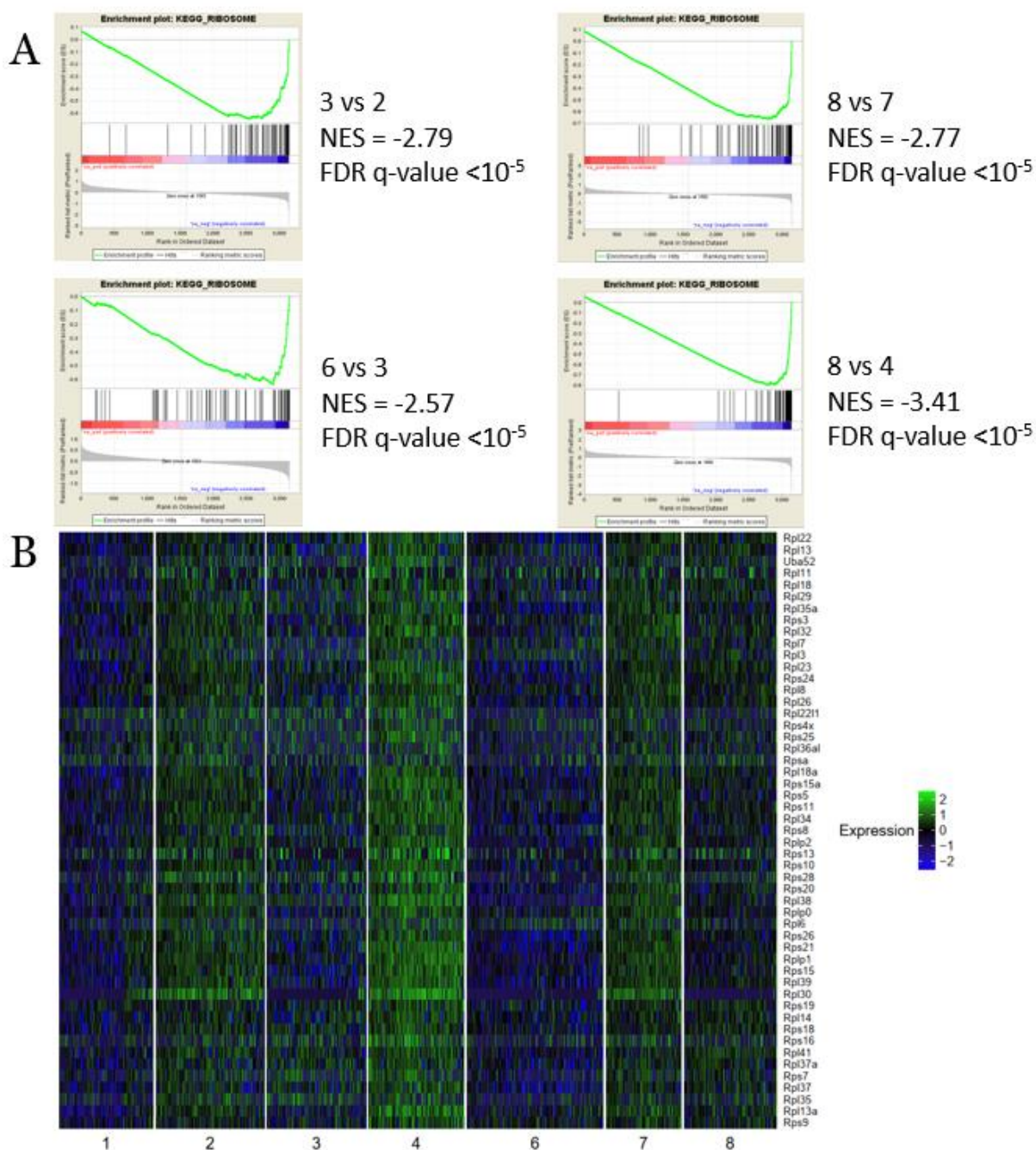


**Figure 4-9 – Genes Encoding Ribosomal protein Gene Set Enrichment Analysis (GSEA) of Drop-Seq data set.**

**A** – Representative GSEA plots of ribosomal proteins found in the KEGG database. Dataset comparisons are displayed with cluster comparison, normalized enrichment score (NES), and false discovery rate (FDR q-value). **B** – Heat map of ribosomal proteins displayed as enriched from GSEA. Cluster 5 from TSNE plot of Drop-Seq data removed due to being an unassigned cluster. X-axis shows cluster identity from t-SNE plots.

#### 4.2.2.1 Comparison of WT SLEC Subsets

As is clear from the heat map, clusters 2, 4 and 7 that are primarily PDK<sup>K465E</sup> dominated, display the highest expression of genes encoding ribosomal proteins. Interestingly, cluster 4 shows the greatest enrichment of these genes, which is of particular interest as this cluster is also the most MPEC like, based on expression of transcripts encoding the transcription factors TCF7 and CD62L. Cluster 6, a non-cycling SLEC like collection of cells, shows the least expression of genes encoding ribosomal proteins. This cluster appears to be more terminally differentiated, based on its lack of Mki67 and increased expression of KLRG1. Whilst the enrichment of the genes encoding ribosomal proteins is at its most definitive between WT and PDK<sup>K465E</sup>, it also occurs between the more effector-like and memory-like subsets within each group.

This enrichment of genes encoding ribosomal proteins is also seen when comparing the two non-cycling SLEC-like populations present in the WT cells. *Figure 4-10A* demonstrates representative GSEA plots comparing the ranked differential gene expression list between clusters 6 and 3, identified in the Drop-Seq experiment.

From this GSEA three data sets in the immunological signatures database provide insight into the differences between these two SLEC like clusters. These data sets were; a comparison of naïve vs day 8 effector cells; untreated vs IL-2 treated CD8 T cells; IL-7R<sup>lo</sup> vs IL-7R<sup>hi</sup> CD8 T cells (GSE9650, GSE39110, GSE8678 datasets respectively). From these data sets, we observe significant similarities between the gene expression of cluster 6 and that of the day 8 effectors, IL-2 treated CD8 T cells and IL-7R<sup>lo</sup> CD8 T cells respectively. The relative upregulation of genes common in cluster 6 and the cell types described above included: *Gzma*, *Gzmb*, *S1pr5*, *Cx3cr1*, *Il2rg*, *Klrg1* and *Stat4*, some of which are displayed in *Figure 4-10B*. These are factors commonly associated with an effector phenotype. One hallmark GSEA figure also associated genes enriched in cluster 6 as being involved with allograft rejection. Further examination of this hallmark dataset of allograft rejection demonstrates an array of genes that are typically associated with increased effector function in CD8 T cells, such as *Gzma*, *Gzmb*, *Stat1* and *Hif1a*. This indicates that despite both expressing markers of a SLEC lineage, cluster 6 possesses a stronger effector phenotype than that of cluster 3. Enrichment of transcripts encoding ribosomal proteins is also evident from the GSEA in this cluster comparison. Specifically, cluster 3 displays enrichment of genes encoding ribosomal proteins compared to cluster 6. This suggests that there is an inverse relationship between effector phenotype and expression of genes encoding ribosomal proteins. This is supported by the

heat map shown in *Figure 4-9*. This could indicate that the enrichment of genes encoding ribosomal proteins is not only a marker of the PDK<sup>K465E</sup> mutation, but also a new indicator of memory phenotypes in CD8 T cells.

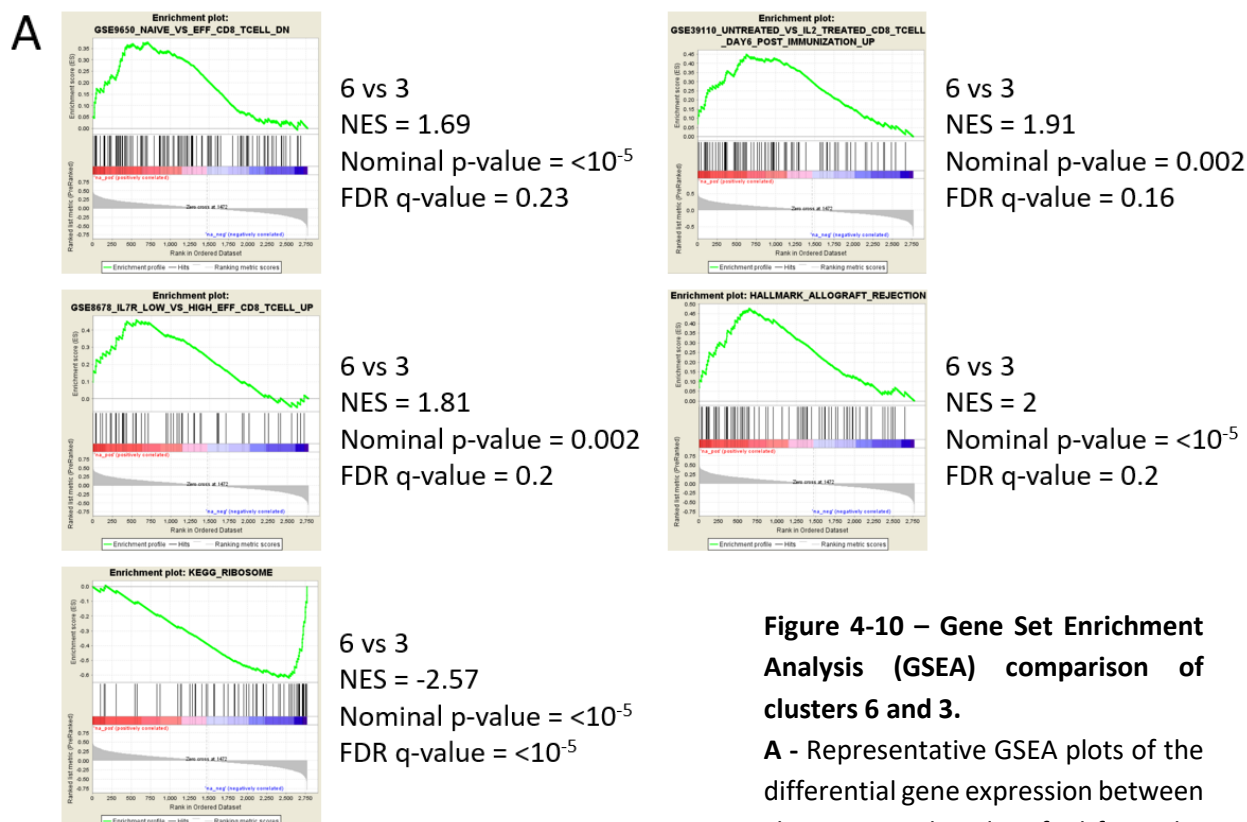
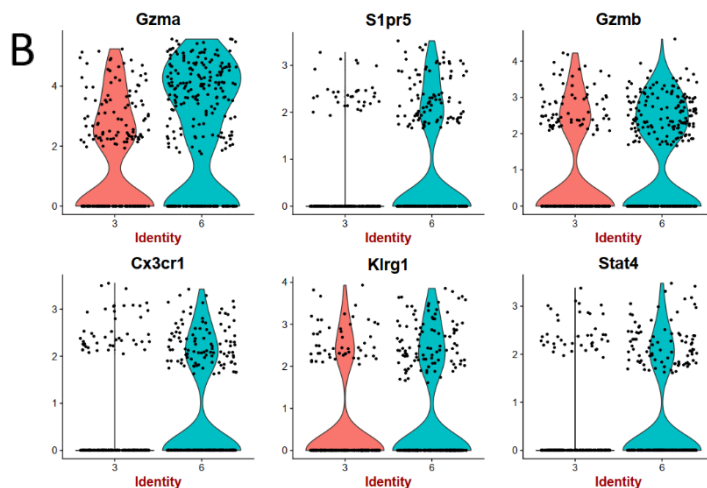


**Figure 4-10 – Gene Set Enrichment Analysis (GSEA) comparison of clusters 6 and 3.**

**A** - Representative GSEA plots of the differential gene expression between clusters 6 and 3 identified from the Drop-Seq data set. Normalised enrichment score (NES), nominal p-value and False Discovery Rate (FDR) displayed. FDR q-value is set under 25%, the score recommended by GSEA. Databases sampled, C1 – Hallmarks, C2 – Kegg and C7 – Immunological signatures. **B** – Violin plots of key effector molecules comparing cluster 3 and 6.



#### 4.2.2.2 Effects of PDK<sup>K465E</sup> Mutation on Metabolic Processes

The GSEA also revealed another effect of the PDK<sup>K465E</sup> mutation on the differentiation of CD8 T cells. By comparing WT and PDK<sup>K465E</sup> cells within similarly differentiated clusters, it is possible to observe an enrichment of genes related to oxidative phosphorylation in the PDK<sup>K465E</sup> cells, as shown in *Figure 4-11*. Whilst this seems to correlate with the ribosomal enrichment described earlier, there is a key difference. This alteration to metabolic genes seems only to be present when comparing WT to PDK<sup>K465E</sup> cells. When clusters 6 and 3 are compared, despite cluster 3 displaying a weaker effector phenotype, this mitochondrial gene enrichment is absent. Whilst increased oxidative phosphorylation is a known feature of CD8 memory cells<sup>274</sup>, it is interesting to note that when effector clusters were compared to memory clusters within WT or PDK<sup>K465E</sup> groups there was no significant enrichment of these mitochondrial genes. This indicates that the PDK<sup>K465E</sup> mutation and subsequent reduced Akt activity is a key driving force behind the increased expression of genes related to oxidative phosphorylation at this time point.

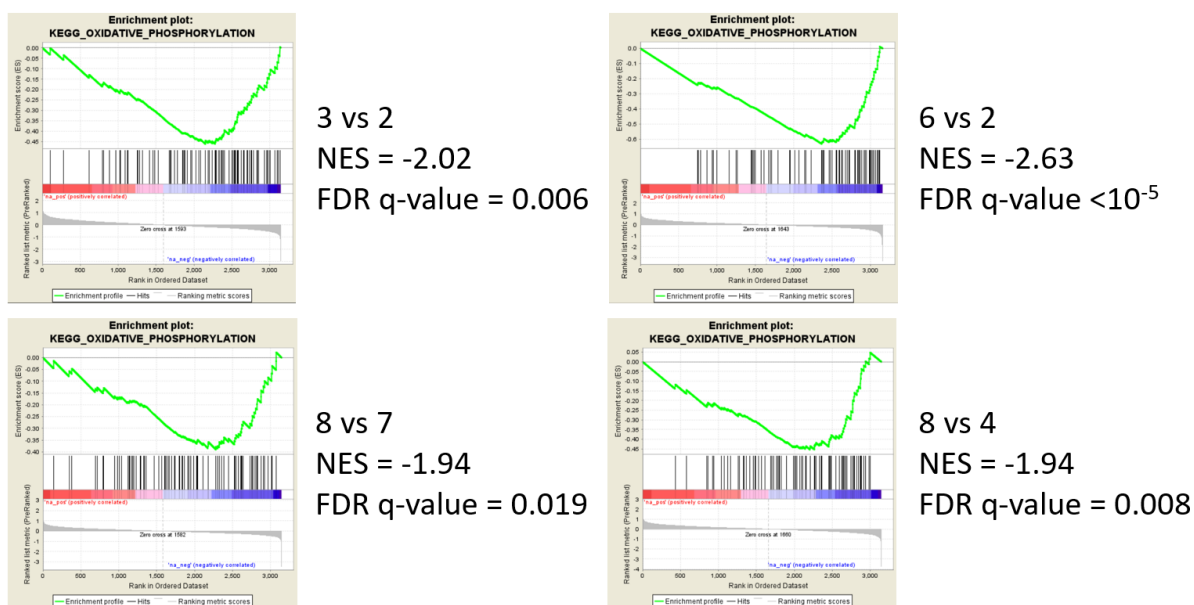


**Figure 4-11 – Gene Set Enrichment Analysis (GSEA) of Oxidative Phosphorylation.**

Representative GSEA plots. Cluster comparisons, Normalised enrichment score (NES) and False Discovery Rate (FDR) displayed. FDR q-value is set under 25%, the score recommended by GSEA.

#### 4.2.2.3 Effect of the PDK<sup>K465E</sup> Mutation on SLECs

The clusters 6, 3 and 2 were then further analysed using GSEA to determine if there were any effects of the PDK<sup>K465E</sup> mutation within the SLEC-like contingent of cells. When either the WT clusters 6 or 3 was compared to the PDK<sup>K465E</sup> cluster 2, the datasets considered enriched in both

clusters 6 and 3 were almost identical. *Figure 4-12* displays GSEA plots only from the cluster 6 versus 2 comparison, as these graphs display the best representative images of the difference in SLEC like cells between WT and PDK<sup>K465E</sup> CD8 T cells. Initially, when looking at the GSEA for the two WT clusters (6 and 3) compared with the PDK<sup>K465E</sup> cells (cluster 2), it is evident that the two primary comparisons are KLRG1<sup>hi</sup> vs KLRG1<sup>lo</sup> effectors (GSE41978) and primary vs quaternary memory CD8 T cells (GSE21360). In these data sets the WT cells were found to share gene expression with the KLRG1<sup>hi</sup> and quaternary memory CD8 T cells respectively. Increased expression of KLRG1 is a known marker of increased effector function, so it is unsurprising that the WT cells are found to have transcriptomic similarity to this dataset. Repeated stimulation of memory cells gradually decreases their proliferative potential and increases cytotoxic capacity<sup>275</sup>. Based on this, it is again predictable that both cluster 6 and 3 would have more in common with quaternary memory compared to primary memory cells. As such, these data sets confirm that despite all clusters displaying a SLEC-like phenotype compared to the total population, both the WT clusters 6 and 3 are more enriched for these effector genes, compared to the PDK<sup>K465E</sup> cluster 2.

This comparison becomes more interesting when looking at genes that are highly expressed in cluster 2. When comparing datasets of naïve and memory CD8 T cells (GSE10239), cluster 2 is defined as having a more similar transcriptomic profile to that of memory cells CD8 T cells. When individually identified genes are examined more closely, markers of certain effector function are evident<sup>276</sup>, such as IFN $\gamma$ , CRIP1 and CASP1, indicating that it is the activated nature of memory cells that is similar to cluster 2 cells. Interestingly, when studying the other GSEA plots in *Figure 4-12*, the listed genes are primarily encoding ribosomal proteins. This indicates that ribosomal enrichment is a common feature identified in other data sets. The group of Gattinoni *et al*<sup>277</sup> have previously compared the transcriptomes of CD8 T cells from WT and ID3<sup>-/-</sup> pmel-1 mice, 5 days post infection with recombinant vaccinia virus expressing human gp100 peptide. Comparing the genes differentially expressed between the ID3<sup>-/-</sup> and WT against the genes expressed in cluster 2 shows cluster 2 to be more similar to ID3<sup>-/-</sup> CD8 T cells. This is relevant because ID3 becomes more highly expressed as cells become late effectors and transition into memory CD8 T cells. Again, whilst ribosomal factors are upregulated in the WT subset of this WT vs ID3<sup>-/-</sup> comparison, markers of memory are also observed, which indicates that the PDK<sup>K465E</sup> SLEC-like compartment is more memory-like than its WT counterparts.

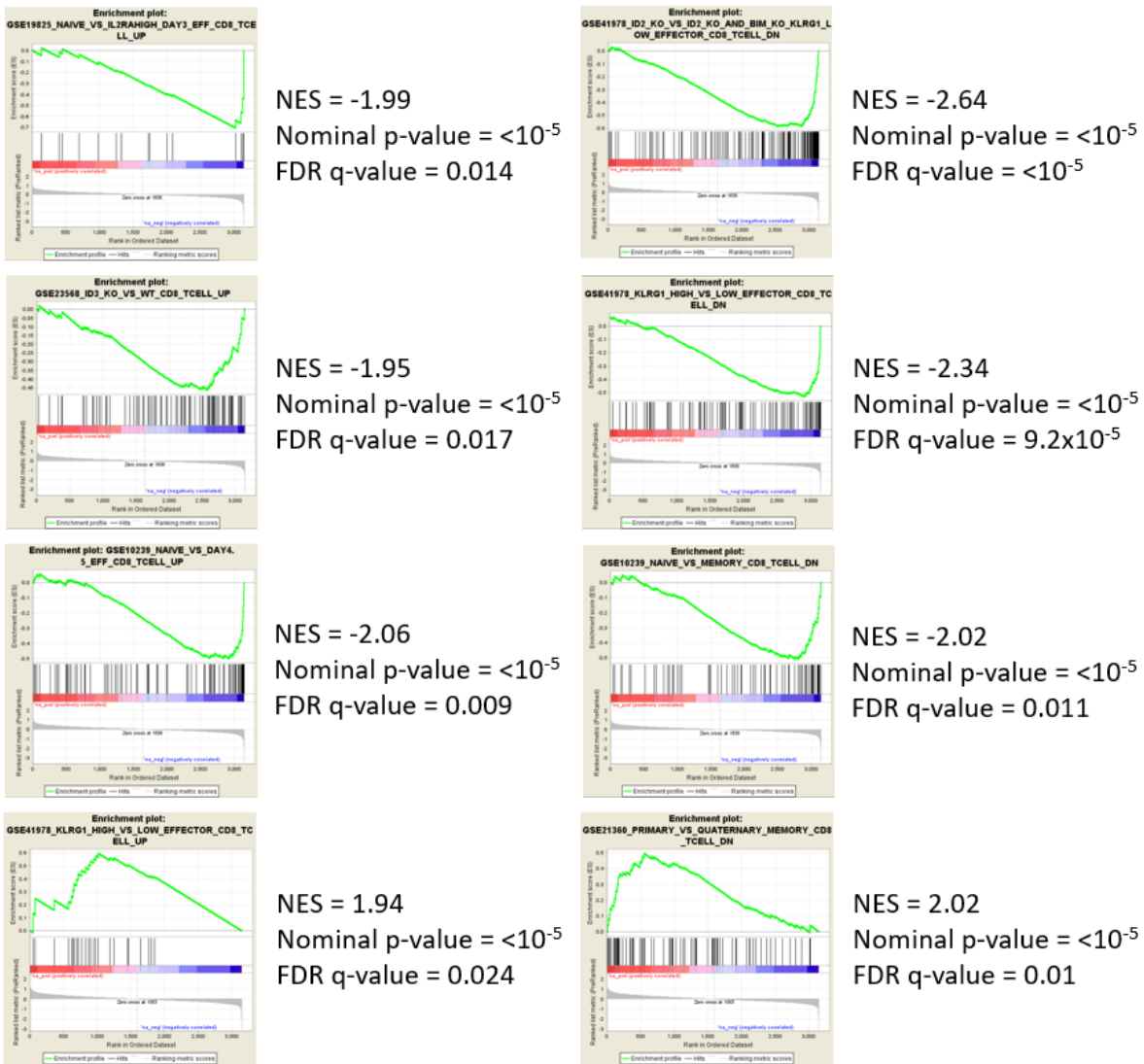


**Figure 4-12 – Gene Set Enrichment Analysis (GSEA) comparing cluster 6 with cluster 2.**

Representative GSEA plots from C7 Immunological signatures data sets. Normalised enrichment score (NES) and False Discovery Rate (FDR) displayed. FDR q-value is set under 25%, the score recommended by GSEA.

**4.2.2.4 Comparison of MPEC Subsets**

To gain greater insight into the effects of the PDK<sup>K465E</sup> mutation on the MPEC subset, the GSEA of cells from clusters 4, 7 and 8 was examined. The comparison of the two PDK<sup>K465E</sup> clusters (4 and 7) with the WT cluster 8, showed near identical GSEA plots. As such, only the plots comparing clusters 8 and 4 are shown in *Figure 4-13*, as they are the best representations of the differences in these MPEC populations. Despite clusters 4, 7 and 8 containing more MPEC-like cells compared with the total population (*Figure 4-6*), the analysis returned very similar results to that of the

comparison between the more SLEC like clusters 2, 3 and 6; in as much as the WT cells (cluster 8) were relatively enriched for genes containing effector like molecules compared to the PDK<sup>K465E</sup> cells (cluster 4 and 7). Two of the GSEA data sets, Goldrath effector vs memory CD8 T cells<sup>278</sup> and Kaech day 8 effector vs memory CD8 T cells<sup>279</sup> provided insight into the gene expression of the MPEC clusters. Reviewing the individual genes from the GSEA of the Goldrath and Kaech datasets shows that cluster 4 displays significant similarity in gene expression with the memory CD8 T cells in both of these data set comparisons. Enrichment of memory phenotype genes such as, CD62L, TCF7, KLF6, FOS and IL-7R was primarily responsible for this similarity. By comparison, the WT cells of cluster 8 resemble effector cells, based on relatively increased expression of GZMB, GZMA, Mki67 and KLRG1 which parallels the gene expression observed in the Goldrath effector cells (Figure 4-13). However, cluster 8 (predominantly WT) by comparison to the WT total cell population has the highest expression of TCF7 and IL-7R, markers associated with the MPEC phenotype. From this it can be inferred that the PDK<sup>K465E</sup> mutation enhances the MPEC like phenotype of cells that differentiate along the path towards becoming memory cells. The differences observed between clusters 8 and 4 are also present in the comparison of clusters 8

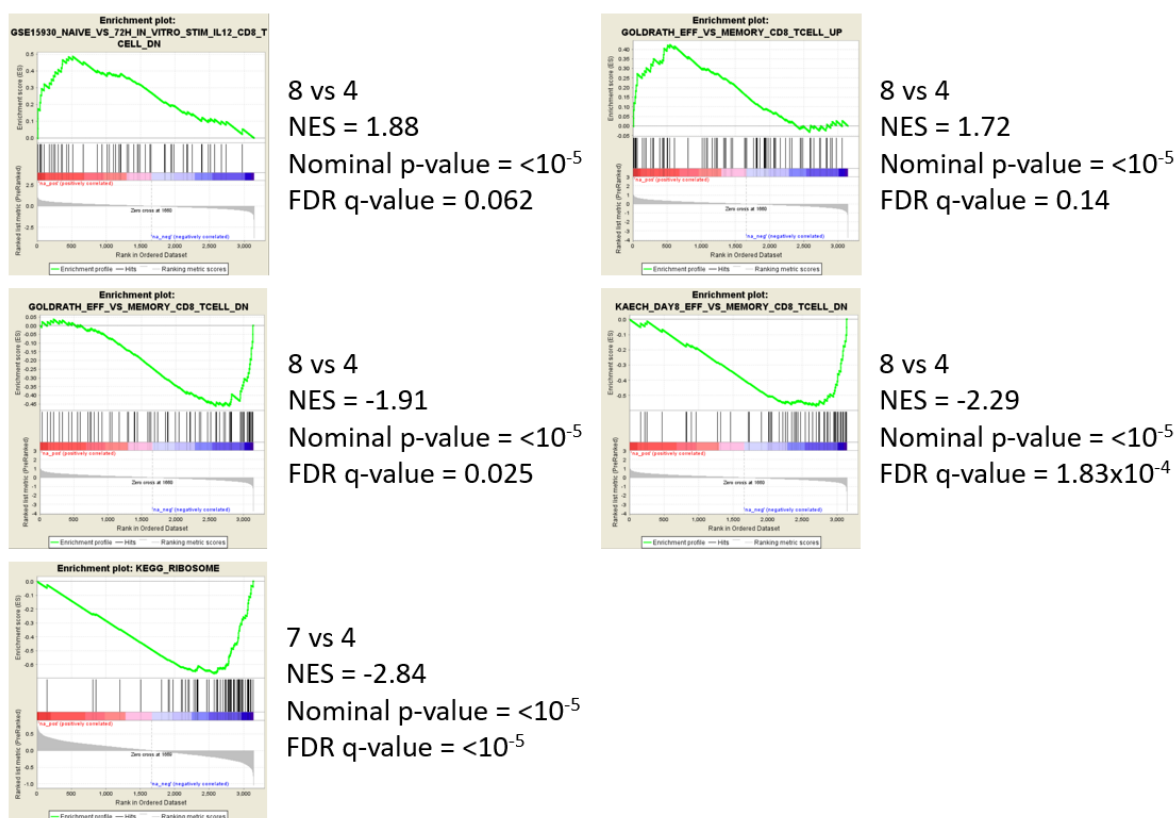


**Figure 4-13 – Gene Set Enrichment Analysis (GSEA) comparing clusters 4, 7 and 8**

Representative GSEA plots from C2 Kegg and C7 Immunological signatures data sets. Cluster comparison, normalised enrichment score (NES) and False Discovery Rate (FDR) displayed. FDR q-value is set under 25%, the score recommended by GSEA.

## Chapter 4

and 7. However, the differences are less pronounced, indicating that much in the same way that there is a stronger SLEC phenotype out of the two WT clusters 6 and 3, there is also a stronger MPEC phenotype in cluster 4 compared to cluster 7. Whilst it can be inferred from the earlier data in *Figure 4-9* it should also be noted that there is also ribosomal enrichment in cluster 4 when compared to cluster 7, further strengthening the idea that expression of ribosomal proteins is connected to increased MPEC phenotype. The GSEA plot for this ribosomal data from the Kegg database is included in *Figure 4-13*.

If there was more time available, this work could have been continued to confirm the pattern of expression observed using qPCR. Assessing whether the alterations in expression of both ribosomal and mitochondrial proteins are detectable by qPCR would greatly aid in future testing of our hypotheses regarding the role of ribosomes and metabolism in CD8 T cells. Beyond the most substantial changes, it could also be possible to recognise the signature expression patterns of the clusters at the peak of the response. This would enable us to determine whether the more complex differentiation states we observe in the Drop-Seq are present in different models.

### 4.3 Summation and Discussion

From the data shown in this chapter it is possible to come to some conclusions regarding the effects of Akt in the early differentiation of CD8 T cells.

At an earlier time point of 45 hours post infection with an attenuated OVA-expressing *Listeria Monocytogenes*, one can be confident that the overall effect of the PDK<sup>K465E</sup> mutation is minimal at best. CFSE staining revealed no clear difference in the proliferative ability of the cells. Surface and intracellular staining through flow cytometry revealed no change in the expression of IL-7R, T-bet, CD62L, Granzyme B, TCF7 and CD25. This suggests that at this early time point reduced Akt activity as a consequence of PDK<sup>K465E</sup> mutation does not affect the differentiation of CD8 T cells.

Previously, using this infection model, many changes were shown in markers of differentiation at the day 6 time point<sup>240</sup>. CD62L and CD127 were increased in PDK<sup>K465E</sup> CD8 T cells, whereas granzyme B showed a reduction in expression<sup>240</sup>. As a result, in this thesis the infection model experiment was repeated but this time the CD8 T cells were subjected to single cell RNA sequencing. The transcriptomes of these cells were then captured through the Drop-Seq process, then analysed through next generation sequencing and bioinformatics techniques. A relatively recent study published in Nature Immunology by Kakaradov *et al*<sup>280</sup> examined CD8 T cells using similar methods and managed to acquire a dataset of nearly 250 single cells spread across multiple time points. In comparison, in this thesis the process led to approximately 2000 individual Ag-specific CD8<sup>+</sup> T cells being sequenced, which makes this one of the largest single cell analyses, specifically looking at CD8 T cells at a single time point. As such, there is greater confidence in the clusters observed due to the prevalence of this much larger dataset. From these data, it is possible to observe many alterations in gene expression between the WT and PDK<sup>K465E</sup> cells. Based on current phenotypic markers used to assign cells at the peak of the response to either a SLEC or MPEC phenotype, a substantial increase in the number of PDK<sup>K465E</sup> cells expressing MPEC markers are observed. Beyond just a phenotypic change, also evident is an enrichment of mitochondrial genes primarily related to the process of oxidative phosphorylation. This metabolic shift is both a feature and cause of memory cell differentiation<sup>281,282</sup>. Again, this strengthens the argument that this PDK<sup>K465E</sup> mutation promotes an overall shift towards memory differentiation. Lastly, and most unexpectedly, is the increase in the expression of genes encoding ribosomal proteins. This enrichment appears in the comparison of WT and PDK<sup>K465E</sup> cells, within

## Chapter 4

any phenotypic group and typically comprises the most significantly differentially expressed genes. Of particular interest is the fact that this increased expression of genes encoding ribosomal proteins is also observed in the WT cells; both in the comparison of SLEC-like vs MPEC-like cells, but also between strong SLECs and weaker SLECs. As the highest expression of genes encoding ribosomal proteins is observed in the most MPEC-like PDK<sup>K465E</sup> cells, and their lowest expression is in the strongest SLEC-like cells of the WT, it is hypothesized that this PDK<sup>K465E</sup> mutation limits the progression of effector cells towards terminal differentiation and also re-enforces the differentiation in favour of MPECs. Subsequently, it can be inferred that the enrichment of these genes encoding ribosomal proteins is a new indicator of an MPEC phenotype.

However, what is the reasoning behind these changes? The overall change in subset populations would most certainly support an alteration in the differentiation of these cells. But are the changes to metabolic and genes encoding ribosomal protein expression the cause of this shift, or are they simply consequences of this mutation enforcing the stronger phenotype?

On the front of cellular metabolism there are two primary pathways to consider, glycolysis and oxidative phosphorylation. Currently, it is known that at various stages of activation and differentiation, CD8 T cells utilise different metabolic processes in order to fuel their functions. Naïve CD8 T cells are metabolically flexible and primarily catabolic in nature, exploiting glucose, amino acids and lipids to fuel the TCA cycle for ATP generation<sup>283,284</sup>. Upon TCR activation and presence of co-stimulation, CD8 T cells become more energetically demanding, so as to sustain enhanced proliferation and effector functions that they develop. This is marked by a substantial increase in levels of aerobic glycolysis; whilst less technically efficient than oxidative phosphorylation, it provides a more immediate source of ATP and metabolic intermediates necessary to allow rapid proliferation<sup>285</sup>. Recently, data has come to light, demonstrating that the most immediate metabolic changes post CD8 T cell activation are in order to induce early onset of primary effector functions. Menk *et al* demonstrated that the immediate metabolic alteration following TCR stimulation is generation of lactate through activation of pyruvate dehydrogenase (PDHK1) and engagement of lactate dehydrogenase (LDH)<sup>286</sup>. They also showed that LDH, much like GAPDH, is capable of binding to AU-rich elements in specific cytokine transcripts of IL-2, IFN $\gamma$  and TNF $\alpha$ , which prevents their translation<sup>286,287</sup>. As such, this would indicate that this immediate activation of PDHK1 acts to relieve the inhibition of these effector function related cytokines. As CD8 T cells enter the contraction phase of the immune response and develop into a memory phenotype, there is a switch towards oxidative phosphorylation once more. This time, however,

the process is more reliant on the upregulation of factors associated with fatty acid oxidation as a primary source of energy<sup>284</sup>.

The shift to a more glycolytic metabolic profile has been shown to be somewhat reliant on Akt signalling, primarily by preventing the internalisation and recycling of the GLUT1 from the cell surface<sup>288</sup>. Akt has also been shown to phosphorylate and augment that activity of the enzyme hexokinase II, as a rate limiting step in glycolysis this causes an increase in glycolytic capacity<sup>1,289</sup>. Typically, Akt would also enhance glycolytic processes in other cell types through its regulatory control of mTORC1 signalling. However, in the context of CD8 T cells, mTORC1 has been shown to be independent of Akt<sup>290</sup>. The effect of Akt on oxidative phosphorylation in CD8 T cells has not been well documented and will be examined later in this thesis. As such, it is interesting to observe that the PDK<sup>K465E</sup> mutation would appear to lead to increased expression of genes related to this process. It has been shown by multiple studies that overall increase in the level of oxidative phosphorylation relative to glycolysis within CD8 T cells can promote a shift in differentiation which favours memory cell development<sup>145,291,292</sup>. Based on the shift of PDK<sup>K465E</sup> cells to favour a memory phenotype, it is not surprising that a corresponding increase in oxidative phosphorylation is observed.

The most defining alteration in expression in this Drop-Seq dataset was the enrichment of mRNA encoding ribosomal proteins in PDK<sup>K465E</sup> cells. During CD8 T cell activation there is rapid increase in the expression of ribosomal proteins and ribosome biogenesis, in order to support the energetic and metabolic demands of an activating cell<sup>293</sup>. Analysis by mass spectroscopy has shown that approximately 250 proteins contribute to the vast majority of the proteome of activated CD8 T cells, with ribosomal proteins contributing significantly to this population<sup>294</sup>. However, the role of ribosomal proteins at later time points in CD8 T cell function and differentiation has not been extensively documented. Recently, Araki *et al*<sup>295</sup> investigated the change in translation that occurs in CD8 T cells during the course of activation. By performing microarray analyses on mRNA bound to polysomes and also the total cellular mRNA of CD8 T cells at a variety of time points, they were able to identify four separate groups of mRNAs, based on their level of expression and recruitment efficiency to the polysomes. Of particular note, the authors found that mRNAs encoding ribosomal proteins shared the same group, which was defined as having high expression but poor recruitment to polysomes. Interestingly, this group of mRNAs also contained encoded proteins relating to oxidative phosphorylation. Overall, the results of this analysis demonstrated that translation of ribosomal and oxidative phosphorylation mRNAs was upregulated following

## Chapter 4

TCR activation, but steadily decreased past the peak of the response and into the memory phase. Subsequent experiments in the same paper examined CD8 effector cells at day 8 following infection with LCMV; day 8 being considered the peak of the response in this model. Cells were separated into IL-7R<sup>hi</sup> and IL-7R<sup>lo</sup> effectors, and the proportion of ribosomal proteins mRNAs bound to each of the ribosomal fractions was examined. From this experiment, it was determined that whilst there was an overall decrease in the expression of mRNAs encoding ribosomal proteins, there was an increase in the proportion of mRNAs bound by the monosome fraction in IL-7R<sup>hi</sup> effector cells. This would suggest that through a currently unknown mechanism, the shift to monosome based translation of ribosomal protein mRNAs, as observed in the MPEC-like IL-7R<sup>hi</sup> day 8 effector cells, aids in their differentiation into memory cells.

Additionally, it has been reported that transcriptional downregulation of genes encoding ribosomal proteins is observed in exhausted CD8 T cells as a result of chronic viral infection<sup>296</sup>. Similarly, memory CD8 T cells that have undergone multiple rounds of repeat stimulation display a reduction in expression of mRNA encoding ribosomal proteins<sup>297</sup>. A key feature that is shared by chronically exhausted CD8 T cells and memory cells following repeated rounds of stimulation is impaired proliferative capacity. As enhanced protein synthesis is a critical function for proliferating CD8 T cells, perhaps the transcriptional downregulation of ribosomal proteins is in some way responsible for the restricted proliferation capacity of both exhausted and repeatedly stimulated memory cells. If this is correct, then the enhanced expression of genes encoding ribosomal proteins observed in the PDK<sup>K465E</sup> CD8 T cells could be a reflection of their skewed differentiation profile that favours a more memory-like phenotype; particularly as memory cells are known to possess a greater proliferative potential than effector and naïve cells<sup>298</sup>.

As to how the PDK<sup>K465E</sup> mutation is coupled to the regulation of ribosomal proteins, this is currently unknown. Araki *et al*<sup>295</sup> also demonstrated, through the use of rapamycin, that polysomes associated translation of ribosomal proteins was in some small part dependent on the activity of mTORC1. However, as has been shown previously, Akt does not regulate mTORC1 in CD8 T cells, nor does the PDK<sup>K465E</sup> mutation affect its activity<sup>146,240</sup>. As such, this would suggest that the regulation of these ribosomal proteins is tightly controlled, with multiple points of regulation, from both mTORC1, Akt and possibly PDK as well. Ribosomal proteins have been shown to be substrates for Akt in neuronal cells<sup>299</sup>. Specifically, RPS3 has been shown to induce apoptosis upon binding E2F1, however this interaction could be inhibited through phosphorylation of RPS3 by Akt<sup>299</sup>. RPS3 has also been shown to interact with elements of NF-κB complex, to directly enhance

its downstream gene targets<sup>300</sup>. Whilst this does suggest evidence that Akt signalling and ribosomal proteins do have interactions, the mechanism that leads alteration in expression of their genes has not been elucidated.

Whilst the mechanism behind the enrichment of these ribosomal proteins is unknown, there may be purpose to increasing the expression of specific proteins. As already mentioned, RPS3 has been shown to have extra-ribosomal function, not purely shackled to the translation process<sup>299</sup>. Interestingly, in recent years, it has been shown that whilst the majority of ribosomal proteins are stably expressed in most actively translating ribosomes, there is a subset of ribosomal proteins that are not equally expressed or utilised<sup>301</sup>. This indicates that ribosomes, even within the same cell, are more heterogeneous than previously thought. When heterogeneous ribosomes and their bound mRNAs were analysed, it was demonstrated that there was variance in the mRNA transcripts that were being translated<sup>301</sup>. This indicates that ribosomes containing specific ribosomal proteins can target different subsets of mRNA transcripts, much in the same way that RPS3 can preferentially target NF- $\kappa$ B related genes<sup>299</sup>.

The idea of specialised ribosomes is relatively new and at present, the number of studies regarding the effects of altered ribosomal protein proportions is minimal. One such study investigated the effects of differentially expressed paralogs of ribosomal proteins, within yeast cells<sup>302</sup>. Segev and Gerst demonstrated that despite having extremely high sequence homology, ribosomal protein paralogs displayed differential affinity for mRNA encoding proteins related to mitochondria and oxidative phosphorylation<sup>302</sup>. Whilst these experiments were conducted in yeast cells, it still shows enrichment of oxidative phosphorylation genes can be related to alterations in ribosomal protein composition; which parallels the Drop-Seq data presented in this chapter. Another study by Ito *et al*<sup>303</sup> examined the effect of specialised ribosomes more directly. Trypsin was used to stimulate the endocytosis process in human dermal fibroblasts (HDFs), which caused uptake of exogenous ribosomes. Upon uptake of these exogenous ribosomes, HDFs demonstrated a new capacity to transdifferentiate into a variety of new cell types, displaying new pluripotency. This displays a novel capability of specialised ribosomes, when introduced, to cause substantive changes in the ability of cells to differentiate.

From these studies, it has been demonstrated that during the course of an immune reaction, ribosomal proteins are upregulated in CD8 T cells to support the requirements of an activated

## Chapter 4

phenotype<sup>293</sup>. As cells move from the peak of the response towards memory cells, they gradually decrease expression of ribosomal proteins; as it represents an energetic investment that memory cells cannot afford<sup>295</sup>. However, some mRNAs encoding ribosomal proteins have been shown to shift a monosome based translation in cells predisposed to form long term memory cells<sup>295</sup>. Alteration in relative abundance of specific ribosomal proteins can lead to the development of specialised ribosomes, which in turn, can display preferential selection for specific groups of mRNAs<sup>302,303</sup>.

Based on the data presented in this chapter it is hypothesised that the enrichment of ribosomal proteins, in MPEC relative to SLEC, represents a new marker of the MPEC phenotype. Expanding upon this theory, it would then be suggested that the PDK<sup>K465E</sup> mutation, through a currently unknown mechanism, enhances this ribosomal enrichment further. This increased expression of ribosomal proteins alters the composition of cellular ribosomes, which in turn leads to the preferential translation of mRNAs encoding genes relating to the MPEC phenotype. This enforced stronger MPEC phenotype present in the PDK<sup>K465E</sup> cells precludes the maintenance of an effector-memory subset of CD8 T cells following the infection model. Alternatively, the enrichment of mRNA encoding ribosomal proteins could be a reflection of their increased proliferative potential as they shift into the memory phenotypes. This is based on the transcriptional downregulation of ribosomal proteins observed in chronically exhausted CD8 T cells as well as repeatedly stimulated memory cells; which demonstrate impaired proliferation.

## Chapter 5 Effect of Akt Signalling on CD8 T Cell Metabolism and Adoptive Cell Therapy of Cancer

### 5.1 Introduction

Metabolism has been touched on already in previous chapters. However, its role in CD8 T cells and the role of Akt in the multiple different metabolic pathways has not been discussed.

Within CD8 T cells there is a balance of metabolic pathways that contributes towards proper functionality of the cell. Naïve CD8 T cells are metabolically versatile, able to employ glucose, amino acids and lipids, to generate ATP through primarily catabolic processes that fuel oxidative phosphorylation<sup>304</sup>. Oxidative phosphorylation is the most effective form of energy production in mitochondria and generates ATP from oxidising electron donors, such as NADH and FADH<sub>2</sub>, produced through glycolysis, the tricarboxylic acid (TCA) cycle or fatty acid oxidation (FAO)<sup>305</sup>. This adaptability of resting naïve cells stems largely from the fact that their metabolic demands are very minor, only requiring enough to maintain homeostatic proliferation and migration<sup>306</sup>. The tonic signals from IL-7 and the TCR mediate the basal uptake of necessary glucose required to maintain cell survival<sup>307</sup>. An overview of the metabolic pathways present in CD8 T cells is shown in *Figure 5-1*.

Upon antigen encounter, TCR stimulation and co-stimulation, the metabolic profile of CD8 T cells radically shifts. As mentioned in the previous chapter, the initial metabolic change in CD8 T cells has recently been shown to be TCR mediated diversion of PDHK1 activity, to generate lactate through lactate dehydrogenase (LDH)<sup>286</sup>. This engagement of LDH relieves its binding to the ARE elements of IFN $\gamma$ , TNF $\alpha$  and IL-2 mRNA, thus allowing their translation. Therefore, the initial metabolic change serves to primarily increase the effector functions of emerging activated CD8 T cells.

CD8 T cells, at this early stage, also undergo rapid proliferation whilst increasing their cellular biomass. To support this sudden alteration in cellular function, CD8 T cells expeditiously accelerate the glycolytic pathway in order to meet the necessary energetic demands of the cell.

## Chapter 5

This is achieved primarily through the increased expression of the Glut1 receptor at the plasma membrane, ensuring an increased uptake of glucose<sup>308</sup>. This is mediated in part by Akt signalling, which prevents the internalisation and degradation of Glut1<sup>241</sup>. However, primary upregulation of the Glut1 glucose transporter is dependent on co-stimulatory signals from CD28<sup>42</sup>. The rate of glycolysis is also augmented by the phosphorylation of hexokinase enzymes by Akt<sup>309</sup>. These enzymes are responsible for converting glucose to glucose-6-phosphate (G6P) and are considered a rate-limiting step in the process. Where the principal by-product pyruvate is converted to lactate, this form of glycolysis is known as aerobic glycolysis and is the primary metabolic pathway utilised by recently activated effector CD8 T cells. This pathway generates metabolic intermediaries, such as G6P and 3-Phosphoglyceric acid (3PG). These two molecules can be utilised in the pentose phosphate and serine biosynthesis pathways respectively<sup>310</sup>. This contributes to the generation of precursors to nucleotides and amino acids, which support the increased proliferation and increase in biomass<sup>310</sup>. Whilst there is a relatively substantial increase in the levels of aerobic glycolysis in activated CD8 T cells, they do not solely rely on it for energy as there is also an increase in oxidative phosphorylation. Oxidative phosphorylation not only contributes to overall ATP level, but also leads to the generation of reactive oxygen species (ROS), which in turn is important for the activation of the transcription factor NFAT and IL-2 production<sup>311</sup>. Whilst not entirely reliant on aerobic glycolysis, it is indispensable for competent effector functions of CD8 T cells<sup>312</sup>.

mTORC1 also plays a critical role in the establishment of an activated CD8 T cell metabolic profile. This occurs primarily through two key transcription factors; hypoxia-inducible factor 1-alpha (HIF1 $\alpha$ ) and c-Myc<sup>313</sup>. HIF1 $\alpha$  is not required for initial CD8 T cell activation, however, it is needed for maximal glycolytic activity by upregulation of multiple glycolytic enzymes such as pyruvate dehydrogenase kinase 1 and lactate dehydrogenase<sup>314</sup>. The effects of HIF1 $\alpha$  in CD8 T cells have been demonstrated through deletion of its immediate upstream negative regulator von Hippel-Lindau tumour suppressor (VHL). Loss of VHL causes an increase in glycolytic rate as measured by extracellular acidification rate (ECAR), as well as a corresponding increase in certain effector functions<sup>314</sup>

Loss of VHL has also been shown to not impact memory formation, nor secondary effector responses, but did however, skew differentiation in favour of the effector memory subset of CD8 T cells<sup>315</sup>. c-Myc promotes the expression of Glut1, Glut3, hexokinase 2, glutaminase 2 and CD98<sup>316</sup>. All of these proteins contribute to increasing glycolysis, as well as the pentose phosphate

and glutaminolysis pathways, which aid in generating necessary macromolecules that support increases in cellular biomass<sup>316</sup>. Whilst c-Myc and mTORC1 are important factors for glycolysis, they also upregulate sterol regulatory element binding proteins (SREBPs). SREBPs are key transcription factors that promote genes involved with aspects of mitochondrial function; primarily those involved with lipid metabolism<sup>317</sup>.

Following the peak of the response, cells enter the contraction phase, being removed by AICD, or transitioning into memory. The transition into memory is accompanied by another metabolic shift, which reflects the differential requirements of long-lived memory cells compared to their short-lived effector counterparts. As resting memory cells do not require metabolic intermediates for macromolecule production, nor do they need nucleotide precursors to support proliferation, their need for aerobic glycolysis is greatly diminished<sup>315</sup>. The process of aerobic glycolysis is considerably more energetically costly and inefficient compared to mitochondrial oxidative phosphorylation supported by fatty acid oxidation (FAO), only generating 2 molecules of ATP per molecule of glucose; compared to a physiological maximum of 36 from full oxidative phosphorylation. The increased availability of ATP in memory cells is part of what allows their more immediate recall ability in response to antigen re-exposure<sup>284</sup>. The principal difference between the oxidative phosphorylation utilised in naïve CD8 T cells versus memory CD8 T cells, is the primary energy source. Naïve cells are capable of using glucose, amino acids and lipids to generate energy, whereas memory cells utilise FAO to as a primary source of energy. FAO and spare respiratory capacity (SRC), a measure of the ability of mitochondria to improve oxidative phosphorylation under stress, are both key markers of memory CD8 T cells.

Accelerated FAO was primarily thought to be achieved in memory cells through increased expression of carnitine palmitoyl transferase 1  $\alpha$  (CPT1 $\alpha$ ), an enzyme which represents one of the rate limiting steps in FAO<sup>318</sup>. The increased FAO and subsequent improved spare respiratory capacity is important although not critical to the development of competent memory cells, as CPT1 $\alpha$  silencing has been shown to impair but not prevent long term persistence following infection<sup>318</sup>. However, a more recent study have called into question the importance of CPT1 $\alpha$  in FAO for memory T cells<sup>319</sup>. AMP activated protein kinase (AMPK), has been shown to be important for memory generation as it acts in opposition to mTORC1<sup>320</sup>. As cells transition into memory, the factors that promote glycolysis and glucose uptake begin to decline. AMPK is capable of detecting this decline and responds by promoting the catabolic process of autophagy, which has been shown to enhance the shift towards memory<sup>321,322</sup>.

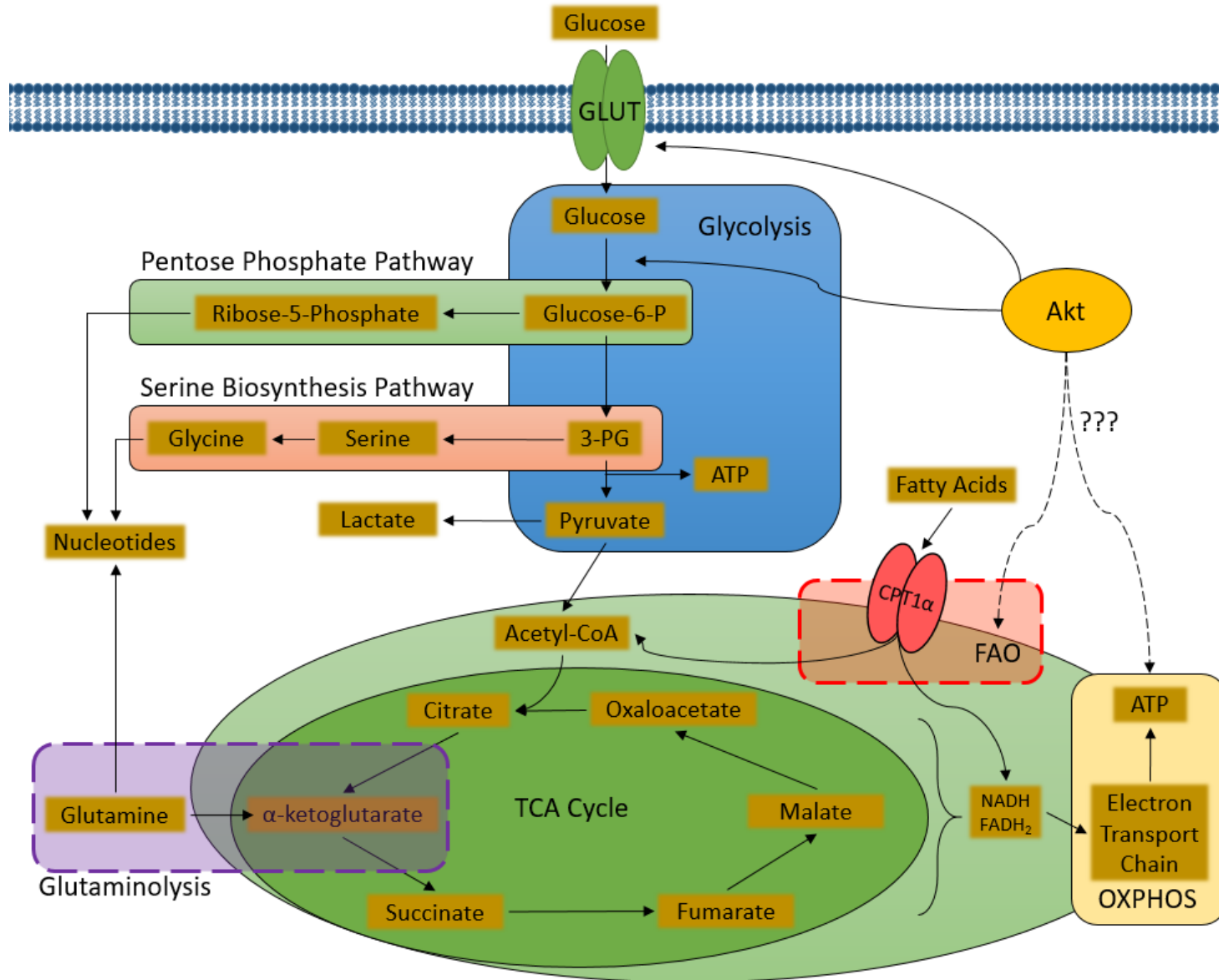


**Figure 5-1 – Metabolic Pathways in CD8 T cells.**

This figure provides an overview of the major metabolic pathways in CD8 T cells. Glycolysis, the pentose phosphate pathway, serine biosynthesis pathway, tricarboxylic acid (TCA) cycle, glutaminolysis, oxidative phosphorylation (OXPHOS) and fatty acid oxidation (FAO) all work in concert to support and influence the differentiation of CD8 T cells. Akt is known to promote expression of GLUT receptors, thus inducing increased glucose uptake. Akt also enhances hexokinases that catalyse the first step in glycolysis. However, the effects of Akt on memory related metabolic processes such as FAO and OXPHOS are not well established. 3-PG – 3-Phosphoglyceric Acid, CPT1 $\alpha$  – Carnitine palmitoyltransferase I. Adapted from Buck *et al*<sup>1</sup>

This is also reinforced by studies showing the deletion of autophagy proteins Atg5 and Atg7, which compromised the formation of competent memory CD8 T cells<sup>322</sup>.

Structural morphology of CD8 T cell mitochondria vastly influences not only their metabolic profile but also their differentiation state<sup>282</sup>. Pearce *et al*<sup>282</sup>, using confocal microscopy, demonstrated that effector CD8 T cells cultured with IL-2, display more rounded mitochondria, whereas memory CD8 T cells cultured in IL-15 show a diffuse and dense network of fused mitochondria<sup>282</sup>. Utilising chemical compounds M1, a mitochondrial fusion promoter and Mdivi-1, a mitochondrial division inhibitor can induce a more fused mitochondrial morphology in CD8 T cells cultured in IL-2<sup>282</sup>. This structural change in the mitochondria not only improves their OCR and SRC, but also induces a phenotypic change that represents a shift towards memory; characterised by increased CD62L expression and survival post transfer in mice<sup>323</sup>. Following this work, CD8 T cells cultured in IL-2, M1 and Mdivi-1 were utilised in ACT for the treatment of lymphoma cell line. The CD8 T cells treated with the compounds to enhance mitochondrial fusion, demonstrated significant delay in the growth of tumours when transferred at day 5 post tumour challenge<sup>282</sup>. However, when a greater number of CD8 T cells were transferred at day 12 post tumour challenge, the CD8 T cells treated with M1 and Mdivi-1 induced tumour regression, unlike their untreated counterparts<sup>282</sup>. Typically, the alteration of CD8 T cell phenotype induces a metabolic shift in order to meet the demands of the cell. However, it is also possible for changes in metabolism to induce a phenotypic alteration. This demonstrates that in CD8 T cells, both differentiation and metabolism are heavily integrated in order to coordinate their functions.

However, these intrinsic factors are not the only influence upon the metabolic state of CD8 T cells. Within tumour microenvironments (TME) the nutrient profile can be radically altered, primarily due to tumour cells own metabolic perturbations. The TME is typically deprived of glucose, due to the high glycolytic rate of tumour cells<sup>194</sup>. In addition, TMEs are frequently hypoxic, have low pH, high levels of reactive oxygen species (ROS) and can be depleted of a variety amino acids<sup>281</sup>. As previously stated, adequate glucose uptake is required to attain and sustain effector functions in CD8 T cells. As such, the glucose deprived nature of the TME can substantially impact their acquisition of effector functions<sup>324</sup>. Another effect of glucose deprivation is the relocation of GAPDH, which during times of glucose deprivation binds to three prime untranslated regions (3'-UTR) of IFN $\gamma$  mRNA, preventing its translation<sup>285</sup>. Lactic acid is one of the primary metabolic by-products of highly glycolytic tumours and has been shown to substantially reduce the effector

## Chapter 5

function of CD8 T cells<sup>325</sup>. Uptake of glutamine and tryptophan is also reportedly higher in cancerous cells. These amino acids are also key for T cell effector function<sup>326,327</sup>, hence the TME limiting their availability is another mechanism of suppression. Previously mentioned in the introduction to this thesis, tumours display inefficient and poorly structured vasculature due to the dysregulation of pro-angiogenic factors. This, in addition to increased oxygen consumption by tumour cells, results in the generation of a hypoxic environment. CTLs reactivated in hypoxic environments have been shown to secrete more immunosuppressive IL-10, but also to possess a higher cytotoxic capacity<sup>328,329</sup>. This indicates that the effects of hypoxia on CD8 T cells in the TME still require fuller elucidation.

Overall, metabolism plays a critical component in CD8 T cell activation and function. Initially, the changes in metabolism over the course of immune response were thought to only be to support the differential requirements of CD8 T cells at the various time points during activation. However, it is now clear that not only does the metabolic state support T cell activation, it can also influence it. In addition to intrinsic pathways, extrinsic pathways that alter cellular metabolism, such as those in TME can also significantly influence CD8 T cells. Akt has been shown to be involved in the initial alterations of glycolytic profile upon T cell activation. However, its role in oxidative phosphorylation, if any, is unclear. Given the enrichment of oxidative phosphorylation genes in PDK<sup>K465E</sup> cells compared to WT cells as shown *Figure 4-11*, the aim of experiments in the current chapter was to gain a better understanding of the involvement of Akt in mitochondrial metabolic functions.

## 5.2 Results

Initially, the aim was to examine the role that Akt plays in metabolic pathways in CD8 T cells, and in particular its effects on oxidative phosphorylation, henceforth referred to as OXPHOS.

Splenocytes from OT-1 transgenic mice were cultured in 20pM SIINFEKL peptide for two days, followed by three days of culture in either IL-2, IL-15 or IL-2 and Akti. IL-2 was used to induce a SLEC like differentiation, whereas IL-15 induced a more MPEC like state<sup>330</sup>. Cells were then subjected to measurement of their metabolic processes by a Seahorse XF analyser. Before metabolic analysis, CD62L expression was assessed in all experiments to confirm the activity of Akti, which is predicted to increase as shown in chapter 3 (*Figure 3-9*). As high Akt activity is associated with high glycolysis and a more SLEC like state, it was hypothesised that the Akti would increase the OXPHOS capacity of CD8 T cells treated with IL-2.

In these assays, cells were analysed to gain a baseline measure of OCR, followed by treatment with oligomycin, an ATP synthase inhibitor, this reduces OCR of affected cells to the absolute minimum; not accounting for proton leaking. Followed by treatment with FCCP, an uncoupling agent, this induces the maximal OCR that is possible. Lastly the cells are treated with rotenone and antimycin A, these inhibit complex I and III in the electron transport chain respectively, effectively shutting down respiration. CD8 T cells were stimulated as previously described using 20pM SIINFEKL for two days followed by cytokine culture for a further three days in the presence or absence of Akti, before their OCR was measured. *Figure 5-2* displays the results of this measurement. *Figure 5-2A* shows the recorded oxygen consumption rate (OCR) of these cells, with repeat measurements being taken every 5 minutes. Oligomycin, FCCP, rotenone and antimycin A were added after the 3<sup>rd</sup>, 6<sup>th</sup> and 9<sup>th</sup> measurement respectively. It was evident that IL-15 treated CD8 T cells had the highest maximal OCR (their baseline OCR is lower though), which is in line with having increased oxidative phosphorylation. IL-2 treated cells have a reduced capacity for oxidative phosphorylation compared with IL-15 treated cells, they are typically larger in size however, and hence display increased basal OCR.

However, maximal OCR is not the best measure of the capacity of oxidative phosphorylation because OCR can vary between experiments based on several variables, from quality of the media, pH, to the health of the cells being analysed and temperature changes. Instead, spare respiratory capacity (SRC) must be utilised. As SRC is normalised within each experiment, it is a more accurate measure of the quality of oxidative phosphorylation within cells. SRC is a measure of the cells ability to increase oxidative phosphorylation in the case of a sudden increase in energy

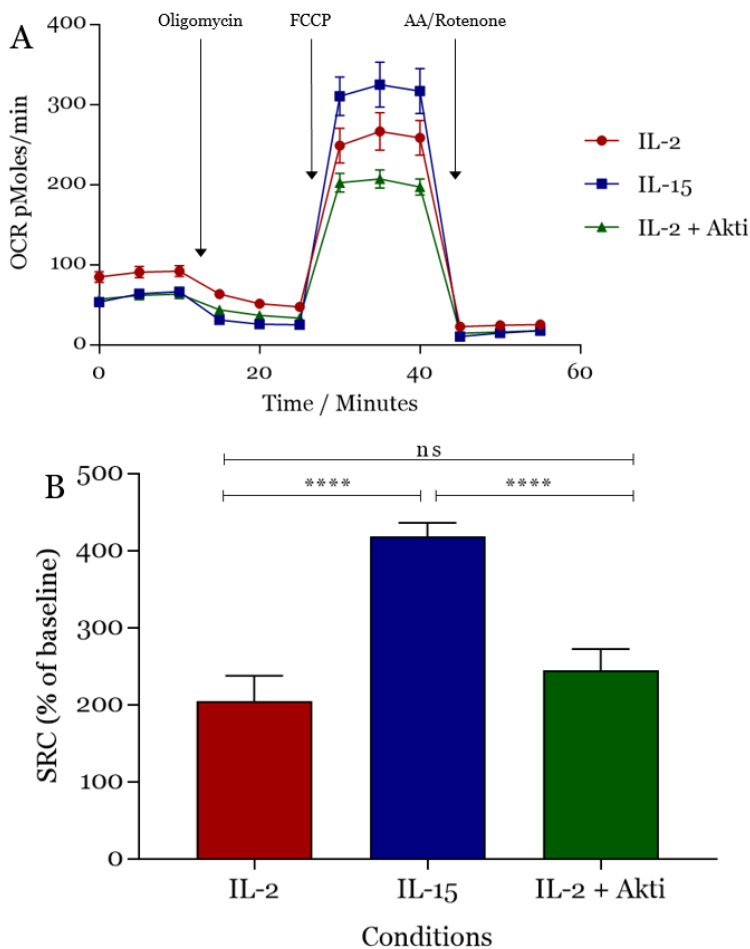


**Figure 5-2 – Effect of Akt activity on oxidative phosphorylation on CD8<sup>+</sup> T cells.**

OT-1 Splenocytes were harvested and stimulated with 20pM of SIINFEKL peptide for 2 days. After 2 days, the cells were washed and resuspended in media containing either 10ng/ml IL-2, 15ng/ml IL-15 or IL-2 in the presence of 1 $\mu$ M of the Akti for an additional 3 days. Oxidative phosphorylation measured using Seahorse XF analyser, using their recommended protocols and reagents, full protocol described in the methods section of chapter 2. 4x10<sup>5</sup> OT-1 T cells were adhered to 96 well plate using CellTak adhesive, six replicate wells per condition. **A** – Graph displaying oxygen consumption rate (OCR) over the 1 hour protocol. Oxygen levels measured every 5 minutes. After every three rounds of oxygen measurement the indicated compound was injected. Graph is representative of two independent experiments with 6 replicates wells per experiment, from one biological sample. **B** – Graph displaying the spare respiratory capacity (SRC) of cells measured in A, for a total of 12 replicates, mean and SEM displayed in both A and B, ns – not significant \*\*\*\* - p-value <0.0001, by Student's two tailed t-test

demand. SRC represents the maximal OCR as a percentage increase over basal OCR ((maximal ORC – basal OCR)/basal OCR)). Therefore SRC takes into consideration differences in basal OCR.

SRC is displayed in *Figure 5-2B*. As expected due to the low basal OCR and high maximal OCR, IL-15 treated cells had the largest SRC which was significantly and substantially higher than the SRC for either the IL-2 or IL-2 +Akti treated cells.

Interestingly, while there was no significant difference between the Akti treated and untreated cells there was a minor trend towards increased SRC in the Akti treated cells. Overall, this indicates that inhibiting Akt in IL-2 treated CD8 T cells has little effect on oxidative phosphorylation.

As a result of these data, it was decided to repeat this experiment using both WT and PDK<sup>K465E</sup> CD8 T cells to determine if the PDK<sup>K465E</sup> mutation impacts the metabolic ability of the cells. Also, in previous data, it is evident that the Akti is more effective in the PDK<sup>K465E</sup> cells, most probably due to the reduced basal activity of Akt in this cell type.

OT-1 WT and PDK<sup>K465E</sup> cells were cultured as described above, with IL-2, IL-15 or IL-2 with the Akti. *Figure 5-3A* shows the OCR of these T cells measured after 5 days in culture. In this experiment WT IL-2 treated cells displayed higher maximal OCR upon exposure to the FCCP compound than

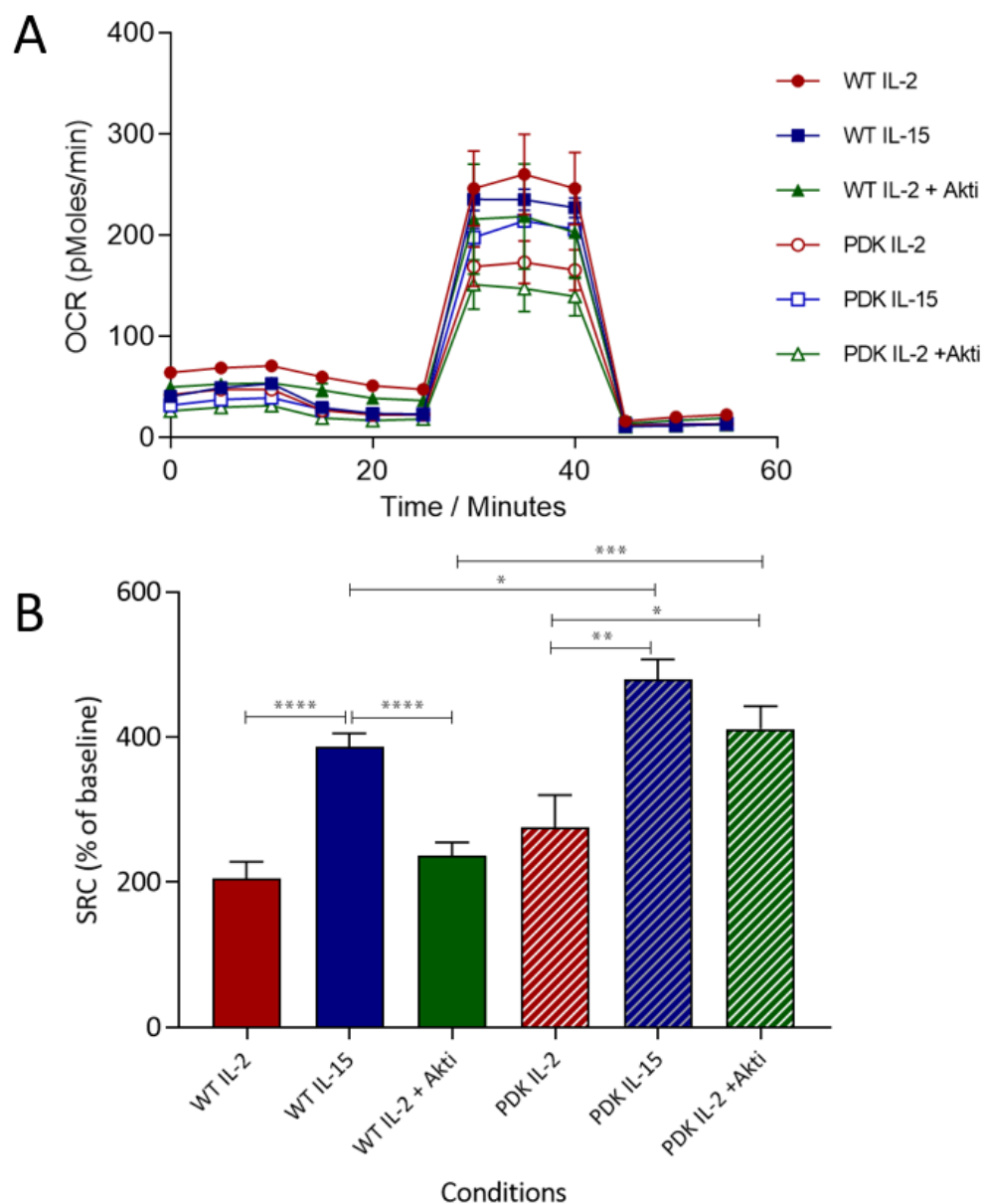


**Figure 5-3 – Effect of PDK<sup>K465E</sup> mutation on oxidative phosphorylation in CD8<sup>+</sup> T cells.**

OT-1 splenocytes from either WT or PDK<sup>K465E</sup> mice were harvested and stimulated with 20pM of SIINFEKL peptide for 2 days. After 2 days the cells were washed and resuspended in media containing either 10ng/ml IL-2, 15ng/ml IL-15 or IL-2 in the presence of 1 $\mu$ M of the Akti for an additional 3 days. Oxidative phosphorylation measured as previously described. **A** – Representative graph of two independent experiments displaying oxygen consumption rate (OCR) over the 1 hour protocol. Oxygen levels measured every 5 minutes. After every three rounds of oxygen measurement the indicated compound was injected. 6 replicates per condition **B** – Graph displaying the spare respiratory capacity (SRC) of cells measured under the same conditions as the representative graph in A. Minimum 12 replicates from two independent experiments, mean and SEM displayed for both graphs. p-value, \*\*\* <0.0005, \*\* <0.005, \* <0.05 by Student's two tailed t-test

IL-15 treated cells in contrast to the results in *Figure 5-2A*. Despite this, the corresponding increase in background OCR caused no overall change in SRC compared to the data displayed in *Figure 5-2B*; demonstrating why SRC is a more useful measure of changes in OXPHOS. Once again IL-15 treated WT OT-1 T cells showed significantly increased SRC compared to the IL-2 and IL-2+Akti treated cells, as seen in *Figure 5-3B*. Again, there was no significant effect of the Akti on the SRC of IL-2 treated WT cells, but there remained a minor increase of 15% in SRC in the Akti and IL-2 treated WT cells compared to the IL-2 treated control cells. These data reinforce the idea that Akti may have a very slight effect on OXPHOS under IL-2 treated conditions. However, studying SRC in the PDK<sup>K465E</sup> cells we observe something different. It was evident that IL-15 treated PDK<sup>K465E</sup> cells have significantly more SRC compared to IL-2 treated PDK<sup>K465E</sup> cells; paralleling the observation in WT cells. However, there was a slight decrease but no significant difference in SRC between IL-15 treated PDK<sup>K465E</sup> cells and the Akti and IL-2 treated PDK<sup>K465E</sup> cells. This indicates that when Akt activity was reduced to a far enough extent, it begins to improve the SRC of CD8 T cells despite being cultured in IL-2.

Since a reduction in Akt signalling has detrimental effects on effector function, including cytotoxicity (Chapter 3, *Figure 3-9/10*), it was predicted that this effect would dominate over the modest improvement in oxidative phosphorylation that could be beneficial for adoptive cell therapy in cancer. Conversely, augmenting the activity of Akt could improve the effector function to an extent that could translate into more efficient clearance of tumour cells, due to improvements in effector function and glycolysis. In this regard, a plasmid was utilised that expresses a myristoylated form of Akt that is constitutively active.

Myristoylation involves adding a myristoyl group, derived from myristic acid, to an N-terminal glycine residue, immediately following the initiating methionine residue. This modification is catalysed by the N-myristoyltransferase enzyme and targets a specific amino acid sequence of GSSKSKPK. The sequence was identified from the transforming effect of the retrovirus AKT8 found in rodent T cell lymphoma<sup>331</sup>. The virus could induce the formation of a constitutively active Akt through fusion of Akt with Gag polypeptide, which contained the myristoylation sequence<sup>331</sup>. The introduction of this myristoyl group to most cytosolic proteins causes immediate and irreversible association with the plasma membrane, due to the extreme hydrophobicity of the myristoyl group. In the case of Akt, it has been shown that addition of a myristoylation sequence causes the enzyme to become constitutively active<sup>332</sup>.

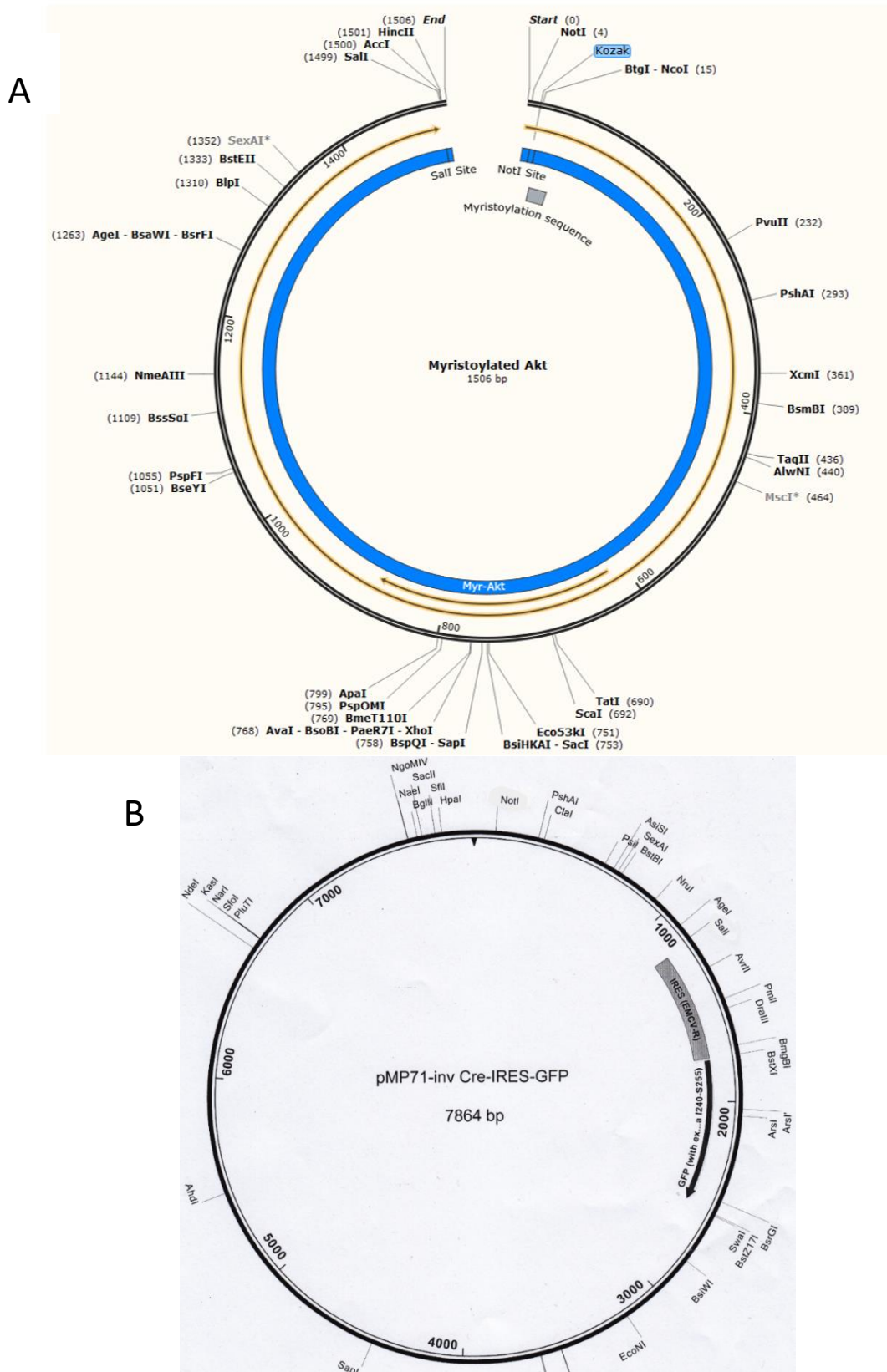


**Figure 5-4 – Schematic of Myristoylated Akt and pMP71 Sequence.**

**A** - Plasmid is designed with the NotI and Sall restriction enzyme sites at the beginning and end of the sequence respectively. These sites allow the Myristoylated Akt (Myr-Akt) sequence to be easily introduced to our control plasmid pMP71. Kozak sequence is present immediately before ATG start codon, to facilitate effective translation. Myristoylation sequence, GSSKSKPK, is added to the N-terminus immediately following the ATG start codon. **B** – pMP71 vector map, this vector contains a GFP reporter gene, ampicillin resistance gene and NotI + Sall sites. Sequence designed in DNASTAR, figure generated within SnapGene.

## Chapter 5

The map displayed in *Figure 5-4A* shows the overall structure of the myristoylated Akt (Myr-Akt) plasmid. As the intention was to utilise the retroviral vector pMP71, restriction sites NotI and Sall were added to the beginning and end of the sequence respectively, in order to allow cloning. A Kozak sequence is contained immediately upstream of the initiating ATG, to ensure translation of the construct. Lastly, the sequence that is recognised by the N-myristoyltransferase, is inserted at the N-terminal end of the Akt sequence between the initiating start codon and the rest of the protein sequence. When inserted into the pMP71 control vector (*Figure 5-4B*), subsequently transduced cells will express this Myr-Akt construct as well as GFP, which is expressed from an internal ribosomal entry sequence (IRES) in pMP71.

Viral particles containing Myr-Akt plasmid were produced through transfection of Phoenix-ECO cells with the Myr-Akt construct as well as pCL-Eco, to enhance the production efficiency of viral particles. Two days post transfection, media from Phoenix cells was used to transduce WT OT-1 splenocytes.  $10 \times 10^6$  WT OT-1 splenocytes were stimulated with  $2 \mu\text{g/ml}$  ConA,  $1 \text{ng/ml}$  IL-7 and  $5 \text{ng/ml}$  IL-12 for 18-24 hours before transduction. For the transduction, the OT-1 cells were resuspended in the virally infected media from the transfected Phoenix-ECO cells and  $10 \text{ng/ml}$  IL-2 was added to promote proliferation and thereby enhance the transduction efficiency. The culture of OT-1s, cytokines and virus media was incubated in retronectin coated wells and spin transduced in a centrifuge at 700g, for 90 minutes at  $37^\circ\text{C}$ . Following this process, the cells are left at  $37^\circ\text{C}$  for 24 hours, at which point the cells are washed and resuspended in either  $10 \text{ng/ml}$  IL-2 or  $15 \text{ng/ml}$  IL-15.

The aim of the next series of experiments was to test the effects of maximal Akt activity in an MPEC inducing culture through IL-15. This was to confirm that the increased activity of Akt induced by IL-2 was responsible for the impairment of CD8 T cell OXPHOS. Despite signalling through near identical signalling pathways, the more restricted expression of IL-15R $\alpha$  limits Akt signalling in a way that IL-2 does not, which in turns induces a more MPEC phenotype<sup>333</sup>.

*Figure 5-5A-D* displays GFP and CD62L expression, respectively. GFP expression was used to confirm presence of vector in transduced T cells and CD62L to confirm the activity of Myr-Akt. IL-15 treated cells transduced with control vector, had the highest expression of CD62L; although this was somewhat reduced compared to typical *in vitro* culture conditions with IL-15 (inferred from *Figure 3-9A*). This was likely, due to the conditions required for transduction of the Myr-Akt and control vector, which require prior treatment with IL-12 and IL-2. The IL-2 treated control

cells showed significantly reduced CD62L expression compared to the IL-15 treated control cells. However, despite culture in IL-15 the Myr-Akt transduced cells showed significantly reduced CD62L expression over both the IL-2 and IL-15 treated control samples. As these samples were gated on GFP positive cells, this confirmed that the Myr-Akt vector had been transduced. In addition, the lack of CD62L expression indicated that the myristoylation induced constitutive Akt activity. This was further reinforced by examination of CD62L expression on the GFP negative cells. *Figure 5-5B* demonstrates that the non-transduced cells within the Myr-Akt treated group possessed stronger expression of CD62L compared to the IL-2 control cells. *Figure 5-5D* displays the CD62L expression from three independent experiments, and demonstrated that the effect of Myr-Akt transduction on CD8 T cells was reproducibly induced. CD62L expression being substantially CD62L expression is only being utilised as a measure of Myr-Akt activity under IL-15 culture, no further downstream Akt targets were examined, as CD62L is directly tied to Akt activity.

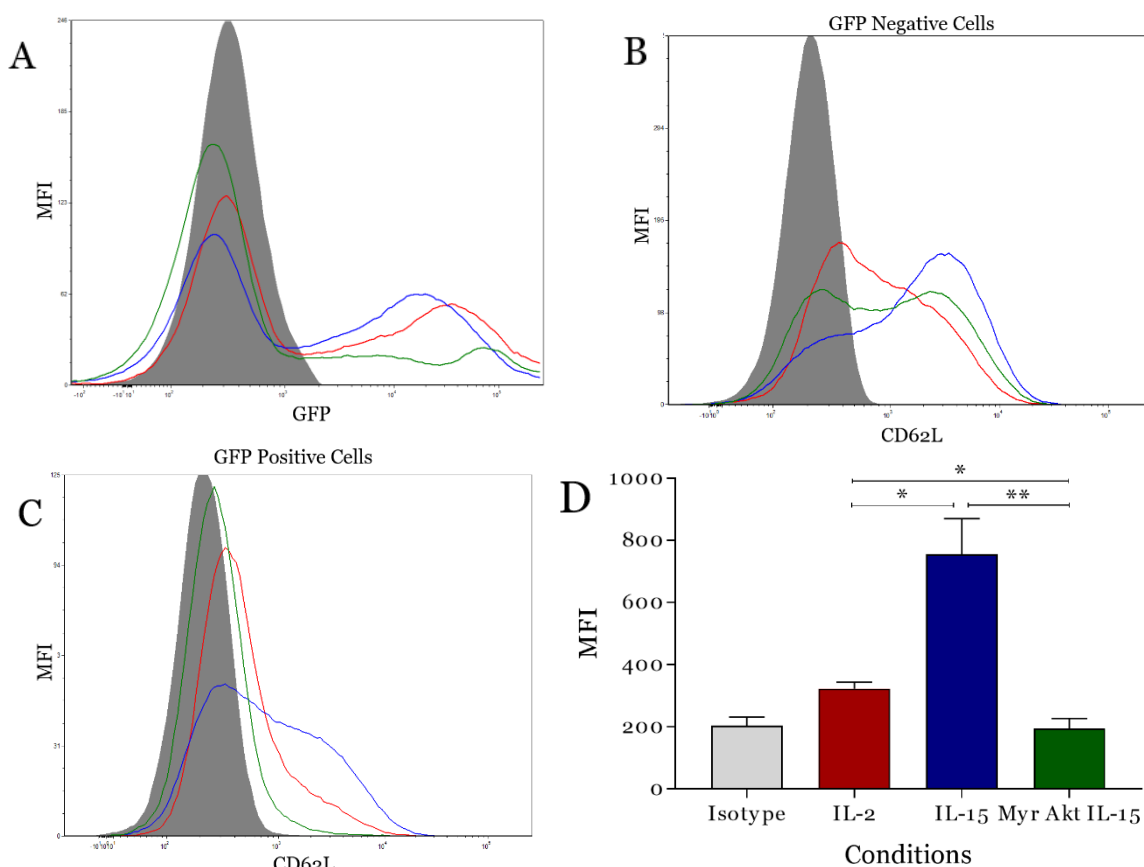


**Figure 5-5 – Representative Expression of CD62L and GFP Post Transduction with Myr-Akt.**

Following transduction protocol and two days in cytokine culture, either 10ng/ml IL-2 or 15ng/ml IL-15 expression of GFP and CD62L is measured on WT OT-1 cells. **A** – GFP expression of CD8 T cell population. **B** – CD62L expression of GFP<sup>-</sup> CD8<sup>+</sup> T cells. **C** – CD62L expression of GFP<sup>+</sup> CD8<sup>+</sup> T cells. Grey – Non-transduced control for A, representative isotype for CD62L (isotypes equivalent across all samples) in B, Red – IL-2 cultured pMP71 transduced control, Blue – IL-15 cultured pMP71 transduced control and Green – IL-15 cultured Myr-Akt transduced cells. **D** – CD62L expression gated on GFP<sup>+</sup> CD8 T cells, \* < 0.05, \*\* < 0.005. **A-C** are representative graphs, **D** is combined from three independent experiments.

## Chapter 5

Post confirmation of this Myr-Akt plasmid, its effects were tested on the metabolic profile of CD8 T cells. OT-1 WT cells were transduced as above and sorted on a FACS Aria, to purify CD8<sup>+</sup> GFP<sup>+</sup> cells transduced with either the pMP71 or Myr-Akt vector. Subsequent to the sorting the pMP71, transduced cells were cultured in either 10ng/ml IL-2 or 15ng/ml IL-15, whereas the Myr-Akt cells were only cultured in 15ng/ml IL-15. After four days further culture, the cells were subjected to metabolic analysis. As shown in *Figure 5-6*, both OCR and SRC were recorded. As before, there was significant difference between IL-2 and IL-15 treated cells, IL-15-treated cells showing substantially increased SRC. The Myr-Akt transduced cells treated with IL-15 show significantly improved SRC over the IL-2 treated cells. Conversely, there is also a significant reduction in the level of SRC in Myr-Akt transduced cells compared to the IL-15 treated control cells. This would indicate that whilst constitutive Akt activity does reduce the SRC of CD8 T cells, it does not impair it through the same mechanism as IL-2.

It is evident, therefore, that Myr-Akt transduced IL-15 treated OT-1 cells have an improved SRC compared to the IL-2 treated control cells. However, another aim was to confirm that the constitutive activity of the Myr-Akt construct did induce a more cytotoxic phenotype that would be more beneficial in an ACT setting. To this end, the cytotoxicity assays that were performed in a previous chapter (Chapter 3, *Figure 3-9/10*) were repeated. Once again, OT-1 cells were transduced with either pMP71 or Myr-Akt vectors, sorted on GFP<sup>+</sup> cells and subjected to the cytotoxicity assay described in chapter 3. One key difference for these experiments was that the ConA stimulus at the beginning of the transduction process was replaced with 100pM SIINFEKL. This concentration of SIINFEKL is five times the typical amount given in order to mimic the stronger stimulus of ConA. Preliminary experiments (not shown) indicated that if the cells were not primed with SIINFEKL they do not respond effectively in this cytotoxicity assay.

The results of this cytotoxicity assay are shown in *Figure 5-7*. With the transduction protocol, there is a slight reduction in effective cytotoxicity compared to previous experiments (*Figure 3-9*). As before, the reduced Akt activity between IL-15 and IL-2 was reflected in the cytotoxic assay, as the IL-15 treated cells showed a complete inability to kill the target cells. At the lowest effector to target ratio, IL-2 treated control cells showed an ability to kill 30% of target cells. This increased at the 1:1 ratio to between 50-60% and was maintained at higher effector to target ratios. The Myr-Akt transduced cells cultured in IL-15 showed an almost identical ability to IL-2 control cells in terms of cytotoxic capacity. As part of this experiment, the expression of Granzyme B was also

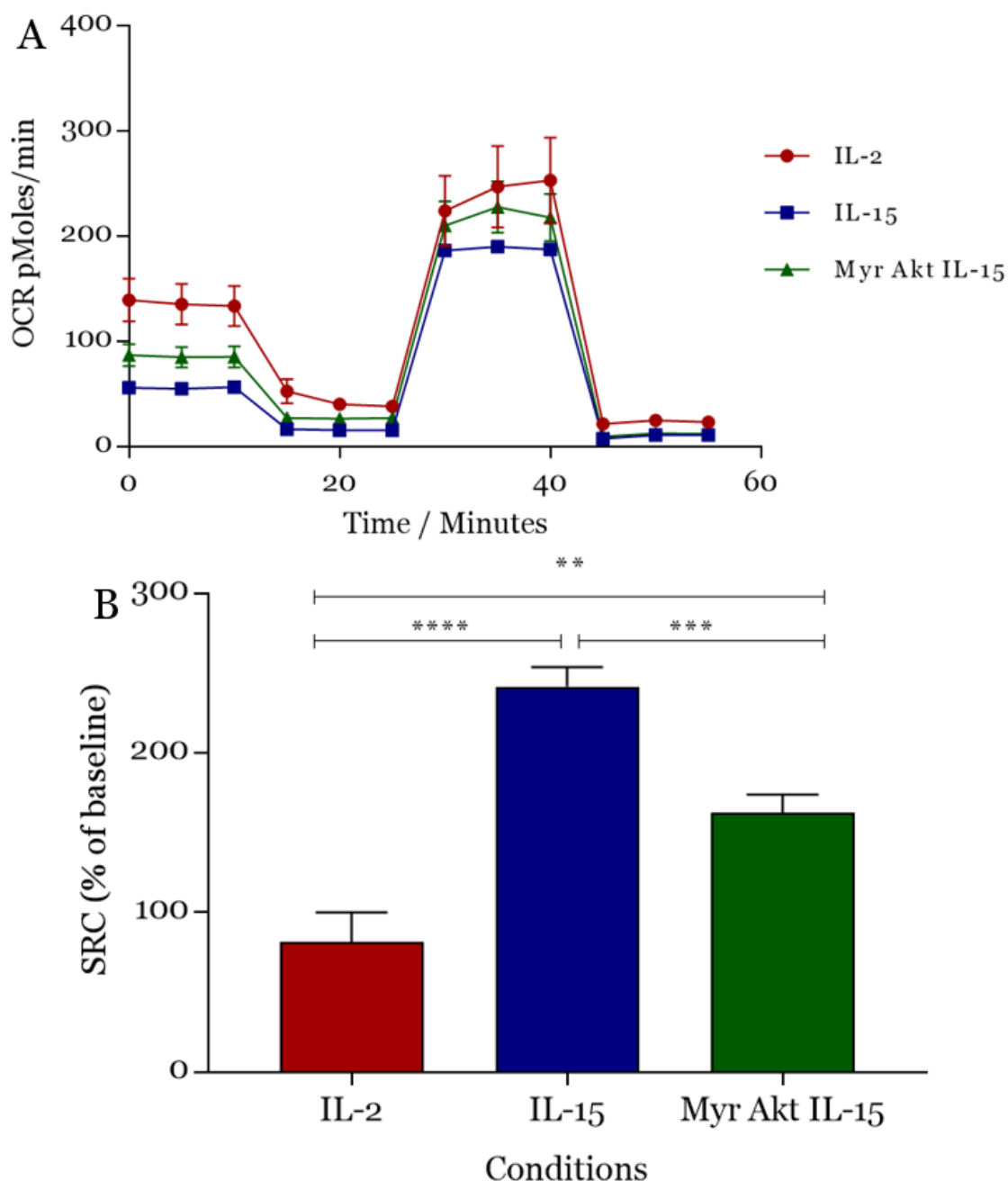


**Figure 5-6 – Effect of transduced myristoylated Akt on oxidative phosphorylation in CD8<sup>+</sup> T cells**

Phoenix-ECO cell line was cultured to 50-70% confluency. Subsequently transfected with pCL-Eco and either Myr-Akt construct or an empty pMP71 vector as a control, cell culture maintained for 2 days. WT spleens were harvested and splenocytes cultured at a density of 2M/ml in 5ml of media containing 2 $\mu$ l ConA, 1ng/ml IL-7 and 5ng/ml IL-12. 18-24 hours post stimulation with ConA and cytokines, splenocytes are washed and resuspended in the supernatant from the Phoenix-ECO culture. New cell suspension cultured in RetroNectin (TaKaRa) coated plates, with addition of 10ng/ml IL-2. Cells undergo spin transduction, 700g for 90 minutes at 37°C. After 24 hours in IL-2, cells are resuspended in fresh media with the cytokines displayed above, 10ng/ml IL-2 or 15ng/ml IL-15 for a further 48 hours before being sorted through flow cytometry and undergoing measurement of oxidative phosphorylation, as previously described. **A** – Graph displaying oxygen consumption rate (OCR) over the 1 hour protocol. Oxygen levels measured every 5 minutes. After every three rounds of oxygen measurement the indicated compound was injected. **B** – Graph displaying the spare respiratory capacity (SRC) of cells measured in A. Both A and B display a combination of two independent experiments, 6 technical replicates from a single biological sample per experiment, mean and SEM displayed across both graphs. p-value \*\*\*\* <0.0001, \*\*\* <0.0005, \*\* <0.005 by Student's two tailed t-test

analysed to determine if Myr-Akt improved its expression. From *Figure 5-7B* it is evident that as

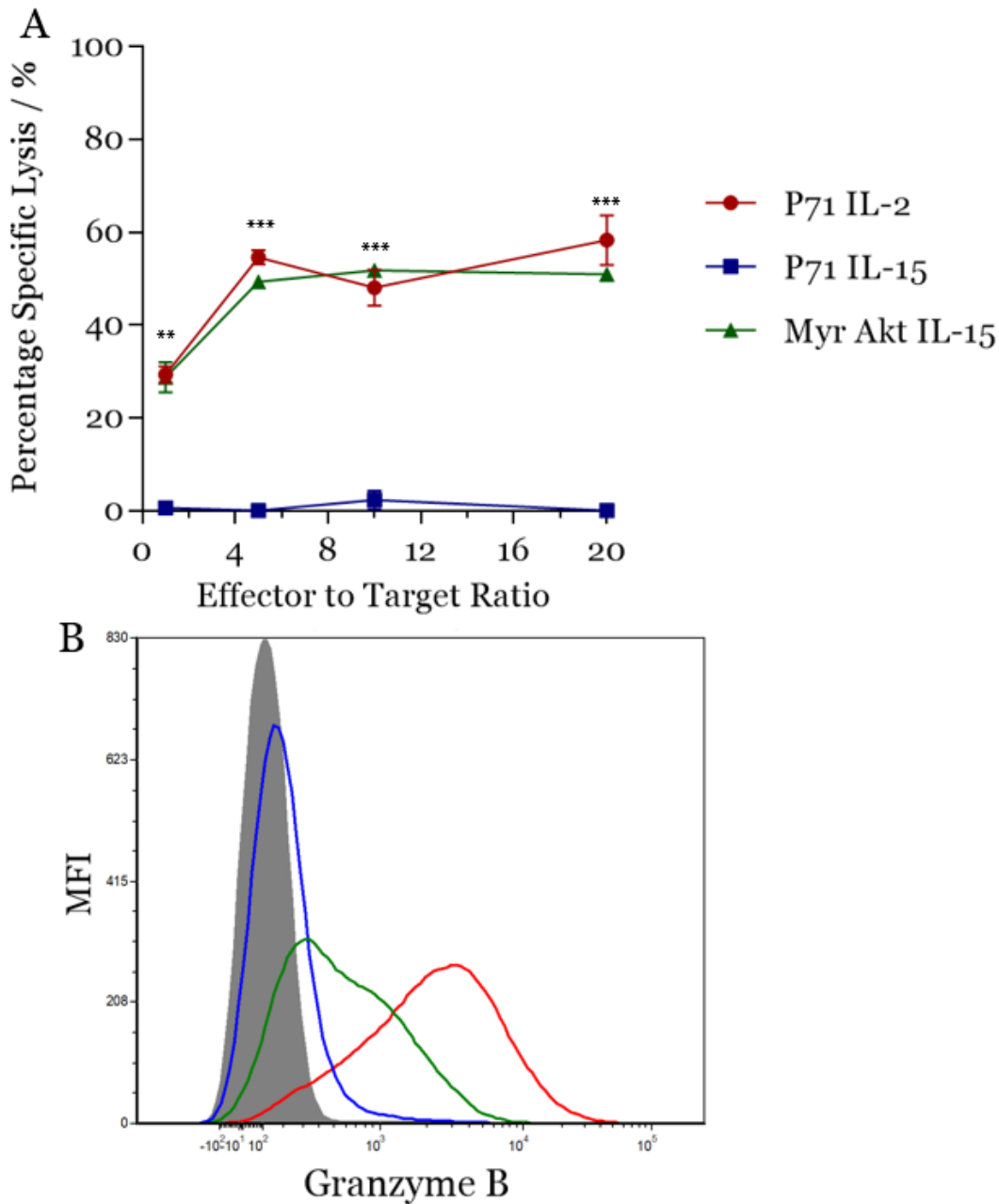


**Figure 5-7 – Effect of transduced myristoylated Akt on CD8 T cell cytotoxicity**

OT-1 transduced cells produced as previously described. Purified transduced cells were subjected to the cytotoxicity assay previously described. **A** – Displaying cytotoxic ability of transduced OT-1 cells,  $1 \times 10^5$  target cells pulsed with  $1 \mu\text{M}$  SIINFEKL, mixed with transduced cells at ratios displayed. Cytotoxicity measured 5 hours later in triplicate from a single sample. p-value \*\*\* < 0.0005, \*\* < 0.005 by Student’s two tailed t-test. **B** – Expression of Granzyme B from transduced OT-1 cells before cytotoxicity assay performed in A. Grey – representative isotype, Red – IL-2 treated pMP71 transduced control, Blue – IL-15 treated pMP71 transduced control and Green – IL-15 treated Myr Akt transduced

expected, IL-15 control cells barely expressed granzyme B, whilst its expression was high in the IL-2 treated control cells.

Again, it is interesting to note that the Myr-Akt transduced cells do have substantially more Granzyme B than the IL-15 control cells. However, the expression sits between the IL-2 and IL-15 control cells. Clearly, the expression seen in the Myr-Akt transduced cells is enough to see the

maximal cytotoxic effect as part of this assay. Indicating that granzyme B may be excessively expressed in IL-2 cells compared to the Myr-Akt transduced cells.

The two previous experiments, showed that by transducing cells with a myristoylated Akt construct and culturing them in IL-15, cells can be generated that possess equal cytotoxic competency to IL-2 treated cells, but without fully impairing oxidative phosphorylation. To address if expression of constitutively active Akt confers an advantage in an ACT setting, a tumour challenge experiment was performed.

C57BL/6 mice were injected subcutaneously with  $0.5 \times 10^6$  EG7-OVA tumour cells and left to propagate for one week. During this time, WT OT-1 splenocytes were harvested and transduced as previously described with either pMP71 or Myr-Akt, sorted and purified for GFP<sup>+</sup> CD8 T cells, and cultured further in IL-2 or IL-15. Following this procedure,  $1 \times 10^6$  of these transduced CD8 T cells were introduced intravenously into the tumour bearing mice.

*Figure 5-8* shows the combined results of two repeats of these experiments. *Figure 5-8A* shows no difference in tumour growth in mice treated with IL-15 expanded T cells compared to mice that did not receive ACT. Initially, there was a significant delay in tumour growth on days 14, 16 and 18, in those mice that received the IL-2 treated cells or IL-15 treated Myr-Akt transduced cells compared to no ACT or IL-15 control groups. However, this delay was not maintained at later time points. When examining overall survival, shown in *Figure 5-8B*, the early growth delay did not lead to increased average survival time. However, in the case either of the repeated experiments, the IL-2 treated and Myr-Akt transduced IL-15 treated cells always resulted in one mouse out of the group of five showing complete regression of the tumour out to 100 days. Whilst this by no means demonstrated a clear and effective therapy, it did show that by using myristoylated Akt the cultured cells were as effective as IL-2 stimulated CTLs, despite being cultured in IL-15.

During these experiments, whilst detectable in blood samples, the Myr-Akt transduced cells were observed at a considerably lower frequency than their control counterparts. Given this, it was decided to investigate whether the Myr-Akt transduced cells were impaired in their ability to survive and/or proliferate *in vivo*.

To analyse whether the Myr-Akt transduced cells do possess a defect in *in vivo* survival and/or proliferation, an *in vivo* restimulation assay was performed. CD45.1<sup>+</sup> WT OT-1 cells were transduced with pMP71 or Myr-Akt constructs, purified by sorting and cultured in IL-2 or IL-15, as previously described. 1x10<sup>6</sup> cells were injected intravenously into recipient C57BL/6 mice and tracked over the course of 2 weeks. 24 hours post injection of the cells the mice received 30

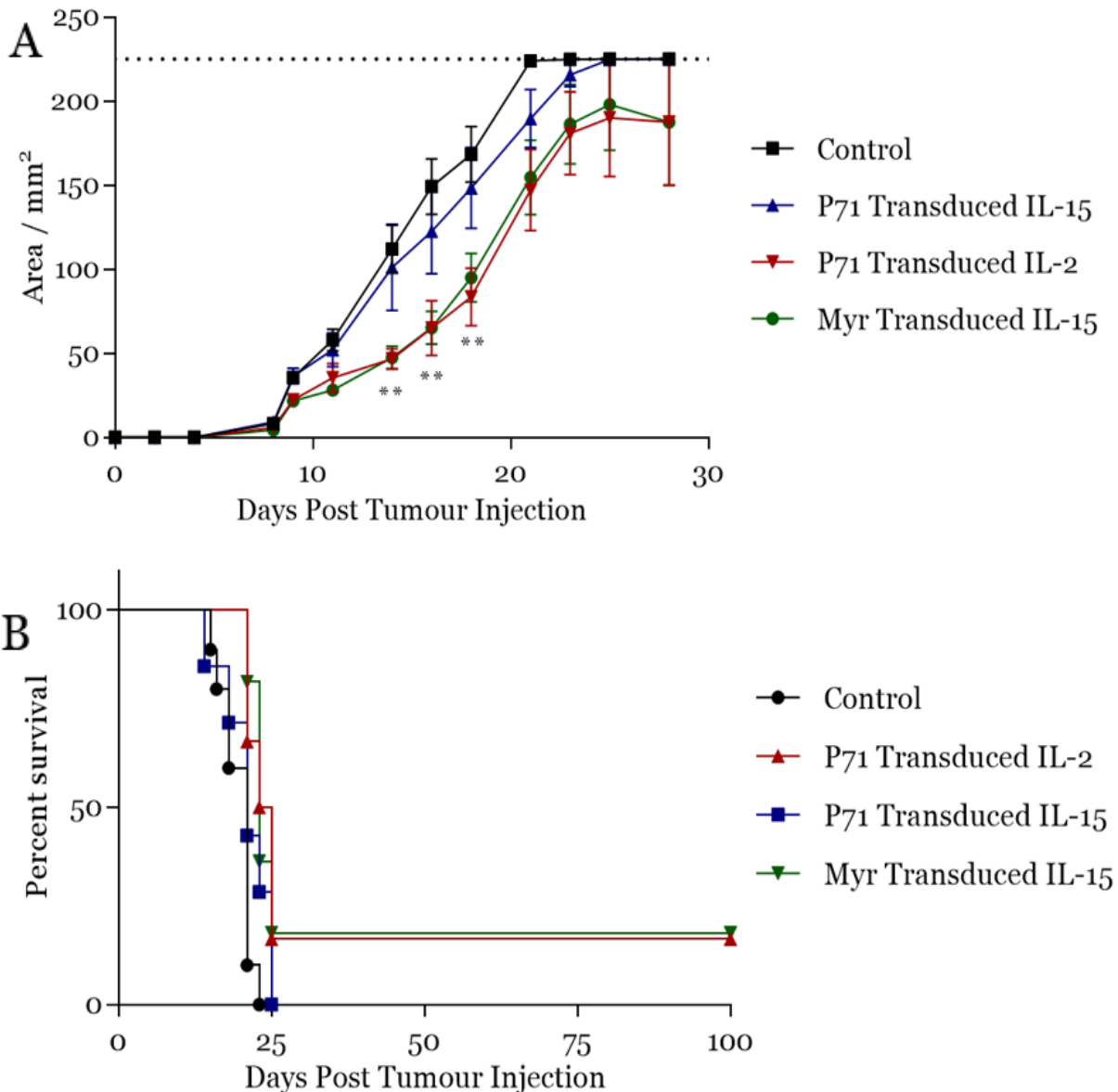


**Figure 5-8 – Adoptive cell transfer utilising Myr-Akt transduction for tumour therapy**  
 pMP71 and Myr-Akt transduced OT-1 cells produced as previously described. Five C57Bl/6 mice per group received 0.5x10<sup>6</sup> EG7-OVA subcutaneously. One week later 1x10<sup>6</sup> transduced and purified OT-1 cells were injected intravenously into three groups of mice; one additional group received PBS alone as a control. **A** – Developing EG7-OVA tumours were measured and area recorded and displayed in the graph above. Points represent group means and SEM. Mice were culled once tumours reached 15x15mm in average size (dashed horizontal line), or at day 100, whichever comes first. p-value \*\* <0.005 by Student’s two tailed t-test, comparing P71 transduced IL-2 and Myr transduced IL-15 with P71 transduced IL-15 and no cell control. **B** – Kaplan-Meier survival curve of mice represented displayed in A. No significant changes in survival by log-rank analysis. Data is combined from two repeat experiments

nanomoles of intravenous SIINFEKL in order to restimulate the cells. The mice were subsequently bled on days 4, 6, 8 and 11 in order to track the cells and assess their basic phenotype.

The tracking of the cells in blood is shown in *Figure 5-9*. *Figure 5-9A* shows percentage of lymphocytes that were both CD8<sup>+</sup> and CD45.1<sup>+</sup>, indicating transferred cells. *Figure 5-9B* shows the frequency of CD8<sup>+</sup> CD45.1<sup>+</sup> GFP<sup>+</sup> cells out of lymphocytes in which is the transferred cells expressing either the control vector pMP71 or Myr-Akt.

In *Figure 5-9A* it is evident that despite the lowest level of activity in cytotoxicity experiments and tumour challenges (*Figures 5-7* and *5-8*), the IL-15 treated cells actually show the greatest recall ability upon restimulation, reaching a total of 30% of the lymphocyte population by day six. By comparison, the IL-2 treated cells only reached 10% of the population at the same time point. The Myr-Akt cells showed a slight reduction in recall ability below the IL-2 treated controls, to approximately 7%. However, when the GFP<sup>+</sup> gating is included, this percentage drops to an almost non-recordable level; as shown in *Figure 5-9B*. This would indicate that even though the Myr-Akt transduced cells were sorted and purified to above 98%, and further cultured in IL-15, the small remaining non-transduced population were able to survive and proliferate *in vivo* far more than the Myr-Akt transduced cells. Taken together, it is clear that IL-15 treated Myr-Akt transduced CD8 T cells do not survive or proliferate *in vivo* following re-challenge in contrast to IL-15 treated cells which undergo significant expansion.

In addition to tracking cell populations in blood, markers of effector and memory cell differentiation were also examined. *Figure 5-10* displays the relative populations of cells expressing the phenotypic markers KLRG1 and CD127 (IL-7R). Blood was taken before the mice were given SIINFEKL peptide to restimulate the transferred cells, in order to examine the resting phenotype. Despite the expectation of transferred cells being present at low frequencies, the Myr-Akt transduced cells were substantially fewer in number than expected. This extremely low frequency of Myr-Akt transduced cells precluded examination of the expression of differentiation markers prior to restimulation. Regardless, at day 0 before restimulation there were clear differences between the cells treated with either IL-2 or IL-15. The IL-15 treated pMP71 transduced cells displayed an increased percentage of CD127<sup>+</sup> cells compared with IL-2 treated pMP71 transduced cells, which was expected. In contrast IL-2 treated pMP71 transduced cells, -

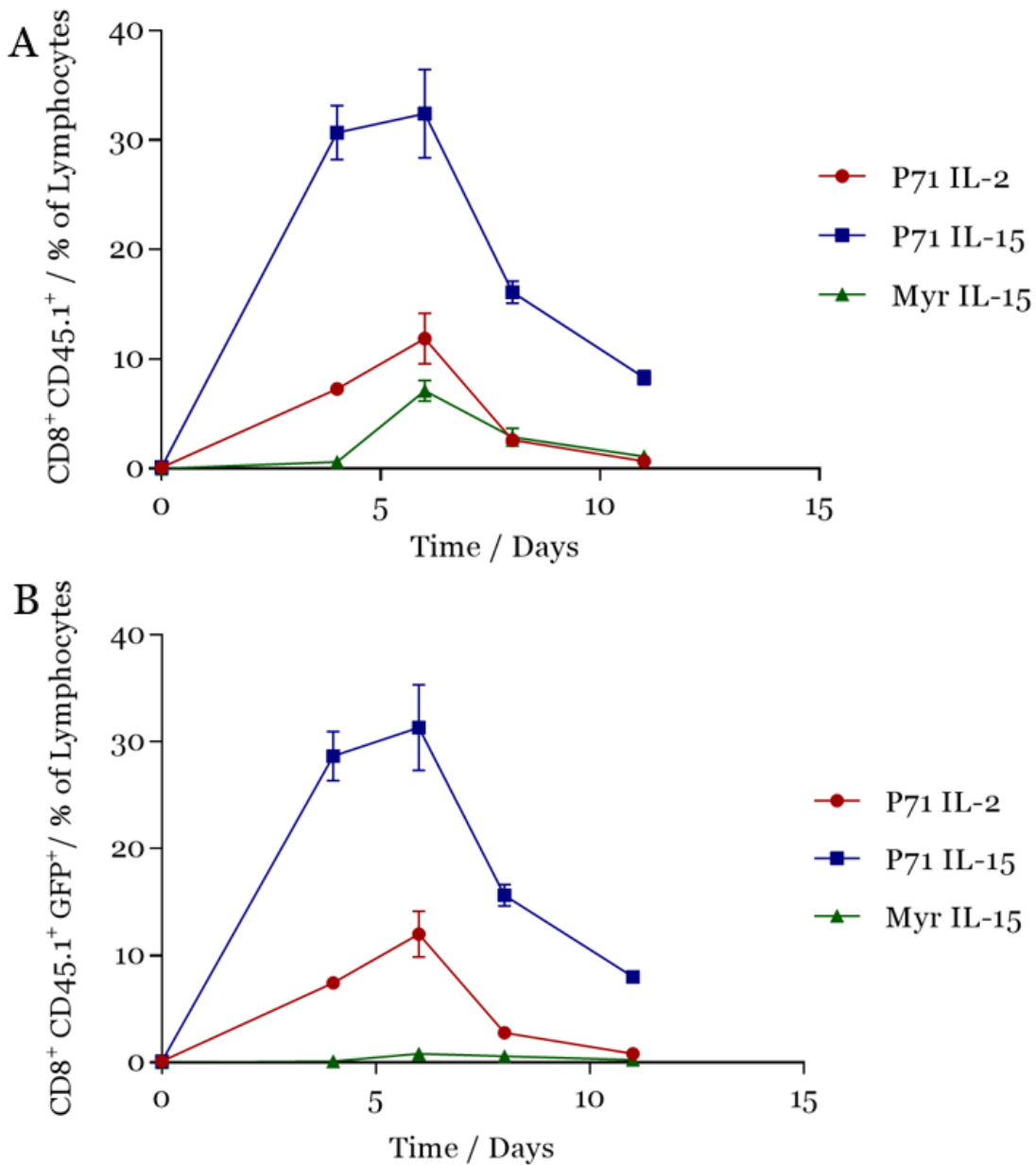


**Figure 5-9 – Tracking survival of Myr-Akt transduced cells.**

pMP71 and Myr-Akt transduced CD45.1<sup>+</sup> OT-1 cells produced as previously described. 1x10<sup>6</sup> of the purified transduced cells were transferred intravenously into recipient C57Bl/6 mice. 24 hours after transfer mice received 30 nanomoles of SIINFEKL peptide to restimulate transferred cells. Transferred cells were tracked in blood. **A** – Transferred cells displayed as percentage of CD8<sup>+</sup> CD45.1<sup>+</sup> out of the lymphocyte population over time. **B** – Same as A, however gate includes GFP<sup>+</sup> marker to isolate specifically transduced transferred cells. Mean and SEM of 4 replicate biological samples displayed

showed a more substantial population of double negative KLRG1<sup>-</sup> CD127<sup>-</sup> cells compared with IL-15 treated pMP71 transduced cells.

At day 4 post re-stimulation, the majority of cells across each of the samples were double negative. The remainder of the cells were primarily single positive for CD127<sup>+</sup>, with IL-15 treated cells and Myr-Akt transduced IL-15 treated cells displaying an increased expression of CD127<sup>+</sup> cells compared to their IL-2 treated counterparts. At day 6, the populations were more varied across

the different treatment groups. IL-2 treated cells showed an equivalent frequency of CD127<sup>+</sup> single positive and CD127<sup>-</sup> KLRG1<sup>-</sup> double negative cells at approximately 40% each. The remainder of the population is primarily single positive KLRG1<sup>+</sup>. In the IL-15 treated pMP71 transduced control, at day 6 the levels of single positive KLRG1<sup>+</sup>, and double positive KLRG1<sup>+</sup> CD127<sup>+</sup> are equivalent to that of the IL-2 treated controls. However, the proportion of single positive CD127<sup>+</sup> cells increased up to 55%, at the expense of the double negative population. Interestingly, in the Myr-Akt transduced cells the opposite was observed; an increase in the double negative cell population at the expense of the CD127<sup>+</sup> single positive group. At day 8, the populations in IL-2 and IL-15 treated controls become more or less identical, approximately 65% KLRG1<sup>-</sup> CD127<sup>+</sup>, 15% KLRG1<sup>+</sup> CD127<sup>+</sup> and 10% each for both KLRG1<sup>+</sup> CD127<sup>-</sup> and double negative populations. The Myr-Akt transduced cells shows a different phenotype pattern at day 8. The

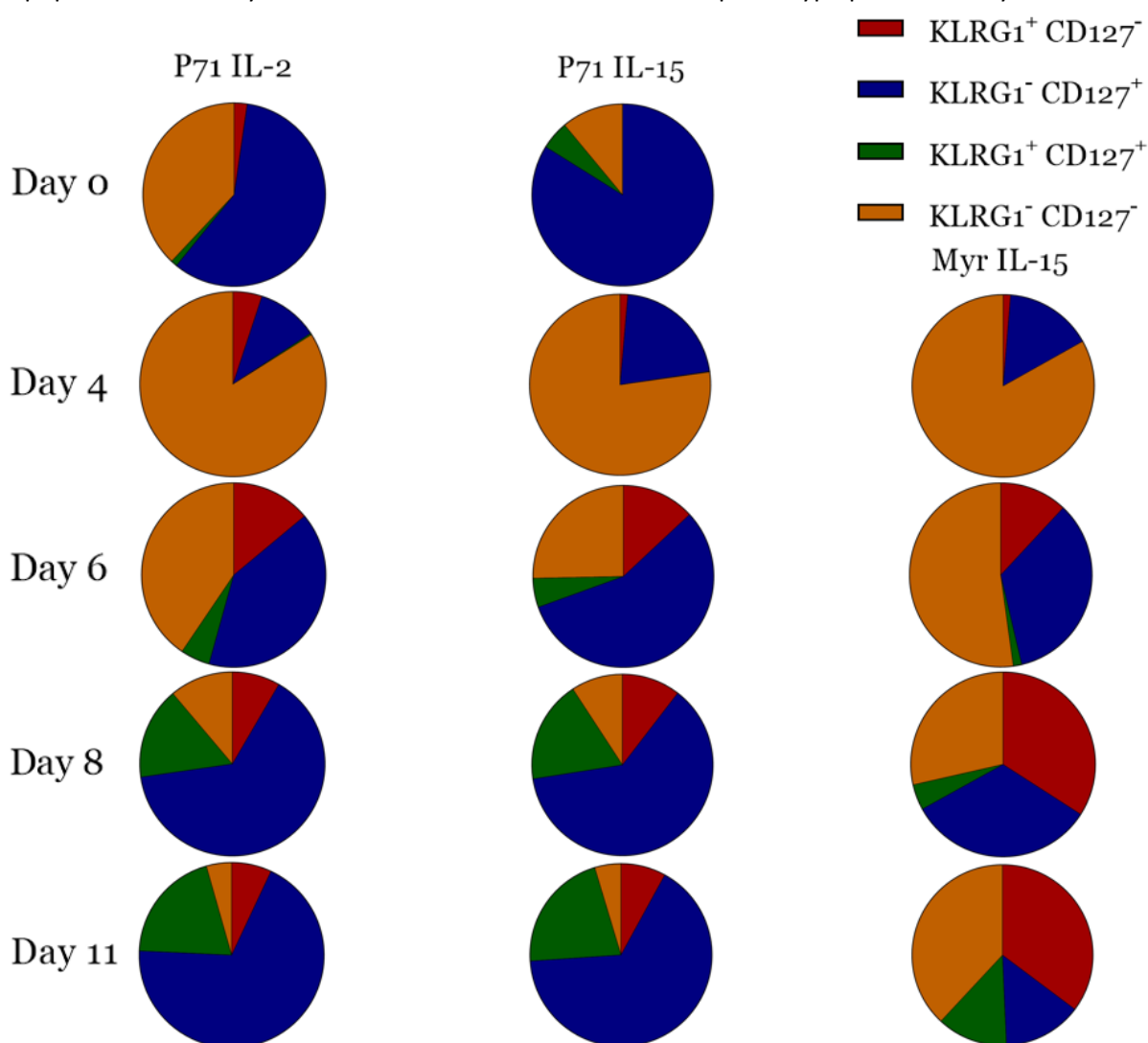


**Figure 5-10 – Phenotype of tracked Myr-Akt transduced cells.**

pMP71 (P71) and Myr-Akt transduced CD45.1<sup>+</sup> OT-1 cells produced as previously described.  $1 \times 10^6$  of the purified transduced cells were transferred intravenously into recipient C57BL/6 mice. 24 hours after transfer mice received 30 nanomoles of SIINFEKL peptide to restimulate transferred cells. Transferred cells were tracked in blood. Phenotypic markers KLRG1 and CD127 were analysed on the transduced cells. Myr-Akt transduced cells could not be measured on day 0 due to limited cell numbers. Data displayed is the average of 4 biological samples.

## Chapter 5

single positive CD127<sup>+</sup> population was reduced to approximately 30%. This reduction corresponds with an increase in the KLRG1<sup>+</sup> single positive and the double negative groups to 35% and 30% respectively. There was also a minor reduction in the double positive population. The difference in the IL-2 and IL-15 treated pMP71 transduced cells at day 11 compared to day 8 is minor; a 5% increase in the double positive and CD127<sup>+</sup> single positive population at the expense of the two other groups. At day 11, the Myr-Akt transduced group again shows substantial differences. The total population of cells expressing CD127, either from the single or double positive phenotypes barely exceeds 25% of the total population of cells. In contrast, the remaining cells are evenly split between single positive KLRG1<sup>+</sup> and double negative phenotypes. Overall, this demonstrates that transduction with Myr-Akt induces a reduced expression of CD127 and a substantial increase in the double negative and KLRG1<sup>+</sup> CD127<sup>-</sup> populations. This is in line with evidence that constitutive Akt activation enforces an enhanced effector function. The lack of CD127 expression could also explain the impaired persistence and proliferation *in vivo*. As signalling through CD127 is an important factor in determining persistence of CD8 T cells during the transition into memory post antigen clearance<sup>334</sup>.

### 5.3 Summation and Discussion

This chapter investigated the effects of Akt on metabolic processes, with a specific focus on oxidative phosphorylation. It further explored whether the effect of Akt on metabolism can be exploited for improved effect in anti-tumour therapy. Initially, the effect of Akt activity was examined through the use of an Akt inhibitor. These data confirmed that IL-2 inhibits SRC when compared to IL-15 culture of cells. In addition, inhibiting Akt provided a small yet insignificant benefit to the spare respiratory capacity of cells whilst they were cultured in IL-2. This effect was more pronounced against a backdrop of PDK<sup>K465E</sup> mutation. This indicates that reducing Akt activity has some positive impact on OXPHOS, at least under these conditions.

Based on the data from the Drop-Seq experiment presented in chapter 4, CD8 T cells exhibiting the PDK<sup>K465E</sup> mutation clearly show enrichment of oxidative phosphorylation genes compared with similarly treated WT cells. Whilst the transcriptomic changes would at least imply a relative improvement in SRC of CD8 T cells bearing the mutation, it is not a certainty. It was evident that WT and PDK<sup>K465E</sup> CD8 T cells possess similar SRC when cultured in IL-2. When treated with IL-15, there was an increase in SRC in both the WT and PDK<sup>K465E</sup> T cells compared to their respective IL-2 treated cells. However, the increase in SRC observed in PDK<sup>K465E</sup> cells was significantly higher than the WT cells in IL-15 culture, in line with an observed increase in oxidative phosphorylation genes. When the Akti was introduced with IL-2 culture, there was a significant increase in the SRC of the PDK<sup>K465E</sup> cells compared to IL-2 culture alone. WT cells displayed a minor increase in SRC with Akti treatment under IL-2 culture, but this increase was non-significant. Previous experiments showed that the Akti inhibitor is more effective at reducing Akt activity in PDK<sup>K465E</sup> mutant T cells than in WT T cells (*Figure 3-10*). This in combination with the observed improvement in SRC of PDK<sup>K465E</sup> cells following Akti treatment, indicates that if Akt activity is reduced to a certain extent it can lead to an improvement in oxidative phosphorylation. However, given the data from chapter 3 confirming impaired cytotoxicity induced by the Akti, the resulting improvement of SRC driven by the Akti is unlikely to aid in anti-tumour activity. As such, it was decided to investigate whether instead of boosting the metabolic ability of cells cultured in IL-2, it was possible to enhance the cytotoxic capacity of cells cultured in IL-15.

To this end, a myristoylated constitutively active Akt construct was utilised and confirmation of its activity was assessed by CD62L expression. As expected, despite being cultured in IL-15, CD8 T

## Chapter 5

cells transduced with Myr-Akt demonstrated significantly reduced expression of CD62L; lower even than that of IL-2 treated cells. When IL-15 treated Myr-Akt transduced CD8 T cell SRC was examined, it was significantly higher than that of IL-2 treated cells, but was still reduced compared to IL-15 treated control-transduced cells. This suggests that at least some of the mechanisms by which IL-15 enhances oxidative phosphorylation are sensitive to inhibition by Akt. Akt activity is known to amplify cytotoxic effector functions in CD8 T cells, and as such Myr-Akt was expected to improve this ability even when cells were cultured in IL-15. A cytotoxicity assay was performed to confirm this. The cytotoxic capacity of Myr-Akt transduced cells cultured in IL-15 was shown to be equivalent to that of IL-2 treated control cells; and significantly improved over IL-15 control cells. Thus, demonstrating that Myr-Akt is enough to restore full effector function, despite the expression of granzyme B being reduced compared to the IL-2 controls.

Use of Myr-Akt in cells cultured with IL-15 has helped to elucidate the effects of IL-2 that can be attributed to Akt activity. Downregulation of CD62L was severe in the Myr-Akt transduced cells, beyond even the effects of IL-2. Granzyme B was upregulated, although it remained at a lower level of expression than IL-2 treated cells. Despite this, the cytotoxic capacity of the Myr-Akt transduced IL-15 treated cells, as assessed by *in vitro* cytotoxicity assays, was equivalent between these cells and their IL-2 treated controls. In addition, the Myr-Akt transduced cells had a more favourable metabolic profile when cultured in IL-15 compared to control cells grown in IL-2. This combination of increased OXPHOS, granzyme B expression and cytotoxic activity suggests that Myr-Akt transduction induces a more effective phenotype for ACT for cancer therapy when cells are cultured in IL-15. In a tumour challenge setting, the Myr-Akt transduced cells were as effective as IL-2 control cells, and both were significantly better than IL-15-treated cells. However, this improvement only delayed the growth temporarily, and did not benefit overall survival. During the assay, it was noted that the Myr-Akt transduced cells were only detectable at low levels in blood, which suggests a lack of proliferation and/or survival. To assess whether any alterations to proliferation or survival occurred in Myr-Akt transduced cells a restimulation assay was performed. This demonstrated that Myr-Akt cells had significant impairments in survival and or proliferation *in vivo*. In addition, there was a substantial decrease in the percentage of cells that became CD127 positive within the Myr-Akt transduced cells compared with cells transduced with a control vector, which could account for the decreased survival observed.

Enhancement of OXPHOS in CD8 T cells can occur through multiple mechanisms. Increased expression of genes encoding enzymes involved in the metabolic processes, such as those at rate-

limiting steps of FAO, can aid in improving OXPHOS. CPT1 $\alpha$  was previously reported to enhance OXPHOS rate in CD8 memory T cells<sup>284</sup>, but recent a recent publication has called this into question<sup>319</sup>. However, oxidative phosphorylation enhancement can also occur due to structural and morphological adaptations of mitochondria. Mitochondria found in IL-2 treated effectors are often small, round and punctate<sup>282</sup>. By comparison, mitochondria found in IL-15 treated cells are often more elongated and possess more dense cristae resulting from fusion of multiple mitochondria, which in turn enhances their metabolic functions<sup>282</sup>. The fusion process is mediated by multiple proteins including mitofusion 1 and 2 (MFN1, MFN2) and optic atrophy 1 (Opa1)<sup>335</sup>.

Data in this chapter show that Akt inhibition in IL-2 treated WT cells causes a marginal improvement in their SRC. However, Akt inhibition in PDK<sup>K465E</sup> cells under the same conditions shows a significant and substantial improvement. This suggests that when Akt activity is reduced it is possible to improve mitochondrial oxidative phosphorylation. However, the mechanism behind this remains unclear. Recently, it has been shown that MFN2 is capable of negatively impacting Akt activity through mTORC2<sup>336</sup>. This is achieved by occupation of an overlapping binding site, by which MFN2 will associate with mTORC2 and hence occlude Akt from being phosphorylated and activated by mTORC2<sup>336</sup>. Whilst this establishes a link between the regulators of mitochondrial fusion, and by extension oxidative phosphorylation enhancement and Akt, it does not explain how severely reduced Akt activity would lead to an increased effectiveness of MFN2. This link was discovered in cancerous cells, so it may not be entirely representative of all cell types. However, if MFN2 does truly regulate Akt, the presence of a negative feedback loop might explain how a strong inhibition could in theory promote mitochondrial fusion through MFN2.

A study has also suggested a link between Opa1 and the Akt signalling pathway in cardiomyocytes. In response to a stimulator of the Akt pathway, in this case insulin, it was demonstrated that there was a substantial change in effectiveness and morphology of the mitochondria consistent with increased fusion<sup>337</sup>. This increased mitochondrial fusion was mediated by Opa1 but sensitive to Akt, mTORC1 and NF- $\kappa$ B inhibition<sup>337</sup>. This suggests that increased Akt activity increases mitochondrial oxidative phosphorylation; a finding perhaps in conflict with data presented in this study. However, given that in CD8 T cells, Akt is not linked directly to mTORC1 signalling, as it is in other cell types, it would be difficult to assert what impact this would have on the regulation of Opa1. A more recent paper has a more defined link between Akt and Opa1<sup>338</sup>. Opa1 exists in two primary isoforms; a short form and long form. It is the balance

between these isoforms that determines the activity of Opa1<sup>339,340</sup>. The long form of Opa1 promotes the fusion process, and cleaving of the long form inhibits this process. Oma1 is a proteolytic enzyme that targets the Opa1 protein and is responsible for converting it to the short isoform<sup>339</sup>. Yang *et al*<sup>338</sup> demonstrated that Oma1 can be targeted for ubiquitination and degradation by glycogen synthase kinase 3 (GSK3). As Oma1 levels decrease the expression of the long form of Opa1 increases, thus promoting mitochondrial fusion. As GSK3 can be phosphorylated and inhibited by Akt, this provides a possible mechanism by which Akt and its inhibition could lead to increased mitochondrial capacity<sup>341</sup>.

When approaching the question of Akt effects on mitochondrial oxidative phosphorylation from the opposite direction, using the Myr-Akt construct, a different effect is observed. Cells transduced with Myr-Akt and cultivated in IL-15 demonstrated significantly better SRC than that of the IL-2 treated cells. However, they also showed reduced SRC compared to IL-15 treated controls. This indicates that whilst Myr-Akt impairs mitochondrial oxidative phosphorylation, there are mechanisms by which IL-15 signalling promotes SRC that are not impacted by constitutive Akt activity. Conversely, it has been shown that the negative effects of IL-2 on oxidative phosphorylation cannot be overcome in WT cells with only Akt inhibition. This suggests that the effects of IL-2 and IL-15 on oxidative phosphorylation metabolism are distinct and only partially linked to Akt, despite IL-2 and IL-15 sharing common receptor chains, as well as downstream signalling pathways<sup>333,342</sup>. Perhaps the restricted expression of IL-15R $\alpha$ , differential affinities for the receptors and temporal differences between the two cytokines could explain the effects observed<sup>333</sup>.

The effects of Myr-Akt on effector function are not that surprising. Increasing Akt activity has long been known to induce a more effector phenotype in CD8 T cells, so a constitutively active form should only act to exacerbate this phenotype. When examining the cytotoxicity assay, it is observed that despite culture in IL-15 the Myr-Akt transduced cells possess equal cytotoxic capacity as that of IL-2 treated control cells, whereas, the control transduced and IL-15 treated cells possessed little to no capacity to eliminate target cells. Interestingly, granzyme B expression in the Myr-Akt transduced cells, whilst increased compared to the IL-15 control, is still substantially lower than the IL-2 treated controls. Whilst Akt does stimulate granzyme B expression, it is not the only factor to do so. IL-2 more strongly induces this compared to IL-15, which aids in explaining the observed difference<sup>91</sup>. However, despite the differential granzyme expression, the cytotoxic abilities of the cells remain identical. Based on the expression of

granzyme B, IL-2 clearly induces an excessive expression of the cytotoxic marker, as the increased expression over IL-15 treated Myr-Akt cells has not noticeably improved killing ability.

Based on its equivalent cytotoxic capacity and improved metabolic profile, the IL-15 treated Myr-Akt cells seemed to possess a beneficial phenotype for anti-tumour therapy. When this potential was examined in an *in vivo* tumour challenge, however the IL-15 treated and Myr-Akt transduced cells conferred only a slight improvement compared to IL-15 treated control cells and were no more effective than IL-2 treated control cells. This would seem to reflect the enhanced cytotoxic abilities of both the Myr-Akt-transduced and IL-2 treated cells. However, whilst long term survival was seen in two mice of each group, there was no significant delay or survival improvement. Phenotypic assessment of these cells during a restimulation assay potentially reveals why no significant survival was conferred by the transfer of Myr-Akt-transduced T cells, despite their more beneficial metabolic profile. Throughout the response, a decrease in the number of cells expressing CD127 was observed. At the latest time point, this was substantially reduced compared to both the IL-2 and IL-15 treated controls. Interestingly, despite being purified through FACs sorting, the frequency of GFP<sup>+</sup> cells immediately showed signs of impaired survival or proliferation. This lack of CD127 would explain the inability of these cells to persist long term *in vivo*, as the cells would be unable to respond to IL-7 for homeostatic proliferation in memory<sup>96</sup>. This could also account for the almost immediate lack of transduced cells following their transfer, as before the restimulation occurs they would have no way of maintaining factors such as Bcl-2<sup>343</sup>. Despite the severe reduction in frequency following *in vivo* transfer, the Myr-Akt cells still showed equal effectiveness in the tumour challenge to that of IL-2 controls. It is possible that the reduced presence of the Myr-Akt cells in the blood is due to their infiltration into the tissues. Akt activity has been linked to expression of factors including CD69 and CD103 that are more commonly associated with a resident memory phenotype<sup>344</sup>. As such, constitutive Akt activation as found in the Myr-Akt cells could induce a higher expression of these factors, thus leading to greater tissue infiltration. Overall, whilst it is possible to have strong effector functions without entirely compromising the beneficial metabolic phenotype of high SRC, the enforced Akt activity compromises survival, most likely through reduced expression of CD127.



## Chapter 6 The Role of SGK in CD8 T Cells

### 6.1 Introduction

PDK is at the centre of an intricate signalling pathway and is sensitive to an array of factors ranging from antigen and cytokines, to glucose levels and other nutrients. As such, developing an understanding of the downstream targets of PDK is important in order to further understand the development, activation and differentiation of T cells. One such target is the serum and glucocorticoid-regulated kinase, or SGK.

#### 6.1.1 SGK

SGK is a family of kinase enzymes consisting of three highly homologous but distinct isoforms, SGK1, SGK2 and SGK3<sup>345</sup>. Both structurally and functionally, SGK and Akt are similar, their catalytic domains in particular show 55% sequence homology. Their consensus target sequences are also similar, and include FOXO1. All the SGK isoforms have 3 domains, the N-terminal domain, the kinase domain and the C-terminal domain. The C-terminal domain, also known as the hydrophobic motif, is highly conserved between the different isoforms. This hydrophobic motif contains a critical serine residue at position 422 in SGK1 (the predominant isoform) and phosphorylation of this serine residue is essential for the activation and function of SGK1<sup>346</sup>. There was initially some debate as to the kinase that was responsible for the phosphorylation of the hydrophobic motif of SGK; some papers showed mTORC1 was responsible<sup>347,348</sup>, whilst others implicated mTORC2<sup>346,349</sup>. It is now accepted that mTORC2 regulates the Ser422 phosphorylation site in SGK1<sup>350</sup>. The phosphorylation of Ser422 does not activate SGK1, it is merely a permissive phosphorylation that allows full activation once the kinase domain has been phosphorylated. The kinase domains across the SGK isoforms show greater than 75% homology, and they all require phosphorylation of a threonine residue at position 256 in SGK1. This Thr256 phosphorylation is caused by PDK1. However, unlike Akt, which is dependent on PI3K activation and the presence of PIP<sub>3</sub> for its activation, SGK is phosphorylated by PDK1 in a PIF-pocket dependent manner<sup>351</sup>. This type of activation is entirely dependent on phosphorylation of the hydrophobic motif, hence the phosphorylation of Ser422 is permissive; it does not activate SGK directly but instead converts it to a substrate for the PIF-pocket interaction with PDK1<sup>351</sup>. Finally, the N-terminus of SGK isoforms can direct cellular localisation. Unlike Akt, SGK lacks any pleckstrin homology domains that cause it to bind PIP<sub>3</sub> and localise to the plasma membrane, thus SGK is considered a cytosolic protein.

## Chapter 6

SGK3 is distinct, in that it contains a Phox homology domain (PX) that causes localisation towards the endosomal membrane<sup>352</sup>. Whilst ubiquitously expressed SGK1 is tightly regulated, in part due to a high rate of protein turn over by the proteasome<sup>353</sup>. As its name suggests, both serum and glucocorticoids cause increased transcription of SGK1 in multiple cell types<sup>354,355</sup>. Other factors such as p38/MAPK, TGF- $\beta$ , IL-6, platelet-derived growth factor (PDGF), NF- $\kappa$ B, NFAT5 and an assortment of pro-inflammatory cytokines also cause increased expression of SGK1<sup>356</sup>. Cellular stresses such as hypoxia, hyperglycaemia and excessive cell shrinkage also contribute to an increased SGK1 transcription rate<sup>357</sup>.

The primary function of SGK1 is the regulation of the epithelial sodium channel (ENaC), as a mechanism of controlling cellular volume<sup>358</sup>. As such, it plays a critical role in the proper function of the kidneys in reclaiming lost sodium ions<sup>359</sup>. Aside from sodium channels, SGK1 also controls a myriad of other ion channels including voltage gated potassium channels, ubiquitous chloride channels and the epithelial calcium channel TRPV5<sup>356</sup>. This confirms the role of SGK1 as a regulator of cell size and volume, enacted through the manipulation of the flow of ions. SGK1 also controls the expression of some transporter proteins including the sodium-glucose cotransporter (SGLT1), sodium-potassium ATPase, creatine transporter (CreaT) as well as a variety of amino acid transporters<sup>356</sup>. SGK1 also possesses regulatory control over transcription factors, such as the cAMP responsive element binding protein or CREB<sup>360</sup>. SGK1 can also enhance activity of other factors such as NF- $\kappa$ B<sup>361</sup>. Whilst not the primary regulator of the forkhead transcription factors FOXO1 and FOXO3a, SGK1 is capable of phosphorylating them in a similar manner to Akt<sup>362</sup>. Although SGK1 and Akt share a similar pool of target proteins, SGK1 does have 2 unique targets: N-myc down-regulated gene 1 (NDRG1), a member of the hydrolase enzyme family; and neural precursor cell expressed developmentally downregulated gene 4-like (Nedd4-2), an E3 ubiquitin ligase<sup>363</sup>. NDRG1 has been linked to enabling SGK1 to control stress responses, cell growth and differentiation, whereas Nedd4-2 is more closely linked to SGK1's regulation of ion channels, primarily ENaC<sup>356</sup>. A diagram of the SGK1 pathway is shown in *Figure 6-1* below.

In immune cells the role of SGK is only beginning to be investigated. Recently, a number of published studies describe the role that SGK1 plays in the differentiation process of CD4 T cells. A study co-authored by Hafler *et al*<sup>364</sup> showed that when cultured under increased NaCl concentrations, CD4 T cells preferentially differentiated into a pathogenic T<sub>H</sub>17 subtype. Culture with equivalent amounts of sodium gluconate, MgCl<sub>2</sub> or mannitol, demonstrated that it was the sodium ion (Na<sup>+</sup>), not the chloride ion (Cl<sup>-</sup>) or the osmotic pressure of the NaCl, that was

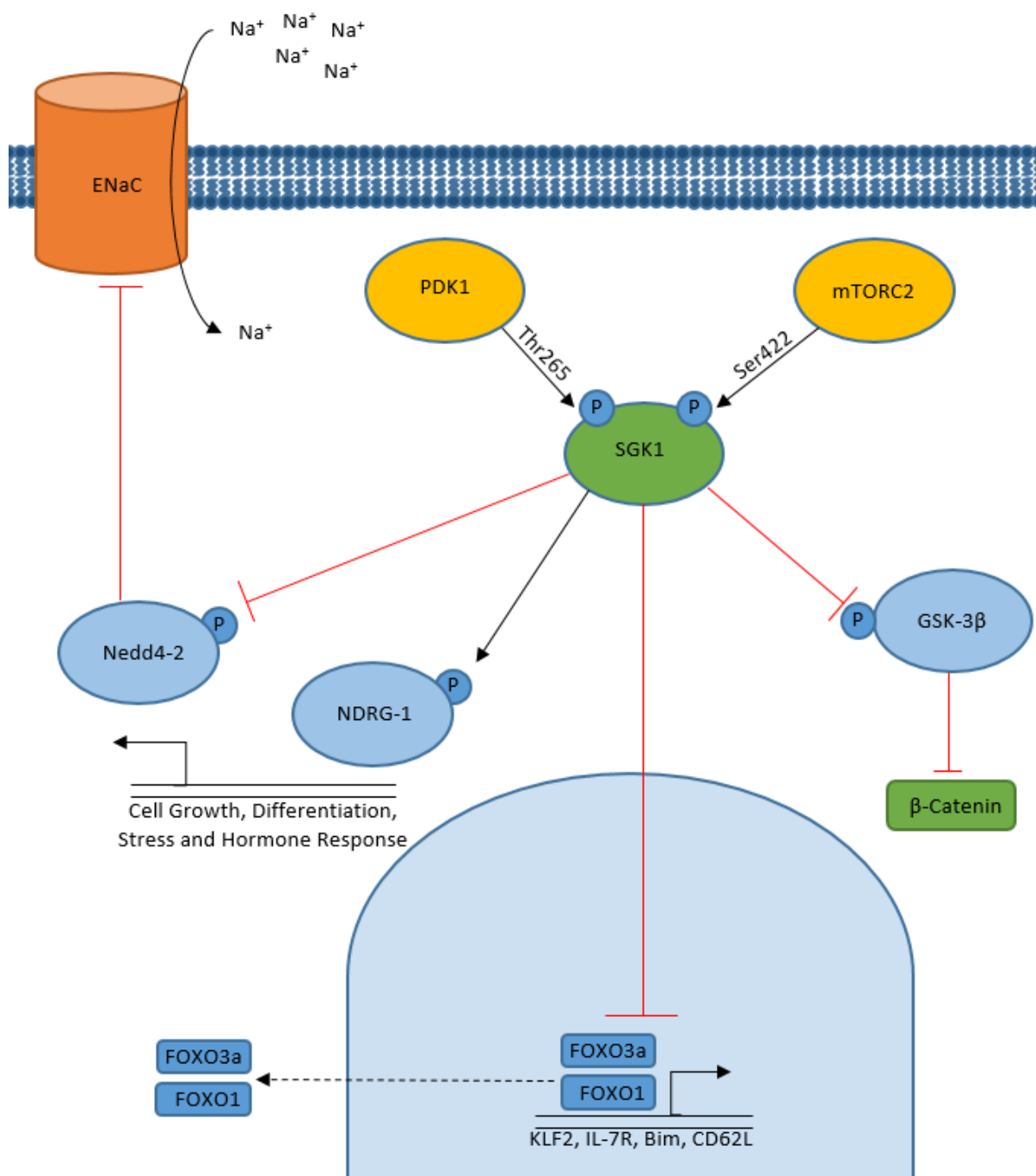


**Figure 6-1 – The SGK Signalling Pathway.**

SGK1 is activated through two independent phosphorylation events. Phosphorylation at serine 422 by mTORC2 allows binding of PDK1 by PIF-pocket interactions to SGK1. This interaction allows PDK1 to activate SGK1 by phosphorylating threonine 265. Due to homology of the kinase domains between Akt and SGK1 they share certain targets, specifically the FOXO family of transcription factors as well as GSK-3 $\beta$ . Nedd4-2, an E3 ubiquitin ligase and NDRG-1, a hydrolase enzyme are unique downstream targets of SGK1. The most well characterised function of Nedd4-2 is the regulation of the epithelial sodium channel (ENaC).

responsible for this altered differentiation. CD4 T cells cultured in high NaCl displayed higher expression of pro-inflammatory cytokines IL-2 and TNF- $\alpha$ , as well as RORC, IL-17F and IL-23R; all classical hallmarks of the T<sub>h</sub>17 subtype<sup>365</sup>. Hafler *et al*<sup>364</sup> also demonstrated that the effects of

## Chapter 6

increased NaCl are transduced through both p38/MAPK and NFAT5 and converge on SGK1. The signalling pathway linking SGK1 to the aggressive T<sub>h</sub>17 phenotype in CD4 T cells was not commented upon in this study.

A paper co-authored by Kuchroo *et al*<sup>366</sup>, coinciding with the publication by Hafler *et al*<sup>364</sup>, posits an explanation to how SGK1 drives T<sub>h</sub>17 phenotypes in high NaCl conditions. Kuchroo *et al*<sup>366</sup> demonstrated, through the use of gene knock outs and genome wide messenger RNA expression profiles, that SGK1 is critical in the IL-23 pathway. IL-23 is an essential cytokine for the stabilisation of the T<sub>h</sub>17 subtype<sup>367</sup>. This study also confirmed that increased salt caused skewing of CD4 T cells to a T<sub>h</sub>17 subtype, which is primarily mediated by SGK1. Under these conditions, SGK1 increases the expression of IL-23R, which in turn increases the expression of SGK1. Increased IL-23R reinforces the T<sub>h</sub>17 subtype, which leads to the increased pathogenic phenotype presented in Hafler *et al*<sup>364</sup>.

In a more recent paper, Hafler and Kuchroo collaborated to demonstrate that high salt conditions also decreased the ability of FOXP3<sup>+</sup> T cells (T<sub>regs</sub>) to suppress autoimmune T cells<sup>368</sup>. As well as dysregulating T<sub>regs</sub> suppressive abilities, the increased salt concentration was shown to induce the T<sub>h</sub>1 subtype as the dominant phenotype amongst CD4 T cells, characterised by increased T-bet expression and IFN $\gamma$  secretion, and that this process was regulated by SGK1<sup>368</sup>.

The role of SGK1 is still somewhat contentious however, as Heikamp *et al*<sup>243</sup> claim that SGK1 in fact suppresses the T<sub>h</sub>1 phenotype and promotes the T<sub>h</sub>2 phenotype<sup>243</sup>. These authors demonstrate that through the phosphorylation of Nedd4-2, and subsequent stabilisation of JunB, SGK1 promotes a T<sub>h</sub>2 phenotype and concurrently increases expression of the long form of the transcription factor TCF-1, which in turn inhibits the production of IFN $\gamma$ .

Whilst the role of SGK1 is well established in kidney and epithelial cells, its role in T cells is poorly characterised. The majority of the research has focussed on CD4 T cells, not CD8 T cells. Considering the similarity between SGK and Akt, it was deemed important to develop experimental approaches to probe the function of SGK in CD8 T cells.

## 6.2 Results

Investigating the role of SGK in CD8 T cells began by utilising a small molecule inhibitor of SGK, namely GSK650394 (Tocris), hereafter referred to as SGKi. This compound has been shown to be an effective inhibitor of both the SGK1 and SGK2 isoforms<sup>369</sup>. The initial approach was to examine the effects of the SGKi on the phosphorylation of NDRG1, a known target of SGK, by western blot. In this case, the activation of SGK with anti-CD3 and anti-CD28 stimulation could not be demonstrated through NDRG1 phosphorylation. However, the SGKi caused an approximate 50%

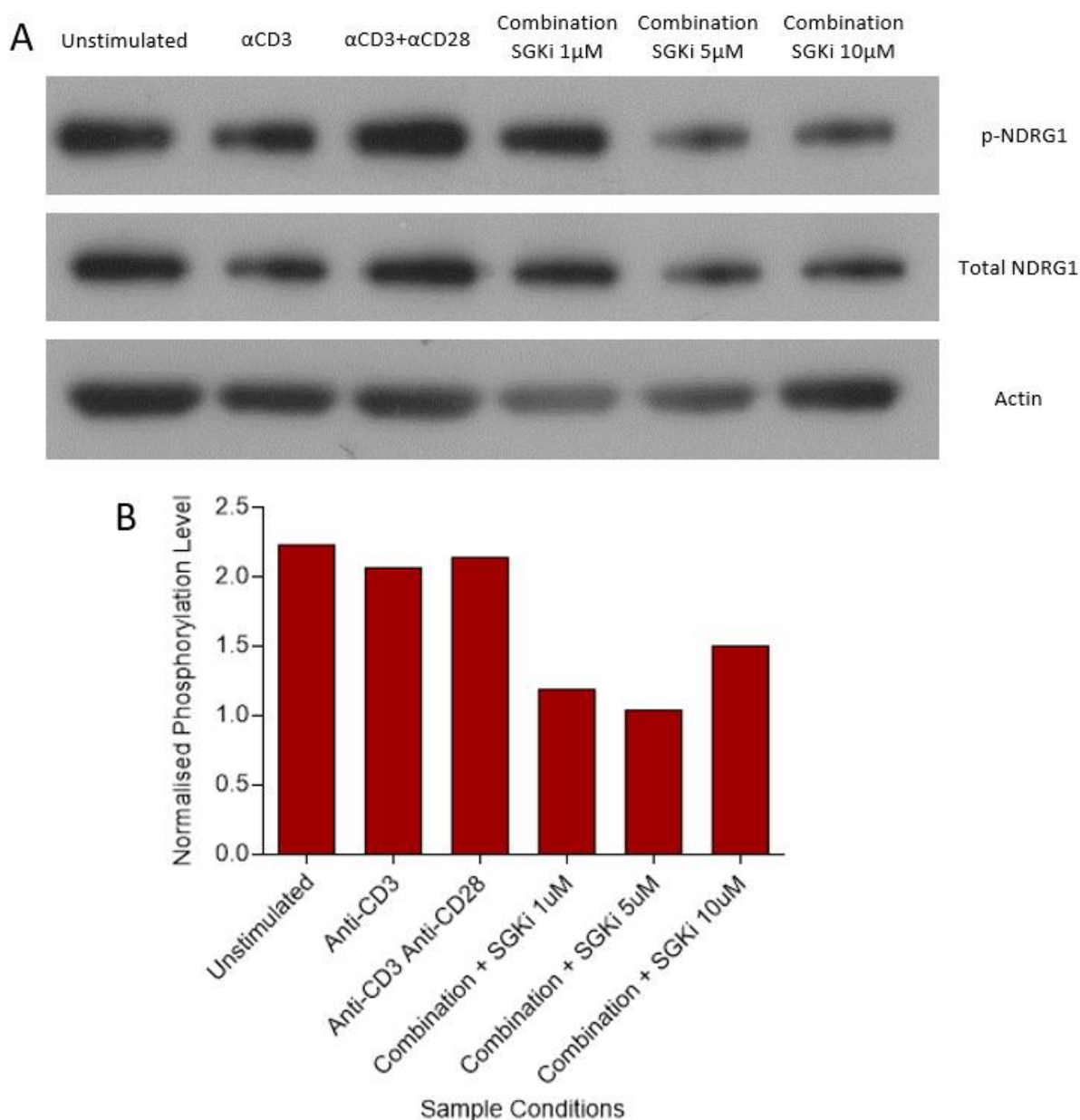


**Figure 6-2 – Effects of SGKi on NDRG1 phosphorylation in CD8<sup>+</sup> T cells.**

OT-1 splenocytes were harvested and CD8<sup>+</sup> T cells purified via MACS negative selection.  $2 \times 10^6$  cells stimulated with  $2 \mu\text{g/ml}$  of platebound anti-CD3, and  $5 \mu\text{g/ml}$  of soluble anti-CD28 for 3 hours in presence or absence of the SGK inhibitor GSK650394 (SGKi). **A** – Western blot displaying levels of phosphorylated NDRG1, Total NDRG1 and Actin. **B** – Level of p-NDRG1 compared to total NDRG1 normalized to actin expression through densitometry calculations in ImageJ. Data from one biological sample

decrease in the normalised level of NDRG1 phosphorylation compared to the total expression of the protein. This finding is shown in *Figure 6-2*.

Subsequently, a thymidine incorporation assay was conducted, to measure the proliferation of CD8 T cells and to assess the effect of SGK inhibition on these cells. Naïve CD8 T cells were purified from OT-1 splenocytes before being stimulated with 1µg/ml plate-bound anti-CD3 or 2µg/ml plate-bound anti-CD3 and 5µg/ml soluble anti-CD28, in the presence or absence of SGKi. Data represented in *Figure 6-3* show that anti-CD3 increased the incorporation of [<sup>3</sup>H]-Thymidine and hence proliferation, when compared to the unstimulated control. This was an effect that was

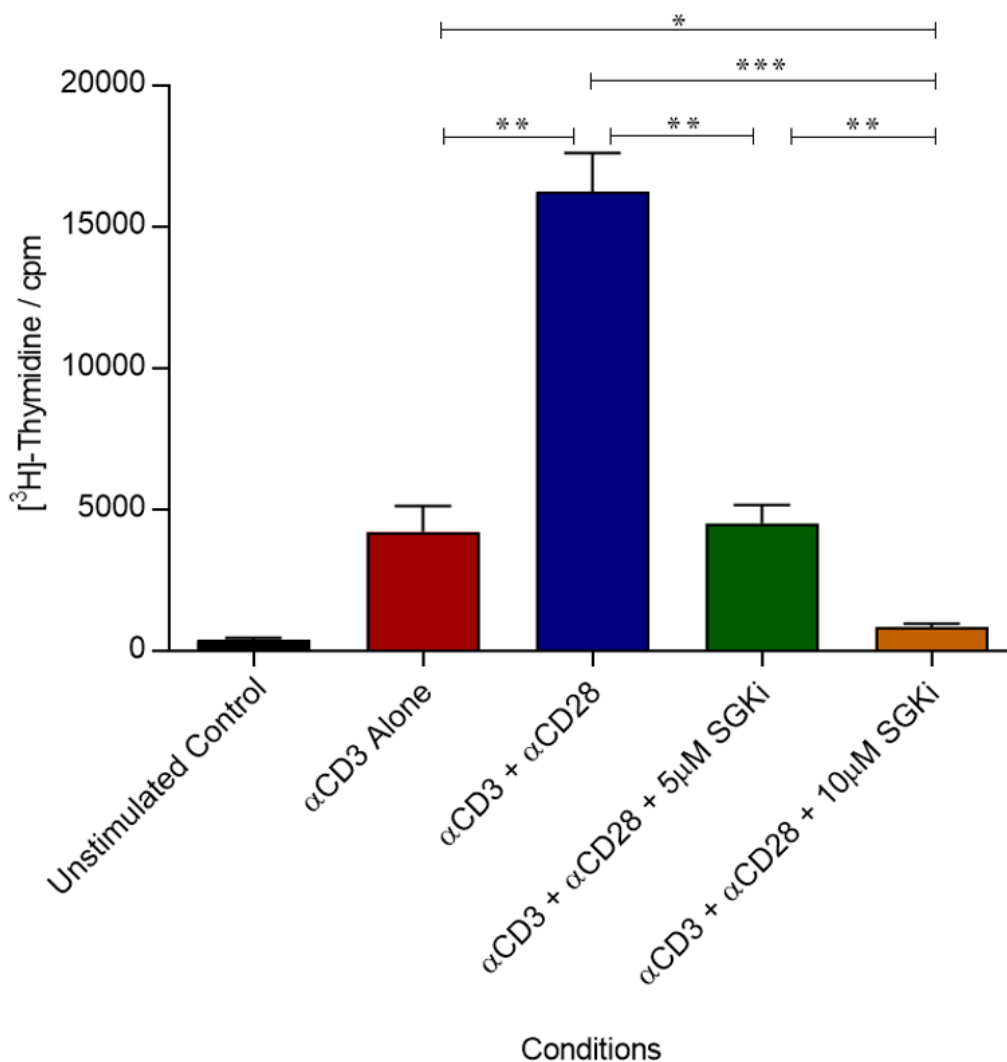


**Figure 6-3 – Effects of SGK inhibition on Tritiated Thymidine Incorporation by CD8<sup>+</sup> T cells.**

OT-1 splenocytes were harvested and CD8<sup>+</sup> T cells purified via MACS negative selection. 200,000 CD8<sup>+</sup> cells were then left unstimulated or stimulated with 2µg/ml platebound anti-CD3 alone or with 5µg/ml soluble anti-CD28 in the presence or absence of 5µM or 10µM of the SGK inhibitor (GSK650394, Torc1s). On day 3 the cells were treated with tritiated thymidine and left for an additional day. Subsequently the level of radiation, and hence thymidine incorporation, was examined by a radiometric counter. Data in triplicate from on biological sample mean and SEM displayed. p values are ≤0.05, 0.005 and 0.0005 for \*, \*\* and \*\*\* respectively

greatly enhanced by the addition of anti-CD28. Two concentrations of SGK were used, 5 $\mu$ M and 10 $\mu$ M, where concentrations between 1 $\mu$ M and 10 $\mu$ M had been used in previous literature<sup>370,371</sup>. The amount of tritiated thymidine that was incorporated, substantially and significantly decreased in the presence of both concentrations of SGK; 5 $\mu$ M of SGK essentially ablated the effects of the addition of anti-CD28, reducing the level of proliferation by over 70% back to the same level as anti-CD3 alone. The addition of 10 $\mu$ M SGK, reduced the level of proliferation even further, until it was indistinguishable from the unstimulated control.

These data suggest that SGK positively regulates CD8 T cell proliferation. However, thymidine incorporation cannot distinguish between proliferation and survival, meaning it may be a result of a combination of these two factors. There also remains the possibility that the SGK was toxic, although these concentrations have been used in previous studies. To address these two concerns, another proliferation assay was performed, this time based on dilution of the dye CFSE. This allowed for a more accurate assessment of the proliferation of only live cells.

Naïve CD8 T cells were purified out of a pool of OT-1 splenocytes. Subsequently, 2x10<sup>5</sup> CD8 T cells were stained with 10 $\mu$ M CFSE. These cells were then stimulated with either 2x10<sup>4</sup> MecSig-OVA B7 cells, or 2 $\mu$ g/ml plate-bound anti-CD3 and 5 $\mu$ g/ml anti-CD28, in the presence or absence of SGK. As the MecSig-OVA B7 cell line is a potent stimulus, the naïve CD8 T cells were only co-cultured with this cell line for 24 hours; previous experiments have shown that prolonged culture with MecSig-OVA causes excessive T cell death (data not shown). The level of CFSE dilution was then assessed by flow cytometry every 24 hours.

Based on the data shown in the thymidine incorporation assay, the concentration of SGK was limited to 5 $\mu$ M. *Figure 6-4A* shows the result of this experiment. Dilution of CFSE was observed in both stimulatory conditions and under both stimulatory conditions 5 $\mu$ M SGK caused substantial inhibition of CD8 T cell proliferation.

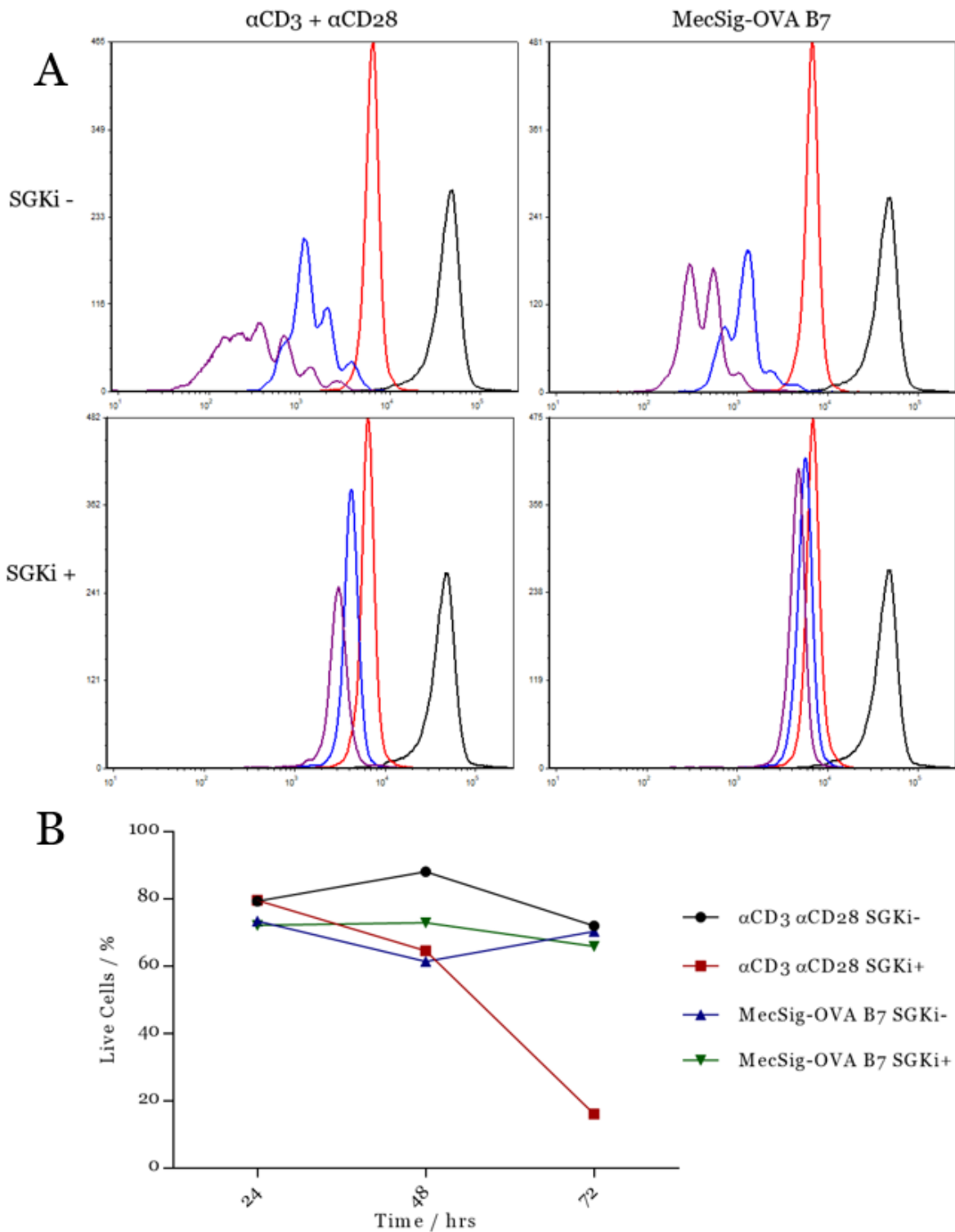


**Figure 6-4 – SGKi prevents cellular proliferation and reduces survival in naïve cells.**

$2 \times 10^5$  naïve OT-1 CD8 T cells stained with membrane dye 10uM CFSE, then cultured with  $2 \times 10^4$  MecSig-OVA B7 cells or 2ug/ml platebound anti-CD3 and 5ug/ml soluble anti-CD28 for 3 days in the presence or absence of 5 $\mu\text{M}$  SGKi and measured by flow cytometry every 24 hours. **A** – Black – 0 hour control, Red – 24 hour sample, Blue – 48 hour sample, Purple – 72 hour sample. **B** – Percentage of live cells in each condition as measured by flow cytometry based on the live cell gate in the proliferation assay. Data from one biological sample

As SGK1 is known to influence factors controlling cellular survival, the percentage of apoptotic cells was also assessed by flow cytometry. These data are shown in *Figure 6-4B* confirm that the SGK inhibitor has no detectable immediate effect on the survival of naïve CD8 T cells. However, after 72 hours there was a considerable decrease in the frequency of live CD8 T cells after treatment with anti-CD3 and anti-CD28 in the presence of 5 $\mu$ M SGK inhibitor, compared to cells similarly stimulated in the absence of the inhibitor. This cell death was not observed in cells treated with the MecSig-OVA B7 cell line. Together, these data indicate that pharmacological inhibition of SGK can hamper both the proliferation and survival of CD8 T cells.

The experiments described so far, demonstrating a potential role for SGK in T cell proliferation, relied upon a small molecule inhibitor of SGK. In order to confirm these findings, alternative approaches were adopted. Using increased NaCl conditions provides another avenue to assess the effects of SGK in CD8 T cells, as other studies have shown that 40 mM NaCl supplemented media upregulates SGK1 expression in CD4 T cells<sup>368</sup>.

OT-1 splenocytes were initially stimulated with 20pM SIINFEKL for two days, before re-suspending 5x10<sup>4</sup> cells in conventional media, media supplemented with 40mM NaCl in order to stimulate SGK, or media supplemented with 80mM mannitol to act as an osmotic control<sup>372</sup>. In addition, cells were incubated in the presence or absence of 10ng/ml IL-2, 1ng/ml IL-2 or 15ng/ml IL-15. Whilst 10ng/ml of IL-2 is considered typical for generating CTLs, 1ng/ml is sub-optimal and is exhausted more quickly, leaving the cells in a cytokine deprived state<sup>373</sup>. CD8 T cells treated with IL-15 do not proliferate as quickly as those treated with IL-2, hence increasing the NaCl concentration within the media of the IL-15 treated group will test whether the SGK1 enhances proliferation. *Figure 6-5A* demonstrates the frequency of dead cells in cultures, as assessed by trypan blue counts. In conventional media, the 10ng/ml IL-2 (IL-2 high) and 15ng/ml IL-15 groups show substantially and significantly reduced cell death when compared to the 1ng/ml IL-2 (IL-2 low) group, likely due to limiting concentrations of IL-2. When stimulated with IL-15 the frequency of dead cells remained similarly low independent of whether cells were cultured in the presence of additional NaCl, mannitol or in conventional media. In the IL-2 high treated cells, the NaCl treated cells showed significantly reduced levels of cell death when compared to cells cultured in standard media or mannitol supplemented media. However, in the IL-2 low treated cells there was a significant and substantial decrease in cell death in the NaCl treated CD8 T cells of approximately 50% compared to culture in standard media, or mannitol supplemented media. *Figure 6-5A* shows that conditions favouring low cell death also drive an increase in the live cell

count, with NaCl treated cells in the IL-2 high and low groups showing an increased number of live cells compared with standard or mannitol supplemented media. To more accurately assess cell death and to consolidate some of these data, a repeat experiment was performed in which only the IL-2 low conditions were included, and in which 7AAD was used to stain dead cells. In *Figure 6-5B*, this experiment shows that there are approximately half as many apoptotic cells in the NaCl treated group compared to the mannitol and standard media controls, consistent with data from

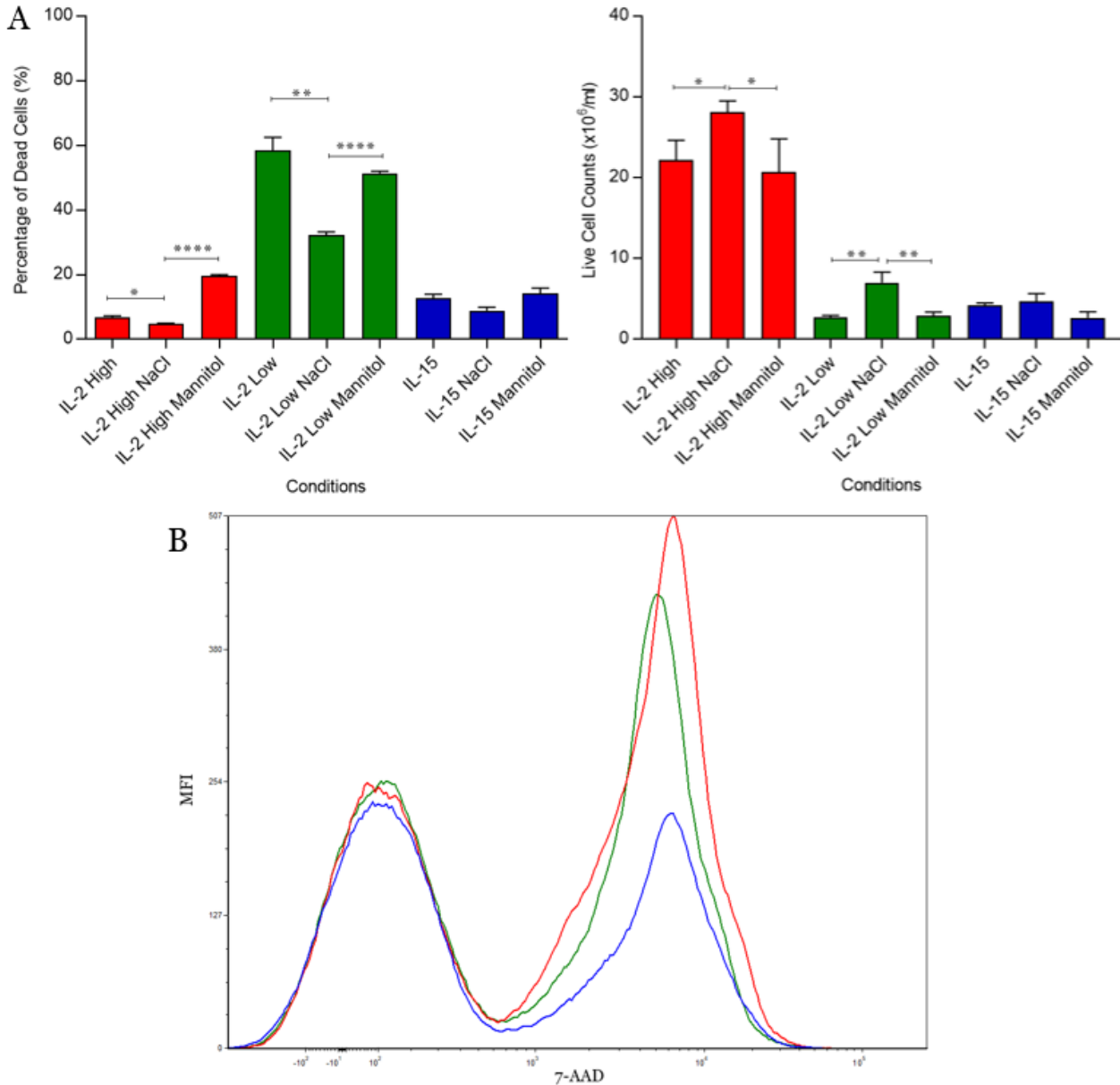


**Figure 6-5 – NaCl protects CD8 T cells under cytokine deprived conditions.**

OT-1 splenocytes stimulated with 20pM SIINFEKL for two days. Subsequently  $5 \times 10^4$  are placed in 96-well plates under multiple cytokine and media conditions. Three cytokine conditions are used, 10ng/uL IL-2 (IL-2 high), 1ng/mL IL-2 (IL-2 low) and 15ng/mL IL-15. 3 media conditions are used, standard media, 40mM NaCl supplemented media and 80mM Mannitol supplemented media. **A** – (left) Percentage of dead cells as assessed by trypan blue cell counts and (right) live cell number as assessed by trypan blue, measured three days after cytokine culture. All cell counts in triplicate from a single biological sample, mean and SEM displayed. P values <0.05, 0.005 and 0.0005 for \*, \*\* and \*\*\*\* respectively. **B** – Apoptosis detecting dye 7AAD staining as assessed by flow cytometry in the IL-2 low group. Red – IL-2 low standard media, Green – IL-2 low mannitol supplemented media, Blue – IL-2 low NaCl supplemented media.

trypan blue staining in *Figure 6-5A*. Together, these results show that increasing NaCl concentration in culture media exerts pro-survival effects in both high and low IL-2 concentrations.

To examine the role of SGK in more detail, two mutated versions of SGK were introduced into T cells. Multiple mutants of SGK have been previously described, and these primarily incorporate mutations at the mTORC2 phosphorylation site at S422. To gain insight into the role of mTORC2 downstream of SGK, the constitutively active S422D and dominant negative S422A forms of SGK that have been reported previously, were used<sup>374-376</sup>. The mutation of serine to aspartic acid (S422D) simulates the phosphorylation of mTORC2, whilst mutation to an alanine residue (S422A) renders SGK resistant to effects of mTORC2. These mutant constructs were synthesised commercially and supplied in the pMA vector that is not suitable for downstream applications. A vector map of the supplied dominant negative form of SGK in this vector is shown in *Figure 6-6A*.

Both the SGK dominant negative and constitutively active constructs (hereafter referred to as DN and CA respectively) are 1351bp in length and are flanked by NotI and Sall restrictions sites 5' and 3' respectively. The Sall site, whilst not listed in the vector map, is located at position 1739. The SGK DN and CA constructs also contain an HA tag at their N-terminus. To introduce these sequences into CD8 T cells, the SGK sequences were sub-cloned into a retroviral vector. The pMP71 vector was elected for use, in house, due to prior experience and for which the sequence is known (see *Figure 6-6B* for a vector map).

Through a previous project this group was already in possession of a NotI/Sall digested pMP71. Therefore, the SGK DN and CA vectors were digested using NotI/Sall restriction enzymes before analysing both the cut SGK constructs and the pre-cut pMP71 vector on an agarose gel, as shown in *Figure 6-7*.

The 1350bp bands of the SGK constructs and the 6800bp band of the pMP71 vector were purified from the agarose gel. Subsequently, the SGK inserts were ligated into the now empty pMP71 vector to generate expression vectors containing the SGK inserts upstream of a GFP reporter gene and an ampicillin resistance gene. These final constructs, and some parental and uncut pMP71 vector control, were then analysed again by Sall/NotI restriction digest to confirm the final



were grown in bacteria and stocks of plasmid were stored for future testing in T cells. Initial transfections into Phoenix-ECO cells confirmed that these constructs lead to expression of GFP (data not shown). Subsequently, transduction of these constructs in CD8 T cells was carried out, as described previously in an earlier chapter (*Figure 5-5*).

*Figure 6-9A* shows GFP expression in CD8 T cells 24 hours post transduction. This indicates that both of the SGK vectors were expressed in approximately 40% of cells. After a further 96 hours of culture in IL-2 or IL-15, expression of GFP was maintained (data not shown) and expression of CD62L, CD127 and CD25 were examined. *Figures 6-9B-E* show that as expected there is an increase in the expression of CD62L and CD127 following IL-15 treatment compared to IL-2 treated cells. *Figures 6-9F+G*, as expected, showed an increase in expression of CD25 in the IL-2 treated cells, compared to the IL-15 treated group.

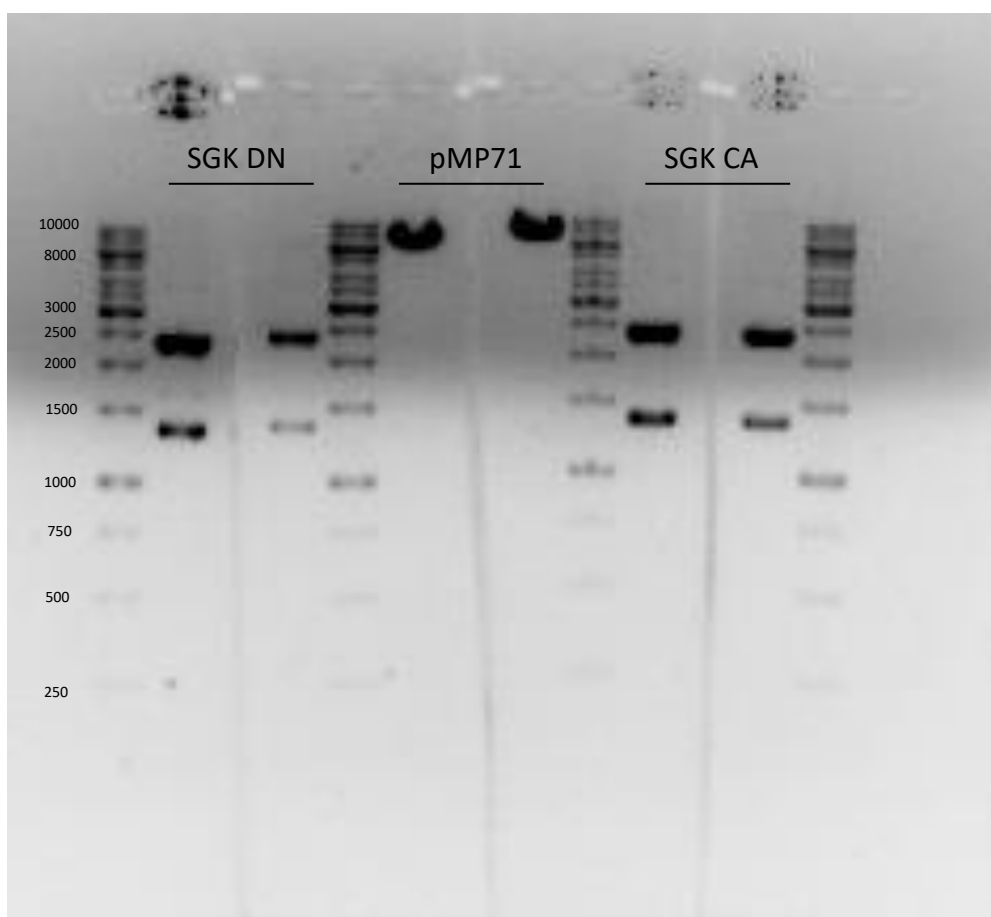


**Figure 6-7 – Restriction digest of SGK DN and SGK CA**

Run on a 1% agarose gel. DNA bands illuminated by presence of ethidium bromide and UV light. Segments cut and removed from gel before exposure to UV so as to protect the DNA samples that go forward to subsequent gel purification. Bands pictured here are used as guide markers, to allow more accurate extraction of DNA for gel purification samples

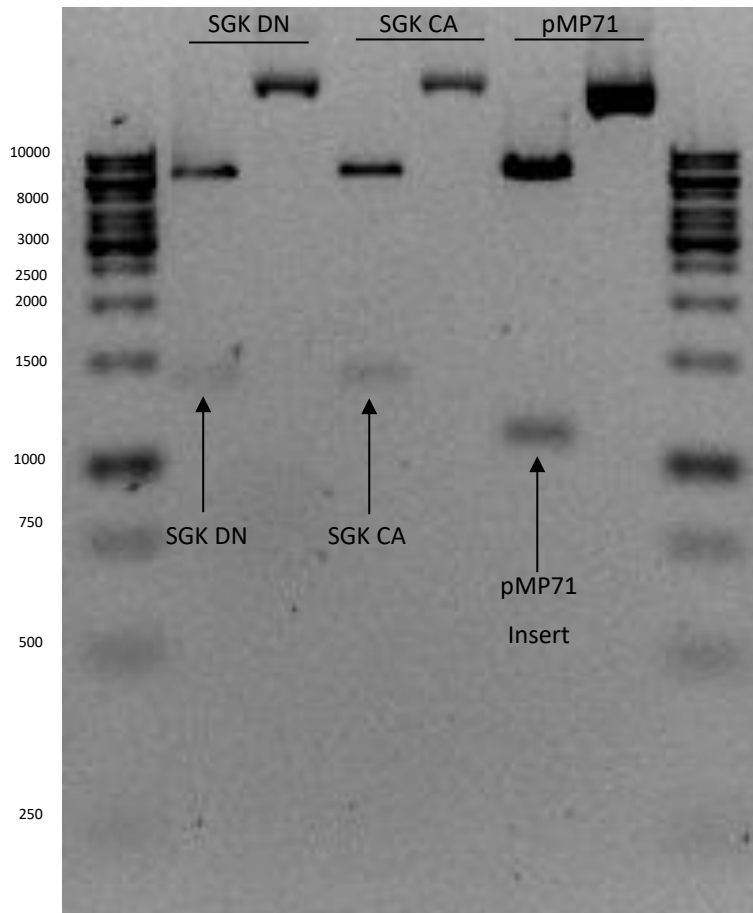


**Figure 6-8 – Restriction digest of SGK DN, pMP71 and SGK CA samples**

Run on a 1% agarose gel. Each sample has undergone a restriction digest with NotI/Sall, which is shown in the first lane for each vector. The second lane for each vector shows the undigested vector, where supercoiling has caused it to run at a substantially higher molecular weight. Bands at 1350bp indicate presence of SGK insert, bands at 1100bp are indicative of original pMP71 insert, bands between 6000-8000bp are evidence of backbone pMP71 vector.

Unfortunately, there were no observed differences in expression of any of these markers, under either cytokine condition between the pMP71 transduced control, DN-SGK or CA-SGK constructs. In an attempt to confirm expression of the SGK constructs, multiple western blots against the HA-tag incorporated into the SGK sequence were performed. However, none returned with a clear blot indicating either contamination or antibody defects.

Time permitting, it would be advantageous to continue testing these constructs in order to examine what effects, if any, were caused by the SGK mutants. Further, the use of western blots could proffer confirmation as to whether the mutants have any effect or are even expressed.

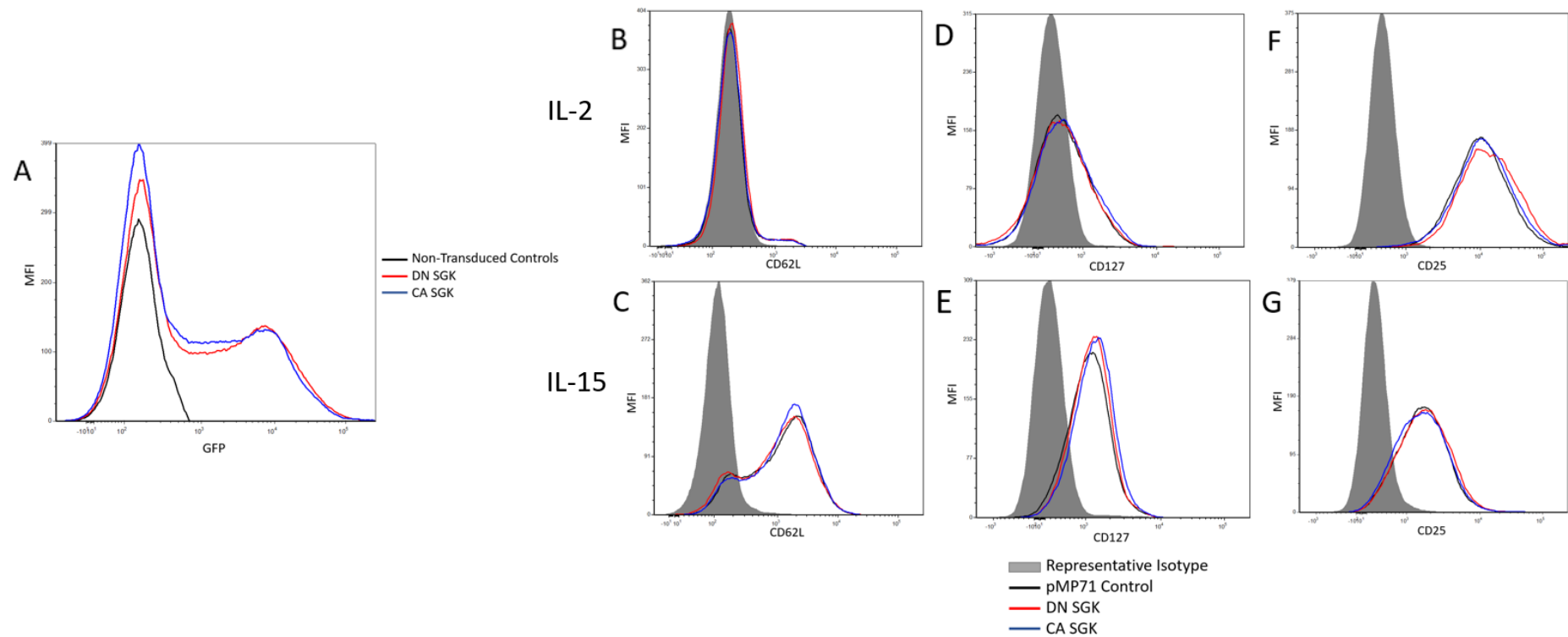


**Figure 6-9 – Effect of dominant negative and constitutively active SGK transduction on CD8 T cells**

CD8 T cells underwent transduction protocol as previously described with either the pMP71 vector as a control or the DN or CA form of SGK. Following transduction protocol cells were kept in 10ng/ml IL-2 for 24 hours at which point, cells were split and either continued their culture in 10ng/ml IL-2 or switched to 15ng/ml IL-15. **A** – GFP expression measured 24 hours post transduction to confirm uptake of the SGK vectors. **B+C** – CD62L expression on GFP<sup>+</sup> CD8<sup>+</sup> T cells 96 hours post culture with either IL-2 or IL-15 respectively. **D+E** – CD127 expression on GFP<sup>+</sup> CD8<sup>+</sup> T cells 96 hours post culture with either IL-2 or IL-15 respectively. **F+G** – CD25 expression on GFP<sup>+</sup> CD8<sup>+</sup> T cells 96 hours post culture with either IL-2 or IL-15 respectively.

### 6.3 Summation and Discussion

This chapter describes the initial approach to dissecting the role of SGK in CD8 T cells. Data in this chapter confirmed that the inhibitor GSK650394 caused a reduction in the level of phosphorylation of an immediate and unique SGK target, NDRG-1. Data presented here also demonstrate that inhibition of SGK causes a marked decrease in the proliferation of naïve CD8 T cells. Inhibition of SGK was also shown to affect the viability of CD8 T cells. To test whether these effects were due to SGK and not off target effects or toxicity, NaCl supplemented media was used as an alternative approach to study the role of SGK. In these experiments, CD8 T cells cultured under high NaCl conditions demonstrated significantly better survival and proliferation compared to untreated and osmotic controls. The SGK<sub>i</sub> studies, combined with the use of NaCl, support the pro-survival effects of SGK that have been demonstrated in other cell types<sup>377</sup>. The precise mechanism by which lymphocytes detect osmotic stress has yet to be elucidated. However, it has been demonstrated that A-kinase anchor protein 13, also known as Brx, is capable of signalling through the established p38 MAPK signalling pathway to both NFAT5 and SGK in response to altered osmolarity<sup>378</sup>. This response is thought to be the mechanism by which increased NaCl concentrations affect CD4 T cells as shown by both the Hafler and Kuchroo studies<sup>364,366,368</sup>. Both NFAT5 and SGK are known mediators of cellular volume and osmolarity control. As such, this pathway seems likely to mediate the osmotic stress response, despite the process by which Brx detects the initial alteration in NaCl remaining unknown.

The increased apoptosis seen in SGK<sub>i</sub> treated cells 72 hours post activation could be due to the lack of pro-survival activity that SGK induces. However, it is also possible that there are other mechanisms behind this enhanced cell death rate. The disruption of survival could be due to a lack of GLUT1, a glucose transporter protein. SGK1 has been shown to regulate the translocation of GLUT1 to the plasma membrane<sup>379</sup>, therefore, inhibition of SGK1 could lead to decreased expression of GLUT1 at the plasma membrane and subsequent lack of glucose uptake. Increased glucose uptake and increased expression of glucose transporters are essential metabolic traits of activated T cells, but not naïve cells. It is possible that it is this decreased expression of GLUT1 that contributes to the increased apoptotic effects observed. As SGK is the primary regulator of both cell volume and size, and both of these factors are noticeably increased when CD8 T cells are treated with the SGK<sub>i</sub> (data not shown), it is conceivable that inhibition of SGK disrupts the expression of ion channels that regulate this process. Given this, due to their increased size during activation, the cells may not be able to respond to sudden shifts in osmolarity, which could cause

the cells to rupture. Overall, SGK inhibition in CD8 T cells caused a marked reduction in proliferation over 48 hours, without impacting cell viability. Going forward, this work could be expanded upon in order to obtain further insight into the effects of SGK activity on components involved in T cell activation. Given its similarity to other AGC kinases, its connections to ERK, NFAT, NF- $\kappa$ B and mTORC1, as well as its effects on proliferation, SGK seems worthy of future study.

Two SGK mutated constructs were also generated; a dominant negative and constitutively active form, termed SGK DN and SGK CA respectively. These constructs were cloned into a GFP-expressing retroviral vector pMP71. Transduction of these SGK constructs was attempted, and GFP expression was demonstrated. However, subsequent examination demonstrated no change in expression of CD62L, CD127 or CD25, which are common markers of CD8 T cell phenotype. Under IL-15 culture, minimal Akt activity would be expected, as such, SGK CA should be capable of phosphorylating FOXOs and reducing their activity. Consequently, it would be expected that factors associated with reduction of FOXO1/3a activity (e.g. CD62L, CD127) would be reduced. Conversely if SGK and Akt coordinate to phosphorylate the FOXO transcription factors, it would be expected the SGK DN would somewhat improve expression of CD62L or CD127 whilst reducing CD25 expression. Follow-up tests to confirm expression of the construct through western blots against the HA-tag were unsuccessful. This could be for a number different reasons. It is possible that despite the expression of GFP, the SGK constructs themselves are not expressed. An alternative explanation is that the SGK constructs are expressed but the mutations are either non-functional or have compromised function. However, this is unlikely as similar constructs have been shown to be functionally expressed<sup>380,381</sup>. It could also be reasoned that SGK simply has no effect on expression of these markers that are typically linked to Akt activity, or that SGK only acts redundantly to compensate for lack of Akt activity. If this is the case, however, it should be possible to observe effects of SGK CA in IL-15 treated cells in which Akt activity is low.

As an alternative approach to study the role of SGK in CD8 T cells a shRNA knockdown of SGK could be performed. ShRNA mediated knockdown of SGK has already been reported in CD4<sup>+</sup> regulatory T cells<sup>368</sup> confirming the applicability of this approach. In T<sub>regs</sub> shRNA of SGK efficiently blocked the effects of high NaCl culture, causing a reduction in IFN $\gamma$  and T-bet expression<sup>368</sup>.

## Chapter 6

In summary the data in this chapter have shown that pharmacological inhibition of SGK restricts the proliferation of CD8 T cells. Under certain conditions this inhibition can negatively impact survival. Use of NaCl supplemented media, a known stimulator of SGK, promotes survival of CD8 T cells under IL-2 culture. The ability of salt to promote survival through SGK is more pronounced when IL-2 is at a sub-optimal concentrations.

## Chapter 7 Discussion

Signalling pathways have greatly contributed to our understanding of the mechanisms behind CD8 T cell activation, differentiation, exhaustion and metabolism. Insight into these mechanisms has enhanced our ability to exploit CD8 T cells for their anti-tumour capabilities.

### 7.1 Models of CD8 T Cell Differentiation

The process of differentiation involves complex integration of signalling pathways in CD8 T cells. This is reflected in the lack of a comprehensive model of CD8 T cell differentiation. As described previously in chapter 1, there are at minimum three models of differentiation; the signal strength model, decreasing potential model and asymmetric cell division. These models are summarised in *Figure 7-1A*. The signal strength model is based on the intensity of the initial stimulatory signal. This model states that stronger initial signals induce SLEC differentiation, whereas MPECs arise from cells that receive less stimulation. The decreasing potential model is similar to the signal strength model, in that cells receiving multiple rounds of antigenic stimulation develop a greater cytotoxic capacity at the expense of memory features, such as proliferative ability and longevity. Conversely, cells that receive fewer stimulatory events retain their ability to persist long term and as a consequence they form memory cells. This model of decreasing potential suggests that naïve cells first form memory cells, and can then differentiate into effector cells. This is supported by analysis showing higher telomerase activity as well as longer telomeres in memory cells compared with effector cells<sup>382</sup>. As such, with reduced telomere length and telomerase activity, it is unlikely that effector cells can differentiate into memory<sup>270</sup>. Lastly is the more recently proposed asymmetric cell division model. The asymmetric cell division model is based on studies showing that certain proteins and cellular components are not equally divided during cellular division, following initial stimulation and activation. This process has been shown to occur *in vitro* and *in vivo* for CD8 T cells, with CD8, mTORC1, Myc and T-bet accumulating preferentially in the daughter cell that is proximal to stimulatory APC<sup>117</sup>. By extrapolation, proximal cells inheriting more factors such as mTORC1, Myc and T-bet are likely to give rise to SLECs, whereas the distal cells go on to form MPECs. All of these models have supporting evidence, which indicates that the true mechanism behind CD8 T cell differentiation is likely to be an integration of these three models.

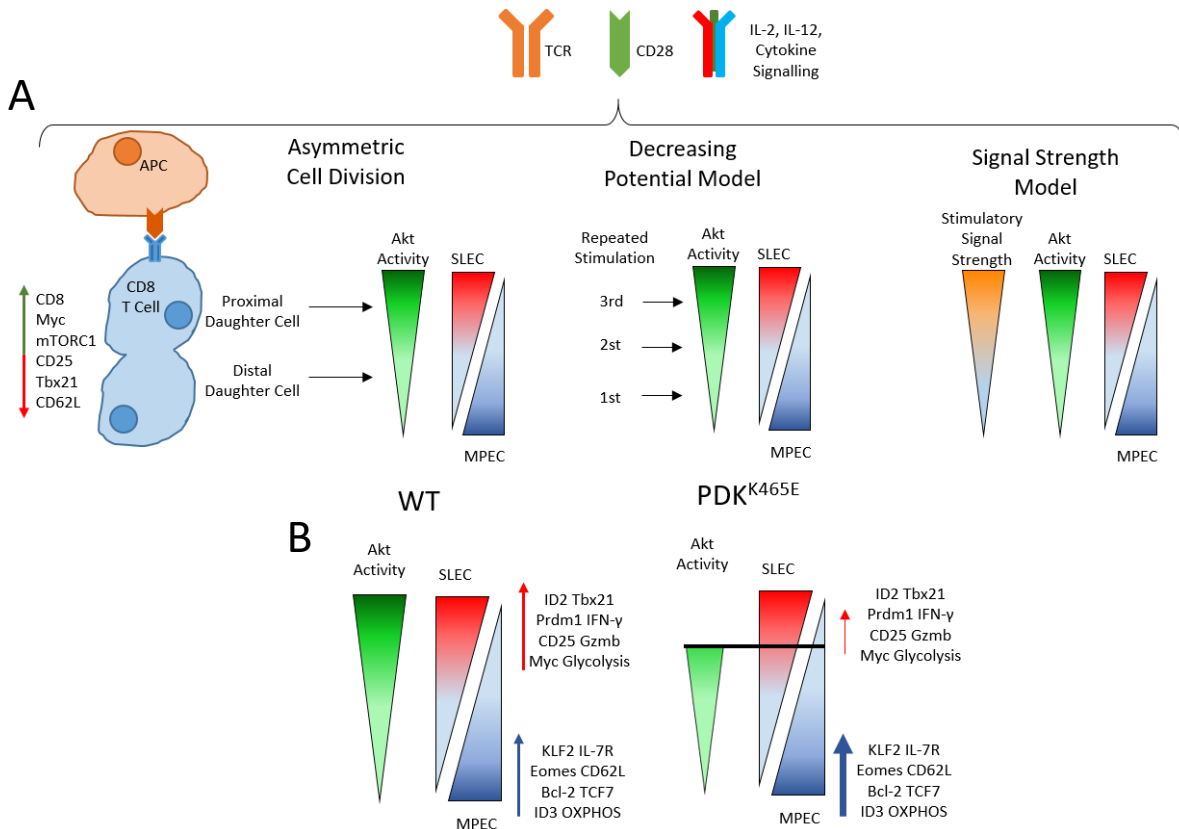


**Figure 7-1 – Models of Differentiation.**

**A** - Diagrams of the three primary models of CD8 T cell differentiation. With restricted Akt activity PDK<sup>K465E</sup> cells show reduced effector capacity and a preference for the MPEC phenotype during differentiation. However, this does not impair the ability of PDK<sup>K465E</sup> CD8 T cells to control infection and tumour. **B** – The effect of the PDK<sup>K465E</sup> mutation on Akt activity

The PDK<sup>K465E</sup> mutation restricts activation induced Akt activity but does not ablate it, as shown in *Figure 7-1B*. This restriction limits the overall ability of CD8 cells to express factors associated with effector function, as demonstrated in chapters 3 and 4. *In vitro* this causes a deficit in cytotoxic capacity, which is overcome under *in vivo* infection and tumour models. The data presented in chapter 4 of this thesis displays the single cell transcriptomic profile of WT and PDK<sup>K465E</sup> CD8 T cells at the peak of the immune response to an *in vivo* LM-OVA infection model. Seven distinct clusters of CD8 T cells were identified based on the pattern of gene expression. Utilising expression of the following markers: TCF7, IL-7R, granzyme B, MKi-67, EZH2 and KLRG1, these clusters could be defined into several phenotypic states. Cluster 1 was defined as cycling SLEC-like due to expression of granzyme B, MKi-67 and EZH2. Clusters 2, 3 and 6 were classified as non-cycling SLEC-like, differentiating them from cluster 1 based on the loss of MKi-67 and EZH2 expression and an increase in KLRG1 expression. Clusters 4, 7 and 8 were defined as MPEC-like, primarily due to high expression of TCF7 and IL-7R and the lack of effector molecule expression. The frequency of PDK<sup>K465E</sup> and WT CD8 T cells in these clusters was not equivalent. This is reflected in the cluster definitions, as two out of the three MPEC-like clusters (4 and 7) are primarily

composed of CD8 T cells of PDK<sup>K465E</sup> origin. This is at the expense of the non-cycling SLEC-like cells, in which the inverse was observed, with two out of three (3 and 6) being of WT origin. Typically at the peak of an immune response CD8 T cells are categorised as either SLECs or MPECs based on the expression of surface markers such as KLRG1 and CD127. However, from the gene expression based clusters generated from the Drop-Seq data there are four separate populations of WT CD8 T cells at the peak of this response. Within the two non-cycling SLEC clusters there was a significant difference in the expression of effector molecules, such as granzyme A, KLRG1, T-bet, S1PR5 and CX3CR1, as well as ribosomal proteins. This indicates that the process of differentiation is more complex than currently understood and the existing surface markers used to identify differential groups of cells are not able to reflect the heterogeneity at the transcriptomic level at this time point. When the effect of the PDK<sup>K465E</sup> mutation on this process is examined, an overall shift in differentiation is observed; with all PDK<sup>K465E</sup> CD8 T cells displaying increased expression of MPEC associated factors compared to their WT counterparts. At the transcriptomic level the effect of this mutation is substantial enough to shift the classification of clusters, adding a new MPEC cluster at the expense of one of the non-cycling SLEC clusters compared to the WT. ACT has been shown to be more effective when the transferred cells are able to generate a competent memory population<sup>383,384</sup>. As such, understanding how Akt signalling integrates into differentiation may provide insight into improving immunotherapies.

Comparison of PDK<sup>K465E</sup> and WT CD8 T cell gene expressions demonstrated a clear enrichment of transcripts encoding ribosomal proteins in the PDK<sup>K465E</sup> cells. This enrichment was also associated with the more MPEC-like cells in both cell types. The effects of altered ribosomal protein expression on CD8 T cell differentiation and function have yet to be elucidated. However, in other cell type enrichment of certain ribosomal proteins has been correlated with extra-ribosomal functions such as cellular proliferation and apoptosis<sup>385,386</sup>. The question remains whether the enrichment of genes encoding ribosomal proteins is a direct consequence of the PDK<sup>K465E</sup> mutation. It could be that increased expression of genes encoding ribosomal proteins is a new marker of memory in CD8 T cells, hence the relative enrichment in PDK<sup>K465E</sup> CD8 T cells merely reflects their skewed differentiation in favour of MPECs. Alternatively, heterogeneity in the composition of ribosomes has been attributed to preferential mRNA selection<sup>299</sup>. It could be possible that the altered expression of genes encoding the ribosomal proteins influences the mRNA molecules targeted for translation, in favour of those encoding proteins associated with the MPEC phenotype. Therefore meaning that increased expression of ribosomal protein could in fact cause a shift towards a memory phenotype. Exhausted CD8 T cells have demonstrated a reduction in ribosomal protein expression, as have repeatedly stimulated CD8 memory cells<sup>296,297</sup>.

These two cell types display impaired proliferative ability in addition to reduced expression of ribosomal proteins<sup>296,297</sup>. As such, it could be that the enrichment of genes encoding ribosomal proteins in the PDK<sup>K465E</sup> cells define their potential proliferative capacity, as MPEC cells are known to possess more robust proliferative abilities than effector cells. Further assessment of the effects of direct overexpression of ribosomal proteins is required to delineate whether any of these possibilities show promise.

Many cell based immunotherapies are more effective when memory cells are utilised. Being able to control and direct the differentiation process of CD8 T cells is key in order to ensure the development of memory cells.

## 7.2 The Role of Akt in CD8 T Cell Differentiation

Akt plays a central role in the generation of effector functionality and the differentiation of CD8 T cells. Its signalling pathway is activated by a myriad of external signals, including the TCR, co-stimulatory molecules, as well as  $\gamma$ -chain cytokine receptors. Akt, as a serine/threonine kinase, elicits its effects through phosphorylation of multiple downstream components. This can include other kinases, transcription factors and enzymes involved in epigenetic modification, described below as well as in *Figures 7.1* and *7.2*.

### 7.2.1 Epigenetic Modification by Akt in T Cells

Epigenetic modification refers to alterations to structures such as chromatin and histone proteins through mechanisms including, but not limited to, acetylation, methylation and phosphorylation. Epigenetics is still very much an emerging field of research. As such, its role in CD8 T cell function and differentiation is yet to be fully elucidated. However, Akt has been shown to phosphorylate enzymes involved with epigenetic modification, namely DNA-methyltransferase 1 (DNMT1) and enhancer of zeste homologue 2 (EZH2).

In the case of DNMT1, serine phosphorylation at position 143 by Akt enhances its activity through reduced degradation and stabilisation<sup>387,388</sup>. Despite its function not being fully established, DNMT1 has been shown to impact two factors in CD8 T cells, specifically, IFN- $\gamma$  production and rapid clonal expansion following antigen stimulation<sup>389,390</sup>. Conditional DNMT1 knockout in CD8 T

cells has been shown to significantly reduce activation induced expansion of antigen-specific cells following LCMV infection<sup>389</sup>. In addition, these DNMT1<sup>-/-</sup> CD8 T cells also display significant impairment of IFN- $\gamma$  production<sup>389</sup>. As increased Akt activity is associated with increased DNMT1 function, through epigenetic modifications Akt can enhance cellular proliferation and IFN- $\gamma$  production. Given that in PDK<sup>K465E</sup> CD8 T cells a reduction in the secretion of IFN- $\gamma$  is observed *in vitro*, it is possible that reduced Akt activity is mediated through epigenetic modifiers such as DNMT1 to impair IFN- $\gamma$  production.

Phosphorylation of EZH2 at serine 21 by Akt, however, has been shown to inhibit its function of methylating lysine at position 27 in histone protein 3 (H3K27)<sup>391</sup>. This phosphorylation was shown not to inhibit the inherent activity of EZH2, nor its association with the greater methylating complex of polycomb-repressive complex 2 (PRC2), but rather cause a reduction in affinity for its specific substrate<sup>391</sup>. Tri-methylation at H3K27 causes repression of genes present at these loci and has been correlated with proliferation, differentiation and survival factors<sup>392</sup>. Whilst active, EZH2 represses the transcription factors ID2, EOMES and PRDM1 (BLIMP-1), whilst enhancing ID3 expression<sup>393</sup>. Upon T cell activation, Akt-mediated phosphorylation of EZH2 could cause increased expression of ID2, EOMES and BLIMP-1, which in turn promotes a more terminally differentiated phenotype in CD8 T cells.

One study utilised Cre-recombinase linked to the granzyme B promoter (GzmB-Cre), along with a floxed form of the EZH2 gene, to generate activation induced loss of EZH2 in T cells<sup>394</sup>. This study demonstrated that loss of EZH2 causes a reduction in the number of antigen specific CD8 T cells at day 8 post-acute LCMV infection<sup>394</sup>. In addition, viral titers were also significantly increased in EZH2<sup>-/-</sup> mice, indicating an impairment of viral clearance<sup>394</sup>. Despite this knockout, there was little effect on cytokine production or proliferation<sup>394</sup>. A separate study using a CD4 linked Cre-recombinase, to generate a pan-T cell knockout of EZH2, demonstrated impaired tumour control<sup>393</sup>. In these experiments, it was determined that the reduced control of tumours was due to an overall reduction in survival of antigen specific CD8 T cells by day 7<sup>393</sup>. In addition, this loss of EZH2 also compromised maintenance of MPECs. These studies suggests that a lack of EZH2 at this early stage impairs survival of effector cells, which in turn prevents virus or tumour clearance. In summary, increasing Akt activity reduces the ability of EZH2 to maintain H3K27 methylation, which in turn could enhance the expression of transcription factors associated with terminal differentiation.

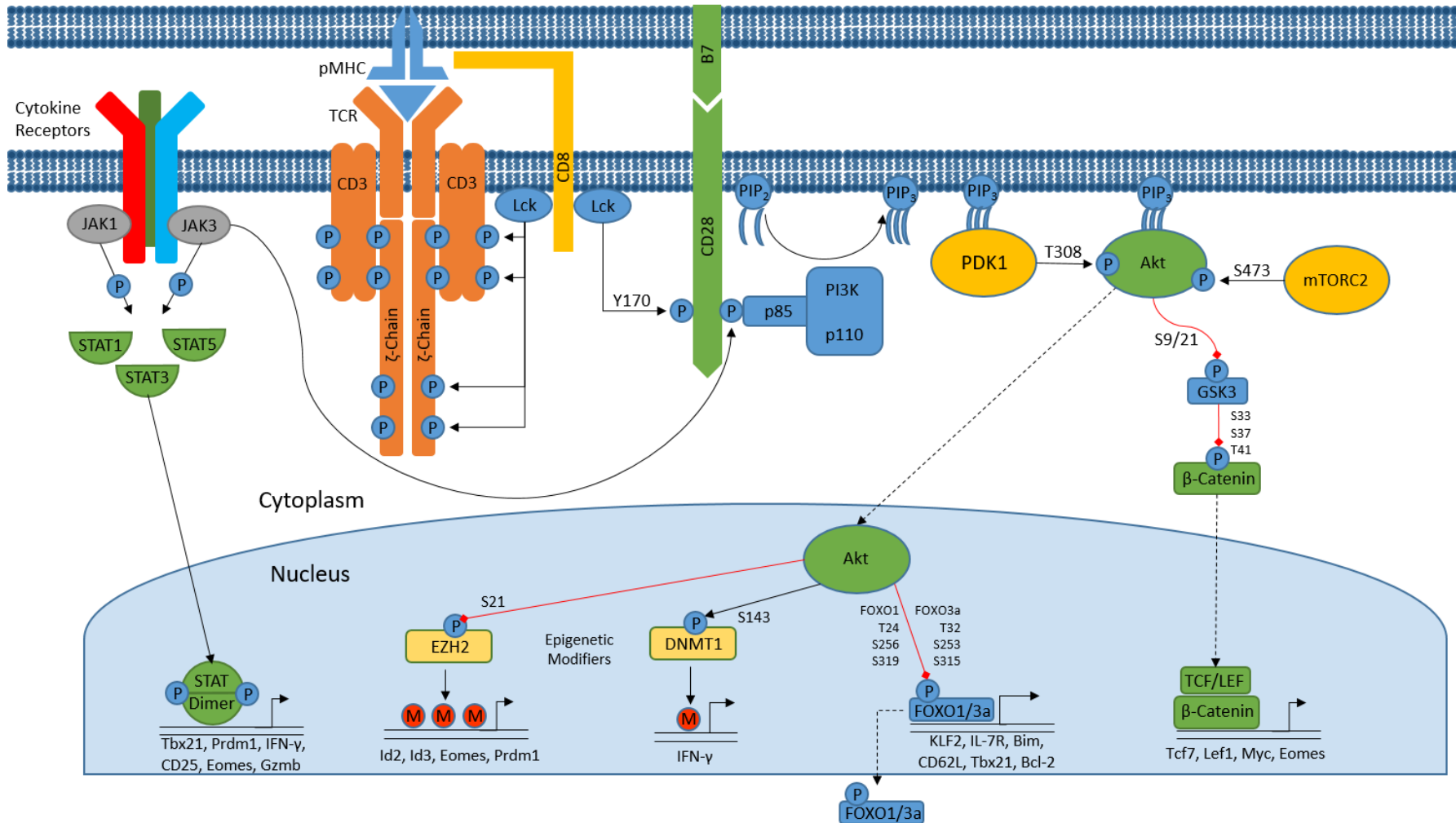


**Figure 7-2 – Akt signalling pathway**

Activation of PI3K through TCR receptor stimulation, CD28 co-stimulation and cytokine engagement induces PDK1/Akt activity. Akt negatively regulates GSK3, permitting  $\beta$ -catenin signalling. FOXO1 and FOXO3a are direct transcription factor targets of Akt. Their phosphorylation by Akt causes exclusion from the nucleus. Akt can also interact with the epigenome through two methyltransferase enzymes, EZH2 and DNMT1. Activity of these two enzymes can alter expression of genes based on alteration of chromatin structure through methylation of histone proteins. Expanded version of Figure 3-1, reflecting factors that stimulate Akt and affect CD8 T cell differentiation in order to summarise possible downstream mechanisms of the PDK<sup>K465E</sup> mutation. Includes phosphorylation sites of the PI3K/Akt signalling pathway.

However, complete loss of EZH2 impairs the survival of both effector cells and MPECs, potentially compromising the control of cancerous cells, infections as well as memory generation.

Interestingly, upon Akt activation you would expect the reduction in activity of EZH2 to increase the expression of EOMES in WT cells. However, in comparisons of WT and PDK<sup>K465E</sup> CD8 T cells in experiments reported in chapter 4, increased expression of EOMES is observed in the PDK<sup>K465E</sup> cells within the comparisons of both SLEC-like and MPEC-like clusters. This suggests that increased EOMES expression is the result of a different pathway outside of epigenetic modifications by EZH2. ID2 expression between the WT SLEC-like cells (clusters 6 and 3) and the PDK<sup>K465E</sup> SLEC-like cells (cluster 2) was not significantly different between any of the comparisons of these three clusters. Transcripts encoding BLIMP-1 were not detectable in this Drop-Seq experiment.

### 7.2.2 Regulation of Transcription Factor Activity by Akt in T Cells

Akt has regulatory control over a series of transcription factors, which in turn influence effector function, metabolism and effector and memory differentiation. Two transcription factors that are direct targets of Akt are FOXO1 and FOXO3a. Akt phosphorylates FOXO1 on a threonine and two serine residues at positions 24, 256 and 319 respectively<sup>395</sup>. This phosphorylation of FOXO1 causes its binding to 14-3-3 proteins, its exclusion from the nucleus, ubiquitination and subsequent degradation<sup>396</sup>. The target genes of the FOXO family of transcription factors include *Bach2*, *Klf2*, *IL7R* (CD127), *Eomes*, *Tbx21* (T-bet), *Sell* (CD62L), *Bcl-2*, in addition to multiple cell cycle kinases, cytokine and chemokine receptors<sup>396</sup>.

Silencing of FOXO1 activity has been shown to increase T-bet expression, and to reduce expression of MPEC associated factors, thus leading to a shift in CD8 T cell differentiation favouring terminal differentiation<sup>397</sup>. In addition, KLRG1<sup>lo</sup> CD8 T cells, from FOXO1<sup>-/-</sup> mice, which are normally considered to be more MPEC-like, retain granzyme B and CD69 expression, without upregulation of TCF7 and EOMES<sup>396</sup>. This renders these memory cells unable to expand upon secondary stimulation. As such, FOXO1 is critical to the development of a competent CD8 T cell memory population capable of immune reactivation<sup>398</sup>. FOXO1 has also been implicated in the persistent expression of PD-1 during chronic LCMV infection<sup>399</sup>. Thus, in addition to promoting memory differentiation, under certain conditions FOXO1 also contributes to the exhaustion

## Chapter 7

processes<sup>399</sup>. Given the reduced Akt activity of the PDK<sup>K465E</sup> mutation, increased FOXO1 activity would contribute to shift in differentiation displayed in the transcriptomic data of chapter 4. Expression of transcripts encoding FOXO1 targets, including TCF7, CD62L and IL-7R, are increased within the MPEC-like PDK<sup>K465E</sup> cells (clusters 4 and 7) compared to the WT MPEC-like cells (cluster 8).

FOXO3a has three similar phosphorylation sites as FOXO1; a single threonine and two serine residues at positions 32, 253 and 315 respectively<sup>400</sup>. Whilst these sites are primarily phosphorylated by Akt, SGK has also been shown to phosphorylate these sites, indicating parallel or possible redundancy mechanisms<sup>377</sup>. FOXO3a can restrain the expansion of effector CD8 T cells<sup>401</sup> and thus FOXO3a deficient effector CD8 T cells accumulate in greater numbers, resulting in an increased MPEC population<sup>402</sup>. This increased memory population does not induce a stronger recall response however, suggesting a role for FOXO3a in regulating secondary responses<sup>402</sup>. The PDK<sup>K465</sup> mutation should result in greater functional activity of FOXO3a, due to the lack of activation induced Akt activity. In experiments previously reported by this group, it has been demonstrated that PDK<sup>K465E</sup> cells show accelerated contraction following vaccination with OVA, anti-CD40 and LPS<sup>240</sup>. This implies that the increased FOXO3a activity is in part responsible for the increased contraction displayed.

Despite coming from the same inhibitor of DNA binding (ID) family of transcription factors, ID2 and ID3 act in direct opposition to each other. ID2 can be induced through cytokine signalling pathways mediated by STATs, as well as through Akt mediated downregulation of EZH2<sup>393</sup>. Loss of ID2 in CD8 T cells is associated with an increase in ID3 expression, as well as a loss of the KLRG1<sup>+</sup> population of cells post LM-OVA infection<sup>403</sup>. In addition, ID2 deficient CD8 T cells have impaired T-bet expression, which overall prevents the generation of competent SLECs<sup>404</sup>. In experiments involving transfer of ID3<sup>lo</sup> and ID3<sup>hi</sup> CD8 T cells, it has been demonstrated that ID3<sup>hi</sup> cells are preferentially skewed towards increased CD127 expression and cytokine production<sup>403</sup>. Furthermore, these ID3<sup>hi</sup> CD8 T cells showed enrichment of genes correlated with MPECs. In accordance with these data, loss of ID3 is associated with defects in long term memory CD8 T cells; with ID3<sup>-/-</sup> mice displaying far fewer memory cells at day 60 post vesicular stomatitis virus-OVA (VSV-OVA) infection<sup>403</sup>. This is despite no outward alteration in the frequency of KLRG1 and CD127 expression. ID2, however, was not significantly differentially expressed between the observed clusters in the Drop-Seq data sets. ID3 was not detected in this analysis.

*Tbx21*, along with its protein product T-bet, is a key transcription factor associated with an effector CD8 T cell phenotype. T-bet induction is correlated to increased expression of multiple effector molecules including granzyme B, IFN- $\gamma$ , KLRG1 and IL-2R $\beta$ <sup>405,406</sup>. Generation of KLRG1<sup>hi</sup> SLECs is entirely dependent on the degree of T-bet expression, as studies on copy-number of *Tbx21* have demonstrated<sup>88</sup>. In certain conditions, EOMES also functions somewhat in concert with T-bet to maintain CD122 expression<sup>406</sup>. As CD8 T cells differentiate from effector into memory cells, T-bet expression gradually decreases, conversely EOMES expression increases<sup>406</sup>. Utilising EOMES knockout mice, it has been demonstrated that following LCMV infection, CD8 T cells display a reduced number of memory CD8 T cells, as well as a reduced frequency of CD62L<sup>+</sup> cells<sup>407</sup>. The balance of T-bet and EOMES has been implicated in the overall differentiation state of CD8 T cells<sup>408</sup>. BLIMP-1 (*Prdm1*) is also induced by inflammatory cytokines in a similar manner to T-bet and further acts to enhance the expression of a similar manner of effector function related genes<sup>409</sup>. BLIMP-1<sup>-/-</sup> CD8 T cells demonstrate increased survival of effector cells, as well as increased MPEC formation<sup>410</sup>. Interestingly, despite increased Akt activity, which through FOXO1 regulates T-bet expression, there is no significant increase in the amount of transcripts encoding T-bet in the WT cells compared to PDK<sup>K465E</sup> cells from the transcriptomic data in chapter 4. However, within the two WT non-cycling SLEC-like clusters (6 and 3), cluster 6 does show increased expression of transcripts encoding T-bet compared to cluster 3.

TCF7 is downstream of the canonical Wnt signalling pathway and a target of  $\beta$ -catenin. Akt can influence this pathway greatly through the phosphorylation of GSK3- $\beta$ . GSK3- $\beta$  typically phosphorylates and degrades  $\beta$ -catenin. However, following phosphorylation by Akt, the activity of GSK3- $\beta$  is inhibited, increasing  $\beta$ -catenin expression and consequently TCF7<sup>341</sup>. Lack of TCF7 expression in CD8 T cells has been demonstrated to impair both the capacity for secondary expansion as well as the ability to differentiate to acquire the central memory phenotype<sup>411</sup>. Whilst central memory phenotype is decreased in TCF7<sup>-/-</sup> CD8 T cells, they still possess an effector memory phenotype. However, these knockout mice display a progressive loss of these effector memory CD8 T cells, which has been attributed to reduced responsiveness to IL-15<sup>411</sup>. Loss of TCF7 is also associated with reduced EOMES expression, which in turn could contribute to the compromised central memory phenotype<sup>411</sup>. Given that PDK<sup>K465E</sup> cells are restricted in Akt activity you would expect TCF7 expression to also be restricted through increased GSK3- $\beta$  activity. However, from the transcriptomic data in chapter 4, TCF7 is more highly expressed in PDK<sup>K465E</sup> cells, as well as the MPEC-like WT cells. Given this, it is likely that some alternative method

besides the canonical Wnt signalling pathway through GSK3- $\beta$  results in this increased expression. FOXO1 is known to target TCF7<sup>412</sup> and as such could explain the observed increase in PDK<sup>K465E</sup> cells. TCF7 is a direct target of EOMES, as this is also increased in MPECs and PDK<sup>K465E</sup> cells, this is another possible cause.

### 7.2.3 Influence of Akt Signalling on CD8 T Cell Metabolism

The role of Akt in glycolysis has been previously established in multiple cell types. However, the function of Akt in metabolism of CD8 T cells specifically, is unique in comparison to other cell types as activation of mTORC1 is not reliant on Akt activity. Typically, mTORC1 is one of the critical activators of the glycolytic pathway through activation of HIF1 $\alpha$  and c-Myc<sup>313</sup>. These two proteins promote the expression of pyruvate dehydrogenase kinase 1, lactate dehydrogenase, Glut1, Glut3, and hexokinase 2, all of which contribute to an increased glycolytic rate<sup>316</sup>. As such, Akt itself affects glycolysis through two main processes. The first process prevents the internalisation and degradation of Glut1, and the second promotes the function of hexokinase enzymes that act as a rate-limiting step in glycolysis<sup>241,309</sup>.

As the focus of the effects of Akt has been on examining glycolysis, its role in oxidative phosphorylation in CD8 T cells is poorly defined. The transcriptomic analysis from chapter 4 demonstrated a significant enrichment of transcripts encoding genes related to oxidative phosphorylation, which implies improved capacity in this metabolic process. Data from chapter 5 examined the effects of pharmacological inhibition of Akt on oxidative phosphorylation in CD8 T cells. Inhibition of Akt in CD8 T cells in IL-2 culture demonstrated a minor improvement in SRC which was not statistically significant. However, when PDK<sup>K465E</sup> CD8 T cells were cultured under similar conditions they displayed significantly improved SRC over the IL-2 treated control cells. Based on this it would seem that if Akt activity can be reduced to severe enough extent, an improvement in oxidative phosphorylation can be seen. Interestingly, there was also an improvement in SRC when PDK<sup>K465E</sup> CD8 T cells were cultured in IL-15 compared to WT cells under the same conditions. There was no observed difference in SRC between the WT and PDK<sup>K465E</sup> CD8 T cells whilst cultured under IL-2 alone. This indicates that the Akt signalling pathway is capable of affecting oxidative phosphorylation, but the mechanism by which this occurs still requires delineation. Studies in other cell types have indicated possible mechanisms through proteins such as MFN2, Opa1 and Oma1, but the links between these proteins and Akt have not been established in CD8 T cells<sup>336,338</sup>.

When the effects of constitutively active Akt in CD8 T cells in IL-15 culture were examined, a significant reduction was observed compared to cells with physiological Akt. This reduction however, was still a significant improvement over IL-2 treated CD8 T cells. This indicates that whilst non-physiologically high levels of Akt activity can impair oxidative phosphorylation, it cannot emulate the effects of IL-2, whilst in IL-15 culture. This would suggest that Akt activity alone is not the primary determinant in the capacity of CD8 T cells to perform oxidative phosphorylation.

In addition to improved SRC, Myr-Akt transduced IL-15 treated CD8 T cells demonstrated equal killing ability to IL-2 treated control cells. However, the granzyme B expression was reduced in the Myr-Akt transduced cells compared to the IL-2 treated control cells, indicating that to achieve full granzyme B expression it requires more than constitutive Akt activity. These IL-15 treated Myr-Akt transduced cells also demonstrate beneficial effect in tumour challenges *in vivo* against IL-15 treated control cells. However, these Myr-Akt transduced cells also displayed impaired survival *in vivo*. Whilst improved SRC is a known feature of memory CD8 T cells, it is not the primary determinant in CD8 T cells persistence. Soon after injection into mice Myr-Akt transduced cells are reduced in frequency in blood. This could be due to the reduced expression of CD127 as a result of constitutive Akt activity. However, the lack of presence in blood is not a certain indicator of lack of survival. Increased Akt activity has also been associated with increased expression of CD69 and CD103<sup>344</sup>. These factors are more commonly associated with the resident memory phenotype, as lectins and integrin proteins are required for long term persistence in non-lymphoid tissues<sup>413</sup>. As such, it is possible that these Myr-Akt transduced cells infiltrate tissue instead of circulating in blood. This might also explain how they are able to remain as effective as IL-2 treated control cells in an *in vivo* tumour challenge, despite showing a reduced frequency in blood.

### 7.3 Summation

In summary, this thesis has focussed on expanding the current understanding of Akt signalling in the context of CD8 T cells. Specifically, it has primarily addressed the role Akt plays in the generation of effector functions, and the processes of differentiation and metabolism. The impairment of effector functions that PDK<sup>K465E</sup> CD8 T cells possess is clear when stimulated *in vitro*, but is not reflected *in vivo*. This suggests that the reduced Akt activity can be compensated for, with other factors stimulated in an *in vivo* system, indicating that full Akt activation is not required for competent effector functions. scRNA-Seq, using Drop-Seq, has demonstrated that at the peak of the immune response, CD8 T cells can be defined into four transcriptionally distinct clusters. This is currently un-reflected in the identifiable groups using the traditional surface markers. Thus indicating that the CD8 T cell differentiation process, at this time point, is more nuanced than first thought. The PDK<sup>K465E</sup> mutation promotes differentiation of CD8 T cells into an MPEC-like phenotype in response to an *in vivo* infection model. This phenotype is characterised by an enrichment of genes encoding both ribosomal proteins and oxidative phosphorylation. Akt activity is inversely correlated with mitochondrial oxidative phosphorylation. However, IL-15 can still enhance oxidative phosphorylation under constitutive Akt activity. Constitutive Akt activity in CD8 T cells under IL-15 culture can provide benefits to anti-tumour activity, but at the cost of persistence in blood. Lastly, it was demonstrated that SGK can promote both survival and proliferation in CD8 T cells.

There remains the question of the application of the data within this thesis and what it adds to the literature surrounding the concept of Akt manipulation in immunotherapy. The use of Akt inhibition or modulation of the Akt pathway for the purposes of immunotherapy has been demonstrated by multiple groups<sup>414-416</sup>. Restifo *et al*<sup>414</sup> demonstrated that using Akt inhibition during culture of anti-CD19 chimeric antigen receptor modified CD8 T cells, when used in adoptive cell transfer, led to improved survival in mice bearing a model of acute lymphoblastic leukaemia. In a similar vein, Dolstra *et al*<sup>415</sup> also showed the benefits of Akt inhibition for ACT in a multiple myeloma model. These studies demonstrate that culture with Akt inhibition throughout the generation of the CTLs for ACT improves the clearance of tumour and survival rates. Beyond this, they express that the improvement in anti-cancer ACT is a direct result of the Akt inhibition inducing a more central memory like phenotype. Based on my data, I would agree that inhibition of Akt activity induces a phenotype similar with that of central memory T cells (T<sub>CM</sub>). The data from the Drop-Seq confirms the overall effect of the PDK<sup>K465E</sup> mutation is an alteration in cellular

differentiation, increasing expression of transcripts encoding oxidative phosphorylation proteins, TCF7, IL-7R, CD62L and CCR7, all of which are associated with a memory phenotype. This would support the use of Akt inhibition in the development of improved ACT competent CTLs. However, these models were primarily performed using either leukemic or lymphoma derived cell lines. The tumours from these cell lines can preferentially target the secondary lymph nodes, as seen in the work of Restifo *et al*<sup>414</sup>. This would mean CD8 T cells cultured in the presence of Akt inhibitors would be more likely to migrate to these sites due to upregulation of factors such as CD62L and CCR7. Therefore, whilst Akt inhibition might be an effective strategy when targeting cancer of a haematopoietic origin, it may not be as effective when dealing with cancers such as melanoma or those of epithelial origin.

It is my opinion that understanding specifically what causes the differentiation of effective CD8 T cell response and the subsequent production of memory is critical to the development of new therapies. As part of the transcriptomic data set presented in this thesis, the state of CD8 T cell differentiation during an immune response has been shown to be more complex than the current system of classification. In addition, it has been demonstrated that a consequence of reduced Akt activity in the PDK<sup>K465E</sup> mutant model is the upregulation of transcripts encoding ribosomal and oxidative phosphorylation proteins. We have somewhat of an understanding of the role that metabolism plays in relation to CD8 T cell differentiation. The induction of a memory like phenotype in CD8 T cells increases mitochondrial oxidative phosphorylation. Conversely, inducing more mitochondrial oxidative phosphorylation in CD8 T cells also produces a more memory like phenotype<sup>282,417</sup>. However, the relationship between ribosomal protein and CD8 T cell differentiation is an unknown quantity. Since the writing of this thesis, experiments from within our lab have demonstrated that when testing the secondary response of both WT and PDK<sup>K465E</sup> CD8 T cells, it was discovered that the PDK<sup>K465E</sup> cells displayed a substantial increase in proliferation upon restimulation compared to their WT counterparts. During primary responses, much of the resources expended by cells is directed to the biosynthesis of ribosomes to support accelerated protein production<sup>293</sup>. As such, it is not unreasonable to suggest that the increased expansion seen in PDK<sup>K465E</sup> mutants during a secondary immune response is due to the increased expression of transcripts encoding ribosomal proteins observed in the Drop-Seq data set. A hallmark of an effective memory response is rapid expansion following re-exposure to the triggering antigen<sup>418</sup>. Therefore, if increased expression of ribosomal proteins does dictate the secondary response rate in memory cells, methods of increasing the number of ribosomes would be a valid strategy in the development of effective memory CD8 T cells.

In addition, data from chapter 6 indicates that signalling through SGK promotes survival of CD8 T cells during times of cytokine deprivation. However, stimulation of SGK in current *in vitro* systems has relied on increasing the concentration of NaCl within the culture media. NaCl, whilst an effective stimulator of SGK activity, does have negative effects in human health, such as hypertension and numerous forms of cardiovascular disease<sup>419</sup>. Hafler and Kuchroo have already demonstrated the effect of NaCl on CD4 T cells, where it depresses the effectiveness of regulatory T cells and promotes the development of the highly inflammatory T<sub>H</sub>17 subset<sup>366,368</sup>. As the tumour microenvironment is often considered an area of both cytokine disruption and nutrient deprivation<sup>420</sup>, it stands to reason the SGK stimulation of CD8 T cells within tumour microenvironments could be beneficial to their survival in such an inhospitable atmosphere. Continuing to study SGK and its associated signalling pathway is therefore critical in order to discover a mechanism of stimulating SGK outside of NaCl, as well as how SGK transduces this increased survival response.

Developing our knowledge of signalling pathways in CD8 T cells allows us to better control and exploit them for therapeutic benefit. As such, this thesis has aimed to expand upon what is currently known about Akt and the effects of its signalling pathway in CD8 T cells.

## Chapter 8 Data Appendix

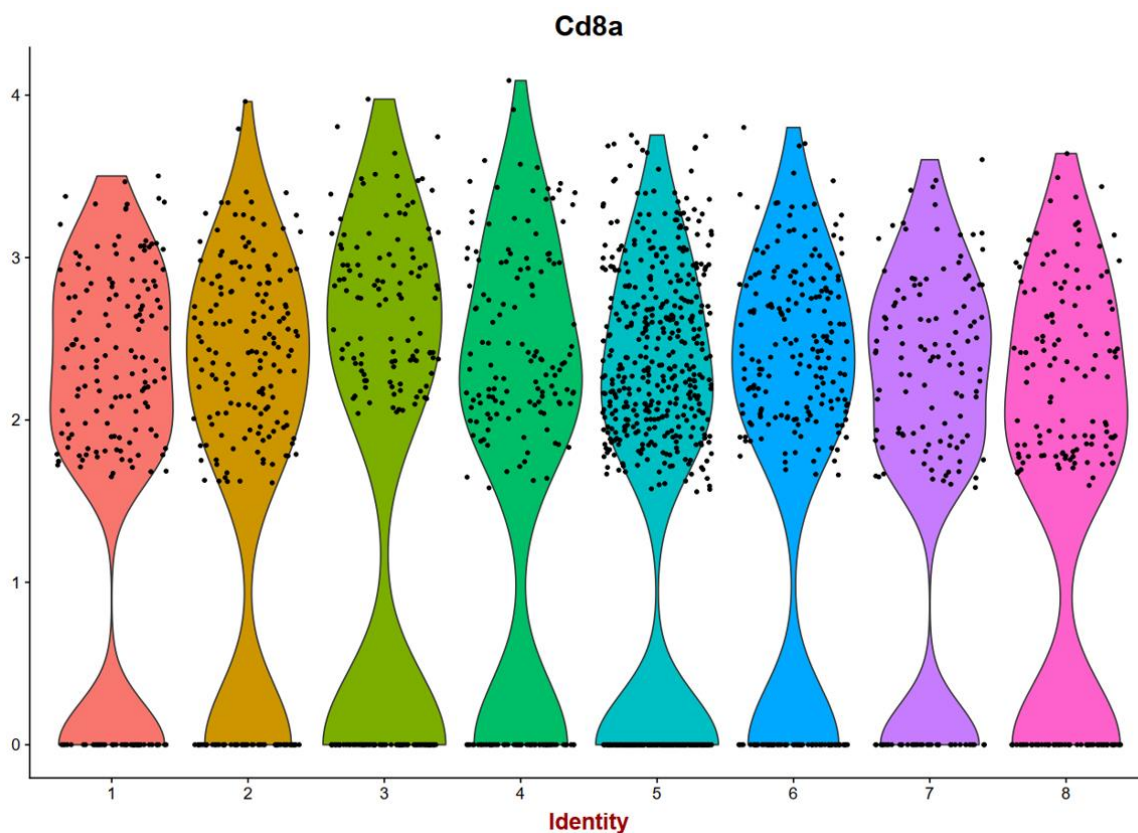


**Figure 8-1 – Expression of CD8a in t-SNE clusters.**

Violin plot demonstrating the expression of CD8 $\alpha$  across the clusters from the t-SNE plot in *Figure 4-3*. x-axis display cluster identity from t-SNE plot, y-axis displays relative expression of target gene.

*Figure 8-1* demonstrates that all clusters across the generated t-SNE plot of *Figure 4-3* showed expression of CD8 $\alpha$ . The frequency of cells expressing CD8 $\alpha$  was equitable across all clusters which indicates broad expression across the cell types regardless of WT or PDK<sup>K465E</sup> origin.



## List of References

- 1 Buck, M. D., O'Sullivan, D. & Pearce, E. L. T cell metabolism drives immunity. *The Journal of experimental medicine* **212**, 1345-1360, doi:10.1084/jem.20151159 (2015).
- 2 Portou, M. J., Baker, D., Abraham, D. & Tsui, J. The innate immune system, toll-like receptors and dermal wound healing: A review. *Vascular pharmacology* **71**, 31-36, doi:10.1016/j.vph.2015.02.007 (2015).
- 3 Hato, T. & Dagher, P. C. How the Innate Immune System Senses Trouble and Causes Trouble. *Clinical journal of the American Society of Nephrology : CJASN* **10**, 1459-1469, doi:10.2215/cjn.04680514 (2015).
- 4 Yatim, K. M. & Lakkis, F. G. A brief journey through the immune system. *Clinical journal of the American Society of Nephrology : CJASN* **10**, 1274-1281, doi:10.2215/cjn.10031014 (2015).
- 5 Reddy, S. T., Swartz, M. A. & Hubbell, J. A. Targeting dendritic cells with biomaterials: developing the next generation of vaccines. *Trends in immunology* **27**, 573-579, doi:10.1016/j.it.2006.10.005 (2006).
- 6 Tang, D., Kang, R., Coyne, C. B., Zeh, H. J. & Lotze, M. T. PAMPs and DAMPs: signal 0s that spur autophagy and immunity. *Immunological reviews* **249**, 158-175, doi:10.1111/j.1600-065X.2012.01146.x (2012).
- 7 Bernard, J. J. *et al.* Ultraviolet radiation damages self noncoding RNA and is detected by TLR3. *Nature medicine* **18**, 1286-1290, doi:10.1038/nm.2861 (2012).
- 8 Braga, T. T. *et al.* Soluble Uric Acid Activates the NLRP3 Inflammasome. *Sci Rep* **7**, 39884, doi:10.1038/srep39884 (2017).
- 9 Abbey, J. L. & O'Neill, H. C. Expression of T-cell receptor genes during early T-cell development. *Immunology and cell biology* **86**, 166-174, doi:10.1038/sj.icb.7100120 (2008).
- 10 Laydon, D. J., Bangham, C. R. & Asquith, B. Estimating T-cell repertoire diversity: limitations of classical estimators and a new approach. *Philosophical transactions of the Royal Society of London. Series B, Biological sciences* **370**, doi:10.1098/rstb.2014.0291 (2015).
- 11 Alexandropoulos, K. & Danzl, N. M. Thymic epithelial cells: antigen presenting cells that regulate T cell repertoire and tolerance development. *Immunologic research* **54**, 177-190, doi:10.1007/s12026-012-8301-y (2012).
- 12 von Boehmer, H. & Fehling, H. J. Structure and function of the pre-T cell receptor. *Annual review of immunology* **15**, 433-452, doi:10.1146/annurev.immunol.15.1.433 (1997).
- 13 Michie, A. M. & Zuniga-Pflucker, J. C. Regulation of thymocyte differentiation: pre-TCR signals and beta-selection. *Seminars in immunology* **14**, 311-323 (2002).
- 14 Huang, C.-Y., Sleckman, B. P. & Kanagawa, O. Revision of T cell receptor  $\alpha$  chain genes is required for normal T lymphocyte development. *Proc. Natl. Acad. Sci. U. S. A.* **102**, 14356-14361, doi:10.1073/pnas.0505564102 (2005).

## List of References

- 15 Germain, R. N. T-cell development and the CD4-CD8 lineage decision. *Nature reviews. Immunology* **2**, 309-322, doi:10.1038/nri798 (2002).
- 16 Xu, X. *et al.* Maturation and emigration of single-positive thymocytes. *Clinical & developmental immunology* **2013**, 282870, doi:10.1155/2013/282870 (2013).
- 17 Kaech, S. M., Wherry, E. J. & Ahmed, R. Effector and memory T-cell differentiation: implications for vaccine development. *Nature reviews. Immunology* **2**, 251-262, doi:10.1038/nri778 (2002).
- 18 D'Cruz, L. M., Rubinstein, M. P. & Goldrath, A. W. Surviving the crash: transitioning from effector to memory CD8+ T cell. *Seminars in immunology* **21**, 92-98, doi:10.1016/j.smim.2009.02.002 (2009).
- 19 Sprent, J. & Tough, D. F. T cell death and memory. *Science* **293**, 245-248, doi:10.1126/science.1062416 (2001).
- 20 Di Pucchio, T. *et al.* Direct proteasome-independent cross-presentation of viral antigen by plasmacytoid dendritic cells on major histocompatibility complex class I. *Nature Immunology* **9**, 551, doi:10.1038/ni.1602  
<https://www.nature.com/articles/ni.1602#supplementary-information> (2008).
- 21 Wang, J. & Maldonado, M. A. The ubiquitin-proteasome system and its role in inflammatory and autoimmune diseases. *Cell Mol Immunol* **3**, 255-261 (2006).
- 22 Savina, A. & Amigorena, S. Phagocytosis and antigen presentation in dendritic cells. *Immunological reviews* **219**, 143-156, doi:10.1111/j.1600-065X.2007.00552.x (2007).
- 23 Li, J., Chai, Q. Y. & Liu, C. H. The ubiquitin system: a critical regulator of innate immunity and pathogen-host interactions. *Cell Mol Immunol* **13**, 560-576, doi:10.1038/cmi.2016.40 (2016).
- 24 Trolle, T. *et al.* The Length Distribution of Class I-Restricted T Cell Epitopes Is Determined by Both Peptide Supply and MHC Allele-Specific Binding Preference. *The Journal of Immunology* **196**, 1480-1487, doi:10.4049/jimmunol.1501721 (2016).
- 25 Evnouchidou, I., Weimershaus, M., Saveanu, L. & van Endert, P. ERAP1-ERAP2 Dimerization Increases Peptide-Trimming Efficiency. *The Journal of Immunology* **193**, 901-908, doi:10.4049/jimmunol.1302855 (2014).
- 26 Wieczorek, M. *et al.* Major Histocompatibility Complex (MHC) Class I and MHC Class II Proteins: Conformational Plasticity in Antigen Presentation. *Frontiers in immunology* **8**, 292, doi:10.3389/fimmu.2017.00292 (2017).
- 27 Zhang, Y. & Williams, D. B. Assembly of MHC class I molecules within the endoplasmic reticulum. *Immunologic research* **35**, 151-162, doi:10.1385/ir:35:1:151 (2006).
- 28 Antoniou, A. N. *et al.* ERp57 interacts with conserved cysteine residues in the MHC class I peptide-binding groove. *FEBS Lett* **581**, 1988-1992, doi:10.1016/j.febslet.2007.04.034 (2007).
- 29 Raghavan, M., Wijeyesakere, S. J., Peters, L. R. & Del Cid, N. Calreticulin in the immune system: ins and outs. *Trends in immunology* **34**, 13-21, doi:10.1016/j.it.2012.08.002 (2013).
- 30 Neefjes, J. J., Momburg, F. & Hammerling, G. J. Selective and ATP-dependent translocation of peptides by the MHC-encoded transporter. *Science* **261**, 769-771 (1993).

- 31 Bleeis, A. *et al.* Structure of the human MHC-I peptide-loading complex. *Nature* **551**, 525-528, doi:10.1038/nature24627 (2017).
- 32 Praveen, P. V., Yaneva, R., Kalbacher, H. & Springer, S. Tapasin edits peptides on MHC class I molecules by accelerating peptide exchange. *European journal of immunology* **40**, 214-224, doi:10.1002/eji.200939342 (2010).
- 33 Reis e Sousa, C. Toll-like receptors and dendritic cells: for whom the bug tolls. *Seminars in immunology* **16**, 27-34 (2004).
- 34 den Haan, J. M. & Bevan, M. J. Antigen presentation to CD8+ T cells: cross-priming in infectious diseases. *Current opinion in immunology* **13**, 437-441 (2001).
- 35 Brownlie, R. J. & Zamoyska, R. T cell receptor signalling networks: branched, diversified and bounded. *Nature reviews. Immunology* **13**, 257-269, doi:10.1038/nri3403 (2013).
- 36 Xu, C. *et al.* Regulation of T cell receptor activation by dynamic membrane binding of the CD3epsilon cytoplasmic tyrosine-based motif. *Cell* **135**, 702-713, doi:10.1016/j.cell.2008.09.044 (2008).
- 37 Davis, S. J. & van der Merwe, P. A. The kinetic-segregation model: TCR triggering and beyond. *Nat Immunol* **7**, 803-809, doi:10.1038/ni1369 (2006).
- 38 Cantrell, D. T cell antigen receptor signal transduction pathways. *Annual review of immunology* **14**, 259-274, doi:10.1146/annurev.immunol.14.1.259 (1996).
- 39 Schwartz, R. H. T cell anergy. *Annual review of immunology* **21**, 305-334, doi:10.1146/annurev.immunol.21.120601.141110 (2003).
- 40 Chen, L. & Flies, D. B. Molecular mechanisms of T cell co-stimulation and co-inhibition. *Nature reviews. Immunology* **13**, 227-242, doi:10.1038/nri3405 (2013).
- 41 Boomer, J. S. & Green, J. M. An enigmatic tail of CD28 signaling. *Cold Spring Harbor perspectives in biology* **2**, a002436, doi:10.1101/cshperspect.a002436 (2010).
- 42 Frauwirth, K. A. *et al.* The CD28 signaling pathway regulates glucose metabolism. *Immunity* **16**, 769-777 (2002).
- 43 Croft, M. The role of TNF superfamily members in T-cell function and diseases. *Nature reviews. Immunology* **9**, 271-285, doi:10.1038/nri2526 (2009).
- 44 Croft, M. The TNF family in T cell differentiation and function--unanswered questions and future directions. *Seminars in immunology* **26**, 183-190, doi:10.1016/j.smim.2014.02.005 (2014).
- 45 Vanamee, É. S. & Faustman, D. L. Structural principles of tumor necrosis factor superfamily signaling. *Science signaling* **11**, doi:10.1126/scisignal.aao4910 (2018).
- 46 Lee, H. W. *et al.* 4-1BB promotes the survival of CD8+ T lymphocytes by increasing expression of Bcl-xL and Bfl-1. *Journal of immunology (Baltimore, Md. : 1950)* **169**, 4882-4888 (2002).
- 47 Rogers, P. R., Song, J., Gramaglia, I., Killeen, N. & Croft, M. OX40 promotes Bcl-xL and Bcl-2 expression and is essential for long-term survival of CD4 T cells. *Immunity* **15**, 445-455 (2001).
- 48 Munitic, I., Kuka, M., Allam, A., Scoville, J. P. & Ashwell, J. D. CD70 deficiency impairs effector CD8 T cell generation and viral clearance but is dispensable for the recall

## List of References

- response to lymphocytic choriomeningitis virus. *Journal of immunology (Baltimore, Md. : 1950)* **190**, 1169-1179, doi:10.4049/jimmunol.1202353 (2013).
- 49 Hendriks, J. *et al.* During viral infection of the respiratory tract, CD27, 4-1BB, and OX40 collectively determine formation of CD8+ memory T cells and their capacity for secondary expansion. *Journal of immunology (Baltimore, Md. : 1950)* **175**, 1665-1676 (2005).
- 50 Tan, J. T. *et al.* 4-1BB costimulation is required for protective anti-viral immunity after peptide vaccination. *Journal of immunology (Baltimore, Md. : 1950)* **164**, 2320-2325 (2000).
- 51 Zhao, Y., Tahiliani, V., Salek-Ardakani, S. & Croft, M. Targeting 4-1BB (CD137) to enhance CD8 T cell responses with poxviruses and viral antigens. *Frontiers in immunology* **3**, 332, doi:10.3389/fimmu.2012.00332 (2012).
- 52 Paterson, D. J. *et al.* Antigens of activated rat T lymphocytes including a molecule of 50,000 Mr detected only on CD4 positive T blasts. *Molecular immunology* **24**, 1281-1290 (1987).
- 53 Gramaglia, I., Weinberg, A. D., Lemon, M. & Croft, M. Ox-40 ligand: a potent costimulatory molecule for sustaining primary CD4 T cell responses. *Journal of immunology (Baltimore, Md. : 1950)* **161**, 6510-6517 (1998).
- 54 Ohshima, Y. *et al.* Expression and function of OX40 ligand on human dendritic cells. *The Journal of Immunology* **159**, 3838-3848 (1997).
- 55 Croft, M., So, T., Duan, W. & Soroosh, P. The significance of OX40 and OX40L to T-cell biology and immune disease. *Immunological reviews* **229**, 173-191, doi:10.1111/j.1600-065X.2009.00766.x (2009).
- 56 Bansal-Pakala, P., Halteman, B. S., Cheng, M. H. & Croft, M. Costimulation of CD8 T cell responses by OX40. *Journal of immunology (Baltimore, Md. : 1950)* **172**, 4821-4825 (2004).
- 57 Mehta, A. K., Gracias, D. T. & Croft, M. TNF activity and T cells. *Cytokine*, doi:10.1016/j.cyto.2016.08.003 (2016).
- 58 Buchbinder, E. I. & Desai, A. CTLA-4 and PD-1 Pathways: Similarities, Differences, and Implications of Their Inhibition. *American journal of clinical oncology* **39**, 98-106, doi:10.1097/coc.000000000000239 (2016).
- 59 Rudd, C. E., Taylor, A. & Schneider, H. CD28 and CTLA-4 coreceptor expression and signal transduction. *Immunological reviews* **229**, 12-26, doi:10.1111/j.1600-065X.2009.00770.x (2009).
- 60 Riley, J. L. PD-1 signaling in primary T cells. *Immunological reviews* **229**, 114-125, doi:10.1111/j.1600-065X.2009.00767.x (2009).
- 61 Geginat, J. *et al.* The CD4-centered universe of human T cell subsets. *Seminars in immunology* **25**, 252-262, doi:10.1016/j.smim.2013.10.012 (2013).
- 62 Lugo-Villarino, G., Maldonado-Lopez, R., Possemato, R., Penaranda, C. & Glimcher, L. H. T-bet is required for optimal production of IFN-gamma and antigen-specific T cell activation by dendritic cells. *Proc Natl Acad Sci U S A* **100**, 7749-7754, doi:10.1073/pnas.1332767100 (2003).

- 63 Groom, J. R. & Luster, A. D. CXCR3 in T cell function. *Experimental cell research* **317**, 620-631, doi:10.1016/j.yexcr.2010.12.017 (2011).
- 64 Murphy, K. M. *et al.* Signaling and transcription in T helper development. *Annual review of immunology* **18**, 451-494, doi:10.1146/annurev.immunol.18.1.451 (2000).
- 65 Thierfelder, W. E. *et al.* Requirement for Stat4 in interleukin-12-mediated responses of natural killer and T cells. *Nature* **382**, 171-174, doi:10.1038/382171a0 (1996).
- 66 Zheng, W. & Flavell, R. A. The transcription factor GATA-3 is necessary and sufficient for Th2 cytokine gene expression in CD4 T cells. *Cell* **89**, 587-596 (1997).
- 67 Usui, T., Nishikomori, R., Kitani, A. & Strober, W. GATA-3 suppresses Th1 development by downregulation of Stat4 and not through effects on IL-12Rbeta2 chain or T-bet. *Immunity* **18**, 415-428 (2003).
- 68 Zhou, L. *et al.* IL-6 programs T(H)-17 cell differentiation by promoting sequential engagement of the IL-21 and IL-23 pathways. *Nat Immunol* **8**, 967-974, doi:10.1038/ni1488 (2007).
- 69 Crotty, S. T follicular helper cell differentiation, function, and roles in disease. *Immunity* **41**, 529-542, doi:10.1016/j.immuni.2014.10.004 (2014).
- 70 Kanamori, M., Nakatsukasa, H., Okada, M., Lu, Q. & Yoshimura, A. Induced Regulatory T Cells: Their Development, Stability, and Applications. *Trends in immunology* **37**, 803-811, doi:10.1016/j.it.2016.08.012 (2016).
- 71 Marie, J. C., Letterio, J. J., Gavin, M. & Rudensky, A. Y. TGF-beta1 maintains suppressor function and Foxp3 expression in CD4+CD25+ regulatory T cells. *The Journal of experimental medicine* **201**, 1061-1067, doi:10.1084/jem.20042276 (2005).
- 72 Haribhai, D. *et al.* A requisite role for induced regulatory T cells in tolerance based on expanding antigen receptor diversity. *Immunity* **35**, 109-122, doi:10.1016/j.immuni.2011.03.029 (2011).
- 73 Hivroz, C., Chemin, K., Turret, M. & Bohineust, A. Crosstalk between T lymphocytes and dendritic cells. *Critical reviews in immunology* **32**, 139-155 (2012).
- 74 Ma, D. Y. & Clark, E. A. The role of CD40 and CD154/CD40L in dendritic cells. *Seminars in immunology* **21**, 265-272, doi:10.1016/j.smim.2009.05.010 (2009).
- 75 Taraban, V. Y., Rowley, T. F. & Al-Shamkhani, A. Cutting edge: a critical role for CD70 in CD8 T cell priming by CD40-licensed APCs. *Journal of immunology (Baltimore, Md. : 1950)* **173**, 6542-6546 (2004).
- 76 Smith, C. M. *et al.* Cognate CD4(+) T cell licensing of dendritic cells in CD8(+) T cell immunity. *Nat Immunol* **5**, 1143-1148, doi:10.1038/ni1129 (2004).
- 77 Bourgeois, C., Rocha, B. & Tanchot, C. A role for CD40 expression on CD8+ T cells in the generation of CD8+ T cell memory. *Science* **297**, 2060-2063, doi:10.1126/science.1072615 (2002).
- 78 Haabeth, O. A. *et al.* How Do CD4(+) T Cells Detect and Eliminate Tumor Cells That Either Lack or Express MHC Class II Molecules? *Frontiers in immunology* **5**, 174, doi:10.3389/fimmu.2014.00174 (2014).

## List of References

- 79 Shklovskaya, E. *et al.* Tumour-specific CD4 T cells eradicate melanoma via indirect recognition of tumour-derived antigen. *Immunology and cell biology* **94**, 593-603, doi:10.1038/icb.2016.14 (2016).
- 80 Chamuleau, M. E., Ossenkoppele, G. J. & van de Loosdrecht, A. A. MHC class II molecules in tumour immunology: prognostic marker and target for immune modulation. *Immunobiology* **211**, 619-625, doi:10.1016/j.imbio.2006.05.005 (2006).
- 81 Protti, M. P., Monte, L. D. & Lullo, G. D. Tumor antigen-specific CD4+ T cells in cancer immunity: from antigen identification to tumor prognosis and development of therapeutic strategies. *Tissue antigens* **83**, 237-246, doi:10.1111/tan.12329 (2014).
- 82 Wang, B. *et al.* Multiple paths for activation of naive CD8+ T cells: CD4-independent help. *Journal of immunology (Baltimore, Md. : 1950)* **167**, 1283-1289 (2001).
- 83 Voskoboinik, I., Whisstock, J. C. & Trapani, J. A. Perforin and granzymes: function, dysfunction and human pathology. *Nature reviews. Immunology* **15**, 388-400, doi:10.1038/nri3839 (2015).
- 84 Kaech, S. M. & Cui, W. Transcriptional control of effector and memory CD8+ T cell differentiation. *Nature reviews. Immunology* **12**, 749-761, doi:10.1038/nri3307 (2012).
- 85 Badovinac, V. P., Porter, B. B. & Harty, J. T. Programmed contraction of CD8(+) T cells after infection. *Nat Immunol* **3**, 619-626, doi:10.1038/ni804 (2002).
- 86 Badovinac, V. P., Porter, B. B. & Harty, J. T. CD8+ T cell contraction is controlled by early inflammation. *Nat Immunol* **5**, 809-817, doi:10.1038/ni1098 (2004).
- 87 Cox, M. A., Harrington, L. E. & Zajac, A. J. Cytokines and the inception of CD8 T cell responses. *Trends in immunology* **32**, 180-186, doi:10.1016/j.it.2011.01.004 (2011).
- 88 Joshi, N. S. *et al.* Inflammation directs memory precursor and short-lived effector CD8(+) T cell fates via the graded expression of T-bet transcription factor. *Immunity* **27**, 281-295, doi:10.1016/j.immuni.2007.07.010 (2007).
- 89 Boyman, O., Cho, J. H. & Sprent, J. The role of interleukin-2 in memory CD8 cell differentiation. *Advances in experimental medicine and biology* **684**, 28-41 (2010).
- 90 Cox, M. A., Kahan, S. M. & Zajac, A. J. Anti-viral CD8 T cells and the cytokines that they love. *Virology* **435**, 157-169, doi:10.1016/j.virol.2012.09.012 (2013).
- 91 Malek, T. R. & Castro, I. Interleukin-2 receptor signaling: at the interface between tolerance and immunity. *Immunity* **33**, 153-165, doi:10.1016/j.immuni.2010.08.004 (2010).
- 92 Liao, W., Lin, J. X. & Leonard, W. J. IL-2 family cytokines: new insights into the complex roles of IL-2 as a broad regulator of T helper cell differentiation. *Current opinion in immunology* **23**, 598-604, doi:10.1016/j.coi.2011.08.003 (2011).
- 93 Bachmann, M. F. & Oxenius, A. Interleukin 2: from immunostimulation to immunoregulation and back again. *EMBO reports* **8**, 1142-1148, doi:10.1038/sj.embor.7401099 (2007).
- 94 Kalia, V. *et al.* Prolonged interleukin-2/Ralpha expression on virus-specific CD8+ T cells favors terminal-effector differentiation in vivo. *Immunity* **32**, 91-103, doi:10.1016/j.immuni.2009.11.010 (2010).

- 95 Pipkin, M. E. *et al.* Interleukin-2 and inflammation induce distinct transcriptional programs that promote the differentiation of effector cytolytic T cells. *Immunity* **32**, 79-90, doi:10.1016/j.immuni.2009.11.012 (2010).
- 96 Tan, J. T. *et al.* Interleukin (IL)-15 and IL-7 jointly regulate homeostatic proliferation of memory phenotype CD8+ cells but are not required for memory phenotype CD4+ cells. *The Journal of experimental medicine* **195**, 1523-1532 (2002).
- 97 Verbist, K. C. & Klonowski, K. D. Functions of IL-15 in anti-viral immunity: multiplicity and variety. *Cytokine* **59**, 467-478, doi:10.1016/j.cyto.2012.05.020 (2012).
- 98 Budagian, V., Bulanova, E., Paus, R. & Bulfone-Paus, S. IL-15/IL-15 receptor biology: a guided tour through an expanding universe. *Cytokine & growth factor reviews* **17**, 259-280, doi:10.1016/j.cytogfr.2006.05.001 (2006).
- 99 Rohr, J. C., Gerlach, C., Kok, L. & Schumacher, T. N. Single cell behavior in T cell differentiation. *Trends in immunology* **35**, 170-177, doi:10.1016/j.it.2014.02.006 (2014).
- 100 Banerjee, A. *et al.* Cutting edge: The transcription factor eomesodermin enables CD8+ T cells to compete for the memory cell niche. *Journal of immunology (Baltimore, Md. : 1950)* **185**, 4988-4992, doi:10.4049/jimmunol.1002042 (2010).
- 101 Sallusto, F., Lenig, D., Forster, R., Lipp, M. & Lanzavecchia, A. Two subsets of memory T lymphocytes with distinct homing potentials and effector functions. *Nature* **401**, 708-712, doi:10.1038/44385 (1999).
- 102 Obar, J. J. & Lefrancois, L. Memory CD8+ T cell differentiation. *Annals of the New York Academy of Sciences* **1183**, 251-266, doi:10.1111/j.1749-6632.2009.05126.x (2010).
- 103 Mahnke, Y. D., Brodie, T. M., Sallusto, F., Roederer, M. & Lugli, E. The who's who of T-cell differentiation: human memory T-cell subsets. *European journal of immunology* **43**, 2797-2809, doi:10.1002/eji.201343751 (2013).
- 104 Parish, I. A. & Kaech, S. M. Diversity in CD8(+) T cell differentiation. *Current opinion in immunology* **21**, 291-297, doi:10.1016/j.coi.2009.05.008 (2009).
- 105 Masopust, D., Vezys, V., Marzo, A. L. & Lefrancois, L. Preferential localization of effector memory cells in nonlymphoid tissue. *Science* **291**, 2413-2417, doi:10.1126/science.1058867 (2001).
- 106 Hamilton, S. E. & Jameson, S. C. CD8 T cell memory: it takes all kinds. *Frontiers in immunology* **3**, 353, doi:10.3389/fimmu.2012.00353 (2012).
- 107 Mueller, S. N. & Mackay, L. K. Tissue-resident memory T cells: local specialists in immune defence. *Nature reviews. Immunology* **16**, 79-89, doi:10.1038/nri.2015.3 (2016).
- 108 Masopust, D. & Picker, L. J. Hidden memories: frontline memory T cells and early pathogen interception. *Journal of immunology (Baltimore, Md. : 1950)* **188**, 5811-5817, doi:10.4049/jimmunol.1102695 (2012).
- 109 Gattinoni, L. *et al.* Wnt signaling arrests effector T cell differentiation and generates CD8+ memory stem cells. *Nature medicine* **15**, 808-813, doi:10.1038/nm.1982 (2009).
- 110 Gattinoni, L. *et al.* A human memory T cell subset with stem cell-like properties. *Nature medicine* **17**, 1290-1297, doi:10.1038/nm.2446 (2011).

## List of References

- 111 Fuertes Marraco, S. A. *et al.* Long-lasting stem cell-like memory CD8<sup>+</sup> T cells with a naive-like profile upon yellow fever vaccination. *Science translational medicine* **7**, 282ra248, doi:10.1126/scitranslmed.aaa3700 (2015).
- 112 Stemberger, C. *et al.* A single naive CD8<sup>+</sup> T cell precursor can develop into diverse effector and memory subsets. *Immunity* **27**, 985-997, doi:10.1016/j.immuni.2007.10.012 (2007).
- 113 Gerlach, C. *et al.* One naive T cell, multiple fates in CD8<sup>+</sup> T cell differentiation. *The Journal of experimental medicine* **207**, 1235-1246, doi:10.1084/jem.20091175 (2010).
- 114 Badovinac, V. P., Messingham, K. A., Jabbari, A., Haring, J. S. & Harty, J. T. Accelerated CD8<sup>+</sup> T-cell memory and prime-boost response after dendritic-cell vaccination. *Nature medicine* **11**, 748-756, doi:10.1038/nm1257 (2005).
- 115 Schietinger, A. & Greenberg, P. D. Tolerance and exhaustion: defining mechanisms of T cell dysfunction. *Trends in immunology* **35**, 51-60, doi:10.1016/j.it.2013.10.001 (2014).
- 116 Gett, A. V., Sallusto, F., Lanzavecchia, A. & Geginat, J. T cell fitness determined by signal strength. *Nat Immunol* **4**, 355-360, doi:10.1038/ni908 (2003).
- 117 Pollizzi, K. N. *et al.* Asymmetric inheritance of mTORC1 kinase activity during division dictates CD8(+) T cell differentiation. *Nat Immunol* **17**, 704-711, doi:10.1038/ni.3438 (2016).
- 118 Verbist, K. C. *et al.* Metabolic maintenance of cell asymmetry following division in activated T lymphocytes. *Nature* **532**, 389-393, doi:10.1038/nature17442 (2016).
- 119 Vantourout, P. & Hayday, A. Six-of-the-best: unique contributions of gammadelta T cells to immunology. *Nature reviews. Immunology* **13**, 88-100, doi:10.1038/nri3384 (2013).
- 120 Nielsen, M. M., Witherden, D. A. & Havran, W. L. gammadelta T cells in homeostasis and host defence of epithelial barrier tissues. *Nature reviews. Immunology* **17**, 733-745, doi:10.1038/nri.2017.101 (2017).
- 121 Zhao, Y., Niu, C. & Cui, J. Gamma-delta (gammadelta) T cells: friend or foe in cancer development? *Journal of translational medicine* **16**, 3, doi:10.1186/s12967-017-1378-2 (2018).
- 122 Chien, Y. H. & Konigshofer, Y. Antigen recognition by gammadelta T cells. *Immunological reviews* **215**, 46-58, doi:10.1111/j.1600-065X.2006.00470.x (2007).
- 123 Pollizzi, K. N. *et al.* mTORC1 and mTORC2 selectively regulate CD8(+) T cell differentiation. *The Journal of clinical investigation* **125**, 2090-2108, doi:10.1172/jci77746 (2015).
- 124 Xue, L., Chiang, L., Kang, C. & Winoto, A. The role of the PI3K-AKT kinase pathway in T-cell development beyond the beta checkpoint. *European journal of immunology* **38**, 3200-3207, doi:10.1002/eji.200838614 (2008).
- 125 Soond, D. R. *et al.* PI3K p110delta regulates T-cell cytokine production during primary and secondary immune responses in mice and humans. *Blood* **115**, 2203-2213, doi:10.1182/blood-2009-07-232330 (2010).
- 126 Ladygina, N. *et al.* PI3Kgamma kinase activity is required for optimal T-cell activation and differentiation. *European journal of immunology* **43**, 3183-3196, doi:10.1002/eji.201343812 (2013).

- 127 Gracias, D. T. *et al.* Phosphatidylinositol 3-Kinase p110delta Isoform Regulates CD8+ T Cell Responses during Acute Viral and Intracellular Bacterial Infections. *Journal of immunology (Baltimore, Md. : 1950)* **196**, 1186-1198, doi:10.4049/jimmunol.1501890 (2016).
- 128 Martini, M., De Santis, M. C., Braccini, L., Gulluni, F. & Hirsch, E. PI3K/AKT signaling pathway and cancer: an updated review. *Annals of medicine* **46**, 372-383, doi:10.3109/07853890.2014.912836 (2014).
- 129 Kok, K., Geering, B. & Vanhaesebroeck, B. Regulation of phosphoinositide 3-kinase expression in health and disease. *Trends Biochem Sci* **34**, 115-127, doi:10.1016/j.tibs.2009.01.003 (2009).
- 130 Vadas, O., Burke, J. E., Zhang, X., Berndt, A. & Williams, R. L. Structural basis for activation and inhibition of class I phosphoinositide 3-kinases. *Science signaling* **4**, re2, doi:10.1126/scisignal.2002165 (2011).
- 131 Jimenez, C., Hernandez, C., Pimentel, B. & Carrera, A. C. The p85 regulatory subunit controls sequential activation of phosphoinositide 3-kinase by Tyr kinases and Ras. *The Journal of biological chemistry* **277**, 41556-41562, doi:10.1074/jbc.M205893200 (2002).
- 132 Huang, C. H. *et al.* The structure of a human p110alpha/p85alpha complex elucidates the effects of oncogenic PI3Kalpha mutations. *Science* **318**, 1744-1748, doi:10.1126/science.1150799 (2007).
- 133 Dbouk, H. A., Pang, H., Fiser, A. & Backer, J. M. A biochemical mechanism for the oncogenic potential of the p110beta catalytic subunit of phosphoinositide 3-kinase. *Proc Natl Acad Sci U S A* **107**, 19897-19902, doi:10.1073/pnas.1008739107 (2010).
- 134 Burke, J. E. *et al.* Dynamics of the phosphoinositide 3-kinase p110delta interaction with p85alpha and membranes reveals aspects of regulation distinct from p110alpha. *Structure (London, England : 1993)* **19**, 1127-1137, doi:10.1016/j.str.2011.06.003 (2011).
- 135 Vanhaesebroeck, B., Stephens, L. & Hawkins, P. PI3K signalling: the path to discovery and understanding. *Nature reviews. Molecular cell biology* **13**, 195-203, doi:10.1038/nrm3290 (2012).
- 136 Webb, L. M. C., Vigorito, E., Wymann, M. P., Hirsch, E. & Turner, M. Cutting Edge: T Cell Development Requires the Combined Activities of the p110 $\gamma$  and p110 $\delta$  Catalytic Isoforms of Phosphatidylinositol 3-Kinase. *The Journal of Immunology* **175**, 2783-2787, doi:10.4049/jimmunol.175.5.2783 (2005).
- 137 Hagenbeek, T. J. *et al.* The loss of PTEN allows TCR alphabeta lineage thymocytes to bypass IL-7 and Pre-TCR-mediated signaling. *The Journal of experimental medicine* **200**, 883-894, doi:10.1084/jem.20040495 (2004).
- 138 Bayascas, J. R. Dissecting the role of the 3-phosphoinositide-dependent protein kinase-1 (PDK1) signalling pathways. *Cell Cycle* **7**, 2978-2982, doi:10.4161/cc.7.19.6810 (2008).
- 139 Pearce, L. R., Komander, D. & Alessi, D. R. The nuts and bolts of AGC protein kinases. *Nature reviews. Molecular cell biology* **11**, 9-22, doi:10.1038/nrm2822 (2010).
- 140 Lemmon, M. A. Pleckstrin homology (PH) domains and phosphoinositides. *Biochemical Society symposium*, 81-93, doi:10.1042/bss0740081 (2007).
- 141 Barile, E., De, S. K. & Pellecchia, M. PDK1 inhibitors. *Pharmaceutical Patent Analyst* **1**, 145-163, doi:10.4155/ppa.12.17 (2012).

## List of References

- 142 Biondi, R. M. *et al.* High resolution crystal structure of the human PDK1 catalytic domain defines the regulatory phosphopeptide docking site. *The EMBO journal* **21**, 4219-4228, doi:10.1093/emboj/cdf437 (2002).
- 143 Macintyre, A. N. *et al.* Protein kinase B controls transcriptional programs that direct cytotoxic T cell fate but is dispensable for T cell metabolism. *Immunity* **34**, 224-236, doi:10.1016/j.immuni.2011.01.012 (2011).
- 144 Finlay, D. K. *et al.* PDK1 regulation of mTOR and hypoxia-inducible factor 1 integrate metabolism and migration of CD8<sup>+</sup> T cells. *The Journal of experimental medicine* **209**, 2441-2453, doi:10.1084/jem.20112607 (2012).
- 145 Sukumar, M. *et al.* Inhibiting glycolytic metabolism enhances CD8<sup>+</sup> T cell memory and antitumor function. *The Journal of clinical investigation* **123**, 4479-4488, doi:10.1172/jci69589 (2013).
- 146 Finlay, D. K. *et al.* PDK1 regulation of mTOR and hypoxia-inducible factor 1 integrate metabolism and migration of CD8<sup>+</sup> T cells. *The Journal of experimental medicine* **209**, 2441-2453, doi:10.1084/jem.20112607 (2012).
- 147 Burgering, B. M. T. & Coffey, P. J. Protein kinase B (c-Akt) in phosphatidylinositol-3-OH kinase signal transduction. *Nature* **376**, 599-602, doi:10.1038/376599a0 (1995).
- 148 Kohn, A. D., Kovacina, K. S. & Roth, R. A. Insulin stimulates the kinase activity of RAC-PK, a pleckstrin homology domain containing ser/thr kinase. *The EMBO journal* **14**, 4288-4295 (1995).
- 149 Cho, H., Thorvaldsen, J. L., Chu, Q., Feng, F. & Birnbaum, M. J. Akt1/PKB $\alpha$  is required for normal growth but dispensable for maintenance of glucose homeostasis in mice. *The Journal of biological chemistry* **276**, 38349-38352, doi:10.1074/jbc.C100462200 (2001).
- 150 Garofalo, R. S. *et al.* Severe diabetes, age-dependent loss of adipose tissue, and mild growth deficiency in mice lacking Akt2/PKB $\beta$ . *The Journal of clinical investigation* **112**, 197-208, doi:10.1172/jci16885 (2003).
- 151 Yang, Z. Z. *et al.* Protein kinase B  $\alpha$ /Akt1 regulates placental development and fetal growth. *The Journal of biological chemistry* **278**, 32124-32131, doi:10.1074/jbc.M302847200 (2003).
- 152 Alessi, D. R. *et al.* Mechanism of activation of protein kinase B by insulin and IGF-1. *The EMBO journal* **15**, 6541-6551 (1996).
- 153 Andjelkovic, M. *et al.* Activation and phosphorylation of a pleckstrin homology domain containing protein kinase (RAC-PK/PKB) promoted by serum and protein phosphatase inhibitors. *Proc Natl Acad Sci U S A* **93**, 5699-5704 (1996).
- 154 Brognard, J., Sierrecki, E., Gao, T. & Newton, A. C. PHLPP and a second isoform, PHLPP2, differentially attenuate the amplitude of Akt signaling by regulating distinct Akt isoforms. *Mol Cell* **25**, 917-931, doi:10.1016/j.molcel.2007.02.017 (2007).
- 155 Tomiyama, H., Matsuda, T. & Takiguchi, M. Differentiation of human CD8<sup>(+)</sup> T cells from a memory to memory/effector phenotype. *Journal of immunology (Baltimore, Md. : 1950)* **168**, 5538-5550 (2002).
- 156 Crompton, J. G. *et al.* Akt inhibition enhances expansion of potent tumor-specific lymphocytes with memory cell characteristics. *Cancer Res* **75**, 296-305, doi:10.1158/0008-5472.can-14-2277 (2015).

- 157 Manning, B. D. & Cantley, L. C. AKT/PKB signaling: navigating downstream. *Cell* **129**, 1261-1274, doi:10.1016/j.cell.2007.06.009 (2007).
- 158 Mao, C. *et al.* Unequal contribution of Akt isoforms in the double-negative to double-positive thymocyte transition. *Journal of immunology (Baltimore, Md. : 1950)* **178**, 5443-5453 (2007).
- 159 Kerdiles, Y. M. *et al.* Foxo1 links homing and survival of naive T cells by regulating L-selectin, CCR7 and interleukin 7 receptor. *Nat Immunol* **10**, 176-184, doi:10.1038/ni.1689 (2009).
- 160 Ouyang, W., Beckett, O., Flavell, R. A. & Li, M. O. An essential role of the Forkhead-box transcription factor Foxo1 in control of T cell homeostasis and tolerance. *Immunity* **30**, 358-371, doi:10.1016/j.immuni.2009.02.003 (2009).
- 161 McLane, L. M. *et al.* Differential localization of T-bet and Eomes in CD8 T cell memory populations. *Journal of immunology (Baltimore, Md. : 1950)* **190**, 3207-3215, doi:10.4049/jimmunol.1201556 (2013).
- 162 Rao, R. R., Li, Q., Gubbels Bupp, M. R. & Shrikant, P. A. Transcription factor Foxo1 represses T-bet-mediated effector functions and promotes memory CD8(+) T cell differentiation. *Immunity* **36**, 374-387, doi:10.1016/j.immuni.2012.01.015 (2012).
- 163 Hamilton, S. E. & Jameson, S. C. CD8(+) T cell differentiation: choosing a path through T-bet. *Immunity* **27**, 180-182, doi:10.1016/j.immuni.2007.08.003 (2007).
- 164 Kim, E. H. *et al.* Signal integration by Akt regulates CD8 T cell effector and memory differentiation. *Journal of immunology (Baltimore, Md. : 1950)* **188**, 4305-4314, doi:10.4049/jimmunol.1103568 (2012).
- 165 Togher, S., Larange, A., Schoenberger, S. P. & Feau, S. FoxO3 is a negative regulator of primary CD8+ T-cell expansion but not of memory formation. *Immunology and cell biology* **93**, 120-125, doi:10.1038/icb.2014.78 (2015).
- 166 Gangemi, S., Allegra, A. & Musolino, C. Lymphoproliferative disease and cancer among patients with common variable immunodeficiency. *Leukemia research* **39**, 389-396, doi:10.1016/j.leukres.2015.02.002 (2015).
- 167 Cunningham-Rundles, C. The many faces of common variable immunodeficiency. *Hematology / the Education Program of the American Society of Hematology. American Society of Hematology. Education Program* **2012**, 301-305, doi:10.1182/asheducation-2012.1.301 (2012).
- 168 Schreiber, R. D., Old, L. J. & Smyth, M. J. Cancer Immunoediting: Integrating Immunity's Roles in Cancer Suppression and Promotion. *Science* **331**, 1565-1570, doi:10.1126/science.1203486 (2011).
- 169 Dunn, G. P., Old, L. J. & Schreiber, R. D. The three Es of cancer immunoediting. *Annual review of immunology* **22**, 329-360, doi:10.1146/annurev.immunol.22.012703.104803 (2004).
- 170 Vesely, M. D., Kershaw, M. H., Schreiber, R. D. & Smyth, M. J. Natural innate and adaptive immunity to cancer. *Annual review of immunology* **29**, 235-271, doi:10.1146/annurev-immunol-031210-101324 (2011).
- 171 Loeb, L. A., Loeb, K. R. & Anderson, J. P. Multiple mutations and cancer. *Proc Natl Acad Sci U S A* **100**, 776-781, doi:10.1073/pnas.0334858100 (2003).

## List of References

- 172 Marincola, F. M., Jaffee, E. M., Hicklin, D. J. & Ferrone, S. Escape of human solid tumors from T-cell recognition: molecular mechanisms and functional significance. *Advances in immunology* **74**, 181-273 (2000).
- 173 Groh, V., Wu, J., Yee, C. & Spies, T. Tumour-derived soluble MIC ligands impair expression of NKG2D and T-cell activation. *Nature* **419**, 734-738, doi:10.1038/nature01112 (2002).
- 174 Vajdic, C. M. *et al.* Cancer incidence before and after kidney transplantation. *Jama* **296**, 2823-2831, doi:10.1001/jama.296.23.2823 (2006).
- 175 Zorn, E. & Hercend, T. A natural cytotoxic T cell response in a spontaneously regressing human melanoma targets a neoantigen resulting from a somatic point mutation. *European journal of immunology* **29**, 592-601, doi:10.1002/(sici)1521-4141(199902)29:02<592::aid-immu592>3.0.co;2-2 (1999).
- 176 Swann, J. B. & Smyth, M. J. Immune surveillance of tumors. *The Journal of clinical investigation* **117**, 1137-1146, doi:10.1172/jci31405 (2007).
- 177 Hoption Cann, S. A., van Netten, J. P., van Netten, C. & Glover, D. W. Spontaneous regression: a hidden treasure buried in time. *Medical hypotheses* **58**, 115-119, doi:10.1054/mehy.2001.1469 (2002).
- 178 Jessy, T. Immunity over inability: The spontaneous regression of cancer. *Journal of natural science, biology, and medicine* **2**, 43-49, doi:10.4103/0976-9668.82318 (2011).
- 179 Stern, C. *et al.* Induction of CD4+ and CD8+ anti-tumor effector T cell responses by bacteria mediated tumor therapy. *International Journal of Cancer* **137**, 2019-2028, doi:10.1002/ijc.29567 (2015).
- 180 Dhodapkar, M. V. MGUS to myeloma: a mysterious gammopathy of underexplored significance. *Blood* **128**, 2599-2606, doi:10.1182/blood-2016-09-692954 (2016).
- 181 Dhodapkar, M. V., Krasovsky, J., Osman, K. & Geller, M. D. Vigorous premalignancy-specific effector T cell response in the bone marrow of patients with monoclonal gammopathy. *The Journal of experimental medicine* **198**, 1753-1757, doi:10.1084/jem.20031030 (2003).
- 182 van Oijen, M. *et al.* On the role of melanoma-specific CD8+ T-cell immunity in disease progression of advanced-stage melanoma patients. *Clinical cancer research : an official journal of the American Association for Cancer Research* **10**, 4754-4760, doi:10.1158/1078-0432.ccr-04-0260 (2004).
- 183 Corthay, A. Does the Immune System Naturally Protect Against Cancer? *Frontiers in immunology* **5**, doi:10.3389/fimmu.2014.00197 (2014).
- 184 Hanahan, D. & Weinberg, R. A. Hallmarks of cancer: the next generation. *Cell* **144**, 646-674, doi:10.1016/j.cell.2011.02.013 (2011).
- 185 Rashidi, A. & Uy, G. L. Targeting the microenvironment in acute myeloid leukemia. *Current hematologic malignancy reports* **10**, 126-131, doi:10.1007/s11899-015-0255-4 (2015).
- 186 Tomasek, J. J., Gabbiani, G., Hinz, B., Chaponnier, C. & Brown, R. A. Myofibroblasts and mechano-regulation of connective tissue remodelling. *Nature Reviews Molecular Cell Biology* **3**, 349, doi:10.1038/nrm809 (2002).
- 187 Kalluri, R. & Zeisberg, M. Fibroblasts in cancer. *Nature Reviews Cancer* **6**, 392, doi:10.1038/nrc1877 (2006).

- 188 Boire, A. *et al.* PAR1 is a matrix metalloprotease-1 receptor that promotes invasion and tumorigenesis of breast cancer cells. *Cell* **120**, 303-313, doi:10.1016/j.cell.2004.12.018 (2005).
- 189 Lochter, A. *et al.* Matrix Metalloproteinase Stromelysin-1 Triggers a Cascade of Molecular Alterations That Leads to Stable Epithelial-to-Mesenchymal Conversion and a Premalignant Phenotype in Mammary Epithelial Cells. *The Journal of cell biology* **139**, 1861-1872, doi:10.1083/jcb.139.7.1861 (1997).
- 190 Pinchuk, I. V. *et al.* PD-1 ligand expression by human colonic myofibroblasts/fibroblasts regulates CD4+ T-cell activity. *Gastroenterology* **135**, 1228-1237, 1237.e1221-1222, doi:10.1053/j.gastro.2008.07.016 (2008).
- 191 Bardos, J. I. & Ashcroft, M. Hypoxia-inducible factor-1 and oncogenic signalling. *BioEssays : news and reviews in molecular, cellular and developmental biology* **26**, 262-269, doi:10.1002/bies.20002 (2004).
- 192 Belli, C. *et al.* Targeting the microenvironment in solid tumors. *Cancer treatment reviews* **65**, 22-32, doi:10.1016/j.ctrv.2018.02.004 (2018).
- 193 Carmen, O. M., Beatriz, M.-P., R., Q. A. & Ángel, M. M. Metabolism within the tumor microenvironment and its implication on cancer progression: An ongoing therapeutic target. *Medicinal Research Reviews* **0**, doi:doi:10.1002/med.21511.
- 194 Chang, C. H. *et al.* Metabolic Competition in the Tumor Microenvironment Is a Driver of Cancer Progression. *Cell* **162**, 1229-1241, doi:10.1016/j.cell.2015.08.016 (2015).
- 195 Heldin, C.-H., Rubin, K., Pietras, K. & Östman, A. High interstitial fluid pressure — an obstacle in cancer therapy. *Nature Reviews Cancer* **4**, 806, doi:10.1038/nrc1456 (2004).
- 196 Dunn, G. P., Old, L. J. & Schreiber, R. D. The immunobiology of cancer immunosurveillance and immunoediting. *Immunity* **21**, 137-148, doi:10.1016/j.immuni.2004.07.017 (2004).
- 197 Garrido, F., Ruiz-Cabello, F. & Aptsiauri, N. Rejection versus escape: the tumor MHC dilemma. *Cancer immunology, immunotherapy : CII* **66**, 259-271, doi:10.1007/s00262-016-1947-x (2017).
- 198 Rezvani, K., Rouce, R., Liu, E. & Shpall, E. Engineering Natural Killer Cells for Cancer Immunotherapy. *Molecular therapy : the journal of the American Society of Gene Therapy* **25**, 1769-1781, doi:10.1016/j.ymthe.2017.06.012 (2017).
- 199 Saini, K. S. *et al.* Rituximab in Hodgkin lymphoma: is the target always a hit? *Cancer treatment reviews* **37**, 385-390, doi:10.1016/j.ctrv.2010.11.005 (2011).
- 200 Dotan, E., Aggarwal, C. & Smith, M. R. Impact of Rituximab (Rituxan) on the Treatment of B-Cell Non-Hodgkin's Lymphoma. *P & T : a peer-reviewed journal for formulary management* **35**, 148-157 (2010).
- 201 Eko, S. L. & van Vollenhoven, R. F. Rituximab and lupus--a promising pair? *Current rheumatology reports* **16**, 444, doi:10.1007/s11926-014-0444-5 (2014).
- 202 Hauser, S. L. *et al.* B-cell depletion with rituximab in relapsing-remitting multiple sclerosis. *The New England journal of medicine* **358**, 676-688, doi:10.1056/NEJMoa0706383 (2008).
- 203 D'Arena, G. *et al.* Rituximab to treat chronic lymphoproliferative disorder-associated pure red cell aplasia. *European journal of haematology* **82**, 235-239, doi:10.1111/j.1600-0609.2008.01187.x (2009).

## List of References

- 204 Johnson, P. & Glennie, M. The mechanisms of action of rituximab in the elimination of tumor cells. *Seminars in oncology* **30**, 3-8, doi:10.1053/sonc.2003.50025 (2003).
- 205 Guan, M., Zhou, Y. P., Sun, J. L. & Chen, S. C. Adverse events of monoclonal antibodies used for cancer therapy. *BioMed research international* **2015**, 428169, doi:10.1155/2015/428169 (2015).
- 206 Hudis, C. A. Trastuzumab--mechanism of action and use in clinical practice. *The New England journal of medicine* **357**, 39-51, doi:10.1056/NEJMra043186 (2007).
- 207 Mitri, Z., Constantine, T. & O'Regan, R. The HER2 Receptor in Breast Cancer: Pathophysiology, Clinical Use, and New Advances in Therapy. *Chemotherapy research and practice* **2012**, 743193, doi:10.1155/2012/743193 (2012).
- 208 Blick, S. K. & Scott, L. J. Cetuximab: a review of its use in squamous cell carcinoma of the head and neck and metastatic colorectal cancer. *Drugs* **67**, 2585-2607 (2007).
- 209 Di Fiore, F. *et al.* Clinical relevance of KRAS mutation detection in metastatic colorectal cancer treated by Cetuximab plus chemotherapy. *British journal of cancer* **96**, 1166-1169, doi:10.1038/sj.bjc.6603685 (2007).
- 210 Raica, M., Cimpean, A. M. & Ribatti, D. Angiogenesis in pre-malignant conditions. *European journal of cancer (Oxford, England : 1990)* **45**, 1924-1934, doi:10.1016/j.ejca.2009.04.007 (2009).
- 211 Baluk, P., Hashizume, H. & McDonald, D. M. Cellular abnormalities of blood vessels as targets in cancer. *Current opinion in genetics & development* **15**, 102-111, doi:10.1016/j.gde.2004.12.005 (2005).
- 212 Sullivan, L. A. & Brekken, R. A. The VEGF family in cancer and antibody-based strategies for their inhibition. *mAbs* **2**, 165-175 (2010).
- 213 Al-Husein, B., Abdalla, M., Trepte, M., Deremer, D. L. & Somanath, P. R. Antiangiogenic therapy for cancer: an update. *Pharmacotherapy* **32**, 1095-1111, doi:10.1002/phar.1147 (2012).
- 214 Wang, W.-M. *et al.* Epidermal Growth Factor Receptor Inhibition Reduces Angiogenesis via Hypoxia-Inducible Factor-1 $\alpha$  and Notch1 in Head Neck Squamous Cell Carcinoma. *PLOS ONE* **10**, e0119723, doi:10.1371/journal.pone.0119723 (2015).
- 215 Garnock-Jones, K. P., Keating, G. M. & Scott, L. J. Trastuzumab: A review of its use as adjuvant treatment in human epidermal growth factor receptor 2 (HER2)-positive early breast cancer. *Drugs* **70**, 215-239, doi:10.2165/11203700-000000000-00000 (2010).
- 216 Popovic, A., Jaffee, E. M. & Zaidi, N. Emerging strategies for combination checkpoint modulators in cancer immunotherapy. *The Journal of clinical investigation* **128**, 3209-3218, doi:10.1172/jci120775 (2018).
- 217 Fife, B. T. & Bluestone, J. A. Control of peripheral T-cell tolerance and autoimmunity via the CTLA-4 and PD-1 pathways. *Immunological reviews* **224**, 166-182, doi:10.1111/j.1600-065X.2008.00662.x (2008).
- 218 Nishimura, H., Minato, N., Nakano, T. & Honjo, T. Immunological studies on PD-1 deficient mice: implication of PD-1 as a negative regulator for B cell responses. *Int Immunol* **10**, 1563-1572 (1998).

- 219 Freeman, G. J. *et al.* Engagement of the PD-1 immunoinhibitory receptor by a novel B7 family member leads to negative regulation of lymphocyte activation. *The Journal of experimental medicine* **192**, 1027-1034 (2000).
- 220 Okazaki, T. & Honjo, T. PD-1 and PD-1 ligands: from discovery to clinical application. *International Immunology* **19**, 813-824, doi:10.1093/intimm/dxm057 (2007).
- 221 Long, E. O. Regulation of immune responses through inhibitory receptors. *Annual review of immunology* **17**, 875-904, doi:10.1146/annurev.immunol.17.1.875 (1999).
- 222 Wherry, E. J. T cell exhaustion. *Nat Immunol* **12**, 492-499 (2011).
- 223 Lipson, E. J. & Drake, C. G. Ipilimumab: an anti-CTLA-4 antibody for metastatic melanoma. *Clinical cancer research : an official journal of the American Association for Cancer Research* **17**, 6958-6962, doi:10.1158/1078-0432.ccr-11-1595 (2011).
- 224 Simpson, T. R. *et al.* Fc-dependent depletion of tumor-infiltrating regulatory T cells co-defines the efficacy of anti-CTLA-4 therapy against melanoma. *The Journal of experimental medicine* **210**, 1695-1710, doi:10.1084/jem.20130579 (2013).
- 225 Jenkins, R. W., Barbie, D. A. & Flaherty, K. T. Mechanisms of resistance to immune checkpoint inhibitors. *British journal of cancer* **118**, 9-16, doi:10.1038/bjc.2017.434 (2018).
- 226 Larkin, J. *et al.* Combined Nivolumab and Ipilimumab or Monotherapy in Untreated Melanoma. *The New England journal of medicine* **373**, 23-34, doi:10.1056/NEJMoa1504030 (2015).
- 227 Carretero-Gonzalez, A. *et al.* Analysis of response rate with ANTI PD1/PD-L1 monoclonal antibodies in advanced solid tumors: a meta-analysis of randomized clinical trials. *Oncotarget* **9**, 8706-8715, doi:10.18632/oncotarget.24283 (2018).
- 228 Blank, C. U., Haanen, J. B., Ribas, A. & Schumacher, T. N. The “cancer immunogram”. *Science* **352**, 658-660, doi:10.1126/science.aaf2834 (2016).
- 229 Rosenberg, S. A. *et al.* Use of tumor-infiltrating lymphocytes and interleukin-2 in the immunotherapy of patients with metastatic melanoma. A preliminary report. *The New England journal of medicine* **319**, 1676-1680, doi:10.1056/nejm198812223192527 (1988).
- 230 Dudley, M. E. *et al.* Cancer regression and autoimmunity in patients after clonal repopulation with antitumor lymphocytes. *Science* **298**, 850-854, doi:10.1126/science.1076514 (2002).
- 231 Gattinoni, L. *et al.* Removal of homeostatic cytokine sinks by lymphodepletion enhances the efficacy of adoptively transferred tumor-specific CD8+ T cells. *The Journal of experimental medicine* **202**, 907-912, doi:10.1084/jem.20050732 (2005).
- 232 Rosenberg, S. A. *et al.* Durable Complete Responses in Heavily Pretreated Patients with Metastatic Melanoma Using T-Cell Transfer Immunotherapy. *Clinical Cancer Research* **17**, 4550-4557, doi:10.1158/1078-0432.ccr-11-0116 (2011).
- 233 Balch, C. M. *et al.* Final version of 2009 AJCC melanoma staging and classification. *Journal of clinical oncology : official journal of the American Society of Clinical Oncology* **27**, 6199-6206, doi:10.1200/jco.2009.23.4799 (2009).

## List of References

- 234 Wu, R. *et al.* Adoptive T-cell therapy using autologous tumor-infiltrating lymphocytes for metastatic melanoma: current status and future outlook. *Cancer journal (Sudbury, Mass.)* **18**, 160-175, doi:10.1097/PPO.0b013e31824d4465 (2012).
- 235 Guo, C. *et al.* Therapeutic cancer vaccines: past, present, and future. *Advances in cancer research* **119**, 421-475, doi:10.1016/b978-0-12-407190-2.00007-1 (2013).
- 236 Hege, K. M., Jooss, K. & Pardoll, D. GM-CSF gene-modified cancer cell immunotherapies: of mice and men. *International reviews of immunology* **25**, 321-352, doi:10.1080/08830180600992498 (2006).
- 237 Quezada, S. A., Peggs, K. S., Curran, M. A. & Allison, J. P. CTLA4 blockade and GM-CSF combination immunotherapy alters the intratumor balance of effector and regulatory T cells. *The Journal of clinical investigation* **116**, 1935-1945, doi:10.1172/jci27745 (2006).
- 238 Curran, M. A., Montalvo, W., Yagita, H. & Allison, J. P. PD-1 and CTLA-4 combination blockade expands infiltrating T cells and reduces regulatory T and myeloid cells within B16 melanoma tumors. *Proc Natl Acad Sci U S A* **107**, 4275-4280, doi:10.1073/pnas.0915174107 (2010).
- 239 Ott, P. A. *et al.* An immunogenic personal neoantigen vaccine for patients with melanoma. *Nature* **547**, 217-221, doi:10.1038/nature22991 (2017).
- 240 Rogel, A. *et al.* Akt signaling is critical for memory CD8<sup>+</sup> T-cell development and tumor immune surveillance. *Proceedings of the National Academy of Sciences* **114**, E1178-E1187, doi:10.1073/pnas.1611299114 (2017).
- 241 Wieman, H. L., Wofford, J. A. & Rathmell, J. C. Cytokine stimulation promotes glucose uptake via phosphatidylinositol-3 kinase/Akt regulation of Glut1 activity and trafficking. *Molecular biology of the cell* **18**, 1437-1446, doi:10.1091/mbc.e06-07-0593 (2007).
- 242 Zhang, B. H. *et al.* Serum- and glucocorticoid-inducible kinase SGK phosphorylates and negatively regulates B-Raf. *The Journal of biological chemistry* **276**, 31620-31626, doi:10.1074/jbc.M102808200 (2001).
- 243 Heikamp, E. B. *et al.* The AGC kinase SGK1 regulates TH1 and TH2 differentiation downstream of the mTORC2 complex. *Nat Immunol* **15**, 457-464, doi:10.1038/ni.2867 (2014).
- 244 Bayascas, J. R. *et al.* Mutation of the PDK1 PH domain inhibits protein kinase B/Akt, leading to small size and insulin resistance. *Mol Cell Biol* **28**, 3258-3272, doi:10.1128/mcb.02032-07 (2008).
- 245 Webb, L. M., Vigorito, E., Wymann, M. P., Hirsch, E. & Turner, M. Cutting edge: T cell development requires the combined activities of the p110gamma and p110delta catalytic isoforms of phosphatidylinositol 3-kinase. *Journal of immunology (Baltimore, Md. : 1950)* **175**, 2783-2787 (2005).
- 246 Hinton, H. J., Alessi, D. R. & Cantrell, D. A. The serine kinase phosphoinositide-dependent kinase 1 (PDK1) regulates T cell development. *Nat Immunol* **5**, 539-545, doi:10.1038/ni1062 (2004).
- 247 Juntilla, M. M. & Koretzky, G. A. Critical roles of the PI3K/Akt signaling pathway in T cell development. *Immunology letters* **116**, 104-110, doi:10.1016/j.imlet.2007.12.008 (2008).
- 248 Waugh, C., Sinclair, L., Finlay, D., Bayascas, J. R. & Cantrell, D. Phosphoinositide (3,4,5)-Triphosphate Binding to Phosphoinositide-Dependent Kinase 1 Regulates a Protein Kinase

- B/Akt Signaling Threshold That Dictates T-Cell Migration, Not Proliferation. *Mol. Cell. Biol.* **29**, 5952-5962, doi:10.1128/mcb.00585-09 (2009).
- 249 Mao, C. *et al.* Unequal Contribution of Akt Isoforms in the Double-Negative to Double-Positive Thymocyte Transition. *The Journal of Immunology* **178**, 5443-5453, doi:10.4049/jimmunol.178.9.5443 (2007).
- 250 Juntilla, M. M., Wofford, J. A., Birnbaum, M. J., Rathmell, J. C. & Koretzky, G. A. Akt1 and Akt2 are required for alphabeta thymocyte survival and differentiation. *Proc Natl Acad Sci U S A* **104**, 12105-12110, doi:10.1073/pnas.0705285104 (2007).
- 251 Zehn, D., Lee, S. Y. & Bevan, M. J. Complete but curtailed T-cell response to very low-affinity antigen. *Nature* **458**, 211-214, doi:10.1038/nature07657 (2009).
- 252 Reeves, R. K. *et al.* Antigen-specific NK cell memory in rhesus macaques. *Nat Immunol* **16**, 927-932, doi:10.1038/ni.3227 (2015).
- 253 Zhao, Z. *et al.* Discovery of 2,3,5-trisubstituted pyridine derivatives as potent Akt1 and Akt2 dual inhibitors. *Bioorganic & medicinal chemistry letters* **15**, 905-909, doi:10.1016/j.bmcl.2004.12.062 (2005).
- 254 Sudhof, T. C. & Rizo, J. Synaptic vesicle exocytosis. *Cold Spring Harbor perspectives in biology* **3**, doi:10.1101/cshperspect.a005637 (2011).
- 255 Elstak, E. D. *et al.* Munc13-4\*rab27 complex tethers secretory lysosomes at the plasma membrane. *Communicative & integrative biology* **5**, 64-67 (2012).
- 256 Zhang, X. *et al.* BAIAP3, a C2 domain-containing Munc13 protein, controls the fate of dense-core vesicles in neuroendocrine cells. *The Journal of cell biology* **216**, 2151-2166, doi:10.1083/jcb.201702099 (2017).
- 257 Yu, M., Ghosh, S. & Farber, D. Ablation of PDK1 reduces CD4 T cell proliferation and alters cytokine production (121.6). *The Journal of Immunology* **188**, 121.126-121.126 (2012).
- 258 Nirula, A., Ho, M., Phee, H., Roose, J. & Weiss, A. Phosphoinositide-dependent kinase 1 targets protein kinase A in a pathway that regulates interleukin 4. *The Journal of experimental medicine* **203**, 1733-1744, doi:10.1084/jem.20051715 (2006).
- 259 Faroudi, M. *et al.* Lytic versus stimulatory synapse in cytotoxic T lymphocyte/target cell interaction: manifestation of a dual activation threshold. *Proc Natl Acad Sci U S A* **100**, 14145-14150, doi:10.1073/pnas.2334336100 (2003).
- 260 Hebeisen, M. *et al.* SHP-1 phosphatase activity counteracts increased T cell receptor affinity. *The Journal of clinical investigation* **123**, 1044-1056, doi:10.1172/jci65325 (2013).
- 261 Hebeisen, M. *et al.* Molecular insights for optimizing T cell receptor specificity against cancer. *Frontiers in immunology* **4**, 154, doi:10.3389/fimmu.2013.00154 (2013).
- 262 Shiratsuchi, T. *et al.* Cloning and characterization of BAP3 (BAI-associated protein 3), a C2 domain-containing protein that interacts with BAI1. *Biochemical and biophysical research communications* **251**, 158-165, doi:10.1006/bbrc.1998.9408 (1998).
- 263 Chapman, E. R. How does synaptotagmin trigger neurotransmitter release? *Annu Rev Biochem* **77**, 615-641, doi:10.1146/annurev.biochem.77.062005.101135 (2008).
- 264 Boswell, K. L. *et al.* Munc13-4 reconstitutes calcium-dependent SNARE-mediated membrane fusion. *The Journal of cell biology* **197**, 301-312, doi:10.1083/jcb.201109132 (2012).

## List of References

- 265 Palmer, R. E. *et al.* in *Cancer cell* Vol. 2 497-505 (2002).
- 266 Palmer, R. E. *et al.* Induction of BAIAP3 by the EWS-WT1 chimeric fusion implicates regulated exocytosis in tumorigenesis. *Cancer cell* **2**, 497-505 (2002).
- 267 Sørensen, J. B. Ride the wave: Retrograde trafficking becomes Ca<sup>2+</sup> dependent with BAIAP3. *The Journal of cell biology* **216**, 1887-1889, doi:10.1083/jcb.201706007 (2017).
- 268 Zhang, X. *et al.* BAIAP3, a C2 domain-containing Munc13 protein, controls the fate of dense-core vesicles in neuroendocrine cells. *The Journal of cell biology* **216**, 2151-2166, doi:10.1083/jcb.201702099 (2017).
- 269 Howarth, J. L., Lee, Y. B. & Uney, J. B. Using viral vectors as gene transfer tools (Cell Biology and Toxicology Special Issue: ETCS-UK 1 day meeting on genetic manipulation of cells). *Cell biology and toxicology* **26**, 1-20, doi:10.1007/s10565-009-9139-5 (2010).
- 270 Gerritsen, B. & Pandit, A. The memory of a killer T cell: models of CD8(+) T cell differentiation. *Immunology and cell biology* **94**, 236-241, doi:10.1038/icb.2015.118 (2016).
- 271 Roychoudhuri, R. *et al.* BACH2 regulates CD8(+) T cell differentiation by controlling access of AP-1 factors to enhancers. *Nat Immunol* **17**, 851-860, doi:10.1038/ni.3441 (2016).
- 272 Stubbington, M. J. T., Rozenblatt-Rosen, O., Regev, A. & Teichmann, S. A. Single-cell transcriptomics to explore the immune system in health and disease. *Science* **358**, 58-63, doi:10.1126/science.aan6828 (2017).
- 273 Kolodziejczyk, A. A., Kim, J. K., Svensson, V., Marioni, J. C. & Teichmann, S. A. The technology and biology of single-cell RNA sequencing. *Mol Cell* **58**, 610-620, doi:10.1016/j.molcel.2015.04.005 (2015).
- 274 van der Windt, Gerritje J. W. *et al.* Mitochondrial Respiratory Capacity Is a Critical Regulator of CD8<sup>+</sup> T Cell Memory Development. *Immunity* **36**, 68-78, doi:10.1016/j.immuni.2011.12.007 (2012).
- 275 Martin, M. D., Condotta, S. A., Harty, J. T. & Badovinac, V. P. Population dynamics of naive and memory CD8 T cell responses after antigen stimulations in vivo. *Journal of immunology (Baltimore, Md. : 1950)* **188**, 1255-1265, doi:10.4049/jimmunol.1101579 (2012).
- 276 Waugh, K. A. *et al.* Molecular Profile of Tumor-Specific CD8+ T Cell Hypofunction in a Transplantable Murine Cancer Model. *Journal of immunology (Baltimore, Md. : 1950)* **197**, 1477-1488, doi:10.4049/jimmunol.1600589 (2016).
- 277 Ji, Y. *et al.* Repression of the DNA-binding inhibitor Id3 by Blimp-1 limits the formation of memory CD8+ T cells. *Nat Immunol* **12**, 1230-1237, doi:10.1038/ni.2153 (2011).
- 278 Luckey, C. J. *et al.* Memory T and memory B cells share a transcriptional program of self-renewal with long-term hematopoietic stem cells. *Proc Natl Acad Sci U S A* **103**, 3304-3309, doi:10.1073/pnas.0511137103 (2006).
- 279 Kaech, S. M., Hemby, S., Kersh, E. & Ahmed, R. Molecular and functional profiling of memory CD8 T cell differentiation. *Cell* **111**, 837-851 (2002).

- 280 Kakaradov, B. *et al.* Early transcriptional and epigenetic regulation of CD8(+) T cell differentiation revealed by single-cell RNA sequencing. *Nat Immunol* **18**, 422-432, doi:10.1038/ni.3688 (2017).
- 281 Zhang, L. & Romero, P. Metabolic Control of CD8<sup>+</sup> T Cell Fate Decisions and Antitumor Immunity. *Trends in Molecular Medicine* **24**, 30-48, doi:10.1016/j.molmed.2017.11.005 (2018).
- 282 Buck, M. D. *et al.* Mitochondrial Dynamics Controls T Cell Fate through Metabolic Programming. *Cell* **166**, 63-76, doi:10.1016/j.cell.2016.05.035 (2016).
- 283 Jones, R. G. & Thompson, C. B. Revving the engine: signal transduction fuels T cell activation. *Immunity* **27**, 173-178, doi:10.1016/j.immuni.2007.07.008 (2007).
- 284 van der Windt, G. J. W. *et al.* CD8 memory T cells have a bioenergetic advantage that underlies their rapid recall ability. *Proceedings of the National Academy of Sciences* **110**, 14336-14341, doi:10.1073/pnas.1221740110 (2013).
- 285 Chang, C. H. *et al.* Posttranscriptional control of T cell effector function by aerobic glycolysis. *Cell* **153**, 1239-1251, doi:10.1016/j.cell.2013.05.016 (2013).
- 286 Menk, A. V. *et al.* Early TCR Signaling Induces Rapid Aerobic Glycolysis Enabling Distinct Acute T Cell Effector Functions. *Cell reports* **22**, 1509-1521, doi:10.1016/j.celrep.2018.01.040 (2018).
- 287 Millet, P., Vachharajani, V., McPhail, L., Yoza, B. & McCall, C. E. GAPDH Binding to TNF- $\alpha$  mRNA Contributes to Posttranscriptional Repression in Monocytes: A Novel Mechanism of Communication between Inflammation and Metabolism. *Journal of immunology (Baltimore, Md. : 1950)* **196**, 2541-2551, doi:10.4049/jimmunol.1501345 (2016).
- 288 Palmer, C. S. *et al.* Regulators of Glucose Metabolism in CD4(+) and CD8(+) T Cells. *International reviews of immunology* **35**, 477-488, doi:10.3109/08830185.2015.1082178 (2016).
- 289 John, S., Weiss, J. N. & Ribalet, B. Subcellular localization of hexokinases I and II directs the metabolic fate of glucose. *PLoS One* **6**, e17674, doi:10.1371/journal.pone.0017674 (2011).
- 290 Finlay, D. K. mTORC1 regulates CD8+ T-cell glucose metabolism and function independently of PI3K and PKB. *Biochem Soc Trans* **41**, 681-686, doi:10.1042/bst20120359 (2013).
- 291 Geiger, R. *et al.* L-Arginine Modulates T Cell Metabolism and Enhances Survival and Anti-tumor Activity. *Cell* **167**, 829-842.e813, doi:10.1016/j.cell.2016.09.031 (2016).
- 292 Zhang, L. *et al.* Mammalian Target of Rapamycin Complex 2 Controls CD8 T Cell Memory Differentiation in a Foxo1-Dependent Manner. *Cell reports* **14**, 1206-1217, doi:10.1016/j.celrep.2015.12.095 (2016).
- 293 Tan, T. C. J. *et al.* Suboptimal T-cell receptor signaling compromises protein translation, ribosome biogenesis, and proliferation of mouse CD8 T cells. *Proceedings of the National Academy of Sciences* **114**, E6117-E6126, doi:10.1073/pnas.1700939114 (2017).
- 294 Hukelmann, J. L. *et al.* The cytotoxic T cell proteome and its shaping by the kinase mTOR. *Nat Immunol* **17**, 104-112, doi:10.1038/ni.3314 (2016).

## List of References

- 295 Araki, K. *et al.* Translation is actively regulated during the differentiation of CD8(+) effector T cells. *Nat Immunol* **18**, 1046-1057, doi:10.1038/ni.3795 (2017).
- 296 Wherry, E. J. *et al.* Molecular signature of CD8+ T cell exhaustion during chronic viral infection. *Immunity* **27**, 670-684, doi:10.1016/j.immuni.2007.09.006 (2007).
- 297 Wirth, T. C. *et al.* Repetitive antigen stimulation induces stepwise transcriptome diversification but preserves a core signature of memory CD8(+) T cell differentiation. *Immunity* **33**, 128-140, doi:10.1016/j.immuni.2010.06.014 (2010).
- 298 Mehlhop-Williams, E. R. & Bevan, M. J. Memory CD8<sup>+</sup> T cells exhibit increased antigen threshold requirements for recall proliferation. *The Journal of experimental medicine* **211**, 345-356, doi:10.1084/jem.20131271 (2014).
- 299 Lee, S. B. *et al.* Ribosomal protein S3, a new substrate of Akt, serves as a signal mediator between neuronal apoptosis and DNA repair. *The Journal of biological chemistry* **285**, 29457-29468, doi:10.1074/jbc.M110.131367 (2010).
- 300 Fahl, S. P., Wang, M., Zhang, Y., Duc, A. C. & Wiest, D. L. Regulatory Roles of Rpl22 in Hematopoiesis: An Old Dog with New Tricks. *Critical reviews in immunology* **35**, 379-400 (2015).
- 301 Shi, Z. *et al.* Heterogeneous Ribosomes Preferentially Translate Distinct Subpools of mRNAs Genome-wide. *Mol Cell* **67**, 71-83.e77, doi:10.1016/j.molcel.2017.05.021 (2017).
- 302 Segev, N. & Gerst, J. E. Specialized ribosomes and specific ribosomal protein paralogs control translation of mitochondrial proteins. *The Journal of cell biology* **217**, 117-126, doi:10.1083/jcb.201706059 (2018).
- 303 Ito, N. *et al.* Ribosome Incorporation into Somatic Cells Promotes Lineage Transdifferentiation towards Multipotency. *Scientific Reports* **8**, 1634, doi:10.1038/s41598-018-20057-1 (2018).
- 304 Krauss, S., Brand, M. D. & Buttgerit, F. Signaling takes a breath--new quantitative perspectives on bioenergetics and signal transduction. *Immunity* **15**, 497-502 (2001).
- 305 Chaban, Y., Boekema, E. J. & Dudkina, N. V. Structures of mitochondrial oxidative phosphorylation supercomplexes and mechanisms for their stabilisation. *Biochimica et Biophysica Acta (BBA) - Bioenergetics* **1837**, 418-426, doi:<https://doi.org/10.1016/j.bbabi.2013.10.004> (2014).
- 306 Raud, B., McGuire, P. J., Jones, R. G., Sparwasser, T. & Berod, L. Fatty acid metabolism in CD8(+) T cell memory: Challenging current concepts. *Immunological reviews* **283**, 213-231, doi:10.1111/jmr.12655 (2018).
- 307 Sprent, J. & Surh, C. D. Normal T cell homeostasis: the conversion of naive cells into memory-phenotype cells. *Nat Immunol* **12**, 478-484 (2011).
- 308 Wofford, J. A., Wieman, H. L., Jacobs, S. R., Zhao, Y. & Rathmell, J. C. IL-7 promotes Glut1 trafficking and glucose uptake via STAT5-mediated activation of Akt to support T-cell survival. *Blood* **111**, 2101-2111, doi:10.1182/blood-2007-06-096297 (2008).
- 309 Roberts, D. J. & Miyamoto, S. Hexokinase II integrates energy metabolism and cellular protection: Acting on mitochondria and TORCing to autophagy. *Cell death and differentiation* **22**, 248-257, doi:10.1038/cdd.2014.173 (2015).

- 310 Wang, R. *et al.* The transcription factor Myc controls metabolic reprogramming upon T lymphocyte activation. *Immunity* **35**, 871-882, doi:10.1016/j.immuni.2011.09.021 (2011).
- 311 Sena, L. A. *et al.* Mitochondria are required for antigen-specific T cell activation through reactive oxygen species signaling. *Immunity* **38**, 225-236, doi:10.1016/j.immuni.2012.10.020 (2013).
- 312 Siska, P. J. *et al.* Suppression of Glut1 and Glucose Metabolism by Decreased Akt/mTORC1 Signaling Drives T Cell Impairment in B Cell Leukemia. *Journal of immunology (Baltimore, Md. : 1950)* **197**, 2532-2540, doi:10.4049/jimmunol.1502464 (2016).
- 313 Duvel, K. *et al.* Activation of a metabolic gene regulatory network downstream of mTOR complex 1. *Mol Cell* **39**, 171-183, doi:10.1016/j.molcel.2010.06.022 (2010).
- 314 Doedens, A. L. *et al.* Hypoxia-inducible factors enhance the effector responses of CD8(+) T cells to persistent antigen. *Nat Immunol* **14**, 1173-1182, doi:10.1038/ni.2714 (2013).
- 315 Phan, A. T. *et al.* Constitutive Glycolytic Metabolism Supports CD8(+) T Cell Effector Memory Differentiation during Viral Infection. *Immunity* **45**, 1024-1037, doi:10.1016/j.immuni.2016.10.017 (2016).
- 316 Pollizzi, K. N. & Powell, J. D. Integrating canonical and metabolic signalling programmes in the regulation of T cell responses. *Nature reviews. Immunology* **14**, 435-446, doi:10.1038/nri3701 (2014).
- 317 Kidani, Y. *et al.* Sterol regulatory element-binding proteins are essential for the metabolic programming of effector T cells and adaptive immunity. *Nat Immunol* **14**, 489-499, doi:10.1038/ni.2570 (2013).
- 318 van der Windt, G. J. *et al.* Mitochondrial respiratory capacity is a critical regulator of CD8+ T cell memory development. *Immunity* **36**, 68-78, doi:10.1016/j.immuni.2011.12.007 (2012).
- 319 Raud, B. *et al.* Etomoxir Actions on Regulatory and Memory T Cells Are Independent of Cpt1a-Mediated Fatty Acid Oxidation. *Cell Metab* **28**, 504-515.e507, doi:10.1016/j.cmet.2018.06.002 (2018).
- 320 MacIver, N. J. *et al.* The liver kinase B1 is a central regulator of T cell development, activation, and metabolism. *Journal of immunology (Baltimore, Md. : 1950)* **187**, 4187-4198, doi:10.4049/jimmunol.1100367 (2011).
- 321 Kim, J., Kundu, M., Viollet, B. & Guan, K. L. AMPK and mTOR regulate autophagy through direct phosphorylation of Ulk1. *Nat Cell Biol* **13**, 132-141, doi:10.1038/ncb2152 (2011).
- 322 Xu, X. *et al.* Autophagy is essential for effector CD8(+) T cell survival and memory formation. *Nat Immunol* **15**, 1152-1161, doi:10.1038/ni.3025 (2014).
- 323 Rambold, A. S. & Pearce, E. L. Mitochondrial Dynamics at the Interface of Immune Cell Metabolism and Function. *Trends in immunology* **39**, 6-18, doi:10.1016/j.it.2017.08.006 (2018).
- 324 Speiser, D. E., Ho, P.-C. & Verdeil, G. Regulatory circuits of T cell function in cancer. *Nature Reviews Immunology* **16**, 599, doi:10.1038/nri.2016.80 (2016).
- 325 Brand, A. *et al.* LDHA-Associated Lactic Acid Production Blunts Tumor Immunosurveillance by T and NK Cells. *Cell Metab* **24**, 657-671, doi:10.1016/j.cmet.2016.08.011 (2016).

## List of References

- 326 Ren, W. *et al.* Amino-acid transporters in T-cell activation and differentiation. *Cell death & disease* **8**, e2655, doi:10.1038/cddis.2016.222 (2017).
- 327 Liu, Z. *et al.* Suppression of memory CD8 T cell generation and function by tryptophan catabolism. *Journal of immunology (Baltimore, Md. : 1950)* **178**, 4260-4266 (2007).
- 328 Vuillefroy de Silly, R., Dietrich, P. Y. & Walker, P. R. Hypoxia and antitumor CD8(+) T cells: An incompatible alliance? *Oncoimmunology* **5**, e1232236, doi:10.1080/2162402x.2016.1232236 (2016).
- 329 Gropper, Y. *et al.* Culturing CTLs under Hypoxic Conditions Enhances Their Cytotoxicity and Improves Their Anti-tumor Function. *Cell reports* **20**, 2547-2555, doi:10.1016/j.celrep.2017.08.071 (2017).
- 330 Mathieu, C. *et al.* IL-2 and IL-15 regulate CD8+ memory T-cell differentiation but are dispensable for protective recall responses. *European journal of immunology* **45**, 3324-3338, doi:10.1002/eji.201546000 (2015).
- 331 Kohn, A. D., Takeuchi, F. & Roth, R. A. Akt, a pleckstrin homology domain containing kinase, is activated primarily by phosphorylation. *The Journal of biological chemistry* **271**, 21920-21926 (1996).
- 332 Kohn, A. D., Summers, S. A., Birnbaum, M. J. & Roth, R. A. Expression of a constitutively active Akt Ser/Thr kinase in 3T3-L1 adipocytes stimulates glucose uptake and glucose transporter 4 translocation. *The Journal of biological chemistry* **271**, 31372-31378 (1996).
- 333 Castro, I., Yu, A., Dee, M. J. & Malek, T. R. The basis of distinctive IL-2- and IL-15-dependent signaling: weak CD122-dependent signaling favors CD8+ T central-memory cell survival but not T effector-memory cell development. *Journal of immunology (Baltimore, Md. : 1950)* **187**, 5170-5182, doi:10.4049/jimmunol.1003961 (2011).
- 334 Tejera, M. M., Kim, E. H., Sullivan, J. A., Plisch, E. H. & Suresh, M. FoxO1 controls effector-to-memory transition and maintenance of functional CD8 T cell memory. *Journal of immunology (Baltimore, Md. : 1950)* **191**, 187-199, doi:10.4049/jimmunol.1300331 (2013).
- 335 Chan, D. C. Fusion and fission: interlinked processes critical for mitochondrial health. *Annual review of genetics* **46**, 265-287, doi:10.1146/annurev-genet-110410-132529 (2012).
- 336 Xu, K. *et al.* MFN2 suppresses cancer progression through inhibition of mTORC2/Akt signaling. *Sci Rep* **7**, 41718, doi:10.1038/srep41718 (2017).
- 337 Parra, V. *et al.* Insulin stimulates mitochondrial fusion and function in cardiomyocytes via the Akt-mTOR-NFkappaB-Opa-1 signaling pathway. *Diabetes* **63**, 75-88, doi:10.2337/db13-0340 (2014).
- 338 Yang, F. *et al.* Leptin increases mitochondrial OPA1 via GSK3-mediated OMA1 ubiquitination to enhance therapeutic effects of mesenchymal stem cell transplantation. *Cell death & disease* **9**, 556, doi:10.1038/s41419-018-0579-9 (2018).
- 339 Ehses, S. *et al.* Regulation of OPA1 processing and mitochondrial fusion by m-AAA protease isoenzymes and OMA1. *The Journal of cell biology* **187**, 1023-1036, doi:10.1083/jcb.200906084 (2009).
- 340 MacVicar, T. & Langer, T. OPA1 processing in cell death and disease - the long and short of it. *Journal of cell science* **129**, 2297-2306, doi:10.1242/jcs.159186 (2016).

- 341 Fang, X. *et al.* Phosphorylation and inactivation of glycogen synthase kinase 3 by protein kinase A. *Proceedings of the National Academy of Sciences* **97**, 11960-11965, doi:10.1073/pnas.220413597 (2000).
- 342 Waldmann, T. A. The shared and contrasting roles of IL2 and IL15 in the life and death of normal and neoplastic lymphocytes: implications for cancer therapy. *Cancer immunology research* **3**, 219-227, doi:10.1158/2326-6066.cir-15-0009 (2015).
- 343 Akashi, K., Kondo, M., von Freeden-Jeffry, U., Murray, R. & Weissman, I. L. Bcl-2 rescues T lymphopoiesis in interleukin-7 receptor-deficient mice. *Cell* **89**, 1033-1041 (1997).
- 344 Skon, C. N. *et al.* Transcriptional downregulation of S1pr1 is required for the establishment of resident memory CD8+ T cells. *Nat Immunol* **14**, 1285-1293, doi:10.1038/ni.2745 (2013).
- 345 Bruhn, M. A., Pearson, R. B., Hannan, R. D. & Sheppard, K. E. Second AKT: the rise of SGK in cancer signalling. *Growth Factors* **28**, 394-408, doi:10.3109/08977194.2010.518616 (2010).
- 346 Garcia-Martinez, J. M. & Alessi, D. R. mTOR complex 2 (mTORC2) controls hydrophobic motif phosphorylation and activation of serum- and glucocorticoid-induced protein kinase 1 (SGK1). *The Biochemical journal* **416**, 375-385, doi:10.1042/bj20081668 (2008).
- 347 Toker, A. mTOR and Akt signaling in cancer: SGK cycles in. *Mol Cell* **31**, 6-8, doi:10.1016/j.molcel.2008.06.007 (2008).
- 348 Hong, F. *et al.* mTOR-raptor binds and activates SGK1 to regulate p27 phosphorylation. *Mol Cell* **30**, 701-711, doi:10.1016/j.molcel.2008.04.027 (2008).
- 349 Lu, M. *et al.* mTOR complex-2 activates ENaC by phosphorylating SGK1. *Journal of the American Society of Nephrology : JASN* **21**, 811-818, doi:10.1681/asn.2009111168 (2010).
- 350 Sommer, E. M. *et al.* Elevated SGK1 predicts resistance of breast cancer cells to Akt inhibitors. *The Biochemical journal* **452**, 499-508, doi:10.1042/bj20130342 (2013).
- 351 Biondi, R. M., Kieloch, A., Currie, R. A., Deak, M. & Alessi, D. R. The PIF-binding pocket in PDK1 is essential for activation of S6K and SGK, but not PKB. *The EMBO journal* **20**, 4380-4390, doi:10.1093/emboj/20.16.4380 (2001).
- 352 Tessier, M. & Woodgett, J. R. Role of the Phox homology domain and phosphorylation in activation of serum and glucocorticoid-regulated kinase-3. *The Journal of biological chemistry* **281**, 23978-23989, doi:10.1074/jbc.M604333200 (2006).
- 353 Lang, F. & Cohen, P. Regulation and physiological roles of serum- and glucocorticoid-induced protein kinase isoforms. *Science's STKE : signal transduction knowledge environment* **2001**, re17, doi:10.1126/stke.2001.108.re17 (2001).
- 354 Webster, M. K., Goya, L., Ge, Y., Maiyar, A. C. & Firestone, G. L. Characterization of sgk, a novel member of the serine/threonine protein kinase gene family which is transcriptionally induced by glucocorticoids and serum. *Mol Cell Biol* **13**, 2031-2040 (1993).
- 355 Naray-Fejes-Toth, A., Fejes-Toth, G., Volk, K. A. & Stokes, J. B. SGK is a primary glucocorticoid-induced gene in the human. *The Journal of steroid biochemistry and molecular biology* **75**, 51-56 (2000).

## List of References

- 356 Lang, F. *et al.* (Patho)physiological significance of the serum- and glucocorticoid-inducible kinase isoforms. *Physiological reviews* **86**, 1151-1178, doi:10.1152/physrev.00050.2005 (2006).
- 357 Bell, L. M. *et al.* Hyperosmotic stress stimulates promoter activity and regulates cellular utilization of the serum- and glucocorticoid-inducible protein kinase (Sgk) by a p38 MAPK-dependent pathway. *The Journal of biological chemistry* **275**, 25262-25272, doi:10.1074/jbc.M002076200 (2000).
- 358 Fejes-Toth, G., Frindt, G., Naray-Fejes-Toth, A. & Palmer, L. G. Epithelial Na<sup>+</sup> channel activation and processing in mice lacking SGK1. *American journal of physiology. Renal physiology* **294**, F1298-1305, doi:10.1152/ajprenal.00579.2007 (2008).
- 359 Wildman, S. S., Kang, E. S. & King, B. F. ENaC, renal sodium excretion and extracellular ATP. *Purinergic signalling* **5**, 481-489, doi:10.1007/s11302-009-9150-6 (2009).
- 360 David, S. & Kalb, R. G. Serum/glucocorticoid-inducible kinase can phosphorylate the cyclic AMP response element binding protein, CREB. *FEBS Lett* **579**, 1534-1538, doi:10.1016/j.febslet.2005.01.040 (2005).
- 361 Zhang, L., Cui, R., Cheng, X. & Du, J. Antiapoptotic effect of serum and glucocorticoid-inducible protein kinase is mediated by novel mechanism activating I{kappa}B kinase. *Cancer Res* **65**, 457-464 (2005).
- 362 Dehner, M., Hadjihannas, M., Weiske, J., Huber, O. & Behrens, J. Wnt signaling inhibits Forkhead box O3a-induced transcription and apoptosis through up-regulation of serum- and glucocorticoid-inducible kinase 1. *The Journal of biological chemistry* **283**, 19201-19210, doi:10.1074/jbc.M710366200 (2008).
- 363 Lang, F., Artunc, F. & Vallon, V. The physiological impact of the serum and glucocorticoid-inducible kinase SGK1. *Current opinion in nephrology and hypertension* **18**, 439-448, doi:10.1097/MNH.0b013e32832f125e (2009).
- 364 Kleinewietfeld, M. *et al.* Sodium chloride drives autoimmune disease by the induction of pathogenic TH17 cells. *Nature* **496**, 518-522, doi:10.1038/nature11868 (2013).
- 365 Korn, T., Bettelli, E., Oukka, M. & Kuchroo, V. K. IL-17 and Th17 Cells. *Annual review of immunology* **27**, 485-517, doi:10.1146/annurev.immunol.021908.132710 (2009).
- 366 Wu, C. *et al.* Induction of pathogenic TH17 cells by inducible salt-sensing kinase SGK1. *Nature* **496**, 513-517, doi:10.1038/nature11984 (2013).
- 367 Stritesky, G. L., Yeh, N. & Kaplan, M. H. IL-23 promotes maintenance but not commitment to the Th17 lineage. *Journal of immunology (Baltimore, Md. : 1950)* **181**, 5948-5955 (2008).
- 368 Hernandez, A. L. *et al.* Sodium chloride inhibits the suppressive function of FOXP3+ regulatory T cells. *The Journal of clinical investigation* **125**, 4212-4222, doi:10.1172/jci81151 (2015).
- 369 Sherk, A. B. *et al.* Development of a small-molecule serum- and glucocorticoid-regulated kinase-1 antagonist and its evaluation as a prostate cancer therapeutic. *Cancer Res* **68**, 7475-7483, doi:10.1158/0008-5472.can-08-1047 (2008).
- 370 Andersen, M. N. *et al.* A phosphoinositide 3-kinase (PI3K)-serum- and glucocorticoid-inducible kinase 1 (SGK1) pathway promotes Kv7.1 channel surface expression by

- inhibiting Nedd4-2 protein. *The Journal of biological chemistry* **288**, 36841-36854, doi:10.1074/jbc.M113.525931 (2013).
- 371 Burgon, J. *et al.* Serum and glucocorticoid-regulated kinase 1 regulates neutrophil clearance during inflammation resolution. *Journal of immunology (Baltimore, Md. : 1950)* **192**, 1796-1805, doi:10.4049/jimmunol.1300087 (2014).
- 372 Jorg, S. *et al.* High salt drives Th17 responses in experimental autoimmune encephalomyelitis without impacting myeloid dendritic cells. *Experimental neurology* **279**, 212-222, doi:10.1016/j.expneurol.2016.03.010 (2016).
- 373 Boyman, O. & Sprent, J. The role of interleukin-2 during homeostasis and activation of the immune system. *Nature reviews. Immunology* **12**, 180-190, doi:10.1038/nri3156 (2012).
- 374 Tsai, K. J., Chen, S. K., Ma, Y. L., Hsu, W. L. & Lee, E. H. sgk, a primary glucocorticoid-induced gene, facilitates memory consolidation of spatial learning in rats. *Proc Natl Acad Sci U S A* **99**, 3990-3995, doi:10.1073/pnas.062405399 (2002).
- 375 Tyan, S. W., Tsai, M. C., Lin, C. L., Ma, Y. L. & Lee, E. H. Serum- and glucocorticoid-inducible kinase 1 enhances zif268 expression through the mediation of SRF and CREB1 associated with spatial memory formation. *Journal of neurochemistry* **105**, 820-832, doi:10.1111/j.1471-4159.2007.05186.x (2008).
- 376 Di Pietro, N. *et al.* Serum- and glucocorticoid-inducible kinase 1 (SGK1) regulates adipocyte differentiation via forkhead box O1. *Molecular endocrinology (Baltimore, Md.)* **24**, 370-380, doi:10.1210/me.2009-0265 (2010).
- 377 Brunet, A. *et al.* Protein kinase SGK mediates survival signals by phosphorylating the forkhead transcription factor FKHRL1 (FOXO3a). *Mol Cell Biol* **21**, 952-965, doi:10.1128/mcb.21.3.952-965.2001 (2001).
- 378 Kino, T. *et al.* Brx mediates the response of lymphocytes to osmotic stress through the activation of NFAT5. *Science signaling* **2**, ra5, doi:10.1126/scisignal.2000081 (2009).
- 379 Palmada, M. *et al.* SGK1 kinase upregulates GLUT1 activity and plasma membrane expression. *Diabetes* **55**, 421-427 (2006).
- 380 Kobayashi, T. & Cohen, P. Activation of serum- and glucocorticoid-regulated protein kinase by agonists that activate phosphatidylinositol 3-kinase is mediated by 3-phosphoinositide-dependent protein kinase-1 (PDK1) and PDK2. *The Biochemical journal* **339 ( Pt 2)**, 319-328 (1999).
- 381 Ma, Y. L., Tsai, M. C., Hsu, W. L. & Lee, E. H. SGK protein kinase facilitates the expression of long-term potentiation in hippocampal neurons. *Learning & memory (Cold Spring Harbor, N.Y.)* **13**, 114-118, doi:10.1101/lm.179206 (2006).
- 382 Romero, P. *et al.* Four Functionally Distinct Populations of Human Effector-Memory CD8<sup>+</sup> T Lymphocytes. *The Journal of Immunology* **178**, 4112-4119, doi:10.4049/jimmunol.178.7.4112 (2007).
- 383 Busch, D. H., Frassle, S. P., Sommermeyer, D., Buchholz, V. R. & Riddell, S. R. Role of memory T cell subsets for adoptive immunotherapy. *Seminars in immunology* **28**, 28-34, doi:10.1016/j.smim.2016.02.001 (2016).
- 384 Berger, C. *et al.* Adoptive transfer of effector CD8<sup>+</sup> T cells derived from central memory cells establishes persistent T cell memory in primates. *The Journal of clinical investigation* **118**, 294-305, doi:10.1172/jci32103 (2008).

## List of References

- 385 Xu, X., Xiong, X. & Sun, Y. The role of ribosomal proteins in the regulation of cell proliferation, tumorigenesis, and genomic integrity. *Science China. Life sciences* **59**, 656-672, doi:10.1007/s11427-016-0018-0 (2016).
- 386 Kowalczyk, P., Woszczynski, M. & Ostrowski, J. Increased expression of ribosomal protein S2 in liver tumors, posthepactomized livers, and proliferating hepatocytes in vitro. *Acta biochimica Polonica* **49**, 615-624, doi:024903615 (2002).
- 387 Denis, H., Ndlovu, M. N. & Fuks, F. Regulation of mammalian DNA methyltransferases: a route to new mechanisms. *EMBO reports* **12**, 647-656, doi:10.1038/embor.2011.110 (2011).
- 388 Esteve, P. O. *et al.* A methylation and phosphorylation switch between an adjacent lysine and serine determines human DNMT1 stability. *Nature structural & molecular biology* **18**, 42-48, doi:10.1038/nsmb.1939 (2011).
- 389 Chappell, C., Beard, C., Altman, J., Jaenisch, R. & Jacob, J. DNA Methylation by DNA Methyltransferase 1 Is Critical for Effector CD8 T Cell Expansion. *The Journal of Immunology* **176**, 4562-4572, doi:10.4049/jimmunol.176.8.4562 (2006).
- 390 de Araujo-Souza, P. S., Hanschke, S. C. & Viola, J. P. Epigenetic control of interferon-gamma expression in CD8 T cells. *Journal of immunology research* **2015**, 849573, doi:10.1155/2015/849573 (2015).
- 391 Cha, T. L. *et al.* Akt-mediated phosphorylation of EZH2 suppresses methylation of lysine 27 in histone H3. *Science* **310**, 306-310, doi:10.1126/science.1118947 (2005).
- 392 Russ, B. E. *et al.* Distinct epigenetic signatures delineate transcriptional programs during virus-specific CD8(+) T cell differentiation. *Immunity* **41**, 853-865, doi:10.1016/j.immuni.2014.11.001 (2014).
- 393 He, S. *et al.* Ezh2 phosphorylation state determines its capacity to maintain CD8(+) T memory precursors for antitumor immunity. *Nature communications* **8**, 2125, doi:10.1038/s41467-017-02187-8 (2017).
- 394 Gray, S. M., Amezquita, R. A., Guan, T., Kleinstein, S. H. & Kaech, S. M. Polycomb Repressive Complex 2-Mediated Chromatin Repression Guides Effector CD8(+) T Cell Terminal Differentiation and Loss of Multipotency. *Immunity* **46**, 596-608, doi:10.1016/j.immuni.2017.03.012 (2017).
- 395 Rena, G., Guo, S., Cichy, S. C., Unterman, T. G. & Cohen, P. Phosphorylation of the transcription factor forkhead family member FKHR by protein kinase B. *The Journal of biological chemistry* **274**, 17179-17183 (1999).
- 396 Hess Michelini, R., Doedens, A. L., Goldrath, A. W. & Hedrick, S. M. Differentiation of CD8 memory T cells depends on Foxo1. *The Journal of experimental medicine* **210**, 1189-1200, doi:10.1084/jem.20130392 (2013).
- 397 Rao, Rajesh R., Li, Q., Bupp, Melanie R. G. & Shrikant, Protul A. Transcription Factor Foxo1 Represses T-bet-Mediated Effector Functions and Promotes Memory CD8+ T Cell Differentiation. *Immunity* **36**, 374-387, doi:<https://doi.org/10.1016/j.immuni.2012.01.015> (2012).
- 398 Deng, Y., Wang, F., Hughes, T. & Yu, J. FOXOs in cancer immunity: Knowns and unknowns. *Seminars in Cancer Biology* **50**, 53-64, doi:<https://doi.org/10.1016/j.semcan.2018.01.005> (2018).

- 399 Staron, M. M. *et al.* The transcription factor FoxO1 sustains expression of the inhibitory receptor PD-1 and survival of antiviral CD8(+) T cells during chronic infection. *Immunity* **41**, 802-814, doi:10.1016/j.immuni.2014.10.013 (2014).
- 400 Brunet, A. *et al.* Akt promotes cell survival by phosphorylating and inhibiting a Forkhead transcription factor. *Cell* **96**, 857-868 (1999).
- 401 Yasuda, K., Ueda, Y., Ozawa, M., Matsuda, T. & Kinashi, T. Enhanced cytotoxic T-cell function and inhibition of tumor progression by Mst1 deficiency. *FEBS Letters* **590**, 68-75, doi:doi:10.1002/1873-3468.12045 (2016).
- 402 Sullivan, J. A., Kim, E. H., Plisch, E. H., Peng, S. L. & Suresh, M. FOXO3 Regulates CD8 T Cell Memory by T Cell-Intrinsic Mechanisms. *PLOS Pathogens* **8**, e1002533, doi:10.1371/journal.ppat.1002533 (2012).
- 403 Yang, C. Y. *et al.* The transcriptional regulators Id2 and Id3 control the formation of distinct memory CD8+ T cell subsets. *Nat Immunol* **12**, 1221-1229, doi:10.1038/ni.2158 (2011).
- 404 Masson, F. *et al.* Id2-Mediated Inhibition of E2A Represses Memory CD8<sup>+</sup> T Cell Differentiation. *The Journal of Immunology* **190**, 4585-4594, doi:10.4049/jimmunol.1300099 (2013).
- 405 Lewis, M. D., Miller, S. A., Miazgowiec, M. M., Beima, K. M. & Weinmann, A. S. T-bet's ability to regulate individual target genes requires the conserved T-box domain to recruit histone methyltransferase activity and a separate family member-specific transactivation domain. *Mol Cell Biol* **27**, 8510-8521, doi:10.1128/mcb.01615-07 (2007).
- 406 Lazarevic, V., Glimcher, L. H. & Lord, G. M. T-bet: a bridge between innate and adaptive immunity. *Nature reviews. Immunology* **13**, 777-789, doi:10.1038/nri3536 (2013).
- 407 Banerjee, A. *et al.* Cutting Edge: The Transcription Factor Eomesodermin Enables CD8<sup>+</sup> T Cells To Compete for the Memory Cell Niche. *The Journal of Immunology* **185**, 4988-4992, doi:10.4049/jimmunol.1002042 (2010).
- 408 Intlekofer, A. M. *et al.* Effector and memory CD8+ T cell fate coupled by T-bet and eomesodermin. *Nat Immunol* **6**, 1236-1244, doi:10.1038/ni1268 (2005).
- 409 Xin, A. *et al.* A molecular threshold for effector CD8+ T cell differentiation controlled by transcription factors Blimp-1 and T-bet. *Nature Immunology* **17**, 422, doi:10.1038/ni.3410 <https://www.nature.com/articles/ni.3410#supplementary-information> (2016).
- 410 Rutishauser, R. L. *et al.* Transcriptional Repressor Blimp-1 Promotes CD8+ T Cell Terminal Differentiation and Represses the Acquisition of Central Memory T Cell Properties. *Immunity* **31**, 296-308, doi:<https://doi.org/10.1016/j.immuni.2009.05.014> (2009).
- 411 Zhou, X. *et al.* Differentiation and Persistence of Memory CD8+ T Cells Depend on T Cell Factor 1. *Immunity* **33**, 229-240, doi:<https://doi.org/10.1016/j.immuni.2010.08.002> (2010).
- 412 Kim, M. V., Ouyang, W., Liao, W., Zhang, M. Q. & Li, M. O. The transcription factor Foxo1 controls central-memory CD8+ T cell responses to infection. *Immunity* **39**, 286-297, doi:10.1016/j.immuni.2013.07.013 (2013).

## List of References

- 413 Mami-Chouaib, F. *et al.* Resident memory T cells, critical components in tumor immunology. *Journal for ImmunoTherapy of Cancer* **6**, 87, doi:10.1186/s40425-018-0399-6 (2018).
- 414 Klebanoff, C. A. *et al.* Inhibition of AKT signaling uncouples T cell differentiation from expansion for receptor-engineered adoptive immunotherapy. *JCI insight* **2**, doi:10.1172/jci.insight.95103 (2017).
- 415 van der Waart, A. B. *et al.* Inhibition of Akt signaling promotes the generation of superior tumor-reactive T cells for adoptive immunotherapy. *Blood* **124**, 3490-3500, doi:10.1182/blood-2014-05-578583 (2014).
- 416 Abu Eid, R. *et al.* Enhanced Therapeutic Efficacy and Memory of Tumor-Specific CD8 T Cells by Ex Vivo PI3K-delta Inhibition. *Cancer Res* **77**, 4135-4145, doi:10.1158/0008-5472.can-16-1925 (2017).
- 417 Zhang, L. & Romero, P. Metabolic Control of CD8(+) T Cell Fate Decisions and Antitumor Immunity. *Trends Mol Med* **24**, 30-48, doi:10.1016/j.molmed.2017.11.005 (2018).
- 418 Jameson, S. & Hamilton, S. CD8 T cell memory: it takes all kinds. *Frontiers in immunology* **3**, doi:10.3389/fimmu.2012.00353 (2012).
- 419 Kotchen, T. A., Cowley, A. W. & Frohlich, E. D. Salt in Health and Disease — A Delicate Balance. *New England Journal of Medicine* **368**, 1229-1237, doi:10.1056/NEJMra1212606 (2013).
- 420 Allison, K. E., Coomber, B. L. & Bridle, B. W. Metabolic reprogramming in the tumour microenvironment: a hallmark shared by cancer cells and T lymphocytes. *Immunology* **152**, 175-184, doi:10.1111/imm.12777 (2017).